University of Alberta

Development of the Human Metabolome Mass Spectrometry Database

by

Melisa A Clements

A thesis submitted to the Faculty of Graduate Studies and Research in partial fulfillment of the requirements for the degree of Master of Science

Department of Chemistry

Edmonton, Alberta

Spring 2008

Your file Votre référence
ISBN: 978-0-494-45795-5
Our file Notre référence
ISBN: 978-0-494-45795-5

Abstract

The objective of this research was to develop new analytical methods for endogenous metabolite identification from urine samples. One of the major challenges in metabolite identification is that the samples being analyzed are complex, containing many different compounds with varying concentrations. In this work two different methods of metabolite identification are described. Initially, known endogenous substrates were incubated with human liver microsomes. The resulting metabolites were then identified, using mass spectrometry (MS), and documented to be used later as pseudo-standards to identify unknowns found in urine. The second method involved the creation of a theoretical metabolite database containing metabolites predicted through known endogenous compounds and biotransformation plus their chemical information. The unknowns identified in urine were matched up to entries in the database using accurate mass measurements and were then confirmed using tandem MS techniques. The potential of these techniques to identify metabolites in human urine was demonstrated.

Acknowledgments

First and foremost, I would like to thank my supervisor, Dr. Liang Li, for giving me the opportunity to further my education in analytical chemistry with his research group. I truly appreciate the guidance, knowledge and opportunities that he has shared with me throughout the past three years and I am sure that everything I have learned from him will continue to benefit me in the future.

I would also like to thank my friends and family for their support over the years and making the entire experience more memorable. I would especially like to thank my parents, Bob and Rose Clements, who encouraged and supported my decisions in furthering my education. My boyfriend, Geoff Brown, for helping me though all of the stressful times and late nights spent working in the lab, I could always count on him to ensure that I had clean clothes and food to eat when I was too busy to take care of it myself. The Li Group, past and present, there was always somebody to talk to and ask for advice, whether it was chemistry related or not. Dr. Sandra Marcus for her help with all of the biology related work I was required to know for this project and Dr. Randy Whittle for his advice and help with the FT-ICR MS.

I would also like to thank the following agencies and groups for the funding that made this research possible including Genome Canada and Genome Alberta through the Human Metabolite Project.

Lastly but not least, I would like to thank my committee members, Dr. Jonathan Curtis and Dr. X. Chris Le, for their time, comments and constructive criticism on my thesis.

Table of Contents

List of Tables

List of Figures

List of Abbreviations

2MBC	2-methylbutyroylcarnitne
3-MCC	3-methylcrotonyl-CoA carboxylase
ASA	argininosuccinic aciduria
BPC	Base peak chromatogram
C2	Acetylcarnitine, $C_9H_{17}NO_4$
C3	Propionylcarnitine, $C_{10}H_{19}NO_4$
C4	Butyrylcarnitine/Isobutyrylcarnitine, $C_{11}H_{21}NO_4$
C5	Valeylcarnitine/Isovaleylcarnitine/2-methylbutyrylcarnitine, $C_{12}H_{23}NO_4$
C6	Hexanoylcarnitine, $C_{13}H_{25}NO_4$
C7	Heptanoylcarnitine, $C_{14}H_{27}NO_4$
C8	Octanoylcarnitine/Valproylcarnitine, $C_{15}H_{29}NO_4$
C9	Nonanoylcarnitine, $C_{16}H_{31}NO_4$
C10	Decanoylcarnitine, $C_{17}H_{33}NO_4$
C11	$C_{18}H_{35}NO_4$
C12	Lauroylcarnitine, $C_{19}H_{37}NO_4$
C13	$C_{20}H_{39}NO_4$
C14	$C_{21}H_{41}NO_4$
C15	$C_{22}H_{43}NO_4$
C16	Palmitoylcarntinte, $C_{23}H_{45}NO_4$
C18	$C_{25}H_{49}NO_4$
C#DC	the # is replaced with a number indicating which acylcarintine and the DC indicates a dicarboxylic acylcarnitine
C#OH	the # is replaced with a number indicating which acylcarintine and the OH indicates that a hydroxyl group has been added to the molecule
C#:x	the # is replaced with a number indicating which acylcarintine and the :x indicates the number of double bonds
CID	Collision induced dissociation
CoA	Coenzyme A
CPT	carnitine palmitoyltransferase
CRM	Charge Residue Model
CSF	Cerebral Spinal Fluid

CYP	Cytochrome P450 enzymes
CYP xyz	Where x is a number which denotes the gene family, y is a letter which denotes the subfamily and z in a number which denotes the individual gene
Da	Dalton
dc	Direct current
DTT	Dithiotreitol
EI	Electron Impact ionization
EIC	Extracted ion chromatogram
ESI	Electrospray ionization
FMO	flavin-contaning monooxygenase
FT-ICR	Fourier Transform Ion Cyclotron Resonance
GA	glutaric acidemia
GC	Gas Chromatography
GC-MS	Gas Chromatography coupled with mass spectrometry
GSH	Glutathione
GST	Glutathione S-transferases
HLM	Human Liver Microsomes
HMDB	Human Metabolome Database
HMG	3-hydroxy-3-methylglutaryl
HML	Human Metabolome Library
HMP	Human Metabolome Project
HPLC	High Pressure Liquid Chromatography
IEM	Ion Evaporation Model
IRMPD	infrared multiphoton dissociation
IVA	isovaleric acidemia
LC	Liquid Chromatography
LCHAD	long-chain hydroxyacyl-CoA dehydrogenase
LC-MS	Liquid Chromatography coupled with mass spectrometry
MADD	multiple acyl-CoA dehydrogenase deficiency
MCAD	Medium-chain acyl-CoA dehydrogenase
MMA	methylmalonic acidemia
MRM	multiple reaction monitoring

MS	Mass Spectrometry
MS/MS	Tandem MS, one ion is isolated and fragmented to create a secondary spectrum
MS^n	A term used in the case of MS/MS experiments, where product ion analysis is extended over a number of generations.
MSUD	Maple Syrup Urinary Disease
m/z	mass to charge
NADPH	reduced nicotinamide adenine dinucleotide phosphate
NAT	N-acetyltransferase
NMR	Nuclear Magnetic Resonance
NRS	NADPH regenerating system
PA	propionic acidemia
PAPS	adenosine-3'-phosphate-5'-phosphosulfate
PKU	phenylketonuria
ppm	Parts per million (current mass - reference mass) / (reference mass $*10^6$)
PS	Pumping station
rf	radio frequency
SAM	S-adenosyl methionine
SCAD	short-chain acyl-CoA dehydrogenase
SIM	Single Ion Monitoring
SPE	Solid Phase Extraction
ST	Sialyltransferase
TC	Total carnitine
TPMT	Thiopurine methyltransferase
UDPGA	Uridine Diphosphate -glucuronic acid
UDPGT	Uridine Diphosphate Glucuronyltransferase
UGT	glucuronosyltransferases
VLCAD	very long-chain acyl-CoA dehydrogenase

Chapter 1

Introduction

1.1. Mass Spectrometry

1.1.1. Electrospray Ionization

Electrospray ionization (ESI) is designed to generate gas phase ions from a solution where they are subsequently focused and transported into the mass analyzer and is one of the more popular interfaces used for sample introduction into a mass spectrometer (MS). It allows a liquid sample to be introduced into the vacuum region of a mass spectrometer without causing a drastic increase in pressure, making it possible to directly interface a Liquid Chromatography system (LC) to an MS.

ESI is achieved by flowing a solution comprised of sample and solvent through a charged needle and spraying the solution into a spray chamber, which is kept at atmospheric pressure, to form a fine mist of charged droplets. To facilitate the spray from a relatively high flow liquid stream (i.e., flow rate>10 μL/min), the needle is housed inside a tube that adds nebulizing gas, typically nitrogen, to the sample stream. The nebulizing gas helps to form a consistent spray and stabilize the ion current. This produces a fine mist of solution in which the solvent is evaporated with the help of a dry gas. The drying gas, also nitrogen, is introduced into the spray chamber by flowing around and heating a part of the capillary. The flow rate and temperature of the drying gas is controlled by the user. Once the solvent is evaporated the remaining analytes, in ion form, are guided towards the entrance of the mass spectrometer by a high-voltage electrostatic gradient.[1] The pressure difference between the spray chamber and the ion focusing and transport region of the mass spectrometer pushes the ions through the entrance aperture to enter the mass analyzer.[1]

There are currently two theories that explain the formation of ions from the small charged droplets formed during solution nebulization, namely the Charge Residue Model (CRM) and the Ion Evaporation Model (IEM). The former suggests that the evaporation of solvent from a charged droplet would increase the surface-charge density until it reaches the Rayleigh limit at which the forces due to Coulombic repulsion and surface tension become comparable. The resulting instability would cause the droplet to burst

creating a number of smaller droplets that would continue to evaporate. A series of these "Coulombic Explosions" would eventually result in droplets so small that they consist of a single solvent molecule and analyte molecule. That analyte would become an ion by retaining some of the droplet charge as the last of the solvent vaporized. [2] The IEM is the more widely acceptable of the two models. The IEM holds that a sequence of Coulombic explosions due to solvent evaporation would result in droplets so small and charge density so high that the resulting electrostatic field at the droplet surface would be strong enough to eject the solute ions from the droplet and into the gas phase. [2]

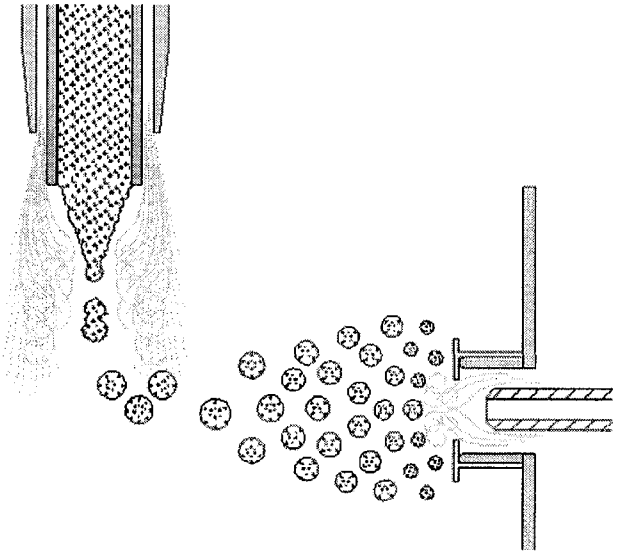

Figure 1.1 - Droplet formation within the Esquire Ion trap. This figure was reproduced with permission from Bruker Daltonics [1]

1.1.2. Ion Trap Mass Spectrometer

In general an ion trap mass spectrometer consists of several basic parts: an interface to generate and transport the ions, a set of filters and lenses to direct the ion beam, a trap to collect and release the ions according to mass/charge (m/z) and a detector to generate the spectrum. The mass analyzer, quadrupole ion trap, is the unique feature in this type of instrument. The quadrupole ion trap consists of three different pieces, the entrance endcap, ring electrode and the exit endcap, as shown in Figure 1.2. These three pieces form a hyperbolic electric potential [3] and work together to perform several important functions, including mass accumulation, selective mass isolation, excitation for collision induced dissociation (MS^n) and sequential mass ejection to produce a mass spectrum.

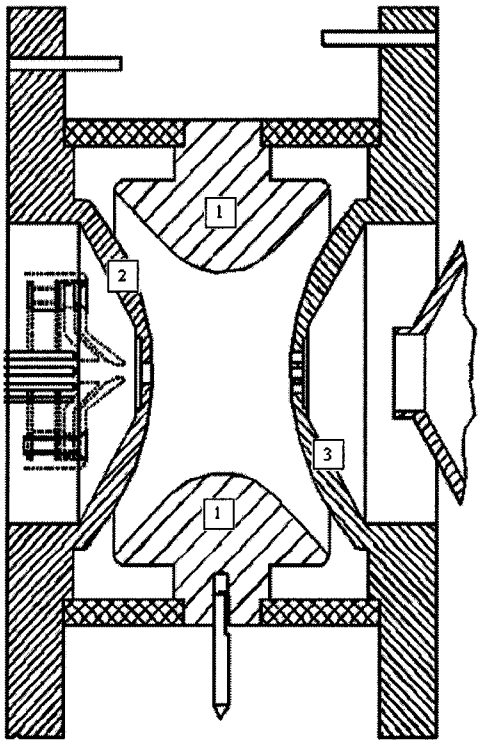

Figure 1.2 - Schematics of the quadrupole ion trap found inside Bruker's Esquire 3000plus. 1) ring electrode, 2) incoming endcap electrode and 3) outcoming endcap electrode. This figure was reproduced with permission from Bruker Daltonics [1]

The quadrupole ion trap is designed to trap ions within an electric field generated by the ring electrode and the endcaps. The ion's ability to be trapped within this field is dependent on the ion stability which is directly related to the rf and dc voltages applied to the trap, as described by the Mathieu equation and stability diagram. [3] The voltages can be set to isolate ions of a single m/z, a small range of m/z or a broad range of m/z depending on the type of experiments to be conducted. The oscillating electric potential applied to the ring electrode, called the "fundamental rf" focuses ions towards the center of the trap.[4] To improve the trapping efficiency helium gas is pumped into the ion trap, at approximately 1 mtorr, collisionally dampening the ion motion and causing the ions to migrate to the center of the ion trap.[3] Thus, once ions are ejected from the ion trap, not only are they bunched together as they leave, but they are also focused tightly along the z-axis so that they are efficiently transmitted to the detector. [5]

Ions are ejected from the ion trap for detection by applying a resonance rf frequency for each m/z. Typically this is done by ramping up the rf voltage applied to the

ring electrode. The energy absorbed by the ions from the resonance rf frequency increases their trajectory along the z-axis (in Figure 1.2 the z-axis runs horizontally) until the ions become unstable and they are ejected through the holes in the outcoming endcap electrode.[4] Once ejected the ions are detected by an electron multiplier to produce a mass spectrum.

To achieve an MS^n spectrum all of the ions except one m/z are ejected from the ion trap. The remaining ions are excited by applying an rf voltage to the ring electrode corresponding to the ions' m/z resonance, but not enough energy to cause the ions to become unstable and be ejected from the trap. This pulls the ions away from the center of the trap and gives them enough energy to undergo energetic collisions with the helium buffer gas resulting in ion fragmentation. The rf voltage is then scanned to eject the fragment ions so that they can be detected and an MS^n spectrum collected.[5]

The Ion Trap Mass Spectrometer used in my thesis work is an Esquire 3000plus made by Bruker Daltonics; the schematics for this system are illustrated in Figure 1.3. This specific instrument is interfaced with an Agilent 1100 LC system using ESI. The nebulizer spray is directed at a 90^o angle with respect to the entrance of the sampling capillary. To help dry the sample a heated dry gas flows around part of the capillary and into the spray chamber. Once the ions are in the gas phase they enter the mass spectrometer through the entrance aperture and a transfer capillary, drawn there by an electrostatic gradient and the pressure differential between the spray chamber and the ion focusing and transport region. Once out of the capillary the ions are sampled by the skimmer which also helps to remove the bulk of the drying gas, helping maintain vacuum in the next stage of the instrument. Following the skimmer is an octopole ion guide which focuses and transports the ions from a relatively high pressure position directly behind the skimmer to the focusing/exit lenses coupling the ion transport to the ion trap; then finally on to the detector where the information is relayed to a computer as a mass spectrum.

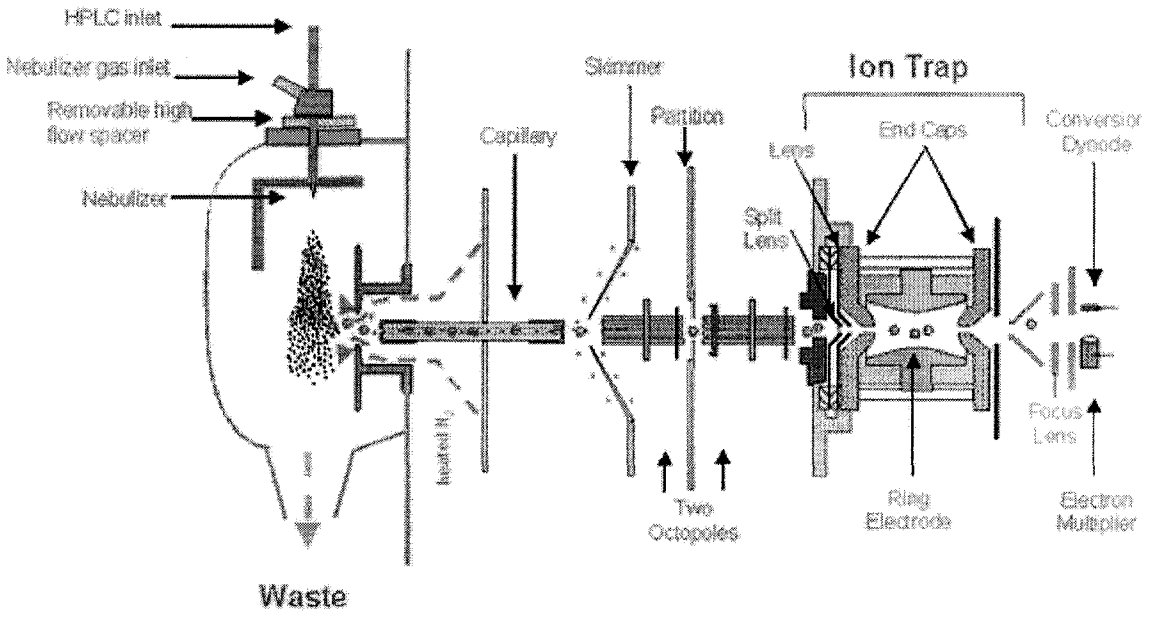

Figure 1.3 - Schematics of the Esquire 3000plus ion trap. This figure was reproduced with permission from Bruker Daltonics [1]

1.1.3. Fourier Transform Mass Spectrometer

Accurate mass measurements and determination of a chemical formula are important and useful factors to verify the identity of unknown compounds in a complex mixture. Fourier Transform Ion Cyclotron Resonance Mass Spectrometers (FT-ICR MS) provides high mass resolving power and mass accuracy.[6] In general an FT-ICR MS instrument goes through a series of steps to produce a mass spectrum. These steps begin with the formation of ions, typically in an external source, followed by the cooling, focusing and accumulation of the ions until they are finally transmitted into the ICR cell. Once in the ICR cell ion isolation experiments can be performed. Then the ions are detected through frequency measurements using dipolar analog detection with simultaneous analog-to-digital conversion and storage of the time-domain analog signal, apodization, fast Fourier transformation, magnitude computation, and frequency-to-m/z conversion with respect to external or internal calibration.[7]

The heart of an FT-ICR MS is the analyzer cell (ICR cell) which can collect an entire spectrum at once, rather than one frequency at a time, as with other scanning mass spectrometers, such as the quadrupole ion trap. The ICR cell can take on different geometries but in general consists of 6 plates: a front and back trapping electrode, two

opposite excitation electrodes and two opposite detection electrodes [8] and resides within a strong homogeneous magnetic field. The magnet traps the ions in a cyclotronic motion perpendicular to the magnetic field, in an xy-plane, but has no trapping effect in the z-direction, hence the front and back trapping electrodes are employed. Together the plates work to trap the ions in a small cloud in the center of the ICR cell; at this point their cyclotronic motion is too small to be detected and their orbits are random, i.e., an ion may start its cyclotron motion at any point around the circle and result in charges canceling each other out. Thus detection is typically preceded by excitation by applying an oscillating electric field, in resonance with the ions, to the two excitation electrodes perpendicular to the magnetic field. The excitation causes the cloud of ions to spiral out from the center of the ICR cell to an orbit with a larger radius as shown in Figure 1.4.

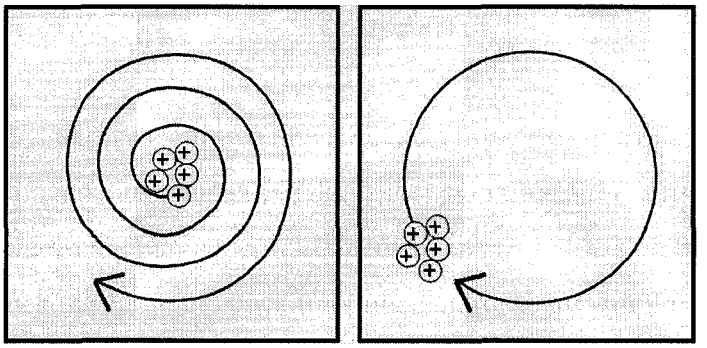

Figure 1.4 - Ion cloud in the center of an ICR cell spiraling to a larger orbital when excited (left). The ion cloud in an orbital with a larger radius for detection (right)

An ion's motion within the ICR cell is completely dependent on the m/z of the ion and not its initial kinetic energy, thus ions of the same m/z will move together in a packet once they are excited to a larger orbital. These ion packets induce a differential current between the two opposing detection plates with a current amplitude proportional to the ion population. The resulting signal is then recorded and transformed to a plot of m/z vs. signal intensity.

The schematic for the FT-ICR MS instrument used for the experiments described in this thesis is illustrated in Figure 1.5. This specific instrument consists of an ESI interface followed by a set of skimmers and ion funnels, a hexapole, a quadrupole mass filter, collision cell and ion transfer optics before the ICR cell.

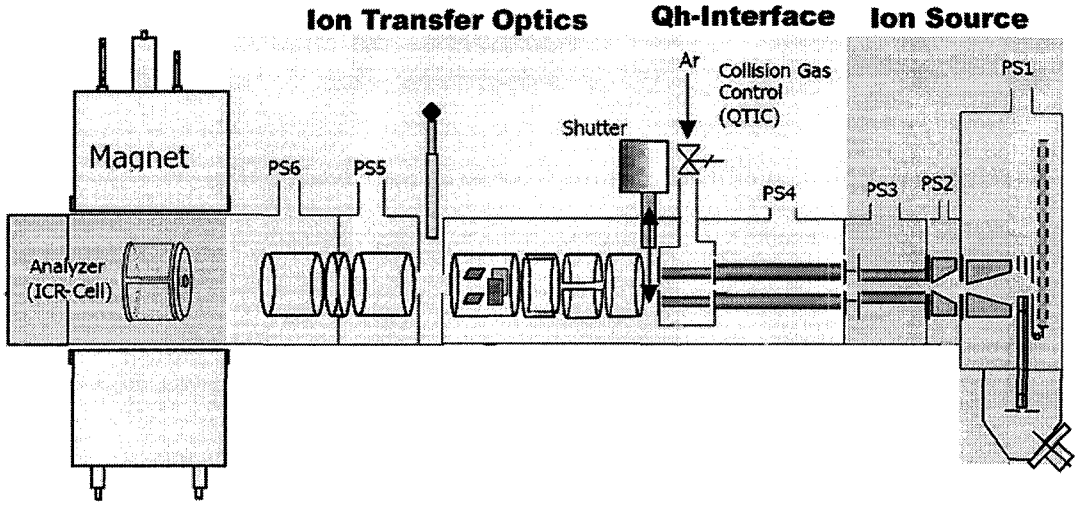

Figure 1.5 - Schematic of Brukers FT-ICR MS. This figure was reproduced with permission from Bruker Daltonics. PS = Pumping station [9]

1.2. Metabolomics

1.2.1. What is it?

In general metabolomics is the study of small molecules within an organism. However since this is fairly new terminology[10] there is some disagreement over the exact definition of "metabolomics'. Some researchers use the term "metabolomics" and "metabonomics" interchangeably to describe the study of an organism's metabolism, while others define them separately. In the journal *Nature Reviews Genetics* "metabolomics" is defined as "the study of metabolome, which is the entire metabolic content of a cell or organism, at a given time"[11]. However, others define the term somewhat differently. The term has also been defined as "the measurement of metabolite concentrations and fluxes in isolated (and usually identical) cell systems or cell complexes".[12] On the other hand, "metabonomics" has been defined as "the study of the total metabolite pool" by the US National Center for Computational Toxicology.[13] But Lindon defines metabonomics as "the comprehensive and simultaneous systematic determination of metabolite levels in whole organisms and their changes over time as a consequence of stimuli such as diet, lifestyle, environment, genetic effects, and pharmaceutical interventions, both beneficial and adverse".[14] And it has also been defined as the "quantitative measurement of time-related multiparametric metabolic responses of multicellular systems to pathophysiological stimuli or genetic

modification".[12] The general consensus seems to be that metabolomics refers to the entire metabolome while metabonomics is used to describe metabolic changes with respect to endogenous or exogenous stimuli.

1.2.2. Phase I and II metabolism

The human body comes in contact with many different chemicals over the course of the day whether synthetic or natural and when these chemicals are taken up the body works to collect energy from them or excrete them so that they do not build up in the system and cause problems. This is all accomplished through metabolic reactions and, since the study of pharmacokinetics is such a large industry, two of the most common forms of metabolism studied are phase I and phase II. Metabolism can occur in all living tissue in the human body. Liver tissue is commonly used for metabolic studies but other tissue such as gut, kidney and lungs are also used.[15] Together the phase I and II metabolic reactions work together to make the small molecules more hydrophilic so that they can be more easily excreted in the urine and do not build up to toxic levels in fatty tissue.[16]

The phase I metabolism reactions involve membrane-associated enzymes found within the endoplasmic reticulum (ER) of hepatocytes, and to a lesser extent cells from other tissue.[16] Phase I reactions entail the introduction or exposure of functional groups on the chemical structure, typically through reactions utilizing oxidases.[16] In general, phase I reactions involve rather small chemical changes that make the compounds more hydrophilic and also provide a functional group that is used to complete phase II reactions.[17] If the compound is still in the body after phase I metabolism occurs then it will often undergo phase II metabolism as well.[18] Phase II reactions involve the addition of large polar groups to the compound. These polar groups are supplied by different cofactors [15] and must be added to most *in vitro* systems for the reaction to occur. The enzymes required for the phase II reactions are located in the cytosol, except UDP- glucuronosyltransferases (UGT), which are microsomal. [15] Phase II reactions do not necessarily need to be preceded by a phase I reaction if an appropriate group is already available for conjugation, such as hydroxyl (-OH), amine ($-NH_2$) or carboxyl (-COOH) moieties.[18]

1.2.3. Common metabolic reactions

A number of different enzymes and cofactors are responsible for the metabolism of all the different compounds in the human body. Some typical examples of phase I metabolism include hydroxylation, which can occur on an aromatic ring or a carbon chain, demethylation from an O, S or N atom, and dehydrogenation that transforms a hydroxyl group to a ketone or aldehyde. These small changes either add or expose polar functional groups to make the compound more hydrophilic and set up the compounds for phase II metabolic reactions.

Table 1.1 - Examples of several phase I metabolic reactions [19, 20]

Rule Name	Target	Result
Hydroxylation		
Demethylation	$R_2N—CH_3$ $RO—CH_3$ $RS—CH_3$	$R_2N—H$ $RO—H$ $RS—H$
Dehydrogenation	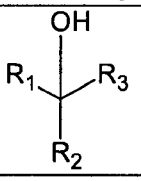	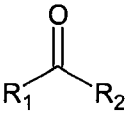

As previously mentioned, phase II metabolism adds large polar groups to make a compound even more hydrophilic to ensure its excretion in urine. This reaction occurs much quicker than phase I metabolism but also requires cofactors to proceed. Several examples include glucuronidation, sulfate conjugation and glutathione conjugation (see Table 1.2). These reactions all require the transfer of part of a cofactor molecule to the compound being metabolized and because of this the enzymes required for this metabolism typically have the word transferase included in their names. A more detailed table of different phase I and II metabolic reactions is included in the Appendix.

Table 1.2 - Examples of several phase II metabolic reactions [19, 20]

Rule Name	Target	Result
Glucuronidation	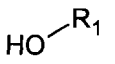	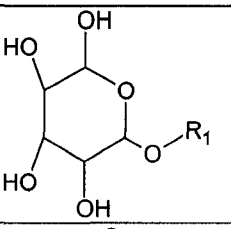
Sulfate Conjugation	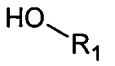	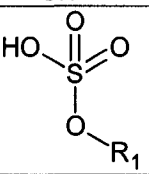
Glutathione Conjugation	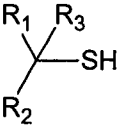	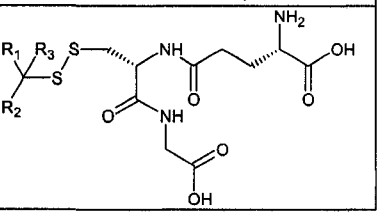

1.3. *In vitro* systems

Metabolites of a substrate can be generated using a number of different *in vivo* and *in vitro* methods. Pharmaceutical companies have been studying the metabolism of different drug candidates for years using these methods. Possible *in vivo* methods include labeling the drug with fluorescent, isotopic or radioactive labels and administering it to a test subject, resulting in easier metabolite identification from such a complex biological system. *In vitro* methods typically use the liver as a starting point since it is the organ where a significant amount of metabolism occurs. However, systems derived from other organs are used as well. Different *in vitro* systems include recombinant enzyme mixtures, cell cultures and cellular fractions. The most common assays use human liver microsomes (HLM) to study human metabolism. [21]

1.3.1. Liver Slices

For studying Phase I and Phase II metabolism *in vitro*, liver slices are a popular choice because they most closely resemble the *in vivo* system. Liver slices, unlike isolated hepatocytes, maintain three-dimensional liver lobule architecture. The three-dimensional liver slice preserves the extracellular matrix, cell-cell communications, transport pathways and minimizes damage and disruption, which reduces the time

required for hepatocytes to adapt to the culture conditions. Also unlike primary or cultured cells, the liver slice contains more than just hepatocytes. Hepatocytes are the major part of the liver representing 65% of the total liver cell population and 80-90% of the total liver mass, whereas the remaining 35% of the liver contains cells such as Kupffer cells.[22-25]

The use of liver slices dates back to the early 20th century, but in later years fell out of favor, most likely due to the difficulty in obtaining slices with uniform dimensions and minimal cell damage, and the development of other *in vitro* models. The use of liver slices was revived with the invention of precision cut tissue slicers that allow for consistent dimensions and rapid production of thin slices (<250 μm thickness).[24] These new developments in instrumentation allow the production of more liver slices than can typically be used for one set of experiments. These liver slices will remain viable in culture for a few days to a few weeks, depending on the culture conditions and the end-point of cell viability. To minimize the waste of unused liver slices research is ongoing to optimize the cryopreservation of liver slices, minimizing cell death due to the freezing and thawing process since the cells that survive cannot be separated from those that do not.[23, 26]

Liver slices in comparison with other *in vitro* systems have a number of advantages as well as disadvantages besides those mentioned above. One advantage compared to isolated hepatocytes is that liver slices are cheaper, easier and faster to prepare. Also, experiments comparing Cytochrome P450 (CYP) enzymes; CYP 2B6, 3A4 and 2C9 show that the protein levels in isolated hepatocyte and human liver slice cultures decline with time in both models, but the rate of decline in the liver slices is considerably slower.[24, 25] Disadvantages compared to other *in vitro* systems include the inadequate penetration of the medium into the inner part of the slice and the samples are not easily applicable to higher throughput screening.[24, 25]

1.3.2. Cells

Isolated hepatocytes are a good alternative to liver slices because they still contain an intact array of enzymes. The isolated cells can be used in the form of freshly isolated cells, cryopreserved cells or a transformed cell line. Isolated hepatocytes, unlike liver slices, lose their lobular architecture and thus the heterogeneous composition of the liver

and only parenchymal cells are retained; other cell types, such as the phagocytic Kupffer cells, are washed out during purification.[22] Each form of the isolated hepatocytes has its own advantages and disadvantages and the type of cells used is dependent on experimental requirements.

Primary cell cultures are obtained from fresh liver samples and are dependent on liver availability. The cells are typically isolated through collagenase digestion which can result in damaged cellular membranes which disrupts the transport system and causes a loss of normal membrane polarity.[22] Primary cell cultures can be kept fresh in suspension, and are viable for a few hours at 37 °C or ice cold for 48 hours in an appropriate medium [24, 27]. When plated in a monolayer they are viable up to 36 days [24]. However, the enzyme activity decreases over time making them unsuitable for some long term studies and impossible to use for repeating experiments with the cells from the same liver. Also, experiments cannot be duplicated using cells from other livers because metabolic activities will change with race, sex, health and age of the donor. [28]

It is also possible to cryopreserve freshly isolated hepatocytes and store them under the appropriate conditions for years so that they can be used at a later date. Cryopreserved cells remove the dependence on liver availability and make it possible to pool cell samples from different donors. The thawed cells are comparable to the freshly isolated hepatocytes and enzyme activity remains above 70% for a number of the enzymes including CYP1A2, CYP2A6, CYP2B6, CYP2C9, CYP2C19, CYP2D6, CYP2E1, CYP3A4, UDPGT and ST. However, it has also been established that while GST activities are similar between freshly isolated and cryopreserved human hepatocytes, intracellular glutathione (GSH) levels are drastically reduced upon cryopreservation. Unfortunately, the viability of cryopreserved cells is only 50% to 80% and not all lots retain active transporters. Also, the cryopreserved cell are known to have poor attachment efficiency and not all lots of these cells can be plated and must be used as a suspension.[24, 27]

Transformed cell line can be used for more reproducible experiments and a more readily available source of hepatocytes. These cell lines are cancer-like in that they continually multiply and are immortal. Unfortunately cell lines are a poor substitute for fresh cells because they have low enzyme expression; however a number of cell lines

have been developed specifically for metabolic studies with slightly elevated enzyme expression levels compared to other cell lines.[29] The HepG2 cell line is one of the more popular cell lines developed for metabolic studies. HepG2 cells were derived from Caucasian human hepatoblastoma with the intention that they would replace fresh human hepatocytes in early toxicology screening during drug development.[30] The HepG2 cell line has been has been characterized and studied by a number of different laboratories and theoretically they should have the same enzyme activity. However, experiments comparing two different stocks of HepG2 cells from different sources showed that the enzyme expression is not the same. Consequently, cell lines should be characterized before undertaking any major metabolic studies to ensure all of the enzymes of interest are active.[30]

1.3.3. Cellular fractions

Cellular fractions are easier to work with and produce simpler and cleaner samples than any of the previously discussed whole cell systems. The three basic cellular fractions used to study human metabolism are microsomes, cytosol and S9 fractions, with microsomes as the most popular choice. Each of these three cellular fractions contains a slightly different set of enzymes but all three can be easily prepared and stored for extended periods below -80 ^{o}C to maintain enzyme activity. Since these systems are easy to store for an extended period and can go through several freeze thaw cycles with minimal damage to their enzyme activity it is feasible to prepare pooled samples from several different donors. Cellular fractions from individuals reflect the idiosyncrasies of the donor and so different preparations are highly variable. Pooled cellular fractions can overcome some of these deficiencies, but only to a limited extent.[31]

The S9 fraction is a post-mitochondrial supernatant fraction composed of both microsomes and cytosol. Consequently, it contains a wide variety of Phase I and Phase II enzymes including P450 enzymes, flavin-monooxygenases, carboxylesterases, epoxide hydrolase, UDP-glucuronosyltransferases, sulfotransferases, methyltransferases, acetyltransferases, glutathione S-transferases and more.[32] Since this is not a full cell system the corresponding co-factors for the different enzymes must be added for the biotransformation to take place.[24] The liver S9 fractions are obtained through centrifugation at 1000 x g of homogenized liver cells/tissue followed by centrifugation at

9000 g to collect the supernatant.[24] The major disadvantage of this system is the overall lower enzyme activity compared to microsomes or cytosol, which may leave some metabolites of interest below detection levels.[24]

Microsomes are small vesicles derived from fragmented endoplasmic reticulum and isolated via centrifugation. Microsomes contain a significant amount of metabolic enzymes and, once isolated from the rest of the cell, microsomes can be used to study the metabolism of different compounds [33]. They are pelleted when the S9 fraction is centrifuged at 100 000 g and contains a number of different enzymes, including P450s (CYPs), flavin-containing monooxygenase (FMOs) and the glucuronosyltransferases (UGTs).[34, 35] Microsomes are mostly used for the evaluation of Phase I metabolism due to the CYP enzymes, which require the addition of a NADPH regenerating system to supply the energy demand of the CYPs.[24, 35] It is also possible to study Phase II glucuronidation biotransformations with the addition of UDP-glucuronic acid (UDPGA) as a cofactor.[35]

The cytosol fraction contains a number of Phase II enzymes including NAT, GST, TPMT and ST, allowing this system to be used to study the biotransformations of these enzymes separately or in combination, depending on the cofactors added. Different cofactors are required for different enzymes, NAT requires a combination of acetyl coenzyme A (acetyl CoA, dithiotreitol (DTT), and acetyl CoA regenerating system, ST requires adenosine-3'-phosphate-5'-phosphosulfate (PAPS), GST needs glutathione (GSH) and TPMT relies on the presence of S-adenosyl methionine (SAM).[24]

1.3.4. Recombinant Enzymes

Recombinant human enzymes offer a slightly different option for studying human metabolism. Recombinant enzymes are obtained by expressing the genetic information encoding the enzyme(s) of interest in recipient cells such as bacterial, yeast, insect or mammalian cells.[36] For example, insect cells which lack endogenous CYP and UGT activity are transfected with cDNA for CYP and UGT human enzymes and the resulting microsomes with the expressed human enzymes allow the investigator to study specific biotransformations and pathways. An alternative to using the microsomes is to purify the enzyme from cells. The cells used must have the ability to be grown to a high density and have high expression levels of the recombinant protein. To facilitate purification the

protein can be easily modified by adding a stretch of histidines to the C-terminal end so it can be purified by immobilized metal affinity chromatography and, if necessary, the His-tag can be removed by cleavage with a protease if the cleavage site is engineered into the tag.[24, 36]

Recently, recombinant models have been developed to reproduce the entire hepatic P450 mediated metabolism of drugs. In this approach, membrane preparations, each containing a different recombinant P450 isoform, were mixed to obtain a final mixture which has a composition similar to that of liver microsomes.[36]

Another approach is to express recombinant human enzymes in a cell line. At the present all known CYPs involved in drug biotransformations as well as UGTs have been successfully over-expressed in cell lines. These transfected cell lines are often as easy to culture as non-transfected cell lines and their main advantage over non-transfected cells is the higher expression of CYP and UGT isozymes.[24]

In general, it has been found that the catalytic properties of the recombinant enzymes, when expressed in the different models, whether they are in bacteria, yeast, insect or mammalian cells, mimic that of their counterparts in human liver microsomes but are typically found at a higher concentration, making it easier for metabolite detection and identification.[36]

The microsomes were the selected *in vitro* system for the experiments described in the following chapters. The microsomes are a compromise between the recombinant enzymes which only comprise of a handful of selected enzymes and the more complex whole cell systems. The cell lines require a significant amount of time to grow before they can be used for metabolic studies. Once prepared microsomes can be frozen and ready to used at a moments notice.

1.4. The Human Metabolome Project

1.4.1. What is the project and its goals?

The Human Metabolite Project (HMP) was launched in 2004 and is a joint effort between several different research groups to identify and quantify all detectable endogenous human metabolites (>1 μM) from healthy individuals and make the information available in a publicly accessible database called the Human Metabolome Database (HMDB).[37] Metabolite information for the database was initially compiled

using previously published data from text books, journal articles, electronic databases and web searches and currently contains more than 2500 endogenous metabolites. Each metabolite in the database contains its chemical information, description, links to relevant databases, such as KEGG and BioCyc, biofluid location, tissue location, biological concentrations and more [37, 38]. Research is ongoing to expand the database through experimental efforts using techniques such as compound synthesis, Nuclear Magnetic Resonance (NMR), Gas Chromatography Mass Spectrometry (GC-MS) and Liquid Chromatography Mass Spectrometry (LC-MS). To help with metabolite identification in complex biofluids, such as urine, plasma and cerebral spinal fluid, more than 900 standards of known endogenous human metabolites have been purchased or synthesized and documented and stored in the Human Metabolome Library (HML) to be used for research purposes.[37, 39] A number of one-dimensional and two-dimensional NMR spectra are in the process of being collected for each of the metabolites in the HML as well as the MS/MS spectra for each metabolite so that spectra can be uploaded to the HMDB and searched.

1.4.2. The HMP's MS/MS database

The present human metabolome MS/MS spectral library consist of approximately 1800 different spectra for about 600 different metabolites which were obtained from the HML. The MS/MS spectra in the spectral library were collected using an Agilent 1100 HPLC system equipped with a 100 well autosampler for flow injection analysis which was coupled to a Waters Micromass Quattro TripleQ (Waters Micromass, UK) equipped with an electrospray ionization source. Fragmentation was achieved using collision-induced dissociation (CID). Three different MS/MS spectra were collected each with different fragmentation energy: low, medium or high, and the resulting MS/MS spectra were uploaded to the MS/MS spectral database. This work was initiated by Nan Guo, a former graduate student of our group, and detailed experimental information on this work is published in her thesis. [40]

The MS/MS spectral database is searchable using a web-based search algorithm that was developed in house by Nelson Young in Dr. David Wishart's laboratory. The functionality of this database is best explained through an example: an MS/MS spectrum of methionine was collected using an ion trap mass spectrometer (see Figure 1.6 left). If

this compound is treated as an unknown then the MS/MS spectral library can be used to identify it. The parent ion mass and the m/z of several of its fragment ions are entered into the online search form and any of the potential matches found during the search are listed in a table and scored based on the number of fragment matches along with links to the corresponding spectra for visual comparison. This example resulted in three possible matches to spectra in the database: methionine low energy MS/MS spectrum (see Figure 1.6 right), methionine medium energy MS/MS spectrum and methionine high energy MS/MS spectrum. Hence this compound was correctly identified using the MS/MS spectral library.

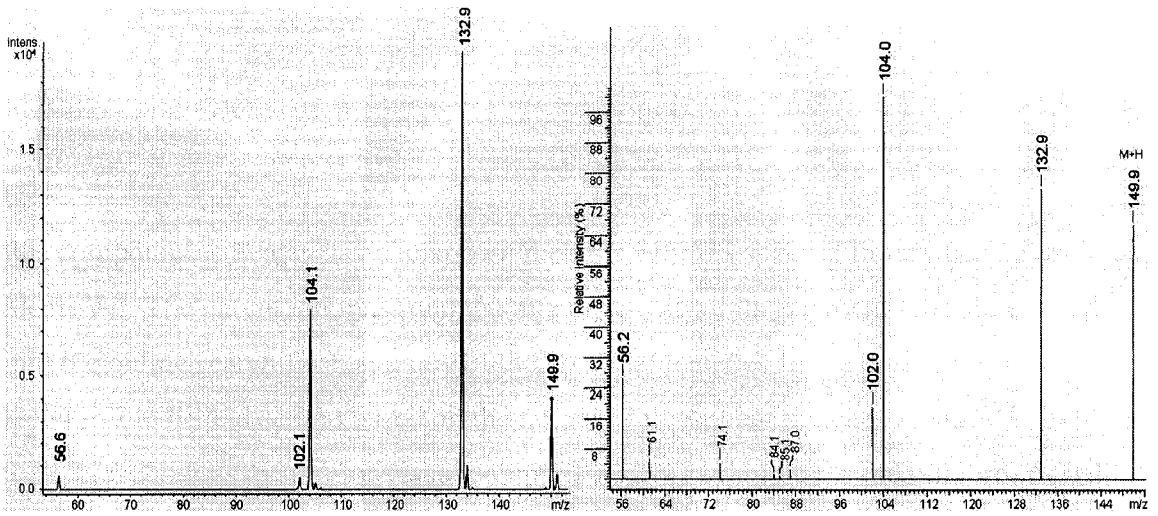

Figure 1.6 - MS/MS spectrum of methionine (Left) as collected on an ion trap mass spectrometer and low energy spectrum as found in the MS/MS library (Right)

Currently construction of the MS/MS spectral library is an ongoing project with the goal to collect the MS/MS spectra for each of the 900 metabolites currently in the HML and any compounds that may be purchased for the HML in the future.

1.5. Overview of Thesis

The present human metabolome MS/MS spectral library only consists of metabolites either commercially available or readily synthesized. This is a small number compared to the size of the human metabolome. The lack of metabolite standards imposes a limitation on the size of the MS/MS spectral library. While synthesis of potential human metabolites can be done in theory and would result in metabolites in relatively large quantity for spectral measurement and other usages, it will be an

expensive endeavor. Two separate strategies are proposed for expanding the spectral library by using a relatively more convenient way to produce metabolite "standards".

In chapters two and three the first strategy is given in detail, where the commercially available or readily synthesized metabolites are used as the starting materials or substrates. These substrates are added to a host such as human liver microsomes (HLM) where metabolic reactions take place to produce metabolites. The structures of the metabolites are characterized, mainly using mass spectrometric tools, and the identified metabolite structures along with spectral data are catalogued. Following identification in the microsome incubations the metabolites are used as pseudo-standards for compound identification in complex biological samples such as human urine. The identification of these metabolites in the microsomal incubations and in urine confirms that they are in fact endogenous human metabolites and they can be used to expand the HMDB.

The microsome incubation method used in chapter two only accounts for the phase I metabolites; the required cofactors necessary for phase II metabolites are not present in the incubations and to add them would at least double the turnover time required for each substrate with minimal benefits. To address the identification of metabolites not formed through microsomal incubations a theoretical database of potential endogenous metabolites was formed. The theoretical metabolite database was derived from the list of known endogenous human metabolites in the HMDB and a set of known biotrasformations, as described in Chapter 4. Once created the theoretical metabolite database was used to help identify metabolites in urine with accurate mass measurements using a Fourier Transform Ion Cyclotron Mass Spectrometer (FT-ICR-MS) as well as MS/MS fragmentation patterns. To facilitate the metabolite identification process and the target analytes, acylcarnitines and their metabolites, in urine sample were extracted using solid phase extraction.

Finally, Chapter 5 summarizes the thesis work and gives a brief discussion on future work.

1.6. References Cited

1. *Esquire series User Manual Volume 1 Theory, Version 5.1.* September 2002, Bruker Daltonics.

2. Fenn, J.B., *Ion formation from charged droplets: roles of geometry, energy, and time.* Journal of the American Society for Mass Spectrometry, 1993. **4**(7): p. 524.

3. Stafford, G., *Ion trap mass spectrometry: a personal perspective.* Journal of the American Society for Mass Spectrometry, 2002. **13**(6): p. 589.

4. Jonscher, K.R. and J.R. Yates, *The Quadrupole Ion Trap Mass Spectrometer--A Small Solution to a Big Challenge.* Analytical Biochemistry, 1997. **244**(1): p. 1.

5. Todd, J.F.J. and A.D. Penman, *The recent evolution of the quadrupole ion trap mass spectrometer--an overview.* International Journal of Mass Spectrometry and Ion Processes, 1991. **106**: p. 1.

6. Zhang, L.K., *Accurate mass measurements by Fourier transform mass spectrometry.* Mass Spectrometry Reviews, 2005. **24**(2): p. 286-309.

7. Marshall, A.G., *Fourier transform ion cyclotron resonance mass spectrometry.* Acc. Chem. Res., 1985. **18**(10): p. 316-322.

8. Heeren, R.M.A., et al., *A mini-review of mass spectrometry using high-performance FTICR-MS methods.* Analytical and Bioanalytical Chemistry, 2004. **378**(4): p. 1048.

9. *Qh-Interface User and Sevice Manual.* October 2006, Bruker Daltonics.

10. Wishart, D.S., *Metabolomics: The Principles and Potential Applications to Transplantation.* American Journal of Transplantation, 2005. **5**: p. 2814-2820.

11. *Glossary.* Nature Reviews Genetics, 2003. **4**(4): p. 1047.

12. Plumb, R.S., et al., *Metabonomics: the use of electrospray mass spectrometry coupled to reversed-phase liquid chromatography shows potential for the screening of rat urine in drug development.* Rapid Communications in Mass Spectrometry, 2002. **16**(20): p. 1991-1996.

13. *National Center for Computational Toxicology (NCCT) Golssary.* 2007 September 10, 2007 [cited 2007 December]; Available from: http://www.epa.gov/comptox/glossary.html.

14. Lindon, J.C., E. Holmes, and J.K. Nicholson, *Metabonomics in pharmaceutical R&D.* FEBS Journal, 2007. **274**(5): p. 1140-1151.

15. Jassal, B. and E.E. Schmidt. *Metabolism of Xenobiotics [Homo sapiens].* 2007 [cited 2007 December]; Available from: http://reactome.org/cgi-bin/eventbrowser?DB=gk_current&FOCUS_SPECIES=Homo%20sapiens&ID=140192&.

16. Howland, R.D. and M.J. Mycek, *Lippincott's Illustrated Reviews: Pharmacology.* 3 ed, ed. R.A. Harvey and P.C. Champe. 2006, Baltimore: Lippincott Williams and Wilkins.

17. Kruidering-Hall, M. *Pharmacokinetics III: Drug Metabolism (Lecture).* [cited 2006 Feburary]; Available from: http://biochemisty.ucsf.edu/~fulton/PTE/Prologue%20Links/Pharmacokinetics%20III.pdf.

18. Korfmacher, W.A., ed. *Using Mass Spectrometry for Drug Metabolism Studies.* 2004, CRC Press: New York.

19. *MetabolitePredict Version 1.1 (Build 44)*, in *Bruker Daltonics Metabolite Tools 1.1.* 2004, Bruker Daltonics.

20. Willoughby, R., E. Sheehan, and S. Mitrovich, *A global view of LC/MS How to solve your most challenging analytical problems.* 1998, Pittsburgh, PA: Global View Publishing.

21. Shou, W.Z., et al., *A novel approach to perform metabolite screening during the quantitative LC-MS/MS analyses of in vitro metabolic stability samples using a hybrid triple-quadrupole linear ion trap mass spectrometer.* Journal of Mass Spectrometry, 2005. **40**(10): p. 1347-1356.

22. Dogterom, P., *Development of a simple incubation system for metabolism studies with precision-cut liver slices.* Drug Metab Dispos, 1993. **21**(4): p. 699-704.

23. Parkinson, A., *An overview of current cytochrome P450 technology for assessing the safety and efficacy of new materials.* Toxicologic Pathology, 1996. **24**(1): p. 48-57.

24. Hariparsad, N., et al., *In vitro methods in human drug biotransformation research: Implications for cancer chemotherapy.* Toxicology in Vitro, 2006. **20**(2): p. 135.

25. Plazar, J., et al., *Detection of xenobiotic-induced DNA damage by the comet assay applied to human and rat precision-cut liver slices.* Toxicology in Vitro, 2007. **21**(6): p. 1134.

26. Martignoni, M., et al., *Phase I and phase II metabolic activities are retained in liver slices from mouse, rat, dog, monkey and human after cryopreservation.* Toxicology in Vitro, 2004. **18**(1): p. 121.

27. Li, A.P., *Human hepatocytes: Isolation, cryopreservation and applications in drug development.* Chemico-Biological Interactions, 2007. **168**(1): p. 16.

28. Schnabl, B., et al., *Replicative senescence of activated human hepatic stellate cells is accompanied by a pronounced inflammatory but less fibrogenic phenotype.* Hepatology, 2003. **37**(3): p. 653-664.

29. Rodriguez-Antona, C., et al., *Cytochrome P450 expression in human hepatocytes and hepatoma cell lines: Molecular mechanisms that determine lower expression in cultured cells.* Xenobiotica, 2002. **32**(6): p. 505.

30. Hewitt, N.J. and P. Hewitt, *Phase I and II enzyme characterization of two sources of HepG2 cell lines.* Xenobiotica, 2004. **34**(3): p. 243 - 256.

31. Kelly, J.H. and N.L. Sussman, *A Fluorescent Cell-Based Assay for Cytochrome P-450 Isozyme 1A2 Induction and Inhibition.* J Biomol Screen, 2000. **5**(4): p. 249-253.

32. *Products: Subcellular Fractions: S9.* [Company Product Sheet] 2007 [cited 2007 November]; Available from: http://www.xenotechllc.com/products/products_s9.asp.

33. Becker, W.M., L.J. Kleinsmith, and J. Hardin, *The world of the cell.* 4th ed. 2000, San Francisco: Benjamin Cummings.

34. Eddershaw, P.J. and M. Dickins, *Advances in in vitro drug metabolism screening.* Pharmaceutical Science & Technology Today, 1999. **2**(1): p. 13.

35. Li, A.P., *Preclinical in vitro screening assays for drug-like properties.* Drug Discovery Today: Technologies, 2005. **2**(2): p. 179.

36. Friedberg, T., *Recombinant in vitro tools to predict drug metabolism and safety.* Pharmaceutical Science & Technology Today, 2000. **3**(3): p. 99.

37. Wishart, D.S., et al., *HMDB: the Human Metabolome Database.* Nucleic Acids Res, 2007. **35**(suppl_1): p. D521-526.

38. *Metabolite Toolbox.* [Electronic Database] 2005-2007 [cited 2007 February]; Available from: http://www.hmdb.ca/.

39. *Human Metabolome Library.* [Chemical Library] 2005-2007 [cited 2007 October]; Available from: http://www.metabolibrary.ca/.

40. Guo, N., *Development of mass spectrometric techniques for protein sequencing and metabolome analysis*, in *Chemistry*. 2006, University of Alberta: Edmonton. p. 142.

Chapter 2

Microsome-Based Metabolite Identification for Expanding the Human Metabolome MS/MS Database

2.1. Introduction

The human metabolome is a part of a complex system of thousands of proteins, enzymes and small molecules in equilibrium with each other. These components are affected by age, sex, the environment and more importantly a person's health. A change in any of these factors can cause the concentration of some compounds to be noticeably different. Analyzing body fluids for small molecules and changes in their concentration can indicate a specific illness, making these molecules useful biomarkers for diseases. Amino acids and acylcarnitines are currently used as biomarkers to help identify several different diseases in infants, such as Maple Syrup Urine Disease (MSUD) and Organic Acidemias. MSUD is detected by a dramatic increase in concentration of the amino acid leucine, the primary biomarker, additional secondary analytes used to test for this disease include isoleucine and valine.[1] Other diseases identified through small molecule analysis include Organic Acidemias. Organic Acidemias are caused by mitochondrial enzyme defects in the catabolism of branched-chain amino acids and fatty acid oxidation defects. This results in increased concentrations of circulating acylcarnitines and increased excretion of acylcarnitines in urine as well as secondary carnitine deficiency.[2] Table 2.1 lists a number of different analytes used as biomarkers and their associated diseases.

Table 2.1 - Analytes used to detect the possibility of a number of different diseases in newborns and the approximate frequency of disease detection in the newborn period (~7 days). [1] All acronyms are defined in at the beginning of the thesis

Analyte	Secondary Analyte	Disorder	Frequency Ranges
Phenylalanine	Tyrosine	PKU	<1:25 000
Leucine	Isoleucine, valine	MSUD	>1:250 001
Methionine		Homocystinuria	>1:250 001
Tyrosine		Tyrosinemia II	>1:250 001
Citrulline		Citrullinemia	1:125 001–1:250 000
Citrulline	Ornithine	ASA	>1:250 001
C8	C6, C10, C10:1	MCAD deficiency	
C8	C4, C5, C10, C12, C14, C16	MADD (GA-II)	>1:250 001
C14:1	C14, C16	VLCAD deficiency	>1:250 001
C4		SCAD deficiency	>1:250 001
C16OH	C18:1OH, C18OH, C16, C14, C14:1	LCHAD deficiency	>1:250 001
C16	FC, C18, C18:1	CPT II deficiency	>1:250 001
C16	FC, C18, C18:1	CPT I deficiency	>1:250 001
C3	C2	PA	1:125 001-1:250 000
C3	C2	MMA	1:75 001-1:125000
C5DC		GA-I	1:125 001-1:250000
C5		IVA	>1:250 001
C5OH		3-MCC deficiency	1:25 001-1:75 000
C5OH		HMG deficiency	>1:250 001

The analytes listed in Table 2.1 are just a few examples of endogenous human metabolites that are analyzed and can indicate an illness. Unfortunately information concerning these compounds, their related diseases and all other known endogenous human metabolites are scattered throughout the literature and are just recently being gathered and entered into large publicly accessible databases, such as the Human Metabolome Database (HMDB). In the past these and other biomarkers have mainly been tested by using gas chromatography (GC) with retention time information, or GC combined with MS (GC-MS), retention time and analyte mass. Much of the current knowledge about organic acidemias and fatty acid oxidation defects is based on findings provided by GC-MS analysis of urine from affected individuals.[1]

GC-MS is commonly used to profile volatile or thermally stable metabolites. Chemical derivatization can be used to expand the applicability of GC-MS to include a

wide variety of non-volatile species.[3] In GC-MS the availability of spectral libraries, for electron impact ionization (EI), are particularly advantageous for the identification of unknown metabolites by matching their fragment ion spectra with those of known compounds from a library. Another complementary technique, liquid chromatography (LC) combined with MS (LC-MS), has been widely used for metabolite detection without the need of chemical derivatization. With electrospray ionization (ESI), LC-MS provides a convenient means of generating molecular mass information on metabolites while tandem MS (MS/MS) can be used to produce fragment ion spectra, potentially useful for identification of unknown metabolites. However, the small number of fragment ion peaks produced, as well as the difficulty of assigning a structural feature to a particular fragment ion peak, is often not sufficient for deducing the compound's structure. Given this limitation, one approach of metabolite identification is through MS/MS spectral matching where an MS/MS spectral library of known metabolites is initially established, much like unknown chemical identification in EI spectral matching. Unfortunately, at the present, there are very few MS/MS spectral library databases publicly available, limiting the application of LC-MS/MS for unknown metabolite identification.

Ventures, such as the Human Metabolome Project (HMP), are trying to create a centralized database containing the entire human metabolome but at the present this database contains only a fraction of all the endogenous metabolites in the human body. Work still needs to be done to identify the unknown endogenous human metabolites; however, identification of unknown compounds in a complex mixture, such as urine, blood and cerebral spinal fluid (CSF), is a difficult task. Using spectral databases with NMR and MS/MS spectra for spectral matching, such as the human metabolome MS/MS database created for the HMP, as discussed in Chapter 1, is a very reliable form of compound identification.

The LC-MS/MS spectral library being created for the HMP is one of the few publicly available databases; however it is not very large. Approximately 900 compounds have been purchased or synthesized for the HMP, only a third of the known compounds currently listed in the HMDB. Purchasing or synthesizing the remaining of the HMDB compounds would be extremely time consuming and expensive and, it is impossible to purchase or synthesize compounds for any unknown human metabolites.

One particular method that pharmaceutical companies use to study drug metabolism and the type of metabolites that are formed in the human body involves the incubation of the drug with human liver microsomes (HLM). The incubation is then followed by analysis of the incubation mixture to identify any drug metabolites. This type of *in vitro* drug testing helps to determine the drug's potential for use *in vivo*. In this chapter, the potential of using this analytical strategy to metabolize known endogenous human metabolites (substrates) using HLM, will be presented. The incubation mixtures were each analyzed using LC-MS and LC-MS/MS and the metabolites ascertained were based on the substrate's structure and LC-MS/MS analysis and interpretation. Metabolites that have been previously identified and listed in the HMDB can have their spectra added to the HMP's MS/MS database. Any new metabolites identified using this method can be documented and used as pseudo-standards for compound identification of unknown compounds in complex biological fluids, such as urine, blood or cerebral spinal fluid (CSF). Once identified in one of these biofluids the metabolite can be added to the HMDB.

2.2. Experimental

2.2.1. Chemicals and Materials

Pooled human liver microsomes and NADPH regenerating system Solution A (26.1 mM NADP+, 66 mM glucose-6-phosphate, and 66 mM $MgCl_2$ in H_2O) and NADPH regenerating system Solution B (40 U/mL glucose-6-phosphate dehydrogenase in 5 mM sodium citrate) were purchased from BD Gentest (Mississauga, ON, Canada). Optima LC/MS grade water and acetonitrile were purchased from Fisher Scientific Canada (Edmonton, AB, Canada). Formic acid and acetic acid were purchased from Sigma Aldrich (Oakville, ON, Canada). Potassium phosphate (KH_2PO_4) was purchased from ACP Chemicals Inc. (Montreal, Quebec, Canada). Phenylacetylglycine methyl ester (PAGME), L-aspartyl-L-phenylalanine (APA), methyl o-methoxyhippuric acid (MMOHA), palmitoylcarnitine (PC), adipic acid, biotin, capric acid, caprylic acid, ferulic acid, hippuric acid, homovanillic acid, indolelactic acid, isovalerylcarnitine, isovalerylglycine, 3-methyladipic acid, 2-methylbutroylcarnitine, 3-methylindole, octanoylcaritine, pantotheinic acid, phenylpropionylglycine, undecanoic acid,

vaillylmandelic and vanillic acid were obtained from the Human Metabolite library through the Human Metabolome Project (Edmonton, AB, Canada).

2.2.2. Instrumentation and Equipment

Microsome sample preparation was conducted in a level two biohazard laboratory which was equipped with the required water bath set to 37 °C, a class II, type A biosafety cabinet and a JEIOtech SI600 shaking incubator set at 37 °C and 150 rotations/min.

All sample analyses were initially conducted using an LC coupled to an ion trap mass spectrometer. The LC system used was an Agilent 1100 equipped with a binary pump, auto sampler and degasser. An ACE 3 μm C18 (50 x 2.1 mm) 100 Å column (Aberdeen, Scotland) was used for sample separation. The flow rate was set to 0.2 mL/minute and separation was performed at ambient temperatures. The LC system was coupled to an Esquire 3000plus quadrupole ion trap (Bruker, Bremen, Germany) equipped with an electrospray interface. A Windows 2000 workstation ran Chemstation and EsquireControl to control the LC-MS system.

When required a 9.4 T Fourier transform ion cyclotron resonance MS (FT-ICR MS) (Bruker, Bremen, Germany) equipped with an electrospray interface was used to collect accurate mass information.

The UPLC system was used with a Waters Acquity UPLC BEH C18 1.7μm (10 x 150 mm) column. The flow rate was set to 0.05 mL/min.

2.2.3. Chromatographic Conditions

The mobile phase system used for analysis under positive ionization mode was water with 4% acetonitrile and 0.1% formic acid in Solvent A and acetonitrile with 0.1% formic acid in Solvent B. The sample injection volume was 20 μL, and the samples were kept at 4 °C in the autosampler until injected. The gradient used was Solvent B held at 0% for 1 min, then increased linearly to 90% in 20 minutes. After Solvent B was held at 90% for 5 minutes, it was brought back down to 0% in 0.1 minutes followed by a 9.9 minute re-equilibration. The total time for one injection was 36 minutes. The same gradient was used for analysis in negative ion mode but the mobile phases were changed to water with 4% acetonitrile in 4 mM ammonium acetate, buffered to pH 8 with ammonium hydroxide for Solvent A, and acetonitrile with 4 mM ammonium acetate, buffered to pH 8 with ammonium hydroxide for Solvent B.

2.2.4. UPLC Chromatographic Conditions

The mobile phase system used for analysis under positive ionization mode was water with 4% acetonitrile and 0.1% formic acid in Solvent A and acetonitrile with 0.1% formic acid in Solvent B. The sample injection volume was 8 μL, and the samples were kept at 4 °C in the autosampler until injected. The gradient used was Solvent B held as 35% for 5 min, then increased linearly to 100% in 25 min. After solvent B was held constant at 100% for 42.5 min. Finally, Solvent B was returned to 35% in 0.01 min to equilibrate for the next ejection.

2.2.5. Mass Spectrometer Conditions

All experiments conducted on the ion trap used electrospray ionization with the nebulizer gas set to 30 psi, the dry gas set to 10 L/min and the dry gas temperature set to 350 °C. The Smart Parameter Settings were optimized for each incubation, the target mass was set to the average mass for the analytes. The compound stability was set according to the substrates stability in the ion trap. The optimization was set to normal and the trap drive level was set according to the manual specifications. The scan speed for the ion trap is 13000 m/z/s, hence for a mass range from 50 to 500 m/z it can collect 28 spectra/s.

Table 2.2 - Trap Drive Level as suggested by the Esquire 3000plus manual [4]

Mass Range (m/z)	Trap Drive Level (%)
50-400	50
400-800	60
800-1200	70
1200-2000	80

The MS/MS experimental conditions are identical to the MS conditions except that the mass of interest was isolated with a 2 Da window and the fragmentation energy was set 0.1 V higher then the energy required to fragment the substrate ion to ensure metabolite fragmentation.

2.2.6. Microsome Handling

To avoid multiple freeze-thaw cycles and maintain enzyme activity the microsomes and NADPH regenerating system were divided into single use fractions and stored at -80 °C until needed.

2.2.7. Microsome Incubation and Sample Preparation

Microsome incubations were performed in Eppendorf tubes (0.6 mL) in a total incubation volume of 125 µL. Incubations contained microsome protein (1 mg/mL), 25 µL NADPH regenerating system (NRS) (17.5 µL 100 mM potassium phosphate (KH_2PO_4) buffer pH 7.4, 6.25 µL Solution A, 1.25µL Solution B), test compound (50 µM) or an equivalent volume of buffer for the controls and 162.5 µL potassium phosphate (KH_2PO_4) buffer (100 mM, pH 7.4). [5, 6]

Prior to the addition of warm NRS (37 °C), samples were incubated in a water bath at 37 °C for 5 minutes. Upon addition of NRS, the samples were placed on a rotator in a 37 °C incubator for a set time (0.5, 1, 3, 6 or 24 hours). The incubations were terminated by adding 50 µL of 5% acetic acid in acetonitrile to the reaction mixture, vortexing and then centrifuging at 16 000 x g for 5 minutes to separate any precipitate. The supernatant was transferred to clean Eppendorf tubes and stored at -20 °C until analyzed. [5, 6]

2.2.8. Data Analysis and Interpretation

Two pieces of software were utilized to help identify potential metabolites in each sample: Bruker's MetabolitePredict™ and MetaboliteDetect™. These programs work together to identify potential metabolites from LC-MS analyses.

To start the process, the structure of the substrate is first entered into MetabolitePredict™, by loading a .mol file or drawing the structure. Subsequently, a list of metabolism rules is defined. The software allows the users to create their own rules or choose from 82 preloaded metabolism rules, see Appendix Table 6.1, which are subdivided into several different subsets. These include: "Acetaminophens", "All Rules Mammals" (includes all Phase 1 and 2 metabolism rules), "All Rules", "Cytochrome P450", "Phase 1 Metabolism" and "Phase 2 Metabolism" (see Appendix Table 6.2). For the purpose of the microsome incubations the list of "Phase 1 Metabolism" rules is selected since the required cofactors for phase II metabolism are not added to the incubation mixture. The prediction is then carried out for a set number of generations; all

predictions for our experiments had three generations of metabolites predicted. The software creates the first generation of metabolites by applying each of the applicable metabolism rules to the substrate resulting in a list of potential first generation metabolites for the substrate. The second generation of metabolites is created by applying the same set of rules to each first generation metabolite; this is repeated until the predetermined number of generations is reached to create a metabolite tree. Figure 2.1 represents a metabolite tree. Each metabolite in the tree has a chemical structure (slightly different from the substrate), a chemical formula, a mass and its unique metabolite number. Once the tree is completed the software is set to compile a mass list eliminating all structural duplications. The completed mass list is exported to MetaboliteDetect™ to help in the identification of potential metabolite peaks in each sample.

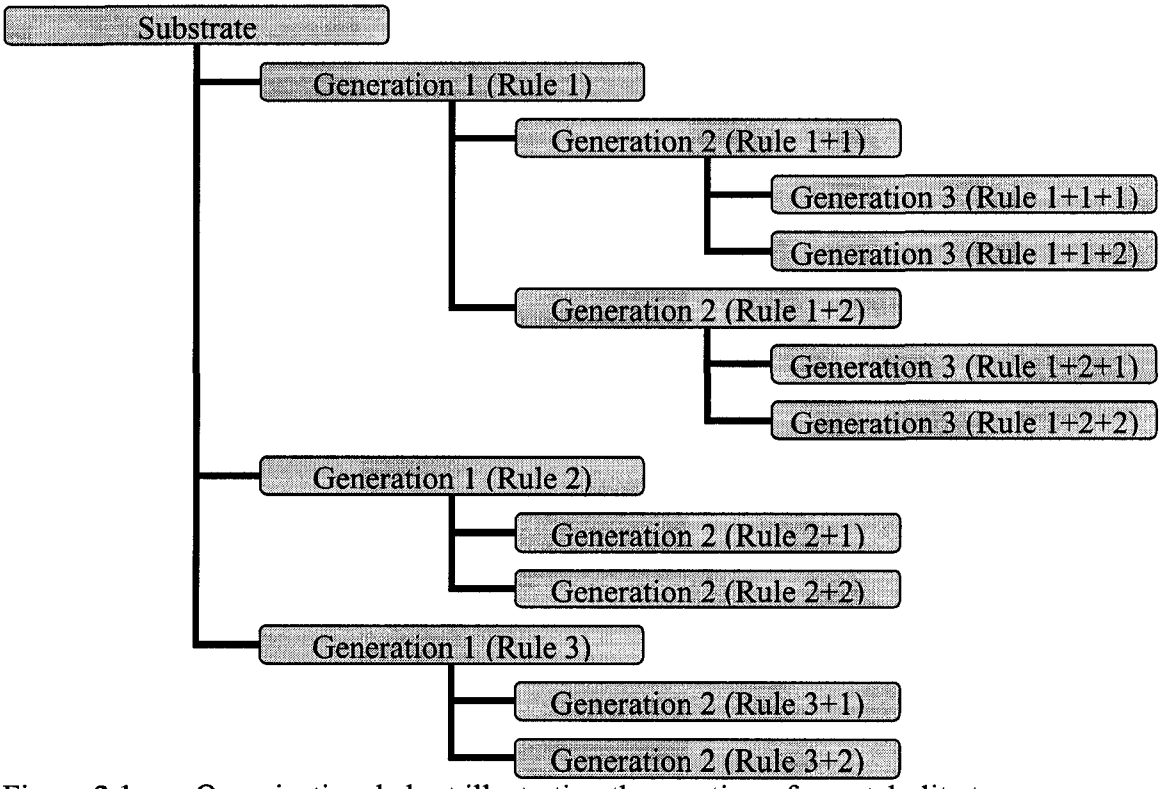

Figure 2.1 - Organizational chart illustrating the creation of a metabolite tree

The predicted metabolite list, sample chromatogram, control chromatogram and MS ionization mode are all loaded into MetaboliteDetect™. The software is then used to subtract the control from the sample chromatogram and highlight any differences between the chromatograms and matches to the predicted mass list from

MetabolitePredict™. All of the peaks of interest are noted and the samples rerun for LC-MS/MS analysis.

2.3. Results and Discussion

2.3.1. Identification of metabolites

Because of the potential batch-to-batch variability of enzyme activity in the microsomes, microsome incubation experiments were carried out with a series of samples and controls, the latter with an equivalent volume of buffer solution instead of substrate. Ion chromatograms of the sample and control were collected under identical LC-MS conditions. For example, Figure 2.2 illustrates a set of base peak chromatograms (BPC) and extracted ion chromatograms (EIC) for the 30 minute microsome incubation of palmitoylcarnitine and its corresponding control. The peak starred in Figure 2.2(b) is from the substrate palmitoylcarnitine (see Figure 2.3); the peaks starred in Figures 2.2(c-f) are the potential metabolites, corresponding peaks are not found in the controls chromatogram indicating that these peaks are most likely metabolites of palmitoylcarnitine. Therefore palmitoylcarnitine has a total of five potential metabolites from the HLM incubations.

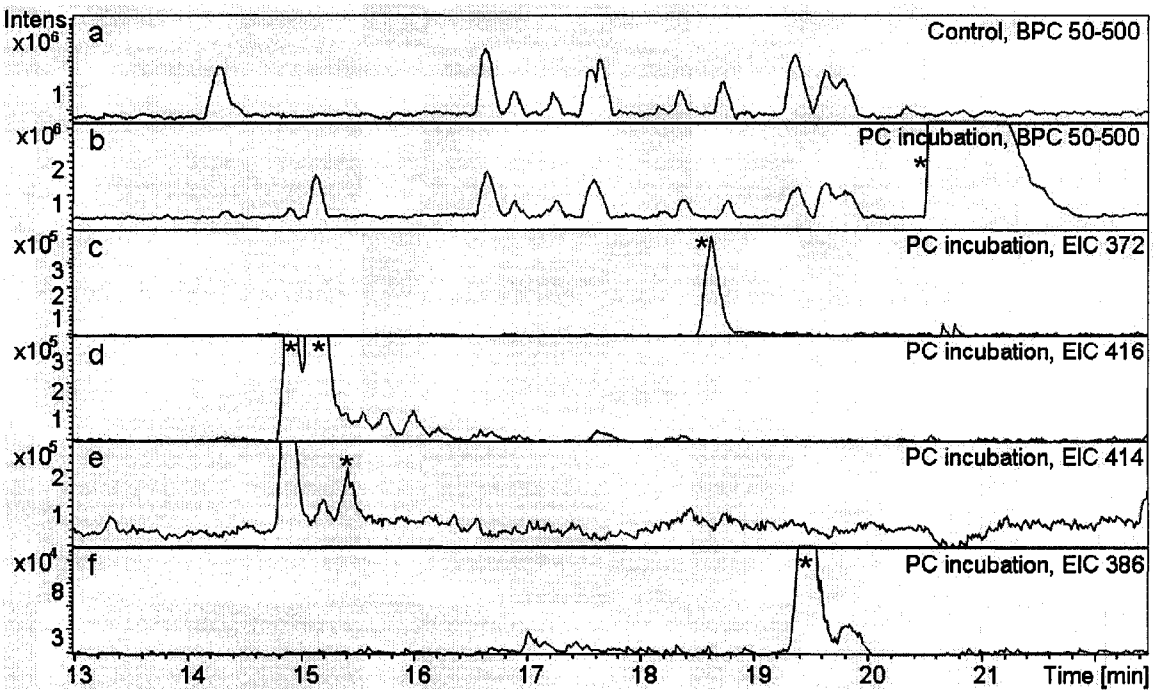

Figure 2.2 - The extracted base peak chromatograms (BPC) and extracted ion chromatograms (EIC) of a 30 minute incubation of palmitoylcarnitine and its corresponding control, a) BPC of control, b) BPC of palmitoylcarnitine incubation, c) EIC 372 of palmitoylcarnitine incubation, d) EIC 416 of palmitoylcarnitine incubation, e) EIC 414 of palmitoylcarnitine incubation and f) EIC 386 of palmitoylcarnitine incubation

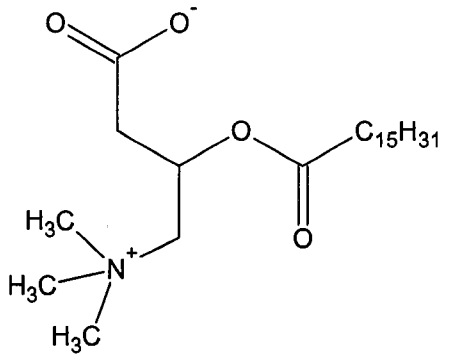

Figure 2.3 - Structure of palmitoylcarnitine

To confirm that the identified peaks, in Figure 2.2(c-f), are metabolites of palmitoylcarnitine the MS/MS spectra of each potential metabolite must be compared to the MS/MS spectrum of palmitoylcarnitine. For the most part the metabolite identification is confirmed if the MS/MS spectrum of the potential metabolite has several neutral losses and fragment ion in common with the substrate and the fragmentation pattern corresponds to the predicted structure. Figure 2.4 show the similarities between

the spectra for palmitoylcarnitine and its potential metabolite m/z 414, the spectra and structure for the other palmitoylcarnitine metabolites can be found in the Appendix Figures 6.1 – 6.29 along with the spectra for other metabolites identified using this method, which are also listed in Table 2.3.

It should be noted that the common neutral loss of 59 Da, commonly seen in the MS/MS spectra of acylcarnitines is due to the loss of trimethylamine, $N(CH_3)_3$ (theoretical mass 59.073499) and not from the loss of CH_2COOH (theoretical mass 59.01330). Using the FT-ICR MS the experimental common neutral loss for palmitoylcarnitine was measured as 59.07374 Da corresponding to the loss of trimethylamine.

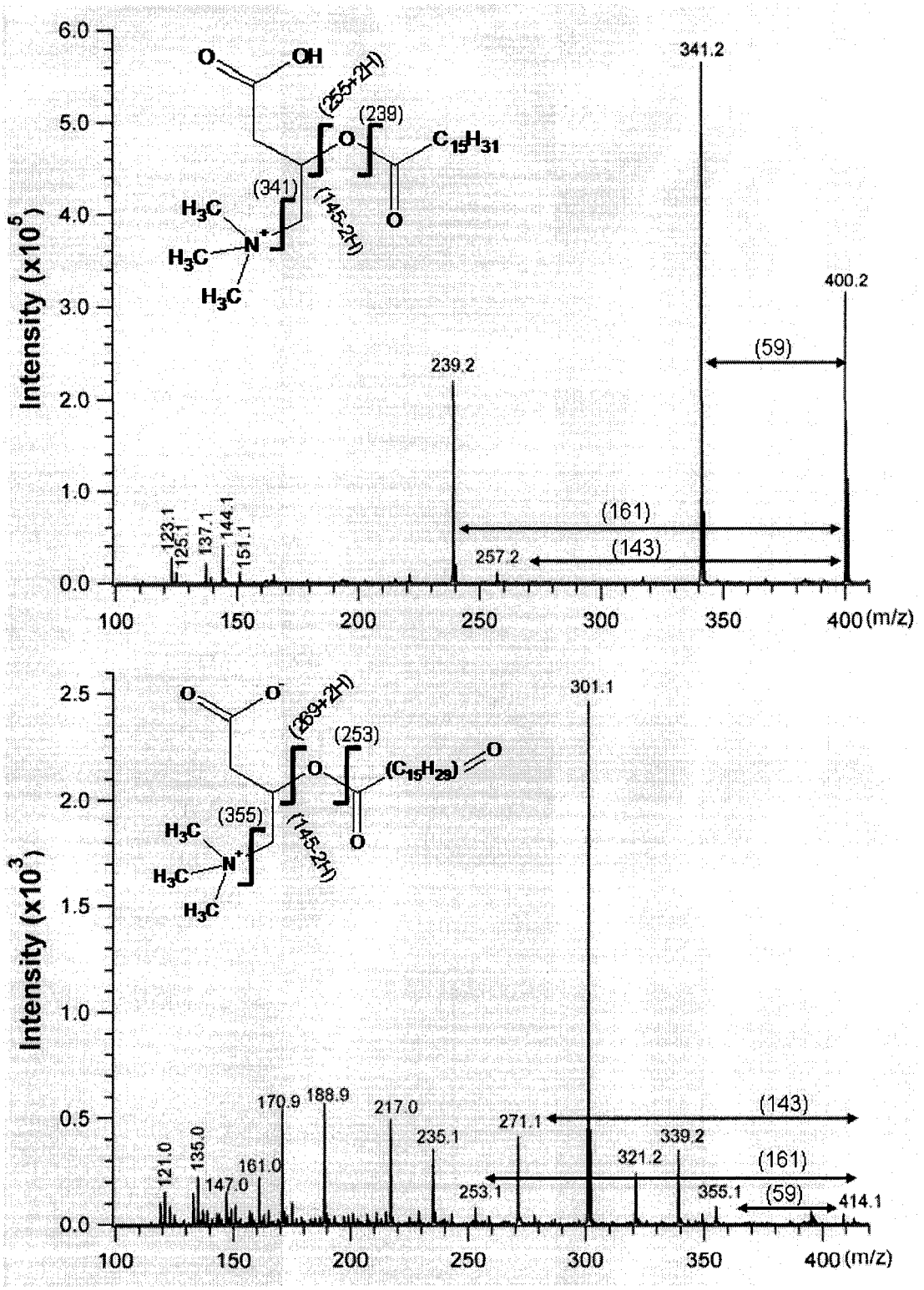

Figure 2.4 - The MS/MS spectrum of palmitoylcarnitine (Top) and the palmitoylcarnitine metabolite m/z 414 (Bottom). The numbers in brackets indicate similar neutral losses.

Table 2.3 - List of identified metabolites from HLM incubations, including the substrate they metabolized from, the metabolite's mass and retention time and any similar fragment ions or neutral losses between the metabolite's fragmentation pattern and that of the substrates.

Substrate	Metabolite m/z	RT (min)	Fragment ions common with substrate (m/z)	Neutral loss commone with substrate (Da)
palmitoylcarnitine	372	18.6	123, 137, 144	59, 143, 161
palmitoylcarnitine	386	19.4	123, 137, 144, 151	59, 161
palmitoylcarnitine	414	15.4		59, 143, 161, 179, 263
palmitoylcarnitine	416a	14.9		59, 161, 179, 235, 249, 263, 277
palmitoylcarnitine	416b	15.1		161, 179, 263, 277
L-aspartyl-L-phenylalanine	166	3.4	120	46
L-aspartyl-L-phenylalanine	309 (neg)	9.7		18, 44, 62
capric acid	187 (neg)	7.2		18
caprylic acid	159 (neg)	3.8		18
ferulic acid	214	9.6	117, 145, 163, 177	14, 32, 60
indolelactic acid	220 (neg)	3.9	130, 158	18, 62
isovalerylcarnitine	259			
2-methylbutroylcarnitine	260	9.2	85	59, 161
methyl o-methoxyhippuric acid	210	9.3	135, 192	18
octanoylcarnitine	304	8.2	85	59, 161, 179
octanoylcarnitine	318	8.8		59
phenylacetylglycine methyl ester	194	8.2	120, 148, 176	118
undecanoic acid	201 (neg)	8.7		18

Table 2.3 lists the potential metabolites for each of the incubated substrates and any similar fragment ions and neutral losses that were used to identify them as a substrate's metabolite. The metabolites for capric acid, caprylic acid and undecanoic acid were not identified based on the MS/MS spectral comparison of substrate versus metabolite. This is because the MS/MS spectra for each of these substrates could not be collected on the ion trap in the negative mode. These substrates did not easily ionize in the negative mode and what was ionized was only blown apart when fragmentation was attempted so that

any remaining signal for the fragments was lost in the noise or below 50 Da, which corresponds previously reported work [7]. Instead the metabolites for these three substrates, capric acid, caprylic acid and undecanoic acid, were identified due to the similarities between the substrates, the similarities between the MS/MS spectra of the metabolites and their predicted structures.

The structure for each of the substrates is a simple straight carbon backbone with a carboxylic acid functional group. Capric acid has a nine carbon backbone, caprylic acid has a seven carbon backbone and undecanoic acid has a ten carbon backbone. Since the substrates have similar structures they should undergo the same metabolism resulting in metabolites with similar structures. The predicted structure for each of these metabolites has an additional alcohol functional group added to somewhere along the carbon backbone; the exact location cannot be exactly identified based on the fragmentation pattern. However, the three metabolites for capric acid, caprylic acid and undecanoic acid all have similar fragmentation patterns with similar neutral losses of 18 (H_2O), 46 (COOH+H) and 60 (CH_2-COOH+H) Da as shown in Figures 2.5-2.7. A potential fragmentation mechanism is drawn in Figure 2.8 explaining fragmentation of these three metabolites.

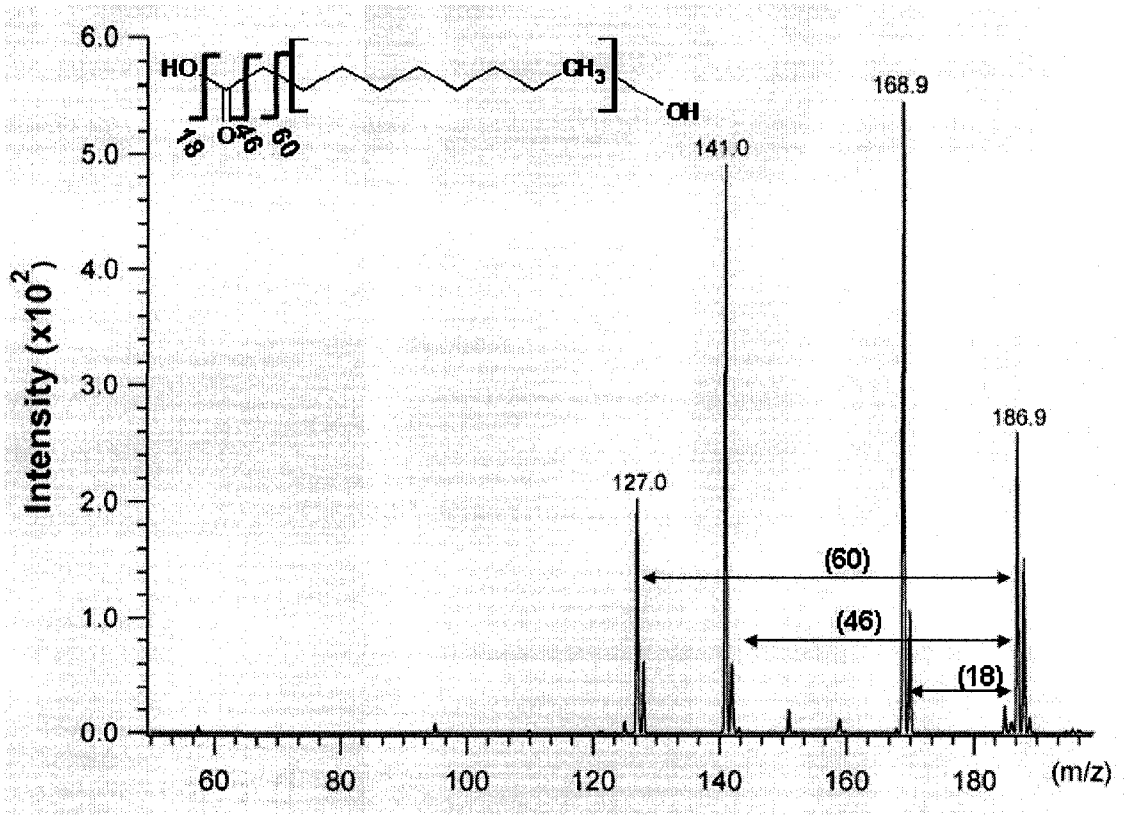

Figure 2.5 - MS/MS of capric acid metabolite m/z 187 (negative mode)

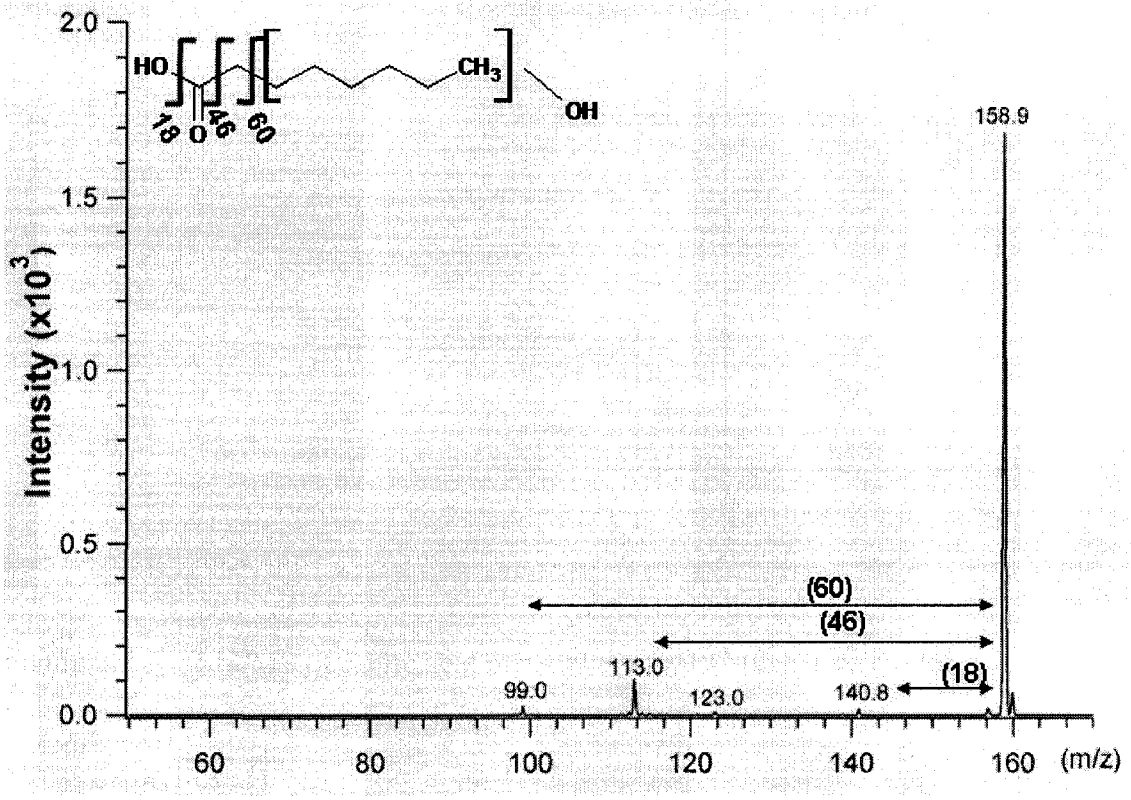

Figure 2.6 - MS/MS of caprylic acid metabolite m/z 159 (negative mode)

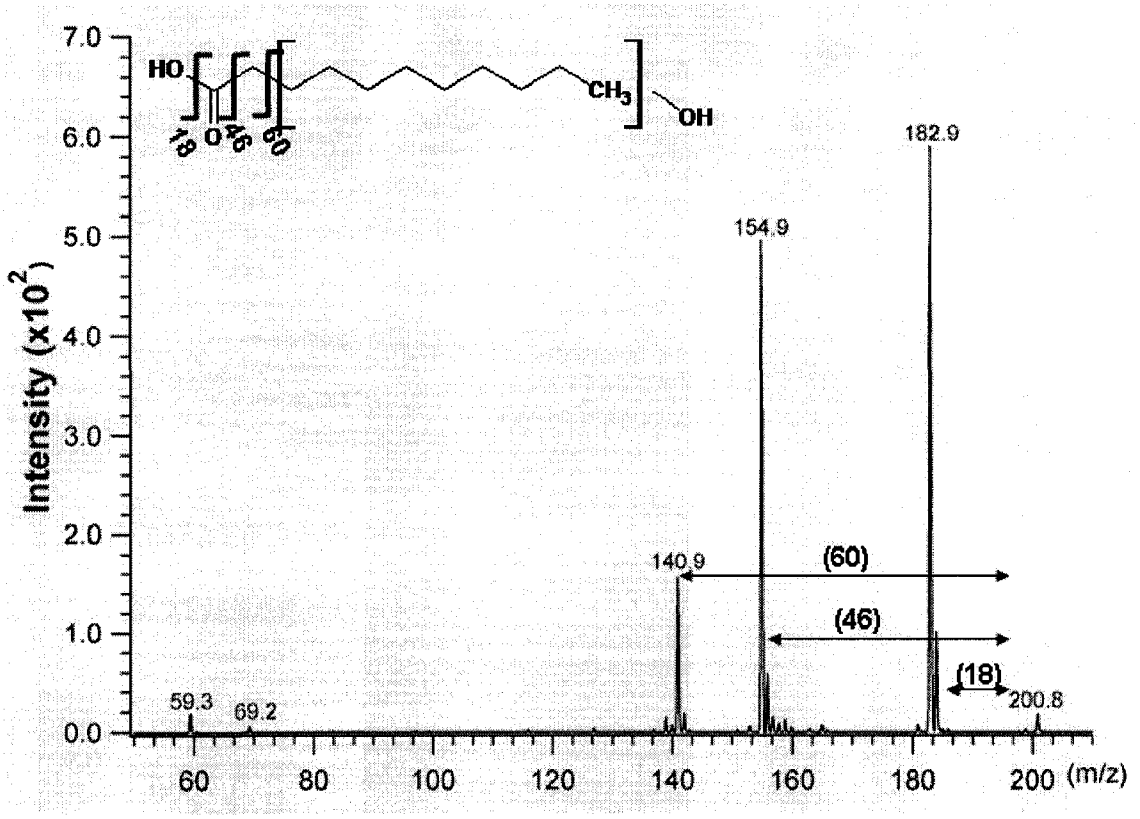

Figure 2.7 - MS/MS of undecanoic acid metabolite m/z 201 (negative mode)

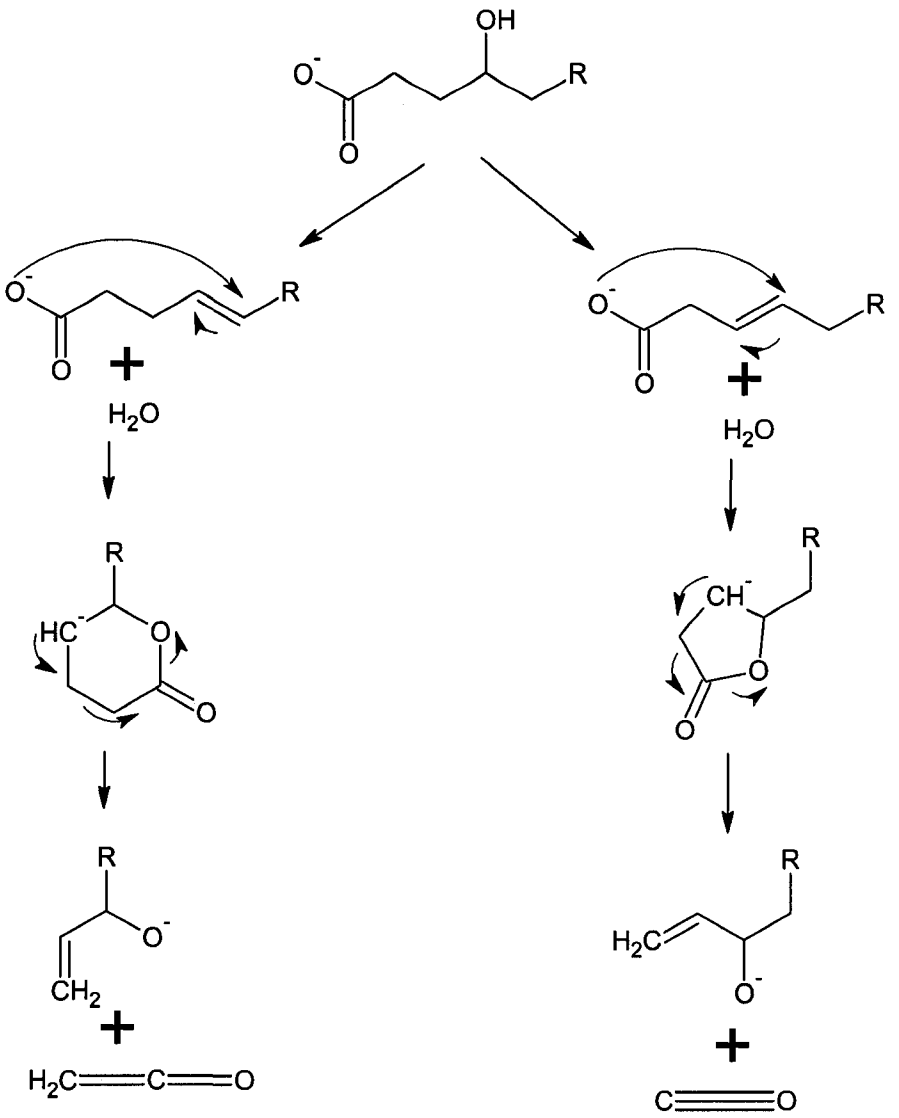

Figure 2.8 - Potential mechanism to cause the fragmentation patterns for the capric acid metabolite m/z 187, the caprylic acid metabolite m/z 159 and the undecanoic acid metabolite m/z 201

2.3.2. Microsomes are the Cause for the Substrates Metabolism

Although the substrates are metabolizing it is possible that it is due to other chemical reactions in the incubation mixture and not the HLM. To test this theory the incubations were repeated for several of the compounds and the controls consisted of everything except the human liver microsomes, in their place an equivalent volume of buffer was used. Several previously used substrates were incubated, including L-aspartyl-L-phenylalanine, methyl o-methoxyhippuric acid, palmitoylcarnitine and

phenylacetylglycine methyl ester, and the presence of previously determined metabolites was investigated.

As shown in Figures 2.9 to 2.15 the L-aspartyl-L-phenylalanine metabolite m/z 166, and the palmitoylcarnitine metabolites m/z 414 and m/z 416 had no metabolite peaks in the sample which did not contain any microsomes. The phenylacetylglycine methyl ester metabolite m/z 194 and the methyl o-methoxyhippuric acid metabolite m/z 210 did have small metabolite peaks appear in the samples with no microsomes but they are small when compared to the samples that included microsomes. The palmitoylcarnitine metabolites m/z 372 and m/z 386 are found in both samples with and without the microsomes so the enzymes in the microsomes are not aiding in the production of these metabolites but they could still be present in the human body so they will not be discarded at this point.

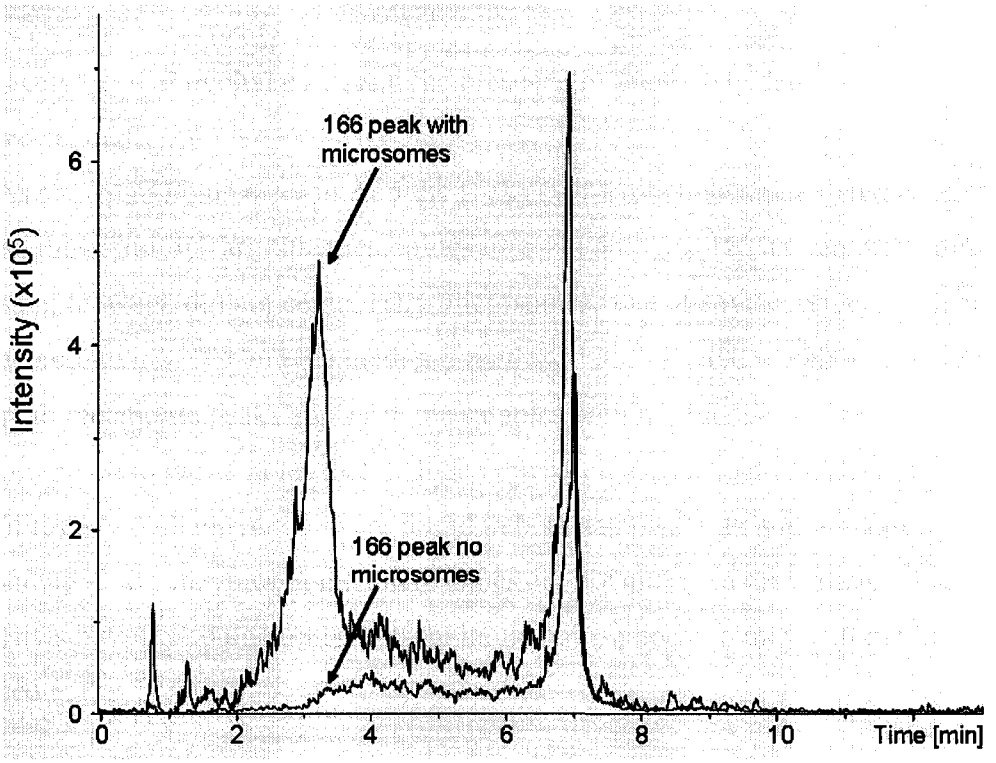

Figure 2.9 - The EIC of m/z 166 from a 1 h HLM incubation with L-aspartyl-L-phenylalanine and the corresponding control with no microsomes added to the incubation mixture

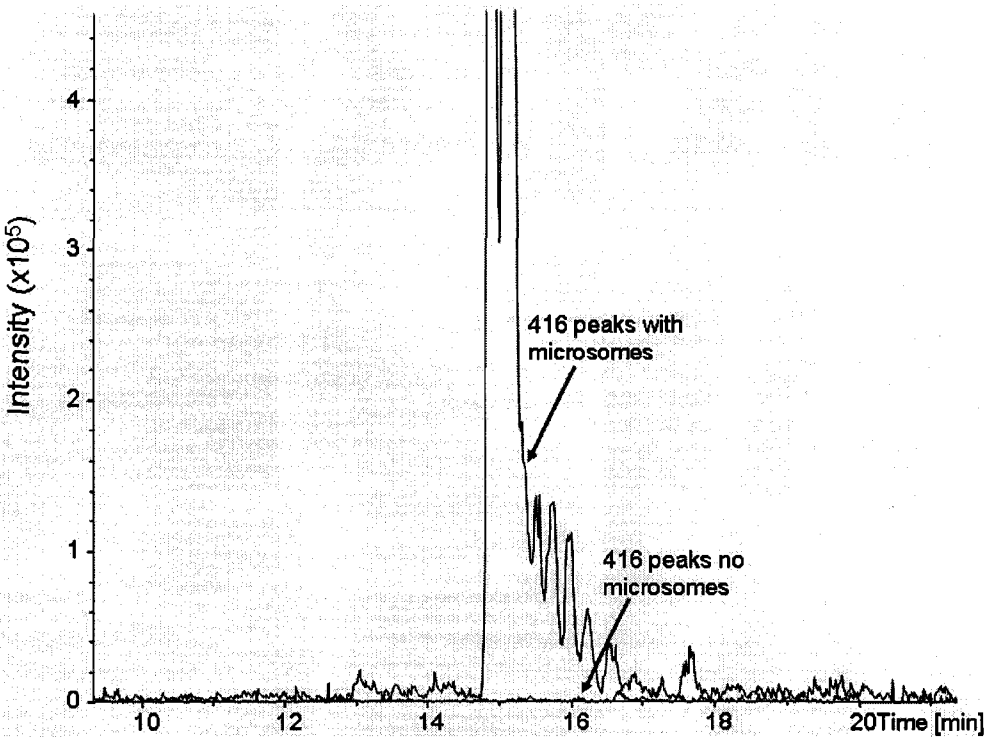

Figure 2.10 - The EIC of m/z 416 from a 1 h HLM incubation with palmitoylcarnitine and the corresponding control with no microsomes added to the incubation mixture

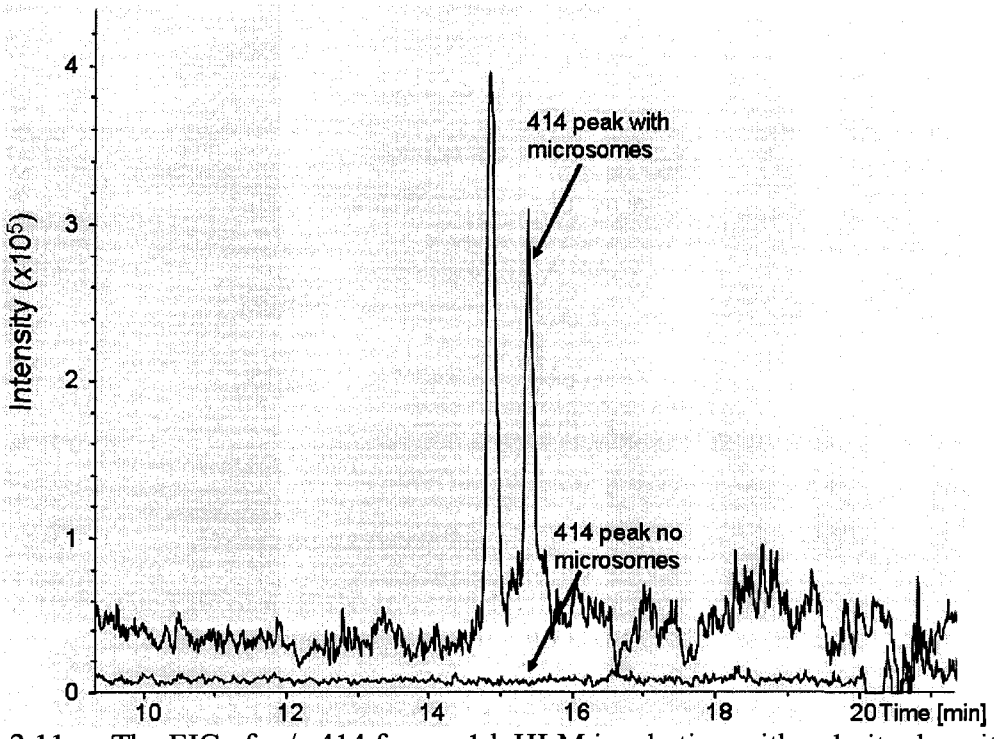

Figure 2.11 - The EIC of m/z 414 from a 1 h HLM incubation with palmitoylcarnitine and the corresponding control without microsomes added to the incubation mixture

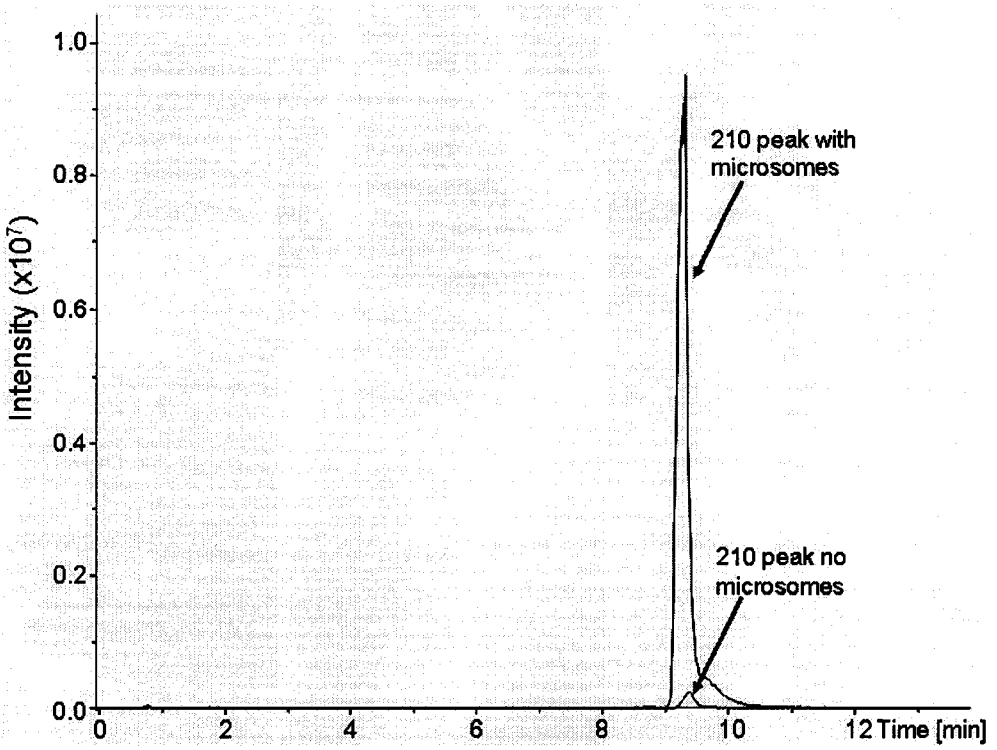

Figure 2.12 - The EIC of m/z 210 from a 1 h HLM incubation with methyl o-methoxyhippuric acid and the corresponding control without microsomes added to the incubation mixture

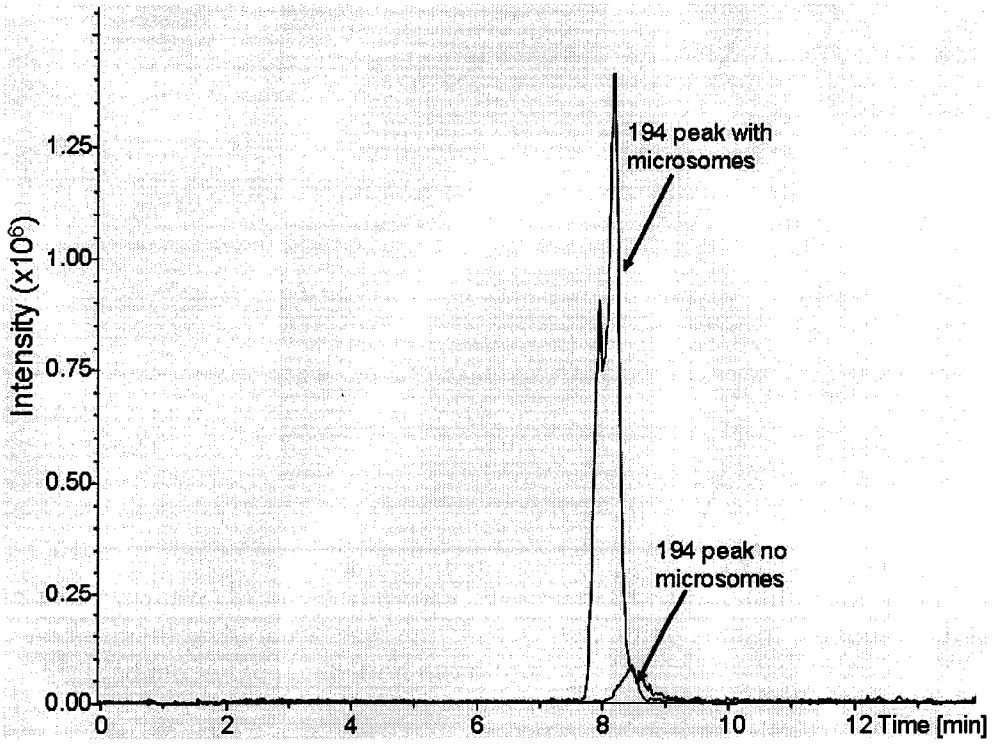

Figure 2.13 - The EIC of m/z 194 from a 1 h HLM incubation with phenylacetylglycine methyl ester and the corresponding control without microsomes added to the incubation mixture

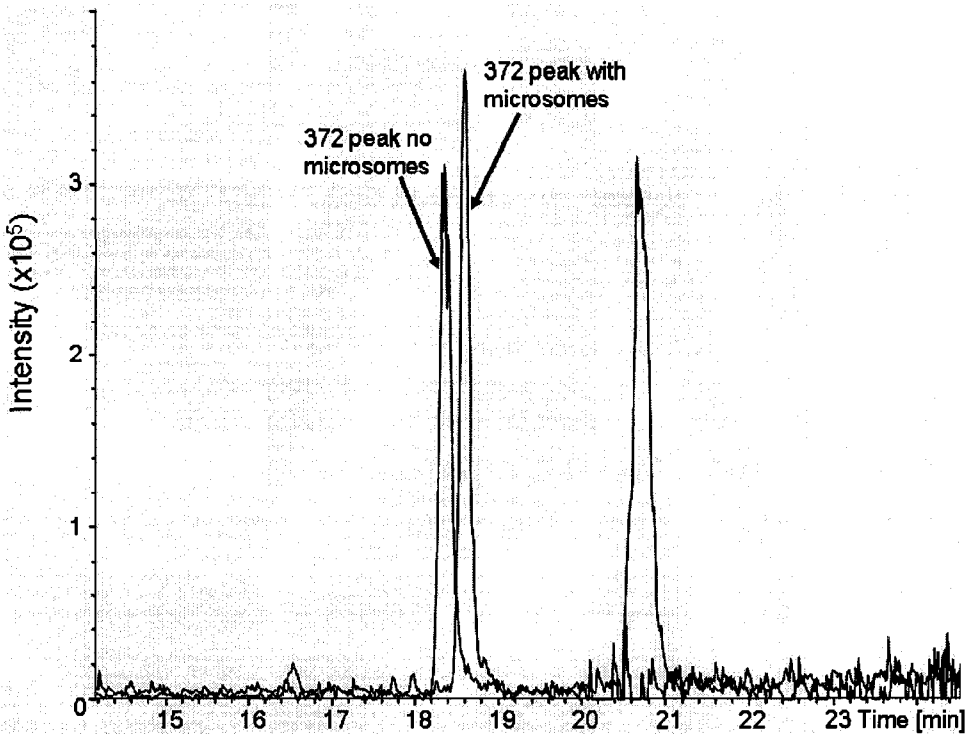

Figure 2.14 - The EIC of m/z 372 from a 1 h HLM incubation with palmitoylcarnitine and the corresponding control without microsomes added to the incubation mixture

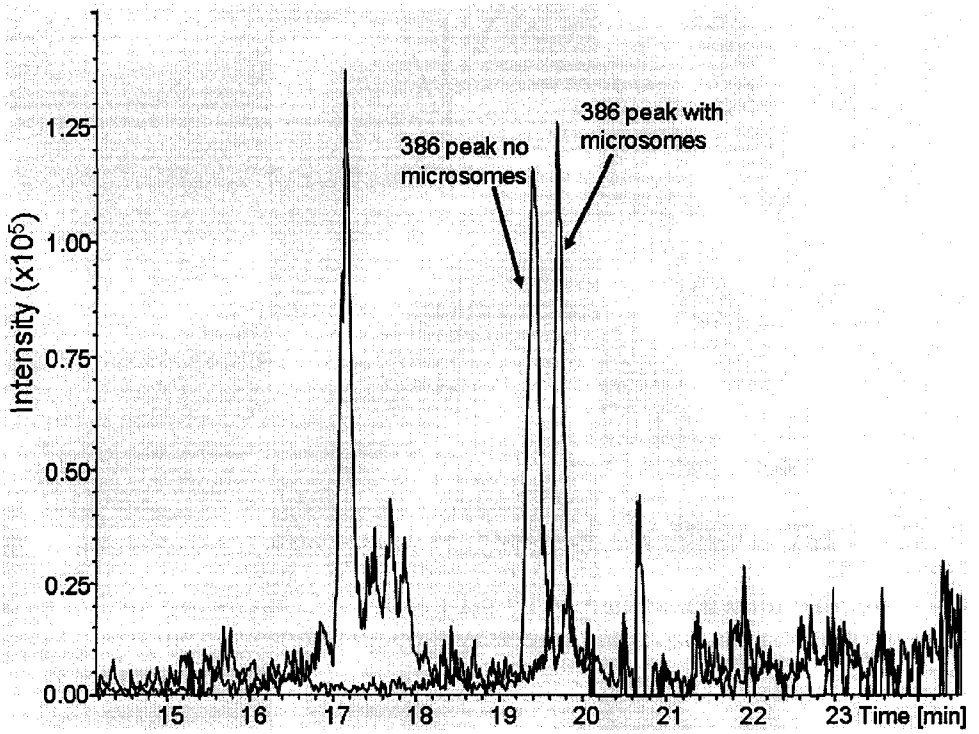

Figure 2.15 - The EIC of m/z 386 from a 1 h HLM incubation with palmitoylcarnitine and the corresponding control without microsomes added to the incubation mixture

2.3.3. The Potential for Methodological Improvements

On average the substrates metabolized using this analytical method only produce one or two metabolites at a detectable limit with the exception of palmitoylcarnitine which produces 5 metabolites when incubated with the HLM. However, if we refer to Figure 2.2(d), the palmitoylcarnitine metabolite m/z 416 has two positively identified metabolites found at 14.9 and 15.1 min. To the right of these two metabolite peaks the EIC shows several smaller peaks between 15.2 and 17.0 min but these peaks are at a concentration too low for subsequent MS/MS analysis. Several adjustments to the method were attempted to increase the concentration of these analytes for MS/MS analysis, including increasing the injection volume, sample concentration and combining several concentrated samples. Unfortunately these attempts also increased the background as well as the ion suppression resulting in no overall improvement. Other areas of improvement involve sample clean up, which was not attempted, and improving the LC separation by using Ultra Performance Liquid Chromatography (UPLC) systems. Figure 2.16 shows the resulting UPLC-MS/MS chromatogram. The UPLC-MS/MS chromatogram has 11 distinct peaks ranging in intensity from 20000 to 2000 counts, suggesting that the two peaks previously identified could have been several different metabolites eluting at the same time. The MS/MS spectrum corresponding to each peak in the chromatogram confirms that 10 of the 11 peaks are metabolites of palmitoylcarnitine and are structural isomers of each other (see Appendix Figures 6.30-6.41); the position of the double bonded oxygen is still undetermined but could reside on any of the carbons indicated in Figure 2.17.

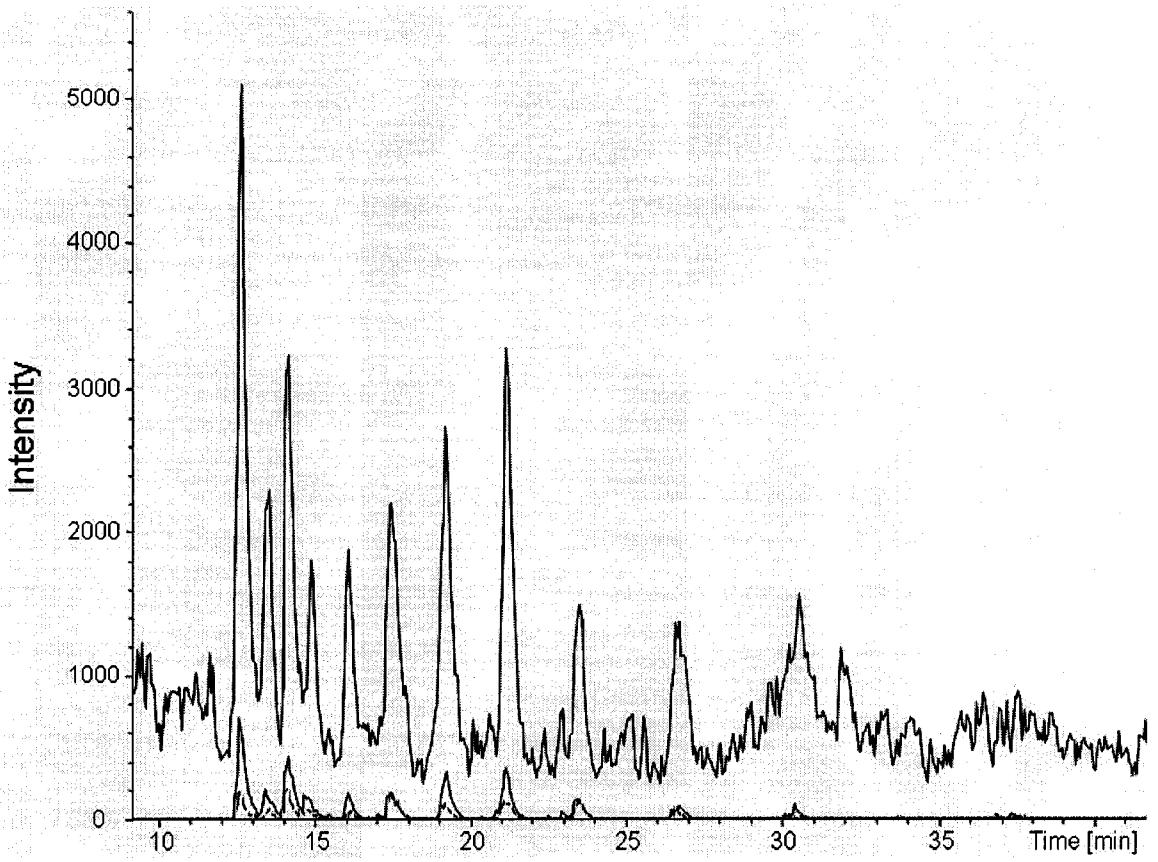

Figure 2.16 - MS/MS of UPLC separation for palmitoylcarnitine metabolite m/z 416. The most intense chromatogram is the MS/MS chromatogram of m/z 416, the small solid line chromatogram is the EIC for m/z 237 and the smaller doted line chromatogram is the EIC for m/z 255

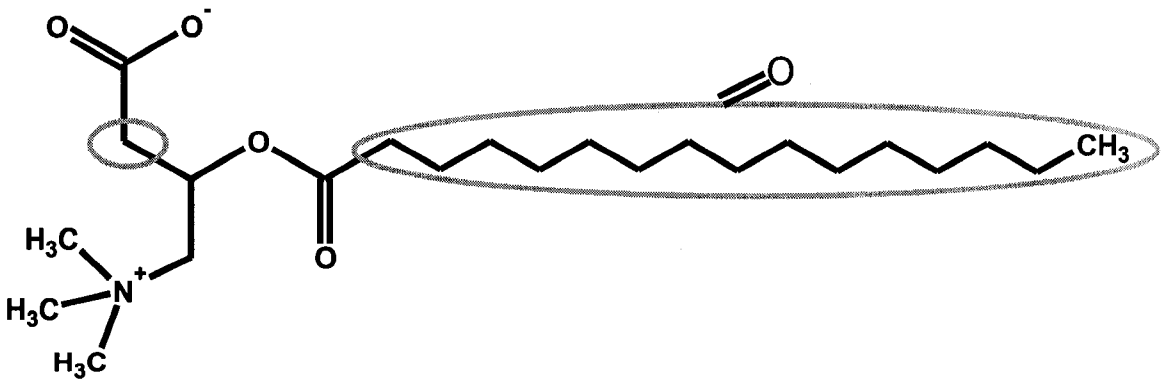

Figure 2.17 - Palmitoylcarnitine metabolite m/z 416, the double bonded O is on one of the circled carbon atoms

2.4. Conclusions

This work examined the strategy of using human liver microsomes to metabolize substrates known to be endogenous human metabolites, followed by analyzing the metabolites using LC-ESI MS and MS/MS for expanding the human metabolome MS/MS spectral library. The potential structures of the metabolites found in microsome incubation experiments were deduced based on the comparison and interpretation of fragment ion spectra of the substrate and its metabolites. The proposed structure along with the MS/MS spectrum of a metabolite could be used for identification of unknown metabolites present in human biofluids and, if found, it could be entered into the human metabolome MS/MS spectral library (see Chapter 3).

Using this method 18 different metabolites were confirmed from 12 different substrates yielding one or two metabolites per substrate, except palmitoylcarnitine that had 5 metabolites identified and showed potential of several more but due to ion suppression the signal was too low for MS/MS analysis. Subsequent analysis using UPLC instead of the typical High Pressure Liquid Chromatography (HPLC) showed that the palmitoylcarnitine metabolite, m/z 416, had 11 different isomers and not just the two that were previously confirmed.

2.5. References Cited

1. Chace, D.H., T.A. Kalas, and E.W. Naylor, *Use of Tandem Mass Spectrometry for Multianalyte Screening of Dried Blood Specimens from Newborns.* Clin Chem, 2003. **49**(11): p. 1797-1817.

2. Rashed, M.S., et al., *Screening blood spots for inborn errors of metabolism by electrospray tandem mass spectrometry with a microplate batch process and a computer algorithm for automated flagging of abnormal profiles.* Clin Chem, 1997. **43**(7): p. 1129-1141.

3. Proestos, C., D. Sereli, and M. Komaitis, *Determination of phenolic compounds in aromatic plants by RP-HPLC and GC-MS.* Food Chemistry, 2006. **95**(1): p. 44.

4. *8.4.4.2 Expert Tune Page, Tuning and Calibration.* HCT/esquire Series user manual, Esquire series User manual V2 Operations. Version 1.0, 2004: p. 8-10.

5. *Human and Animal Liver Microsomes.* [Product Sheet] Revised 18 October 2004 [cited 2006 January]; Available from: http://www.invitrotech.com/filelib/ps_microsomes.pdf.

6. Shou, W.Z., et al., *A novel approach to perform metabolite screening during the quantitative LC-MS/MS analyses of in vitro metabolic stability samples using a hybrid triple-quadrupole linear ion trap mass spectrometer.* J Mass Spectrom, 2005. **40**(10): p. 1347-1356.

7. Bandu Mary, L., et al., *Prediction of MS/MS data. 1. A focus on pharmaceuticals containing carboxylic acids.* Anal Chem FIELD Full Journal Title:Analytical chemistry, 2004. **76**(6): p. 1746-53.

Chapter 3

Using the Human Liver Microsome Metabolites to Identify Compounds in Human Urine

3.1. Introduction

Disease diagnostics can require a multitude of tests and some of these can involve unpleasant and invasive procedures, such as muscle and bone biopsies, which may result in scars and prolonged discomfort. Lumbar punctures are used to extract CSF, a biofluid commonly used to test for a number of different neurological diseases, and if the procedure is performed incorrectly it can leave a patient permanently paralyzed. In some cases a disease may make it impossible to perform routine tests, such as blood work or biopsies. For example, Fibrodysplasia Ossificans Progressive is a disease in which muscle and connective tissue turn to bone upon injury and a simple prick from a needle will cause irreversible damage.

Currently, over 95% of all diagnostic clinical assays test for small molecules [1], such as those compounds mentioned in section 2.1. However, the compounds analyzed for disease diagnostics are only a small fraction of the human metabolome. Researchers, such as those working on the HMP, are working to document all known human metabolites and expand the database by identifying new metabolites and thus increase the number of potential compounds for clinical assays to help with disease diagnosis. It is not yet possible to analyze the metabolome of a whole human. However a large number of studies are underway analyzing many different biological fluids, such as urine, sputum, bronchoalveolar lavage, breath condensate, whole blood, serum, feces, and cerebral spinal fluid.[2] Urine is one of the more popular biofluid for metabolomic investigations due to the quantity that can be collected, the non-invasive collection, the complex metabolic nature of the fluid, and the ability to collect multiple samples from a single individual over a short time period.

Many different methods have been developed to study the human metabolome and the various biological samples that entails. The most popular techniques involve Nuclear Magnetic Resonance (NMR) and MS; both techniques have their advantages and shortcomings. NMR has been used for the characterization of synthetic compounds since

the 1950s and using a combination of 1D and 2D techniques it is an invaluable tool for structural identification of different metabolites.[3] To help with compound identification in complex samples software with pattern recognizing ability has been developed and used in a number of different studies.[3, 4] Unfortunately, NMR is not nearly as sensitive as MS. Stand-alone metabolite identification using NMR requires a significant amount of sample clean up, purification, concentration and reconstitution in deuterated solvent before the NMR analysis.[3] However, research is ongoing and techniques being developed to improve the sensitivity of NMR by using more powerful magnets as well as the incorporation of LC with NMR.[3]

Mass spectrometry is a more sensitive technique than NMR and readily couples to a gas or liquid chromatograph instrument. There are several MS strategies that are commonly used for metabolite identification in complex samples, including precursor ion and constant neutral loss scanning, product ion scanning, multiple-reaction monitoring, accurate mass measurements, isotope ratios, fragmentation libraries, MS/MS libraries and isotope labeling. Typically several of these strategies are used together for the positive identification of metabolites.[3]

The main strategy used to help identify the metabolites, described in Chapter 2, was the product ion scanning method. Specific ions were targeted, based on known biotransformations, and fragmented so that their MS/MS spectra could be recorded and the fragmentation pattern analyzed for characteristic fragmentation patterns and other clues to help to identify the metabolite and its structural features. Common fragmentation interpretations include the nitrogen rule, which states that a molecule with an odd numbered molecular weight stipulates an odd number of nitrogen atoms in the compound while an even numbered molecular weight must contain either no nitrogen atoms or an even number of nitrogen atoms, to determine the number of nitrogen atoms in the chemical formula while specific neutral losses found in the fragmentation pattern can indicate different functional groups.[3] Other common compound identification methods used include precursor ion scanning, the common neutral loss method and the multiple-reaction monitoring (MRM) method.

Precursor ion scanning requires the first mass analyzer to scan the entire mass range followed by fragmentation of each different m/z ion in turn, and then the second mass

analyzer only allows the mass of one specific fragment ion through to the detector to produce a chromatogram of precursor ions that fragment to a common, diagnostic product ion. The common neutral loss method is similar to the precursor ion scan method in that only one fragmentation is being monitored. The difference between the two methods is that the constant mass is being loss, so while the first mass analyzer is being scanned, the second mass analyzer is also being scanned but for an ion of [M-x], where x is a constant defined by the neutral loss. For example, acylcarnitines typically have a neutral loss of 59 Da corresponding to the loss of $N(CH_3)_3$ which can be used to help identify most acylcarnitine metabolites. Common neutral losses may also be used to target metabolites with a specific biotransformation, such as the loss of 176 mass units indicates a glucuronide conjugate. Lastly, the multiple-reaction monitoring method targets two or more fragment ions and/or common neutral losses to help identify members of a specific structural family or metabolites of a specific compound. In the mass spectrometer the first mass analyzer will scan the entire mass range, the ions are then fragmented in the second mass analyzer and the peaks of interest are targeted. Targeting more then one characteristic fragment ion or common neutral loss decreases the chance of a coincidental fragmentation with the same mass as the target compounds but a completely different structure. [5]

Accurate mass measurements from instruments such as Fourier Transform Ion Cyclotron Resonance Mass Spectrometers (FT-ICR MS) are increasing in popularity. With a mass error of less than 5 ppm it is possible to deduce the chemical formula of an unknown metabolite. In the case of several potential chemical formulas the correct one can be identified by comparing the ratio of the isotopic peaks. Each element has several stable isotopes, each with a slightly different mass and a known natural occurrence, and with this knowledge it is possible to predict the isotopic masses for each chemical formula and their relative intensities. Some compounds, such as chlorine (Cl) with three ^{35}Cl to every one ^{37}Cl, have a very distinctive isotope pattern.

When studying the metabolism of a specific substrate it is also possible to label the compound with isotopically heavy or light atoms, like carbon 13, before administering it to the test subject for *in vivo* experiments or by adding it to any cultures or enzyme mixtures for *in vitro* experiments. The difference in the mass for the heavy or light atoms

in the substrates structure helps to identify the metabolism pathway as well as the chemical structures using MS and MS/MS analysis. Another labeling option is to dope the chemical structure with stable radioactive atoms before administration to the test subject.[6] The radioactive labeled substrates can be used to identify the location of the substrate and its metabolites within an individual. However, unlike the other methods discussed, the radioactive labeled substrates are detected using radioautographic imaging instead of NMR or MS.[7]

Other compound identification techniques require databases of experimental information. Companies, for example Thermo, have built fragmentation libraries to meet the expanding requirements of unknown compound identification in complex samples using MS/MS analysis. Thermo has released software, Mass Frontier™, which can predict the fragmentation pattern of a given structure or given an MS/MS spectrum the software can deduce the possible structure of the different fragment ions. The software contains a database of known fragmentation mechanisms which can automatically be searched and compared so that fragmentation patterns can be predicted or a possible structure suggested.[8-10] Like all the other techniques mentioned above this method still requires verification from another metabolite identification methods before positive identification of a compound can be made.

The preferred method for positive identification of metabolites in complex biological samples, such as human urine, is to use a set of standards for direct MS/MS comparison or if the standards are not available then a MS/MS library containing the MS/MS spectra of different compounds under different experimental conditions.[11, 12] Using a library can work well; for example, GC-MS analysis using electron impact fragmentation and the resulting fragmentation patterns are fairly consistent between instruments; unfortunately with the advent of LC-MS the number of different types of mass spectrometers and different methods of fragmentation increased. The MS/MS spectra collected on an ion trap and a time-of-flight instrument may have different fragmentation patterns for the same compound. Having standards allows the user to directly compare retention time as well as the fragmentation pattern of the standard against the unknown on their system.[13] This is the method used in this chapter to identify compounds in urine. The database of metabolites documented in Chapter 2 was

collected on the same instrument used to analyze the urine, as described in this chapter. It was also possible to rerun the microsome incubation under identical conditions as the urine analysis for positive identification using the retention times as well as the fragmentation pattern.

3.2. Experimental

3.2.1. Chemicals and Materials

Fisher brand nylon 0.2 μm syringe filters along with Optima LC/MS grade water and acetonitrile were purchased from Fisher Scientific Canada (Edmonton, AB, Canada). Formic acid and L-phenylalanine were purchased from Sigma Aldrich (Oakville, ON, Canada). O-methoxyhippuric acid was purchased from ChemBridge (San Diego, CA). Phenylacetylglycine was obtained from the Human Metabolome Library through the Human Metabolome Project. (Edmonton, AB, Canada).

3.2.2. Instrument and Equipment

All sample analyses were initially conducted using an LC coupled to an ion trap mass spectrometer. The LC system used was an Agilent 1100 equipped with a binary pump, auto sampler and degasser. An ACE 3 μm C18 (50 x 2.1 mm) 100 Å column (Aberdeen, Scotland) was used for sample separation. The flow rate was set to 0.1 mL/minute and separation was performed at ambient temperatures. The LC system was coupled to an Esquire 3000plus quadrupole ion trap (Bruker, Bremen, Germany) equipped with an electrospray interface. A Windows 2000 workstation ran Chemstation and EsquireControl to control the LC-MS system.

When required a 9.4 T FT-ICR MS (Bruker, Bremen, Germany) equipped with an electrospray interface was used to collect accurate mass information.

3.2.3. Chromatographic Conditions

The flow rate was set and held constant at 0.1 mL/min. The gradient used was B held at 0% for 1 min, then increased to 50% in 80 minutes and 100% in 5 minutes. After B was held at 100% for 10 minutes, it was brought back down to 0% in 0.1 minutes followed by a 9.9 minute re-equilibration. The total time for one injection was 105 minutes. The LC solvents, column and MS parameters were identical to the microsome sample analysis.

3.2.4. Sample Collection and Preparation

A urine sample was collected from a healthy individual and filtered through a Fisher brand Nylon 0.2 μm syringe filter. The sample was then stored at -20 °C until analyzed. An informed consent was obtained from the volunteer and ethics approval for this work was obtained from the University of Alberta in compliance with the Health Information Act (in accordance to Section 54(1)).

3.2.5. Mass Spectrometry Conditions

All experiments conducted on the ion trap used electrospray ionization with the nebulizer gas set to 30 psi, the dry gas set to 10 L/min and the dry gas temperature set to 350 °C. The LC-MS data collected are in Single Ion Monitoring (SIM) mode, i.e., only one target m/z was monitored with a 4 Da window, and the Smart Parameter Settings were optimized for each target m/z. The compound stability was set according to the substrates stability in the ion trap. The optimization was set to normal. And the trap drive level was set according to the manual specifications. The scan speed for the ion trap is 13000 m/z/s, hence for a mass range from 50 to 500 m/z it can collect 28 spectra/s.

Table 3.1 - Trap Drive Level as suggested by the Esquire 3000plus manual [14]

Mass Range (m/z)	Trap Drive Level (%)
50-400	50
400-800	60
800-1200	70
1200-2000	80

The MS/MS experimental conditions are identical to the MS conditions except that the mass of interest was isolated with a 4 Da window and the fragmentation energy was set to the same energies required to fragment the metabolites as discussed in Chapter 2.

3.2.6. Data Analysis and Interpretation

All microsome incubations were run using the same LC-MS conditions as the urine samples and the retention times for each metabolite was used for initial identification of potential matches to the urine sample. Positive identification of a metabolite in urine was confirmed by comparing the MS/MS spectra from the identified metabolites in the microsome samples to those generated from urine.

3.3. Results and Discussion

Four different metabolites were identified in a single human urine sample using this method, including metabolites phenylacetylglycine methyl ester m/z 194, methyl o-methoxyhippuric acid m/z 210, L-aspartyl-L-phenylalanine m/z 166 and 2-methylbutyroylcarnitine m/z 260. Figures 3.1-3.4 show the MS/MS spectra of the metabolite pseudo-standards obtained from the HLM incubations alongside spectra of matching MS/MS fragmentation patterns from a urine sample.

The spectra from the HLM incubation and the urine sample for the phenylacetylglycine methyl ester metabolite m/z 194, see Figure 3.1, match extremely well and also elute from the LC column at identical retention times. Together the retention time, fragment masses and the relative peak intensities of the fragment peaks reveal that these are the same compound. Based on the chemical structure of the substrate, by examining the similarity and differences between the MS/MS spectra of the substrate (see appendix figure 6.25) and that of the metabolite (Figure 3.1), and using the fragmentation for structural assignment, it can readily be concluded that the potential metabolite m/z 194 is from phenylacetylglycine, a known endogenous human metabolite [15]. Apparently, phenylacetylglycine methyl ester metabolizes to phenylacetylglycine with the loss of a methyl group, catalyzed by the cytochrome P450 enzymes. The identity of this compound was further verified by obtaining a phenylacetylglycine standard and analyzing it using the ion trap to determine its retention time and fragmentation pattern.

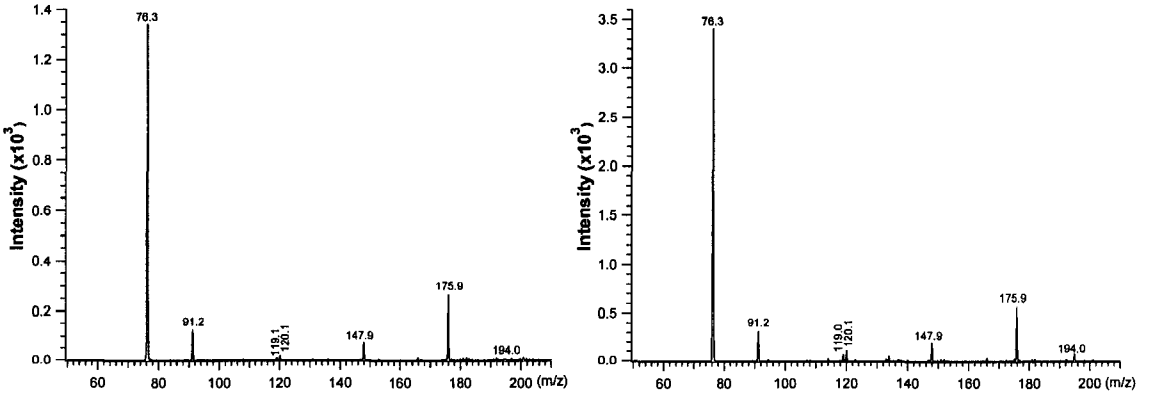

Figure 3.1 - MS/MS spectra of phenylacetylglycine, left from HLM incubations and right from a human urine sample

The L-aspartyl-L-phenylalanine metabolite elutes from the LC column from the microsome sample and urine sample at identical retention times and also has identical

fragmentation patterns (see Figure 3.2). The differences in relative peak heights between the two sets of spectra for phenylalanine are related to the number of ions trapped in the ion trap for each fragmentation experiment. Comparing the MS/MS spectra of L-aspartyl-L-phenylalanine and its potential metabolite at m/z 166 it can be conclude that the compound is phenylalanine, a known endogenous human metabolite [16]. L-aspartyl-L-phenylalanine metabolizes to phenylalanine due to peptidase, which cleaves a carbon nitrogen bond resulting in the loss of $C_4H_4NO_3$ (115 Da). The standard for L-phenylalanine was also available and the corresponding LC-MS experiments further confirm the identity of the metabolite found in urine. Thus, two known endogenous human metabolites, phenylalanine and phenylacetylglycine, were confirmed and identified in urine, proving that this method works for metabolite identification in complex biofluids.

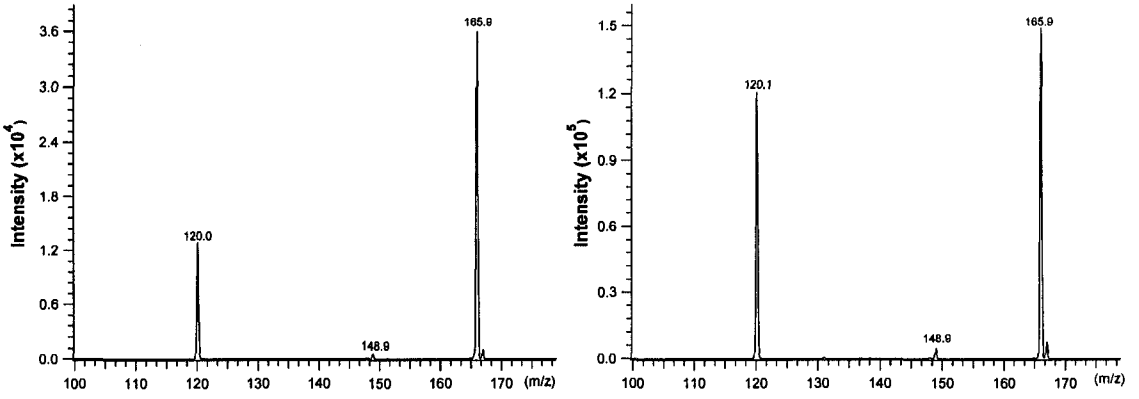

Figure 3.2 - MS/MS spectra of phenylalanine, left from HLM incubations and right from a human urine sample

The peak from the urine sample with the spectrum corresponding to the methyl o-methoxyhippuric acid metabolite m/z 210 eluted from the LC column over a minute sooner in the urine sample than HLM incubation, using the gradient with the 105 minute run time as outlined in the method section. Spiking the urine sample with o-methoxyhippuric acid showed that these two compounds were not identical even though the fragmentation patterns matched. Accurate mass measurements and MS/MS fragmentation using infrared multiphoton dissociation (IRMPD) on a FT-ICR-MS showed that the compound from the incubation is o-methoxyhippuric acid and the compound found in urine is one of its structural isomer p-methoxyhippuric acid or m-methoxyhippuric acid, both of which have previously been identified in urine (see

Appendix Figure 6.41 and 6.42).[17, 18] Methyl o-methoxyhippuric acid metabolizes to o-methoxyhippuric acid due to the loss of a methyl group, likely catalyzed by the cytochrome P450 enzymes. Thus, the metabolites identified from the microsome incubations can also be used to identify structural isomers in complex biofluids, such as urine.

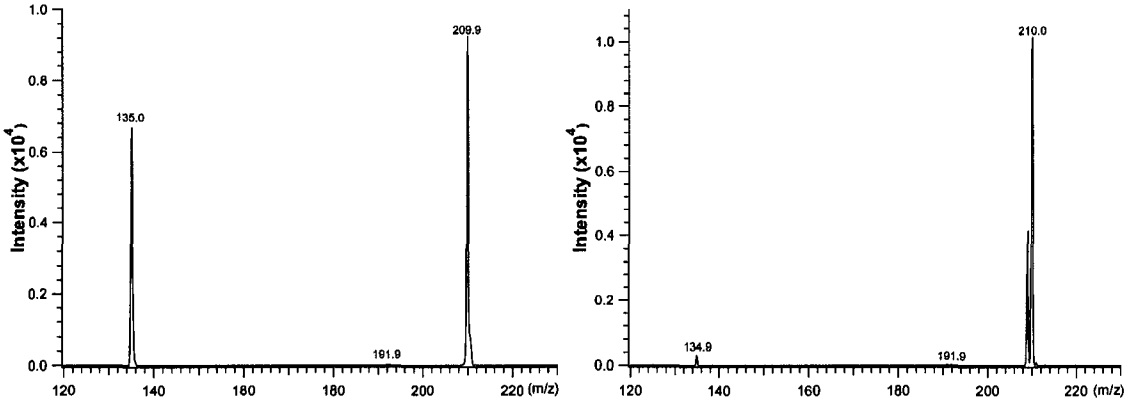

Figure 3.3 - MS/MS spectra of: (left) o-methoxyhippuric acid from HLM incubations and (right) p-methoxyhippuric acid or m-methoxyhippuric acid from a human urine sample

The retention time difference for the 2-methylbutyroylcarnitine metabolite m/z 260 in urine compared to the incubated sample is insignificant and can be explained by experimental error between injections. The fragmentation patterns of m/z 260 from the two different samples are slightly different, see Figure 3.4, the 2-methylbutyroylcarnitine metabolite m/z 260 from the HLM incubation's base peak is m/z 99.1 and has a fragment at m/z 116.1 while the spectrum from the urine has a base peak at m/z 200.9, the m/z 99.1 peak is the second smallest and the spectrum has a peak at m/z 144.0 instead of m/z 116.1, suggesting that these two MS/MS spectra are of isomers and not the same compound. Since structural isomers can have very similar retention times, as shown in Chapter 2 with palmitoylcarnitine, the slight difference in retention times for the 2-methylbutyroylcarnitine metabolite, m/z 260, from the microsome incubation compared to the urine sample is most likely due to a structural difference and not experimental error. The concentration of these two compounds was too low for MS/MS analysis using FT-ICR-MS with IRMPD. The accurate mass was collected for the MS/MS of 2-methylbutyroylcarnitine, which showed two peaks at m/z 85 that would not be resolved using an ion trap MS, one at 85.02846 corresponding to $C_4H_5O_2$ (theoretical mass

85.02895) and the second at 85.06486 corresponding to C_5H_9O (theoretical mass 85.06534). Knowing this it was determined that the 2-methylbutyroylcarnitine metabolite m/z 260 from the HLM incubation has the structure illustrated in Figure 3.5(left) and the 2-methylbutyroylcarnitine metabolite m/z 260 found in the urine sample is its isomer where the O is moved to one of the C* illustrated in Figure 3.5(right), 3-[(2-methyl-3-oxobutanoyl)oxy]-4-trimethylammonio)butanoate, or 3-[(2-methyl-4-oxobutanoyl)oxy]-4-trimethylammonio)butanoate, or 3-[(2-formylbutanoyl)oxy]-4-trimethylammonio)butanoate. The isomer will be referred to as 2MBC metabolite 260b while the metabolite found in the HLM incubation will be referred to as 2MBC metabolite 260a. 2MBC metabolite 260b is a previously undocumented endogenous human metabolite and a standard for this compound could not be purchased through typical chemical suppliers.

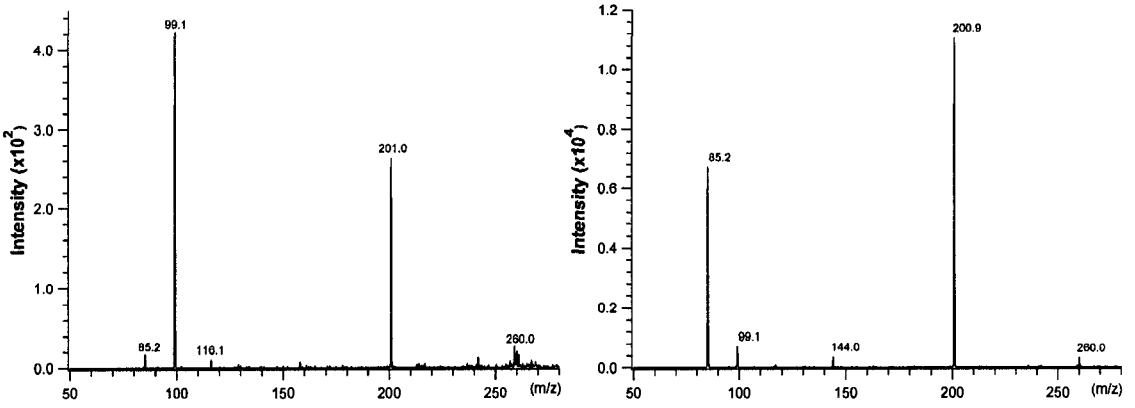

Figure 3.4 - MS/MS spectra of the 2-methylbutyroylcarnitine m/z 260; (left) from HLM incubations and (right) from a human urine sample

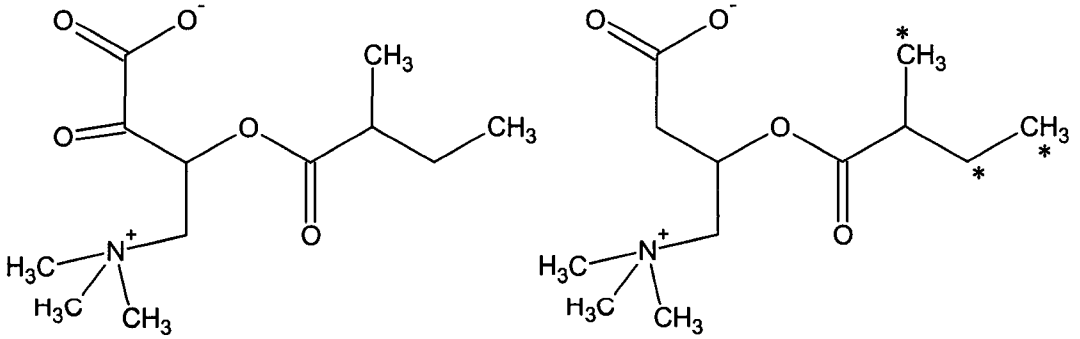

Figure 3.5 - Left is 2MBC metabolite 260a and Right 2MBC metabolite 260b, with a =O found on one of the carbons indicated with a *

3.4. Conclusions

The results shown in this chapter illustrate that the microsome-based system can be used to generate metabolites from a substrate, a known endogenous human metabolite, and subsequent analysis of their metabolites by LC MS/MS in microsome and human biofluids can lead to the identification of potentially new endogenous human metabolites. Metabolites of four substrates, L-aspartyl-L-phenylalanine, phenylacetylglycine methyl ester, methyl o-methoxyhippuric acid and 2-methylbutyroylcarnitine identified from the microsomal incubations experiments were used to identify unknowns in human urine. The metabolites identified in healthy human urine include phenylacetylglycine, phenylalanine, p or m-methoxyhippuric acid and a previously undocumented endogenous human metabolite 2MBC metabolite 260b, a 2-methylbutyroylcarnitine metabolite. A standard for 2MBC metabolite 260b cannot be purchased through typical chemical suppliers and would have to be synthesized. Thus, the unknown metabolite has not been confirmed. Nevertheless, this proof-of-principle work illustrates the usefulness of our strategy for human metabolite identification through the creation and expansion of a human metabolome library using microsome incubation of known substrates. Future work will focus on the optimization of the microsome metabolism experiment and analytical techniques involved in the strategy and apply this method for a wide variety of substrates to produce a relatively more comprehensive human metabolome MS/MS spectral library.

3.5. References Cited

1. Wishart, D., *Proteomics and the Human Metabolome Project.* Expert Rev. Proteomics, 2007. **4**(3): p. 333-5.

2. Saude, E. and B. Sykes, *Urine stability for metabolomic studies: effects of preparation and storage.* Metabolomics, 2007. **3**(1): p. 19.

3. Chandra Prakash, C.L.S.A.N., *Analytical strategies for identifying drug metabolites.* Mass Spectrometry Reviews, 2007. **26**(3): p. 340-369.

4. Griffin, J.L., *Review. The Cinderella story of metabolic profiling: does metabolomics get to go to the functional genomics ball?* Philosophical

Transactions of the Royal Society B: Biological Sciences, 2006. **361**(1465): p. 147.

5. Cox, D.M., et al., *Multiple Reaction Monitoring as a Method for Identifying Protein Posttranslational Modifications.* J Biomol Tech, 2005. **16**(2): p. 83-90.

6. Abdul Mutlib, W.L.J.A.H.C.P.G.W.S., *Application of stable isotope labeled glutathione and rapid scanning mass spectrometers in detecting and characterizing reactive metabolites.* Rapid Communications in Mass Spectrometry, 2005. **19**(23): p. 3482-3492.

7. Hsieh, Y., J. Chen, and W.A. Korfmacher, *Mapping pharmaceuticals in tissues using MALDI imaging mass spectrometry.* Journal of Pharmacological and Toxicological Methods, 2007. **55**(2): p. 193-200.

8. Min He, A.D., Gargi Choudhary, Karen Salomon, Diane Cho, *A High Throughput Approach for Metabolite Profiling and Characterization Using the LXQ Linear Ion Trap Mass Spectrometer.* Thermo Electron Corporation, Application Note: 369.

9. Kagan, M.R., *Analysis of a Verapamil Microsomal Incubation using Metabolite ID and Mass Frontier™.* Thermo Electronic Corporation, Application Note: 320, 2003.

10. Rao, R., *The use of AQAmax™ and Mass Frontier™ in the identification of pesticide isomers by ESI LC/MS.* Thermo Quest, LC/MS Application Report, AN514, 1999.

11. Brown GK, S.O., Jellum E., *Chromatographic profile of high boiling point organic acids in human urine.* Journal of chromatography, 1978. **145**(2): p. 177-84.

12. Zhang, Q., et al., *GC/MS analysis of the rat urine for metabonomic research.* Journal of Chromatography B, 2007. **854**(1-2): p. 20.

13. Li, Y., et al., *Identification of some benproperine metabolites in humans and investigation of their antitussive effect1.* Acta Pharmacologica Sinica, 2005. **26**(12): p. 1519-1526.

14. *8.4.4.2 Expert Tune Page, Tuning and Calibration.* HCT/esquire Series user manual, Esquire series User manual V2 Operations. Version 1.0, 2004: p. 8-10.

15. Ferraz, F.G.P. and M.E. Relvas, *Separation and Identification of Organic Acids in Biological Media by Column and Gas Phase Chromotography.* Clin Chim Acta, 1965. **11**(3): p. 244.

16. Bruckner, H. and A. Schieber, *Determination of amino acid enantiomers in human urine and blood serum by gas chromatography-mass spectrometry.* Biomed Chromatogr, 2001. **15**(3): p. 166-172.

17. Caldwell, J. and J.D. Sutton, *Influence of dose size on the disposition of trans-[methoxy-14C]anethole in human volunteers.* Food and Chemical Toxicology, 1988. **26**(2): p. 87.

18. Grupe, A. and G. Spiteller, *New polar acid metabolites in human urine.* Journal of Chromatography, 1981. **226**(2): p. 301-14.

Chapter 4

Theoretical Metabolite Database for Compound Identification

4.1. Introduction

Urine is a complex fluid containing a large number of endogenous and exogenous compounds, which may undergo biotransformations while in the body. Identifying all of the endogenous compounds in a sample such as urine or plasma is a daunting task that has been made more manageable with the instrumentation and analytical techniques that are currently available. Using an FT-ICR MS to generate accurate mass measurements can help to determine the chemical formula of unknown analytes. However, as the compound increases in size, the number of chemical formulas that match a single mass also increases. Even once the chemical formula is known; it is not always possible to work out the corresponding chemical structure using MS/MS data.

To simplify the data analysis for unknown compound identification from a complex sample, two key steps were taken. In the first step, a theoretical database of potential endogenous human metabolites was created. The metabolites in this database were selected or predicted based on known endogenous human metabolites and biotransformations. If the compounds are known to naturally occur in the human body, any metabolites predicted using known biotransformations also have a high probability of being present. This method of prediction can easily result in tens of thousands of metabolites from one substrate, which creates a huge database and a lot of data to sort through and analyze. To further simplify the identification procedure the urine sample can be cleaned up so that only one family of compounds is targeted. For example, the family of compounds targeted and described in this chapter is the acylcarnitines.

L-carnitine is a low molecular weight endogenous compound present in all mammalian species primarily located in skeletal and cardiac muscle (~98%).[1, 2] This compound originates through absorption from dietary sources, such as red meat, and endogenous biosynthesis from lysine. Most human tissue contains the enzymes necessary to convert lysine to trimethyllysine and subsequently butyrobetaine; however the enzymes required for the finial stage of L-carnitine biosynthesis are only present in the

liver, kidney and brain. The primary role of L-carnitine is to facilitate the transfer of fatty acids across the inner mitochondrial membrane for β-oxidation and consequently to produce energy.[1] Other roles of L-carnitine include controlling the coenzyme A (CoA)/acyl-CoA ratios by accepting short-chain acyl groups from the corresponding acyl-CoA and transporting them out of the mitochondria and ensuring the detoxification of poisonous organic acids by combining with potentially toxic acyl groups inside the mitochondrion so that they can be passed through the mitochondrial membrane, out of the cell, to be excreted by the urine.[1-3] Due to the critical role in fatty acid oxidation, endogenous concentrations of L-carnitine and its acyl derivatives are maintained within narrow limits and any changes in the urinary pattern of these acylcarnitines can indicate any number of diseases, such as those mentioned in section 2.1.

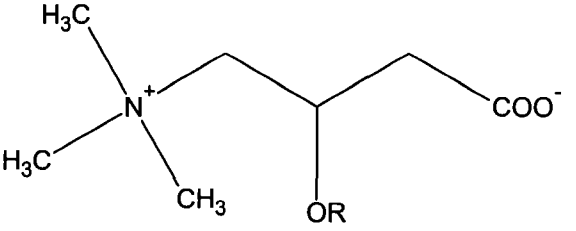

Figure 4.1 - The structure of acylcarnitine where R = H for L-carnitine and R = a fatty acid chain varying in length connected through an ester linkage for all other acylcarnitines

As indicated in Figure 4.1 all acylcarnitines are zwitterionic, making isolation and concentration fairly simple. A prime candidate for sample clean up is Solid Phase Extraction (SPE). SPE uses a solid phase and a liquid phase to isolate one type of analyte from a sample. It uses the same type of stationary phases that are used in liquid chromatography columns but in a relatively cheap, disposable, single-use cartridges. SPE is also an efficient method for isolating and concentrating solutes from relatively large volumes of sample and is generally used to clean up a sample before further analysis. Compounds separated using SPE can subsequently be separated using chromatographic techniques for a two-dimensional separation.

There are many different types of SPE cartridges available, including reversed phase, normal phase, ion exchange and adsorption. Acylcarnitines can be easily targeted using a mixed-mode stationary phase that employs both active cation exchange and

reversed phase sites. The sorbent interaction with a typical acylcarnitine is shown in Figure 4.2.

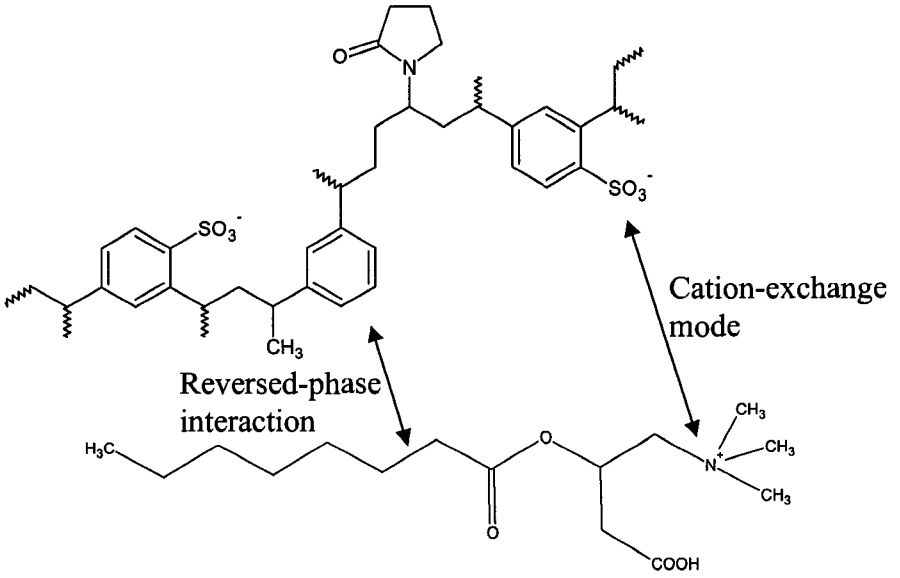

Figure 4.2 - Oasis® MCX SPE exchange sorbent (top) and interaction with a typical acylcarntine (bottom) [4]

In this chapter the use of a theoretical metabolite database for compound identification is explored to determine its potential advantages and disadvantages. Acylcarnitines, as model compounds, are targeted for analysis through SPE sample cleanup in urine, and they are identified using MS and MS/MS, combined with the theoretical metabolite database.

4.2. Experimental

4.2.1. Theoretical Database Creation

The theoretical database was created using Bruker's MetabolitePredict™ software as well as some home-built applications. The compound of interest can be loaded into MetabolitePredict™ and a list of potential metabolites is predicted as described in section 2.2.7, using the rule set "All Rules Mammals". Creating a mass list of metabolites for one compound using the MetabolitePredict™ software could easily take on the order of weeks, depending on the number of predicted metabolites. To speed up the database creation, a mass list was not created within the software. Instead, the MetabolitePredict™ files were opened as text files and the data mined from them using home-built applications which were created by Nelson Young in Dr. David Wishart's laboratory, and

uploaded to a web-based database. A screen shot of the web-based interface is shown in Figure 4.3. To search the database, a text file containing a list of molecular masses (not m/z) is uploaded to "Search For Masses" and the "Search Database" button is then selected. The text file should be a single column of masses. The search algorithm individually compares each entry in the text file to the entire database and reports on any mass matches. The search algorithm is programmed to set the mass tolerance based on the number of significant figures outputted from the mass spectrometer. If the experimental mass list contains more than three figures after the decimal point, then a mass match is determined within ±0.0015 Da. If there are three figures after the decimal point, then the mass match is within ±0.01 Da, and for two figures, then the mass the match is within ±0.1 Da.

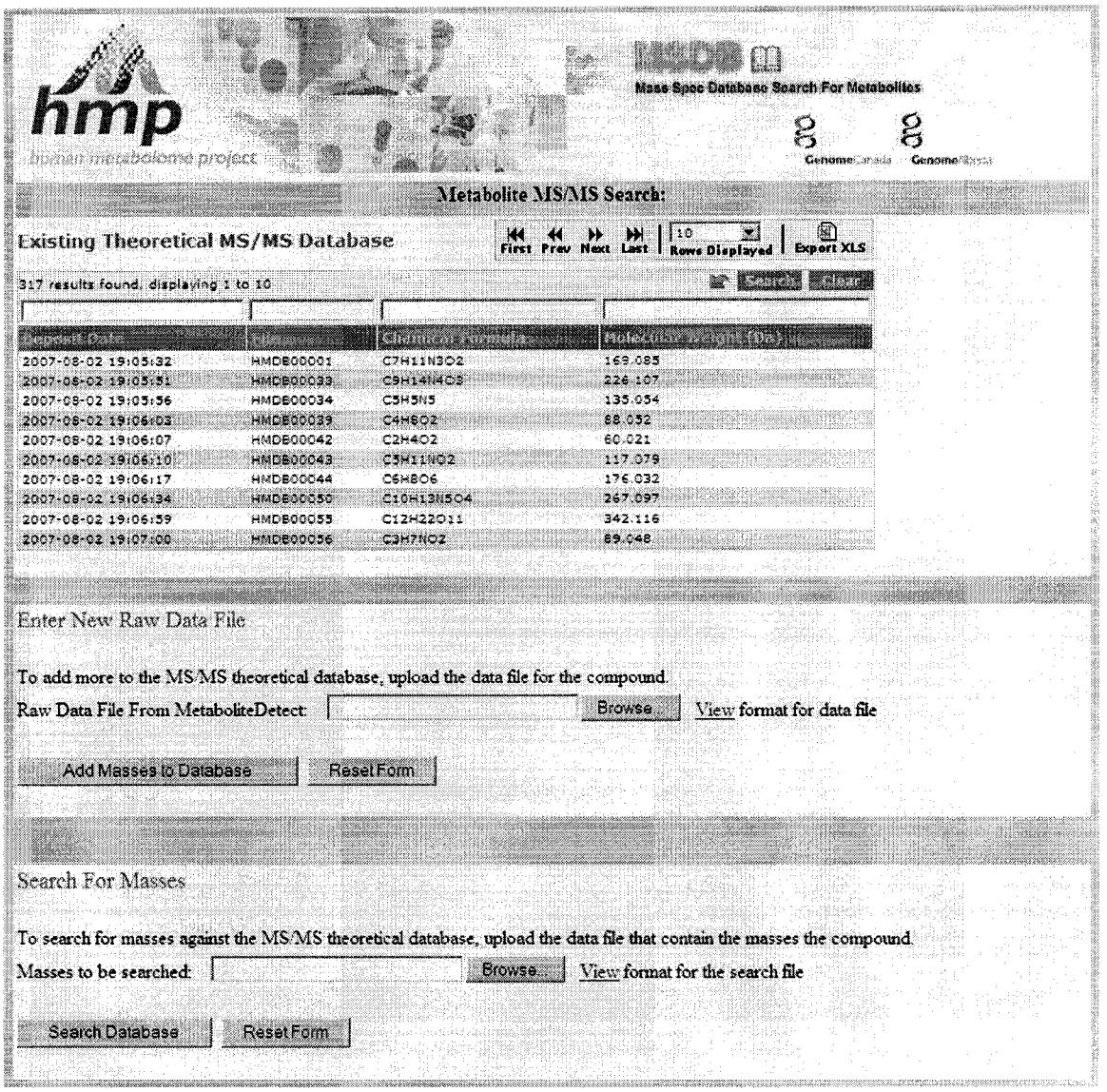

Figure 4.3 - Screen shot of web-based interface for accessing the Theoretical Metabolite Database

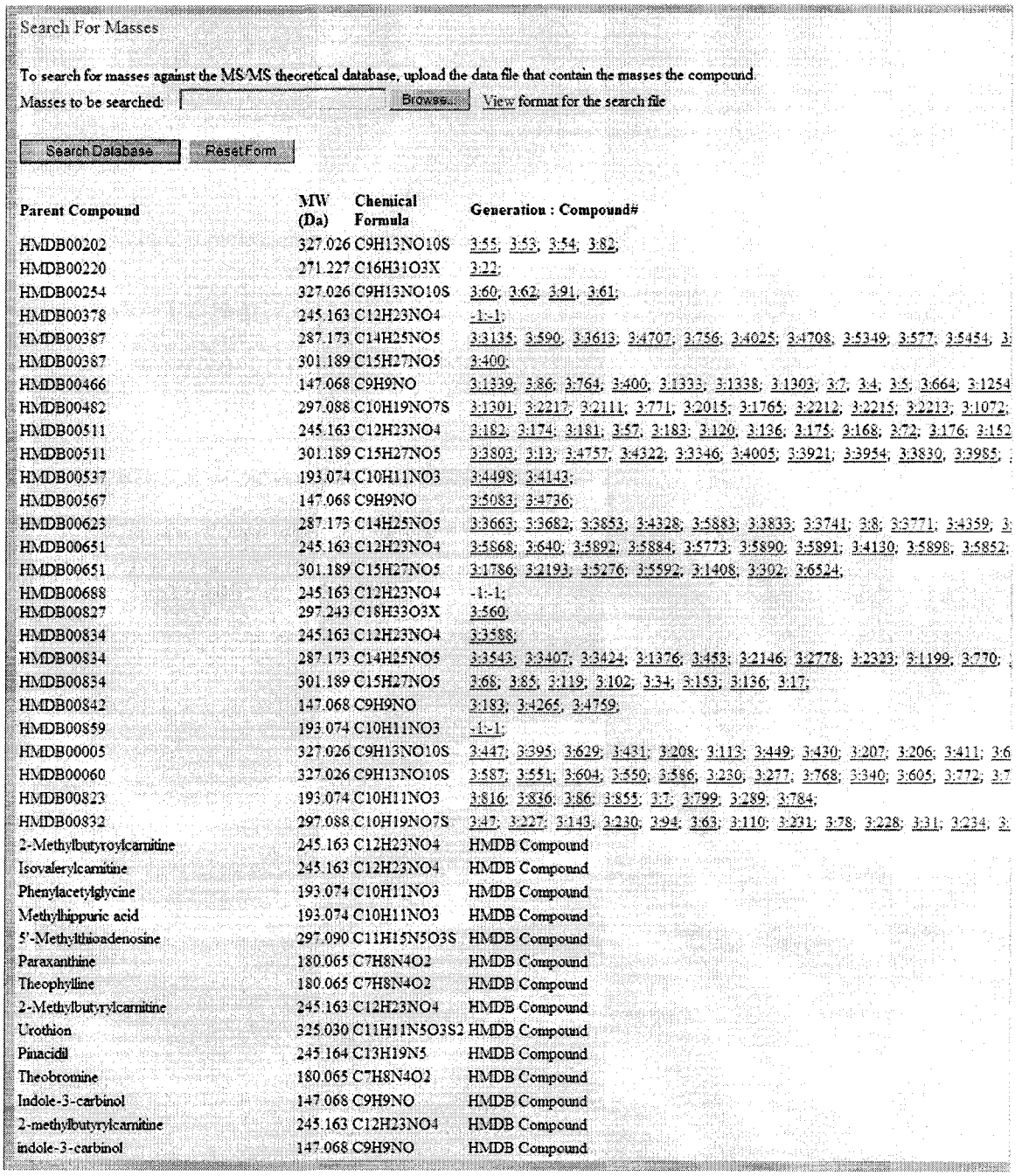

Search For Masses

To search for masses against the MS/MS theoretical database, upload the data file that contain the masses the compound.

Masses to be searched: Browse... View format for the search file

Search Database Reset Form

Parent Compound	MW (Da)	Chemical Formula	Generation : Compound#
HMDB00202	327.026	C9H13NO10S	3:55; 3:53; 3:54; 3:82;
HMDB00220	271.227	C16H31O3X	3:22;
HMDB00254	327.026	C9H13NO10S	3:60; 3:62; 3:91; 3:61;
HMDB00378	245.163	C12H23NO4	-1:-1;
HMDB00387	287.173	C14H25NO5	3:3135; 3:590; 3:3613; 3:4707; 3:756; 3:4025; 3:4708; 3:5349; 3:577; 3:5454; 3:
HMDB00387	301.189	C15H27NO5	3:400;
HMDB00466	147.068	C9H9NO	3:1339; 3:86; 3:764; 3:400; 3:1333; 3:1338; 3:1303; 3:7; 3:4; 3:5; 3:664; 3:1254
HMDB00482	297.088	C10H19NO7S	3:1301; 3:2217; 3:2111; 3:771; 3:2015; 3:1765; 3:2212; 3:2215; 3:2213; 3:1072;
HMDB00511	245.163	C12H23NO4	3:182; 3:174; 3:181; 3:57; 3:183; 3:120; 3:136; 3:175; 3:168; 3:72; 3:176; 3:152
HMDB00511	301.189	C15H27NO5	3:3803; 3:13; 3:4757; 3:4322; 3:3346; 3:4005; 3:3921; 3:3954; 3:3830; 3:3985; ;
HMDB00537	193.074	C10H11NO3	3:4498; 3:4143;
HMDB00567	147.068	C9H9NO	3:5083; 3:4736;
HMDB00623	287.173	C14H25NO5	3:3663; 3:3682; 3:3853; 3:4328; 3:5883; 3:3833; 3:3741; 3:8; 3:3771; 3:4359; 3:
HMDB00651	245.163	C12H23NO4	3:5868; 3:640; 3:5892; 3:5884; 3:5773; 3:5890; 3:5891; 3:4130; 3:5898; 3:5852;
HMDB00651	301.189	C15H27NO5	3:1786; 3:2193; 3:5276; 3:5592; 3:1408; 3:302; 3:6524;
HMDB00688	245.163	C12H23NO4	-1:-1;
HMDB00827	297.243	C18H33O3X	3:560;
HMDB00834	245.163	C12H23NO4	3:3588;
HMDB00834	287.173	C14H25NO5	3:3543; 3:3407; 3:3424; 3:1376; 3:453; 3:2146; 3:2778; 3:2323; 3:1199; 3:770; ;
HMDB00834	301.189	C15H27NO5	3:68; 3:85; 3:119; 3:102; 3:34; 3:153; 3:136; 3:17;
HMDB00842	147.068	C9H9NO	3:183; 3:4265; 3:4759;
HMDB00859	193.074	C10H11NO3	-1:-1;
HMDB00005	327.026	C9H13NO10S	3:447; 3:395; 3:629; 3:431; 3:208; 3:113; 3:449; 3:430; 3:207; 3:206; 3:411; 3:6
HMDB00060	327.026	C9H13NO10S	3:587; 3:551; 3:604; 3:550; 3:586; 3:230; 3:277; 3:768; 3:340; 3:605; 3:772; 3:7
HMDB00823	193.074	C10H11NO3	3:816; 3:836; 3:86; 3:855; 3:7; 3:799; 3:289; 3:784;
HMDB00832	297.088	C10H19NO7S	3:47; 3:227; 3:143; 3:230; 3:94; 3:63; 3:110; 3:231; 3:78; 3:228; 3:31; 3:234; 3:
2-Methylbutyroylcarnitine	245.163	C12H23NO4	HMDB Compound
Isovalerylcarnitine	245.163	C12H23NO4	HMDB Compound
Phenylacetylglycine	193.074	C10H11NO3	HMDB Compound
Methylhippuric acid	193.074	C10H11NO3	HMDB Compound
5'-Methylthioadenosine	297.090	C11H15N5O3S	HMDB Compound
Paraxanthine	180.065	C7H8N4O2	HMDB Compound
Theophylline	180.065	C7H8N4O2	HMDB Compound
2-Methylbutyrylcarnitine	245.163	C12H23NO4	HMDB Compound
Urothion	325.030	C11H11N5O3S2	HMDB Compound
Pinacidil	245.164	C13H19N5	HMDB Compound
Theobromine	180.065	C7H8N4O2	HMDB Compound
Indole-3-carbinol	147.068	C9H9NO	HMDB Compound
2-methylbutyrylcarnitine	245.163	C12H23NO4	HMDB Compound
indole-3-carbinol	147.068	C9H9NO	HMDB Compound

Figure 4.4 - Screen shot of results from a database search

The resulting mass matches are listed at the bottom of the web page, as shown in Figure 4.4. The mass matches with the Theoretical Metabolite Database are listed first, with the Human Metabolome Database (HMDB) number for the parent compound followed by the metabolite mass, chemical formula and a reference number from the MetabolitePredict™ file which uniquely identifies each metabolite and its structure. Each reference number can also be selected to open the corresponding .sdf file, which contains

all of the structural information required to recreate the molecule including all of the atoms and bonds, can be saved as a .mol file which in turn can be opened using software such as ChemSketch. ChemSketch is freeware provided from ACD Labs, which provides a workspace to view and draw chemical structures and reactions.

The Theoretical Database also searches the HMDB for mass matches to known human metabolites. These mass matches are listed at the bottom of the list with the name of the metabolite followed by its molecular masses and chemical formula.

4.2.2. Chemicals and Materials

Fisher brand nylon 0.2μm syringe filters along with Optima LC/MS grade water, methanol and acetonitrile were purchased from Fisher Scientific Canada (Edmonton, AB, Canada). Formic acid was purchased from Sigma Aldrich (Oakville, ON, Canada). Ammonium chloride was obtained from EMD Chemicals Inc. (Gibbstown, NJ, USA).

4.2.3. Instrument and Equipment

Accurate mass measurements were collected using an LC coupled to a FT-ICR mass spectrometer. The LC system used was a capillary Agilent 1100 equipped with an Agilent 20 μL/min H_2O flow splitter, binary pump, auto sampler and degasser. Two columns connected in sequence were used for sample separation. The first column was a 3 μm C8 (50 x 1.0 mm) followed by a 3 μm C18 (150 x 0.5 mm). The flow rate was set to 20 μL/min and separation was performed at ambient temperatures. The LC system was coupled to a 9.4 T FT-ICR MS (Bruker, Bremen, Germany) equipped with an electrospray interface. The MS system was controlled by a Windows XP professional workstation running Apex Control 2.0.0 Build 36 (6-507). The LC was controlled manually by an Agilent control module (product number G1323B).

The MS/MS analyses were collected using the same LC system and columns but coupled to an ion trap mass spectrometer in place of the FT-ICR MS. The LC system and columns were run under identical conditions and settings to those used for the FT-ICR MS analysis. The LC system was coupled to an Esquire 3000plus quadrupole ion trap (Bruker, Bremen, Germany) equipped with an electrospray interface. The MS system was controlled by a Windows 2000 workstation running EsquireControl. The LC was controlled manually by an Agilent control module.

All MS and MS/MS analysis were collected with the instruments set for positive ionization.

4.2.4. Chromatographic Conditions

The mobile phase system used for analysis was water with 4% acetonitrile and 0.1% formic acid in Solvent A and acetonitrile with 0.1% formic acid in Solvent B. The sample injection volume was 10 μL and the flow rate was held constant at 20 μL/min in micro mode. The gradient used was B held at 0% for 2 min, then increased to 40% in 80 minutes and 100% in 10 minutes. After B was held at 100% for 15 minutes, it was brought back down to 0% in 0.1 minutes followed by a 14.9 minute re-equilibration. The total time for one injection was 120 minutes.

4.2.5. Sample Collection and Preparation

A urine sample was collected from a healthy individual and filtered through a Fisher brand Nylon 0.2 μm syringe filter. The sample was then stored at -20 °C until analysis. Informed consent was obtained from the volunteer and ethics approval for this work was obtained from the University of Alberta in compliance with the Health Information Act (in accordance to Section 54(1)).

The urine sample was processed with SPE to concentrate the acylcarnitines. Five 1 mL mixed-mode, cation exchange/reversed-phase cartridges were setup with a vacuum manifold using a vacuum of 4 inches of Hg. Each cartridge was conditioned and equilibrated with 2 mL methanol followed by 2 mL water. One mL of urine was loaded on each cartridge, followed by a wash with water then 20% methanol in water. One mL each of three different solvents was used to elute the samples off the cartridge. The first was 0.1 M NH_4Cl in 40 % methanol, followed by 0.1 M NH_4Cl in 80 % methanol and finally 0.1 M NH_4Cl in 97.5 % methanol. The NH_4Cl is not water soluble, therefore it had to be initially dissolved in water before diluting it with methanol for a final solution containing 97.5% methanol.

The eluants were dried down, combined and reconstituted in 2.5 mL of mobile phase A. All of the loads, washes and eluants were stored at -20 °C pending analysis.

4.2.6. Mass Spectrometry Conditions

4.2.6.1. FT-ICR MS

Three different MS spectra were collected using the FT-ICR MS. Each used a different method which was tuned and calibrated for a different mass range: 50 to 100 Da, 90 to 375 Da and 350 to 650 Da. Collecting three different spectra using three smaller mass ranges instead of collecting one spectra incorporating the entire range, 50 to 650 Da, was used to increase the sensitivity and mass accuracy of the instrument. The scan speed for the FT-ICR MS is approximately 1 spectra/s.

4.2.6.2. FT-ICR MS/MS

The FT-MS tune methods were used as a starting point for the MS/MS tune methods. Each tune method was optimized for isolation with a few minor adjustments to the systems optics. The Auto MS/MS was turned on, utilizing the collision cell, with the "MS/MS Isolation", "Collisional Activation" and the "Fixed Collision Voltage" activated. The collision voltage was set to -6.6 V. The include list was active for mass range 100 to 350 Da. Only one precursor ion was selected per MS scan and that ion intensity must be above a minimum threshold of 1000. The "Active Exclusion" was enabled to exclude an ion after the acquisition of one MS/MS spectrum for the next 1.25 min. Lastly, to help improve the MS/MS signal, "MS/MS Boost" was activated so that the ion accumulation time was increased to 1.0 sec for all MS/MS spectra.

4.2.6.3. Ion trap MS/MS

All experiments conducted on the ion trap used electrospray ionization with the nebulizer gas set to 11 psi, the dry gas set to 5 L/min and the dry gas temperature set to 300 °C. The Smart Parameter Settings were set to accommodate the entire range of masses being scanned with the target mass set to 322 Da. The compound stability was set to 100 % and the Trap Drive Level was set according to the manual specifications (see Table 3.1) at 70 %. The optimization was set to normal. The LC run was split into several different time segments, with each segment targeting a specific ion for MS/MS fragmentation. The ion selected was set in the MS/MS tab with a 3 Da isolation window and fragmentation energy of 1.1 V. The scan speed for the ion trap is 13000 m/z/s, hence for a mass range from 50 to 500 m/z it can collect 28 spectra/s.

4.2.7. Data Analysis and Interpretation

4.2.7.1. MS Analysis and Interpretation

The LC-MS data files were analyzed using Bruker's DataAnalysis™, the unprocessed BPC are illustrated in the Appendix Figures 6.25 and 6.26. The chromatographic peaks from the base peak chromatogram were integrated manually for each MS run on the FT-ICR MS. Mass list parameters were assessed and set according to each LC-MS analysis. The high mass range, 350 to 650 Da, had a mass list consisting of peaks with a signal to noise threshold of 10, relative intensity threshold (basepeak) of 0.0001, absolute intensity threshold of 300 000 and a mass range of 350 to 650 Da. The mid mass range, 90 to 375, had a mass list with a signal to noise threshold of 10, relative intensity threshold (basepeak) of 0.0001 and absolute intensity threshold of 90 000 and persistent peaks were excluded. The low mass range, 50 to 100, was identical to a blank run with no noteworthy chromatographic peaks so the sample and data were not analyzed further. Each mass list was further analyzed to remove any irrelevant peaks including isotope peaks and side peaks due to FT signal being cut off after a defined time.

The mass list from each integrated chromatographic peak was copied into an Excel worksheet. The proton was subtracted from the ion's mass and the mass list uploaded to the theoretical database, where these masses were compared to those in the database. This resulted in a list of matching compounds from the theoretical database with a mass that corresponded to the experimental mass list. The list was manually filtered to include only acylcarnitine metabolites with a permanent positive charge then was copied to an Excel worksheet. If the mass found experimentally matched the theoretical mass with <2 ppm error then the compound was targeted for MS/MS analysis.

4.2.7.2. MS/MS Analysis and Interpretation

Acylcarnitine metabolites were identified based on the typical acylcarnitine neutral losses of 59 Da, due to the loss of $(CH_3)_3N$, and 161, due to the loss of $C_7H_{15}NO_3$. The MS/MS fragmentation patterns were also compared to the predicted structures. The fragment ion of 85 Da, corresponding to $C_5H_4O_2$, is also an indication of an acylcarnitine compound but may not always be present due to automatic cut offs set by the ion trap during MS/MS sample analysis.

4.3. Results and Discussion

4.3.1. Potential Mass matches from MS Analysis

Urine is a complex biofluid that contains a multitude of different metabolites, both endogenous and exogenous. Using SPE to target specific types of metabolites simplifies the task of data collection and analysis. The mixed-mode MCX cartridges worked well for targeting the acylcarnitines. The permanent positive charge, found on the nitrogen atom, is attracted to the cation exchange portion of the cartridge and their varying length hydrophobic tails are attracted to the reversed phase portion of the cartridge. However, the FT-ICR MS analysis still resulted in an overwhelming amount of data in spite of the SPE clean up.

Tuning the FT-ICR MS for small molecules with masses 50-650 Da, is challenging and has several limitations. The low mass cut off is directly related to the mass resolution of the instrument, with the mass resolution decreasing as the low mass cut off decreases. Tuning the instrument for the entire range, 50-650 Da, while retaining the sensitivity required for analyte detection, is not possible with the current instrument setup. When the instrument is optimized for the mid to high end of the mass range, the sensitivity for anything less than 100 Da suffers. Similarly, if the instrument is optimized for anything below 100 Da, the sensitivity for anything above 100 Da decreases. To overcome these limitations, three different tune methods and calibration mixtures were created to cover the entire range of interest in three discreet parts: 50 to 100 Da, 100 to 375 Da and 350 to 650 Da. The calibration mixtures have several overlapping compounds to ensure a good calibration across the entire mass range.

Having three different tune files requires that three different LC-MS runs must be collected for each sample. For the extracted urine sample, only two of the chromatographic runs contain any significant data. The LC-MS run covering 50 to 100 Da showed no chromatographic peaks of interest. The high mass range, 350 to 650, has 84 chromatographic peaks, each with a mass list containing between 10 and 170 entries. The mid mass range, 90 to 375, has 60 chromatographic peaks, each with a mass list containing between 8 and 42 entries. Each chromatographic peak results in a different mass list for a total of 144 different mass lists. Each mass list was individually compared to the theoretical metabolite database.

Using chromatographic peak 11 (26.9-27.2 min) from the mid mass range LC-MS run as an example, the mass list contains 21 different entries (147.0680, 162.0122, 180.0649, 193.0741, 226.1682, 245.1629, 250.1320, 271.2263, 287.1736, 295.1420, 296.1456, 297.0895, 297.2416, 301.1891, 311.2574, 325.0304, 326.0379, 327.0257, 327.0473, 339.2269 and 347.0126 Da). Comparison of this mass list to the theoretical database results in 35 different mass matches as shown in Table 4.1.

Table 4.1 - Results from mass comparison with the theoretical database. Information from the Metabolite Generation : Metabolite Number column was deleted and is indicated with a "..." at the end of the list in any affected cells

Parent Compound	Metabolite Mass	Metabolite Chemical Formula	Metabolite Generation : Metabolite Number
HMDB00005	327.026	C9H13NO10S	3:447; 3:395; 3:629...
HMDB00060	327.026	C9H13NO10S	3:587; 3:551; 3:604 ...
HMDB00202	327.026	C9H13NO10S	3:55; 3:53; 3:54; 3:82;
HMDB00220	271.227	C16H31O3X	3:22;
HMDB00222	271.227	C16H31O3X	3:20410;
HMDB00254	327.026	C9H13NO10S	3:60; 3:62; 3:91; 3:61;
HMDB00378	245.163	C12H23NO4	-1:-1;
HMDB00387	287.173	C14H25NO5	3:3135; 3:590; 3:3613...
HMDB00387	301.189	C15H27NO5	3:400;
HMDB00466	147.068	C9H9NO	3:1339; 3:86; 3:764 ...
HMDB00482	297.088	C10H19NO7S	3:1301; 3:2217; 3:2111 ...
HMDB00511	245.163	C12H23NO4	3:182; 3:174; 3:181 ...
HMDB00511	301.189	C15H27NO5	3:3803; 3:13; 3:4757 ...
HMDB00537	193.074	C10H11NO3	3:4498; 3:4143;
HMDB00567	147.068	C9H9NO	3:5083; 3:4736;
HMDB00623	287.173	C14H25NO5	3:3663; 3:3682; 3:3853 ...
HMDB00651	245.163	C12H23NO4	3:5868; 3:640; 3:5892 ...
HMDB00651	301.189	C15H27NO5	3:1786; 3:2193; 3:5276 ...
HMDB00688	245.163	C12H23NO4	-1:-1;
HMDB00705	245.163	C12H23NO4	3:10; 3:132;
HMDB00711	297.088	C10H19NO7S	3:245; 3:152; 3:153;
HMDB00738	193.074	C10H11NO3	3:1289; 3:957; 3:1088 ...
HMDB00756	245.163	C12H23NO4	3:10; 3:132;
HMDB00791	245.163	C12H23NO4	3:3588;
HMDB00791	287.173	C14H25NO5	3:1540; 3:2349; 3:909 ...
HMDB00791	301.189	C15H27NO5	3:102; 3:136; 3:68 ...
HMDB00823	193.074	C10H11NO3	3:816; 3:836; 3:86 ...
HMDB00827	297.243	C18H33O3X	3:560;
HMDB00832	297.088	C10H19NO7S	3:47; 3:227; 3:143 ...
HMDB00834	245.163	C12H23NO4	3:3588;
HMDB00834	287.173	C14H25NO5	3:3543; 3:3407; 3:3424 ...
HMDB00834	301.189	C15H27NO5	3:68; 3:85; 3:119 ...
HMDB00842	147.068	C9H9NO	3:183; 3:4265; 3:4759;
HMDB00859	193.074	C10H11NO3	-1:-1;

Since the acylcarnitines and their metabolites were being targeted, the metabolites of any other endogenous compound could be removed from Table 4.1. To further simplify the MS/MS data analysis, it could be takeen into account that the SPE MCX cartridge has cation exchange properties which would only retain acylcarnitine

metabolites that still had the permanent charge on the nitrogen atom. Any predicted compound that does not have this trait could also be removed from Table 4.1. Applying these restrictions resulted in a much shorter and more manageable list of potential metabolites for MS/MS analysis (Table 4.2)

Table 4.2 - Resulting acylcarnitines metabolites from a mass list comparison with the theoretical database

Parent Compound	Metabolite Mass	Metabolite Chemical Formula	Metabolite Generation : Metabolite Number
HMDB00378	245.16286	C12H23NO4	-1:-1;
HMDB00688	245.16286	C12H23NO4	-1:-1;
HMDB00705	245.16286	C12H23NO4	3:10; 3:132;
HMDB00791	245.16286	C12H23NO4	3:3588;
HMDB00791	287.17356	C14H25NO5	3:1540; 3:2349; 3:909; ...
HMDB00651	301.18905	C15H27NO5	3:1786; 3:2193; 3:5276; ...
HMDB00791	301.18905	C15H27NO5	3:102; 3:136; 3:68; 3:119; ...

Once all of the mass lists were compared to the theoretical database with the same restrictions discussed above, a total of 477 different mass matches were found. It should be noted that one mass could result in several matches to the theoretical database but would have been the result of different parent compounds or could be a structural isomer from the same substrate. In addition, the chromatographic peak width for one ion may span more than one of the manually integrated peaks in the chromatogram. The mass allowance for a found match in the theoretical database is 0.0015 Da, which translates to a range in error from 30 to 2.3 ppm for a mass range of 50 – 650 Da because [Error (ppm) = (Measured mass – Reference Mass / Reference Mass) x 10^6]. To utilize the high mass measurement accuracy of the FT-ICR MS a mass error of 2 ppm was used as a cut-off for assigning chemical formula and target the ion for MS/MS analysis. This still resulted in 213 potential matches to the theoretical database requiring further experimental analysis.

Table 4.3 - Summary of results from LC-MS data analysis

	LC-MS runs		
	90 to 375	**350 to 650**	**Total**
Chromatographic peaks	60	84	144
# of Masses in each chromatographic peak	8-42	10-170	----
Total number of matches with the Theoretical Database	254	223	477
Matches with Theoretical Database below 2 ppm	75	138	213

4.3.2. Acylcarnitine Metabolites Identified Through Targeted MS/MS Analysis

Due to software limitations on the FT-ICR MS, all MS/MS analyses were performed on an Ion Trap MS. The software that controls the Ion Trap allows for a single ion to be targeted within a specified time segment during an LC run. Specific ions from the FT-ICR MS analysis were targeted for MS/MS analysis on the Ion Trap based on their retention times for a total of 11 different LC-MS/MS runs in an attempt to collect MS/MS spectra on all 213 potential metabolites identified using accurate mass measurements.

The fragmentation pattern for an acylcarnitine metabolite with no changes to the carnitine portion of the molecule has two characteristic neutral losses. The first neutral loss of 59 Da is due to the loss of the neutral molecule $N(CH_3)_3$ and the second neutral loss of 161 Da is due to the fragmentation at the ester linkage between the carnitine portion of the molecule and the hydrophobic tail. For most acylcarnitines, these two neutral losses are enough for initial identification of the compound as an acylcarnitine.

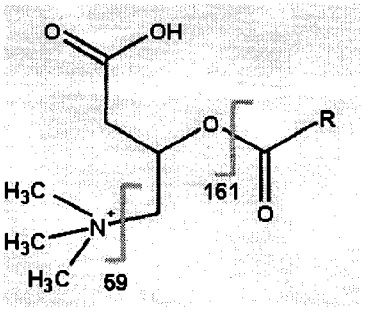

Figure 4.5 - The characteristic carnitine portion of an acylcarnitine molecule and its typical neutral loss fragmentation for acylcarnitines, loss of 59 and 161 Da.

For all other acylcarnitine compounds that do not show the characteristic neutral losses, the proposed structures from the Theoretical Metabolite Database were needed to compare the structures directly to the corresponding MS/MS spectrum for positive identification.

Figure 4.6 is of an EIC of m/z 304.2117 from an FT-MS run that corresponds to an exact mass match between the theoretical metabolite database and a metabolite of octanoylcarnitine (chemical formula $C_{15}H_{30}NO_5$). These ion peaks were targeted for MS/MS analysis using the Ion Trap MS and spectra for several peaks were collected as indicated in Figure 4.6. The proposed metabolite structure from the theoretical metabolite database shows octanoylcarnitine (C8) modified with the addition of a hydroxyl group (C8OH).

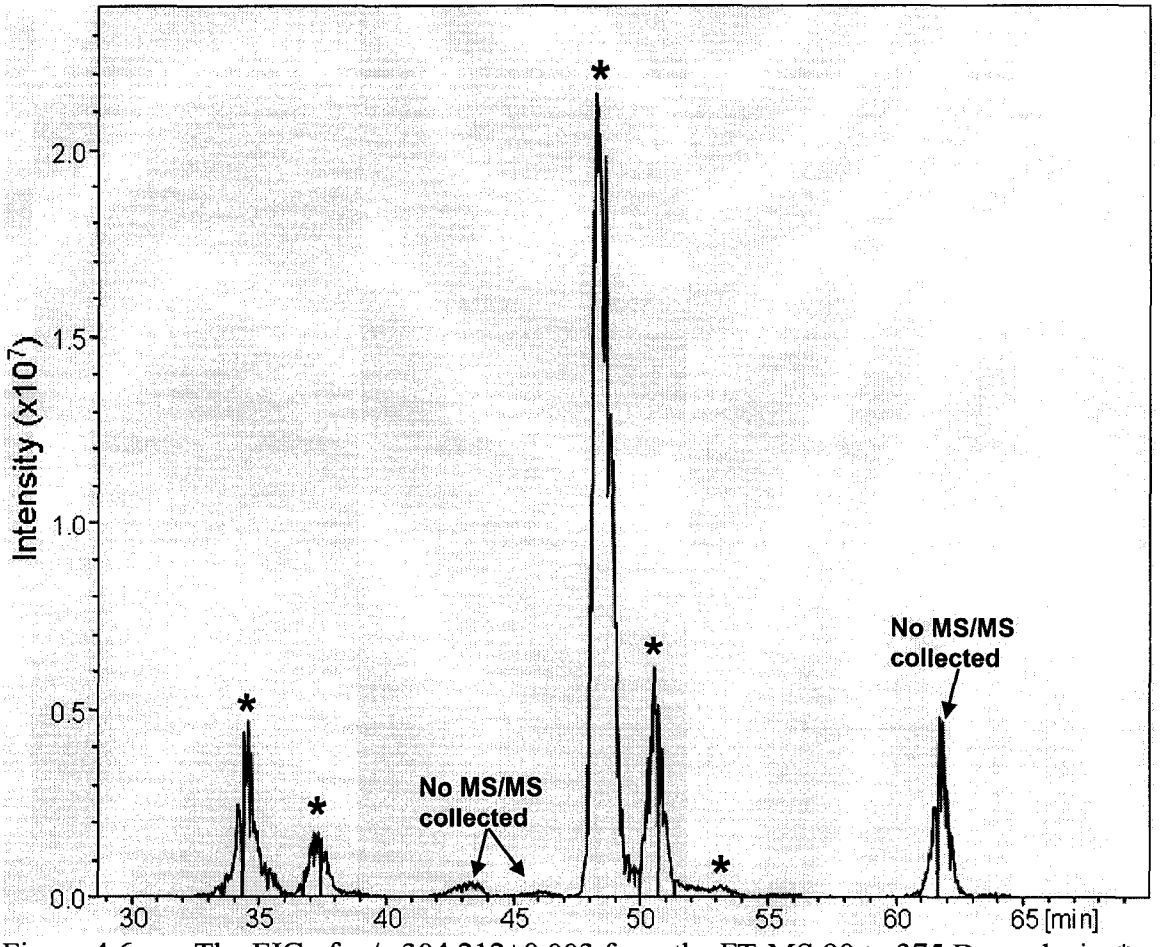

Figure 4.6 - The EIC of m/z 304.212±0.003 from the FT-MS 90 to 375 Da analysis, * indicate peaks for which MS/MS chromatograms were collected

The EIC for m/z 304.212 shows eight distinct chromatographic peaks that must be verified using MS/MS. Assuming that the OH modification is located along the hydrophobic tail of the octanoylcarnitine metabolite, there are several characteristic fragmentations that would confirm the compound's identity, but not the exact position of the hydroxyl group. Acylcarnitines have a characteristic product ion of 85 Da corresponding to $C_4H_6O_2$, as well as two characteristic neutral losses of 59 Da and 161 Da, due to the loss of $N(CH_3)_3$, and $C_7H_{15}NO_3$, respectively, (Figure 4.7) resulting in fragment ions of 304, 245 and 143 Da. The hydroxyl group added during the biotransformation of octanoylcarnitine would also be easily lost during fragmentation and would result in fragment ions of 286, 227 and 125 Da respectively.

Five of the eight chromatographic peaks, as indicated in Figure 4.6 with *, can be confirmed based on the MS/MS fragmentation shown in Figures 4.8-4.12. Acylcarnitines

have several characteristic fragmentations which can be identified in the following spectra, Figures 4.8-4.12. The first fragment is due to a common neutral loss of 59 Da, corresponding to the loss of the trimethylamine, $N(CH_3)_3$. The second characteristic acylcarnitine fragmentation is the fragment ion at 85 Da corresponding to $C_4H_5O_2$ due to the loss of the trimethylamine and hydrophobic tail. The finial characteristic fragmentation is due to a common neutral loss of 161 Da, due to breakage at the ester linkage separating the hydrophobic tail from the rest of the molecule. Finally the addition of an hydroxyl group can easily be detected by the loss of 18 Da, water, in the MS/MS spectrum. The MS/MS spectra for the other three peaks either were not collected or those portions of the chromatogram showed no corresponding chromatographic peak to an MS/MS spectrum with characteristic fragments from an acylcarnitine compound.

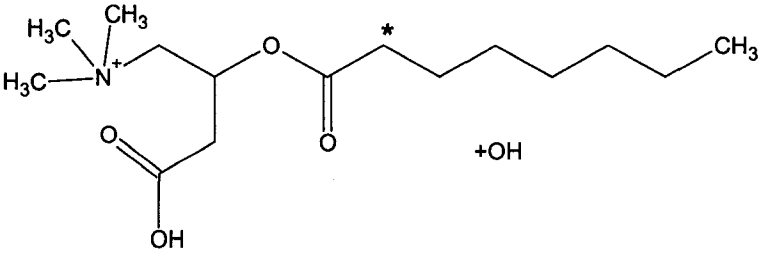

Figure 4.7 - Predicted structure from the theoretical database for m/z 304.2117, the OH could replace a H on any of the C atoms

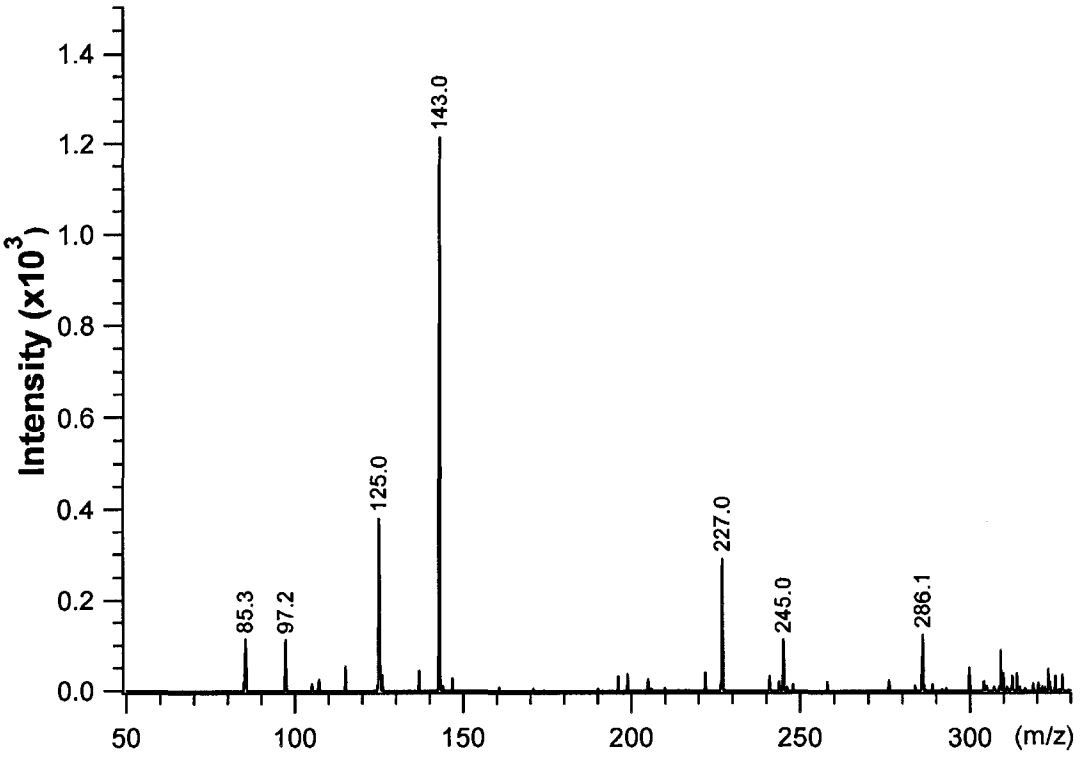

Figure 4.8 - MS/MS analysis of m/z 304 from an Ion Trap MS, RT 34.6 min

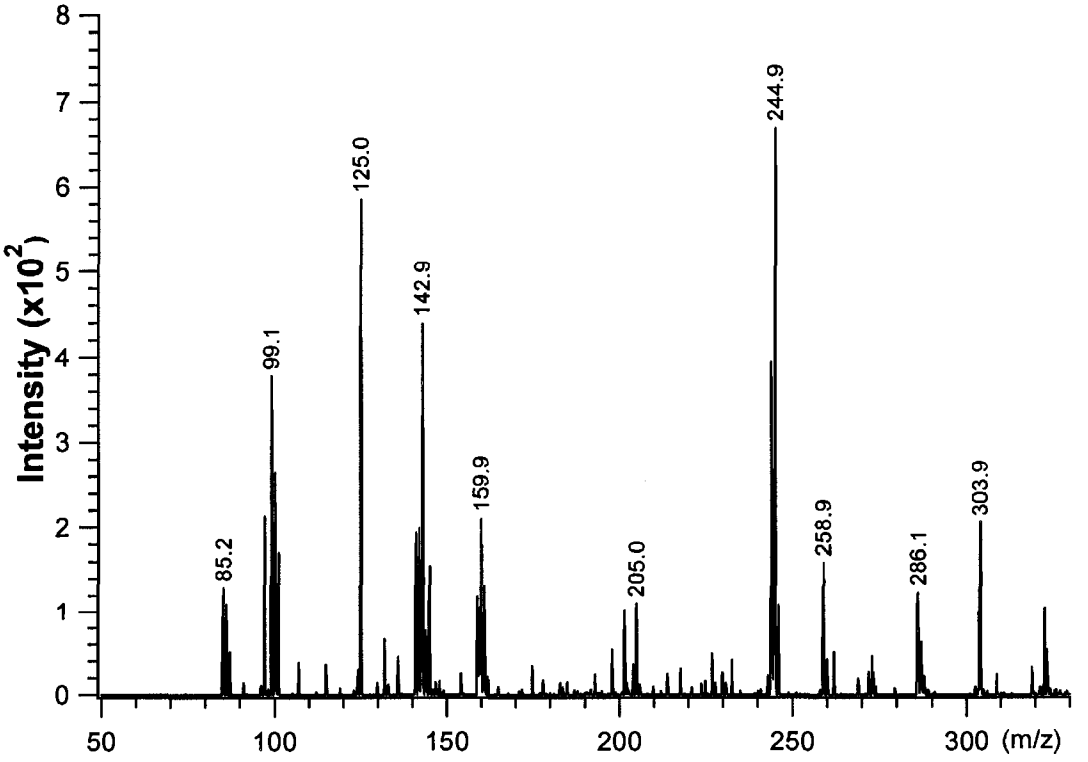

Figure 4.9 - MS/MS analysis of m/z 304 from an Ion Trap MS, RT 39.0 min

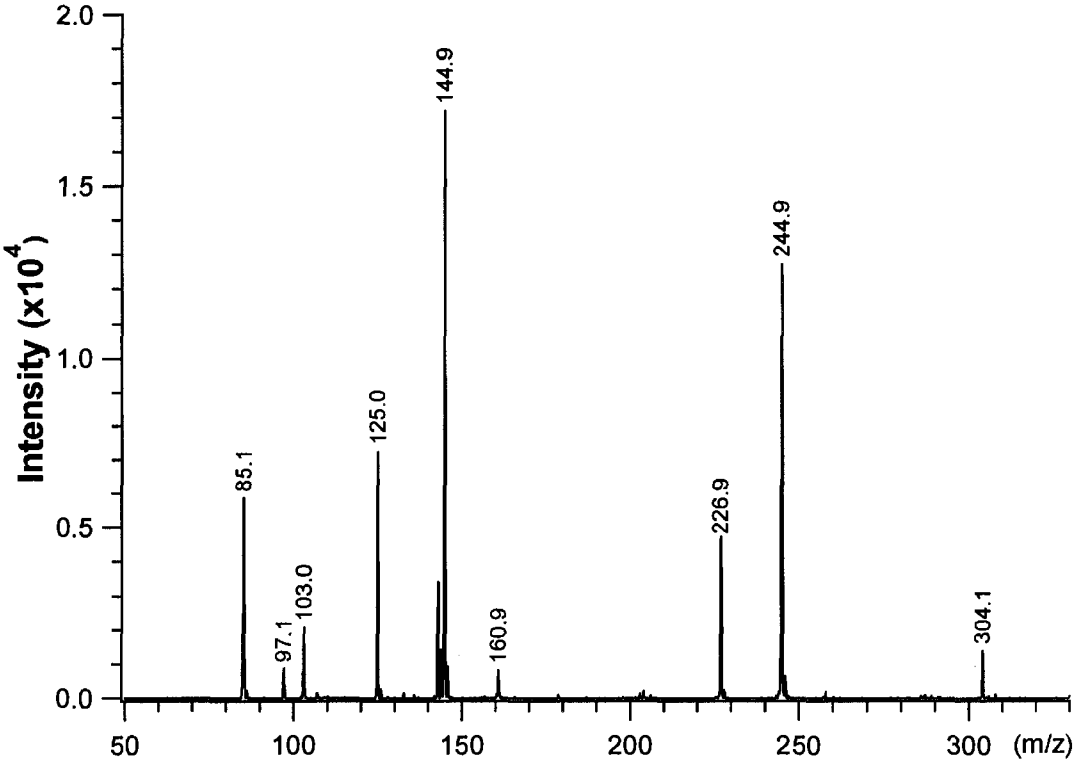

Figure 4.10 - MS/MS analysis of m/z 304 from an Ion Trap MS, RT 47.7 min

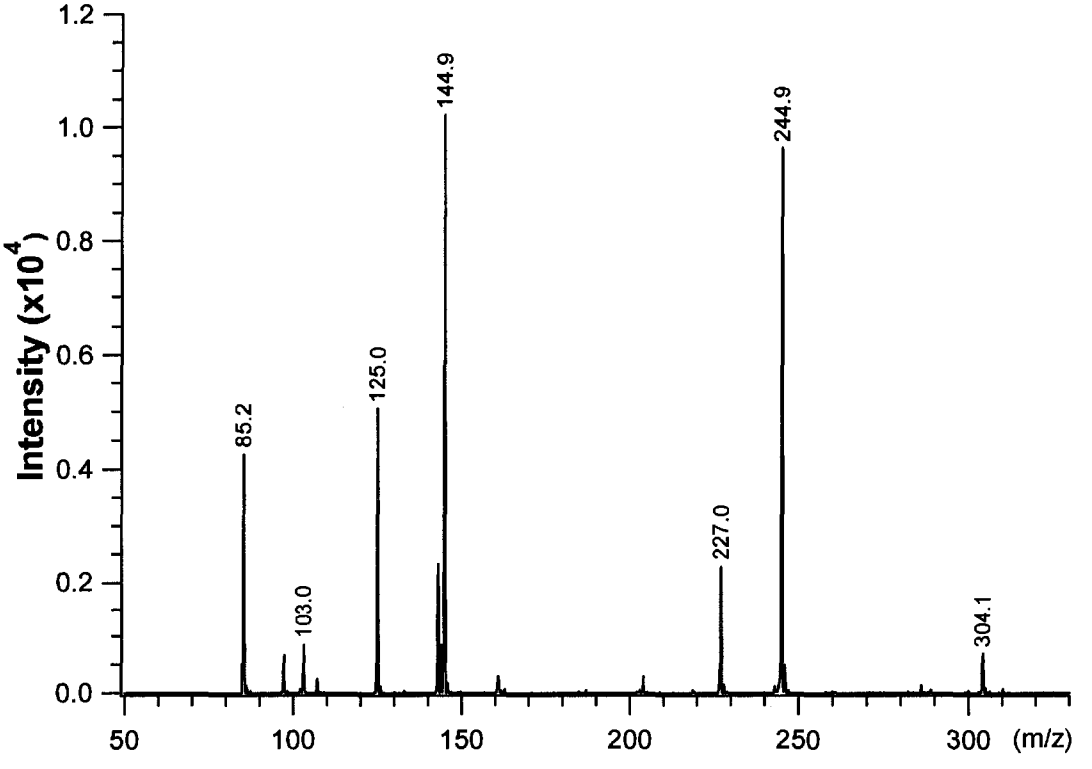

Figure 4.11 - MS/MS analysis of m/z 304 from an Ion Trap MS, RT 48.3 min

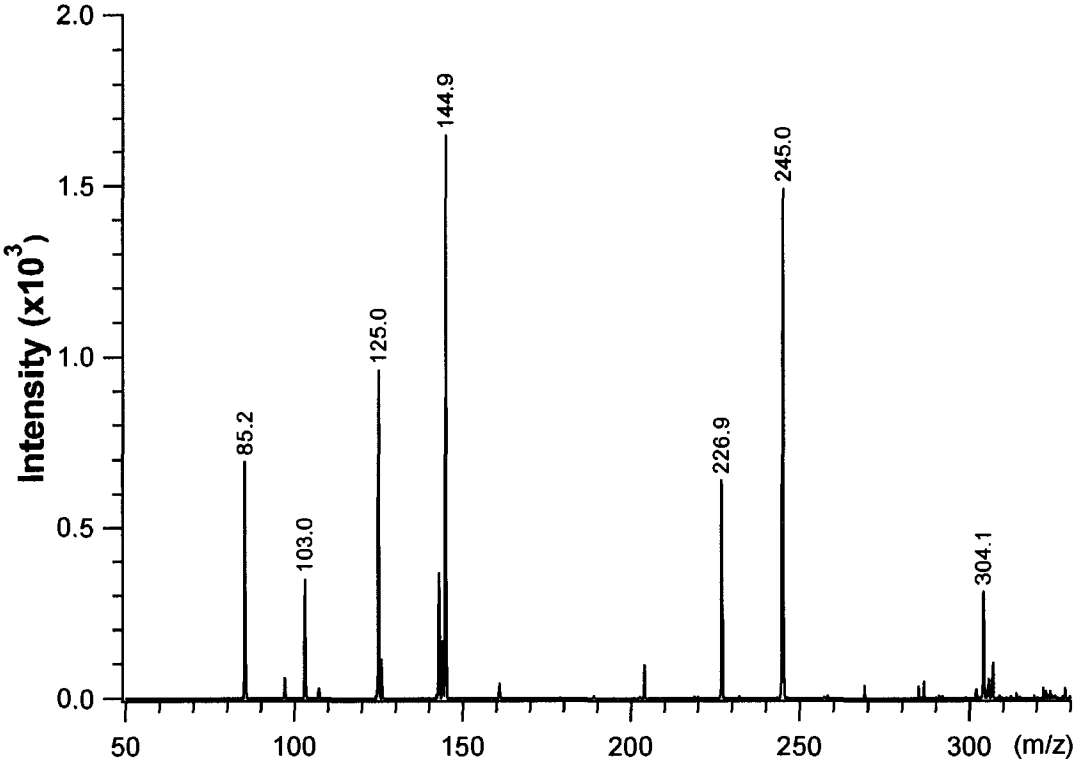

Figure 4.12 - MS/MS analysis of m/z 304 from an Ion Trap MS, RT 50.2 min

Similar analyses were done for the other potential acylcarnitine metabolites identified through accurate mass measurements and the theoretical metabolite database. The confirmed metabolites are listed in Table 4.4 with the parent compound it was derived from, the metabolite's molecular weight, chemical formula, metabolic changes, the number of isomers identified and any relative references containing information on one or more of the isomers.

Table 4.4 - All the metabolites identified based on accurate mass measurements, the theoretical metabolite database and MS/MS analysis.

Parent Compound	Metabolites				
	Formula Weight	Chemical Formula	Changes	# Isomers MS/MS	References
Carnitine	371	$C_{12}H_{24}N_2O_9S$	See appendix	3	none
C7	273	$C_{14}H_{27}NO_4$	None	1	[5, 6]
C8	301	$C_{15}H_{28}NO_5$	=O	3	none
C8	303	$C_{15}H_{30}NO_5$	OH	5	[1]
C8	317	$C_{15}H_{27}NO_6$	OH, =O	1	[7]
C9	301	$C_{16}H_{31}NO_4$	None	1	[3]
C9	315	$C_{16}H_{30}NO_5$	=O	7	none
C9	317	$C_{16}H_{32}NO_5$	OH	3	none
C10	315	$C_{17}H_{33}NO_4$	None	2*	[1, 5]
C10	331	$C_{17}H_{34}NO_5$	OH	1	[8]
C10	329	$C_{17}H_{32}NO_5$	=O	6	none
C10	347	$C_{17}H_{33}NO_6$	OH, OH	1	none
C10	345	$C_{17}H_{32}NO_6$	=O, OH	3	[7]
C10	343	$C_{17}H_{30}NO_6$	=O, =O	1	none
C11	343	$C_{18}H_{33}NO_5$	=O	1	none
C12	359	$C_{19}H_{38}NO_5$	OH	1	[1]
C12	357	$C_{19}H_{35}NO_5$	=O	7	none
C12	373	$C_{19}H_{36}NO_6$	=O, OH	6	[7]
C12	533	$C_{25}H_{44}NO_{11}$	See appendix	1	none
C14 or C16**	399	$C_{21}H_{37}NO_6$	=O, OH, =	2	none
C16	401	$C_{21}H_{37}NO_6$	=O, OH	3	[9]
C16	594	$C_{27}H_{53}N_3O_9S$	See appendix	1	none

* These could be structural isomers of each other

** C16 - $2CH_3$ from the N and 2H atoms put in their place

4.3.3. Acylcarnitine Metabolites Identified Through Auto MS/MS Analysis

To utilize the accurate mass measurement capability of the FT-ICR MS, the SPE sample was run on the FT-ICR MS using the auto MS/MS option. The spectra were then analyzed to identify any acylcarnitines using characteristic product ions, 85 Da, and neutral losses, -59 and -161 Da. Only two LC MS/MS chromatograms were collected because the LC-MS for the low mass range, 50 to 100 Da, showed no peaks of interest. The high mass range, 350 to 650, did not have any MS/MS spectra that contained at least two of the three characteristic fragments/neutral losses, thus the compounds identity could not be confirmed using this method. The LC MS/MS run collected for the mid mass range, 100 to 350 Da, resulted in 66 different MS/MS spectra for 16 different mass

ions with at least 1.25 min between adjacent MS/MS spectra of the same m/z to minimize the number of spectra recorded for the same ion. Comparison of the accurate mass measurements with the theoretical metabolite database resulted in four matches to the database. Of the remaining 12 acylcarnitines' masses identified using this method, there were no mass matches to the theoretical metabolite database because the metabolites were not predicted based on the defined biotransformations, the mass difference fell outside the allowed mass match range of ±0.0015 Da for any mass containing four or more figures after the decimal point, or the substrate compound was not in the HMDB so the compound and its list of metabolites were not included in the theoretical database. Table 4.5 lists the acylcarnitines identified using auto MS/MS.

Table 4.5 - Acylcarnitines identified through Auto MS/MS analysis using the FT-ICR MS

Found m/z	# of MS/MS spectra collected	Error (ppm)	Predicted carnitine*	Theoretical database match	Chemical formula	Comments
246.1702	1	3.2	C5	Yes	C12H23NO4	Not previously targeted because >2 ppm error
288.2159	5	4.5	C8	Yes	C15H29NO4	Not previously targeted because >2 ppm error
302.2313	2	0.4	C9	Yes	C16H31NO4	Previously targeted for MS/MS on the ion trap
316.2120	2	0.4	C9, =O	Yes	C16H29NO5	Previously targeted for MS/MS on the ion trap
274.2013	1	4.4	C7	No	C14H28NO4	Heptanoylcarntine not in the HMDB
272.1856	1	4.4	C7:1	No	C14H26NO4	Heptanoylcarntine not in the HMDB
284.1857	1	3.5	C8:2	No	C15H26NO4	Double bonds not predicted based on structure
286.2011	16	3.1	C8:1	No	C15H28NO4	Double bonds not predicted based on structure
300.2177	9	3.9	C9:1	No	C16H30NO4	Nonanoylcarnitine not in the HMDB
310.1999	11	6.8	C10:3	No	C17H28NO4	Double bonds not predicted based on structure
312.2655	3	9	C10:2	No	C17H30NO4	Double bonds not predicted based on structure
314.2292	6	7.5	C10:1	No	C17H32NO4	Double bonds not predicted based on structure
330.2245	3	6.7	C10, =O	No	C17H32NO5	Outside mass range
336.2140	1	6.5	C12:4	No	C19H30NO4	Double bonds not predicted based on structure
326.1446	1	7.4	C10:3, O	No	C17H28NO5	Double bonds not predicted based on structure
328.2119	3	7.7	C11:1	No	C18H34NO4	Not in the HMDB

* The acylcarnitine structure is predicted by the MetabolitePredict™ software or manually based on known biotransformations

The first two ions listed in Table 4.5, 246.1702 and 288.2159, were matched to masses in the theoretical database and identified in the LC-MS, but the mass match error was >2 ppm so these ions were not targeted for MS/MS analysis using the ion trap. The

following two ions listed, 302.2313 and 316.2120, were previously identified and the MS/MS spectra were collected using the ion trap. Several of the acylcarnitines were not in the HMDB so they were not included in the theoretical database, including C7, C9 and C11. Lastly, any acylcarnitine metabolite with a double bond, excluding the addition of a double bonded oxygen atom, were not predicted by the MetabolitePredict™ software based on the structure of the compound and the listed set of biotransformations (see Appendix) used for the prediction of the metabolites. However, several of these compounds have been referenced in different journal articles [1, 3]. The chemical formula for any compounds not found in the theoretical database is based on the results from the DataAnalysis™ software. This software can generate a molecular formula based on accurate mass measurements, a table of atomic masses and a defined mass error, in ppm, for the parent peak as well as any fragment peak found in a spectrum.

4.4. Conclusions

In this work, the possibility of using accurate mass measurements from an FT-ICR MS along with a theoretical metabolite database to identify potential endogenous human metabolites followed by MS/MS analysis for verification was investigated. To simplify the procedure and analysis, acylcarnitines were targeted during sample cleanup using SPE and during the data analysis. Specific targeting of this family of compounds generated a large amount of data to process and resulted in the identification of 60 different acylcarnitines. By comparing the EIC for the LC-MS analysis with the targeted ions and their retention times, it becomes obvious that MS/MS collection for some structural isomers were missed.

To test the theoretical metabolite database, the same sample was run using auto MS/MS on the FT-ICR MS. All acylcarnitines were initially identified by analyzing the fragmentation pattern and the masses of all the confirmed acycarnitines were compared to the theoretical metabolite database. In total, 16 different masses were compared to the database for a total of 66 MS/MS spectra. Each of these MS/MS spectra with the same parent mass were separated by at least 1.25 minutes but adjacent MS/MS spectra could be the result of the same compound. When compared to the theoretical metabolite database, only four of the masses corresponded to a predicted metabolite and of those, only two had a mass error of <2 ppm. The remaining 12 compounds that were not matched to the

theoretical database were likely due to issues that must be addressed. The theoretical metabolite database is based on known endogenous human metabolites listed in the HMDB. Several of the acylcarnitines are not listed in the HMDB because the database is currently incomplete and/or these compounds are found in the human body at concentrations below 1 μM, the database's concentration cutoff.

The theoretical metabolite database has the potential of being a very useful tool for compound identification once the method is optimized and the database refined. For example, mass errors >2 ppm for the acylcarnitines identified using auto MS/MS is not acceptable for an FT-ICR MS and also need to be improved. The tune method for the FT-ICR MS should be checked, as settings such as the "Excitation Amp" will cause problems with the instrument's calibration if set too high.

4.5. References Cited

1. Reuter, S.E., et al., *Impact of haemodialysis on individual endogenous plasma acylcarnitine concentrations in end-stage renal disease.* Annals of Clinical Biochemistry, 2005. **42**: p. 387.

2. Maeda, Y., et al., *Simultaneous quantification of acylcarnitine isomers containing dicarboxylic acylcarnitines in human serum and urine by high-performance liquid chromatography/electrospray ionization tandem mass spectrometry.* Rapid Communications in Mass Spectrometry, 2007. **21**(5): p. 799-806.

3. Van Bocxlaer, J.F. and A.P. De Leenheer, *Solid-phase extraction technique for gas-chromatographic profiling of acylcarnitines.* Clin Chem, 1993. **39**(9): p. 1911-1917.

4. *Sample Preparation, Oasis MCX SPE Products.* Chromatography Columns, SPE, Supplies and Waters Quality Parts Catalog 2007-2008 [cited 2007; Available from: www.waters.com.

5. Möder, M., et al., *The pattern of urinary acylcarnitines determined by electrospray mass spectrometry: a new tool in the diagnosis of diabetes mellitus.* Analytical and Bioanalytical Chemistry, 2003. **375**(2): p. 200.

6. Maeda, Y., et al., *Simultaneous quantification of acylcarnitine isomers containing dicarboxylic acylcarnitines in human serum and urine by high-performance liquid chromatography/electrospray ionization tandem mass spectrometry.* Rapid Communications in Mass Spectrometry, 2007. **21**(5): p. 799-806.

7. Tracey, B.M., et al., *Urinary C6-C12 dicarboxylic acylcarnitines in Reye's syndrome.* Clinica Chimica Acta, 1988. **175**(1): p. 79.

8. Schaefer, J., et al., *Fatty Acid Oxidation in Peripheral Blood Cells: Characterization and Use for the Diagnosis of Defects of Fatty Acid Oxidation.* Pediatric Research, 1995. **37**(3): p. 354-360.

9. Millington, D.S., et al., *Application of fast atom bombardment with tandem mass spectrometry and liquid chromatography/ mass spectrometry to the analysis of acylcarnitines in human urine, blood, and tissue.* Analytical Biochemistry, 1989. **180**(2): p. 331.

Chapter 5

Overall Conclusions and Future Work

5.1. Metabolite Identification in Microsome Samples

It is relatively easier to identify the metabolites in a microsome incubation than in a biological sample, such as blood, urine or cerebral spinal fluid (CSF). Compared to biological samples, a microsome incubation sample contains fewer compounds making it a less complex system to analyze. Additionally, a corresponding control can be incubated along with the microsome sample for direct comparison. The predecessor of the metabolites in the incubation is known and its MS/MS spectrum can be used for comparison with that of its metabolites. Using a simple incubation method, like those commonly used for xenobiotic analysis, followed by a quick sample clean-up and MS analysis, as described in Chapter 2, only a handful of metabolites were positively identified. A number of the potential metabolites that were initially identified through comparison with the control sample could not be confirmed through MS/MS analysis due to their low concentrations. Also, several of the chromatographic peaks identified as metabolites were oddly shaped suggesting that a single peak found using HPLC separation could actually be several structural isomers with overlapping retention times. Using UPLC could resolve these peaks so that they could then each be uniquely identified.

Work is currently ongoing to improve upon these methods, including the microsome incubation, sample clean-up as well as MS and MS/MS analysis. Changes in the incubation procedures that are currently being looked at include changing the buffering system, changing the microsome concentration, as well as purchasing different microsomes. For example, increasing the microsome concentration for an incubation would make the system reach equilibrium more quickly than a system with a lower microsome concentration. This would be beneficial for any substrates that require more time for metabolism to occur because the microsomes lose functionality over time further slowing the biotransformation process. Another way to potentially improve the number of identified metabolites would be to purchase different types of microsome. All of the work described in Chapter 2 used the same type of human liver microsomes. Different

microsomes can be harvested by selecting a slightly different fraction during their collection, as described in Chapter 1. Each fraction contains different enzyme activities so the use of a different fraction may result in a different metabolite profile. To target specific metabolites it is also possible to purchase recombinant enzymes, a handful of enzymes found within a modified microsome at a higher concentration than in typical microsomes.

Sample clean-up and concentration may also improve the detection of the different metabolites in a microsome incubation. Work using solid phase extraction (SPE) is currently underway; however, the SPE method must be optimized for each family of compounds and the appropriate SPE cartridge must be selected. One major concern with this method is the limited sample volume; a single error may require the incubation to be redone.

Other future work that may benefit the identification of metabolites in a microsomal incubation would be switching to a nanospray introductory system for the mass spectrometer. The smaller spray shows higher sensitivity and also requires less sample consumption for each analysis. It would also be possible to switch away from the microsomes to a whole cell system, such as cryopreserved freshly isolated hepatocytes. Some work was done using HepG2 cell lines, which were replaced with the microsomes for time efficiency. Using cryopreserved freshly isolated hepatocytes may be a good compromise between the two systems.

5.2. Using Metabolites Produced with Human Liver Microsomes as Pseudo-Standards for Compound Identification in a Human Urine Sample

A large number of different endogenous and exogenous compounds, with concentrations ranging in several orders of magnitude, are excreted in urine. The easiest and most conclusive way to identify these compounds is to use standards for direct comparison. However, not all the necessary standards can be easily purchased and synthesizing them would be extremely time-consuming. Using the identified metabolites from the microsome incubations as pseudo-standards, along with a one-dimensional LC separation followed by MS analysis did result in the positive identification of several

different compounds in a single urine sample. However, using a more targeted approach, such as SPE, to target families of compounds for comparison with microsome produced pseudo-standards would most likely result in a higher number of matches. Targeting a single family of compounds allows for easier biological sample clean-up and simplifies the MS/MS data analysis because specific fragment ions and common neutral losses can be targeted. Method development for SPE could initially be done using the microsome incubation samples and then optimized for the biological sample for families of compounds, such as the acylcarnitines. Using SPE to clean up the biological sample would make it easier to identify metabolite matches because there would be fewer compounds to analyze in the sample and less ion suppression caused by co-eluting compounds.

Due to instrument availability, these compounds were identified by targeting a single m/z on the ion trap mass spectrometer and collecting the corresponding MS/MS spectra. The MS/MS spectrum and the compound's retention time were compared to the pseudo-standard for positive identification. Instead of making several LC/MS runs using single ion monitoring (SIM) it may be more prudent to use the FT-ICR MS to scan the entire range of compounds in order to find accurate mass matches to the metabolite pseudo-standards. The experiments could then be repeated under identical LC conditions using the ion trap to target ions based on m/z and retention time, for MS/MS analysis.

5.3. Using the Theoretical Metabolite Database for Unknown Metabolite Identification

Using microsomes to produce metabolite pseudo-standards and then using these pseudo-standards to identify compounds in a complex biological sample works well. However, the microsomes do not contain all of the enzymes involved in metabolism and the experiments described in Chapters 2 and 3 only target phase I metabolites. To investigate phase II metabolism the correct cofactors must be added to the incubation mixture. Most published experimental procedures tend to investigate a single phase II reaction at a time resulting in metabolites that can easily be predicted. In an attempt to speed up the identification process a theoretical metabolite database was created. This database contains many phase I and phase II metabolites from multiple substrates with

their predicted structure, chemical formula and mass allowing for accurate mass matches to be made with complex biological samples.

The theoretical metabolite database currently shows a lot of potential in helping with unknown metabolite identification in a complex sample, such as urine. Several issues were identified that need to be addressed and a significant amount of work needs to be done to make the database more user-friendly.

The web interface for the database needs to be improved. For example, the mass errors that identify a positive mass match are preset. This should be changed so that the user can define the mass error either in Da or ppm. It would also be useful if the output from a search could be exported to an Excel spreadsheet. Lastly, the output list of metabolites currently links to a .mol file that contains all of the structural information for the compound and requires secondary software to view the structure. When these links are selected it would be more useful if the structure was generated immediately rather than the user repeatedly going through the time-consuming process of converting the .mol file to a structure. It would also be useful if these links were exported into the spreadsheet so that they could be saved and revisited at a later date.

While the data were being processed a couple of errors were found in the database. First, several compounds were uploaded to the database twice, resulting in the same information being reported in the search output twice. Also, the output of a search resulted in a single line of what appeared to be random output. What appeared to be a mass match with the predicted metabolites from a single substrate did not have the matching .sdf files. The .sdf files did not have the same chemical formula or molecular weight of what was reported in the output list or to each other. Some work has been done to remove the duplicates in the database and to address the issues with the random output. However, these changes still need to be tested to ensure that the problem has been fixed.

To get the full benefit of this database additional time needs to be spent on method development for sample clean-up using SPE as well as on method development with the FT-ICR MS. The acylcarnitines identified from the SPE sample had a hydrophobic tail of seven or more carbons, but literature shows that urine also contains acylcarnitines with smaller hydrophobic tails. It is possible that these compounds were eluted from the SPE cartridge with one of the washes, most likely the 20% methanol wash. The washes were

stored at -20 °C but have yet to be analyzed and may contain some of the smaller, more polar acylcarnitine compounds.

In short, the theoretical metabolite database shows much potential but a significant amount of work still needs to be done to make it more user-friendly and to explore its complete potential.

Appendix

Table 6.1 - Lists all of the metabolism rules in MetabolitePredict™ with their target structure and resulting changes

Rule #	Rule Name	Target	Result
001	Alcohol Dehydrogenase A R1=H,C R2=H,C	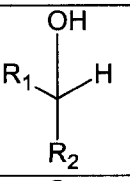	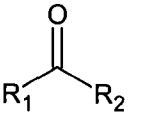
002	Aldehyde Dehydrogenase A R1=H,C	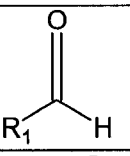	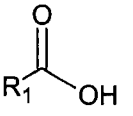
003	beta-Oxidation Hydrogenation 1 A R1=C R2=H,C	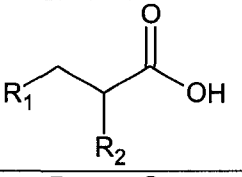	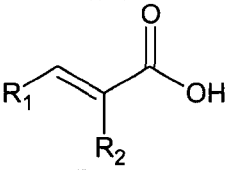
004	beta-Oxidation Hydration A R1=C R3=H,C R2=H,C	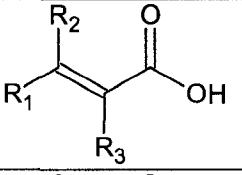	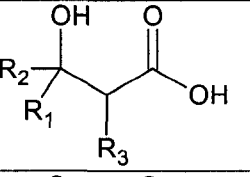
005	beta-Oxidation Hydrogenation 2 A R1=C R2=H,C	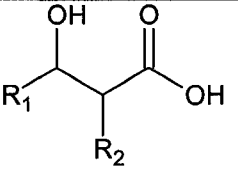	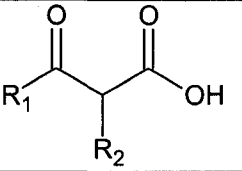
006	beta-Oxidation Cleavage A R1=C R2=H,C	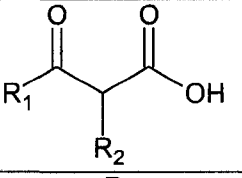	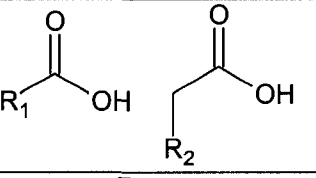
007a	CYP450 Hydroxylation A R1=H,C R2=H,C R3=H,C,N,Cl,Br,I	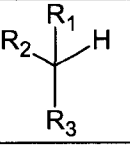	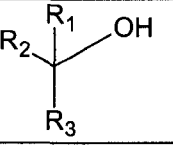
007b	CYP450 Hydroxylation A R1=C_ar		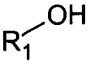
008	CYP450 N-Demethylation A	$H_2N—CH_3$	$H_2N—H$
009	CYP450 O-Demethylation A	$HO—CH_3$	$HO—H$
010	CYP450 S-Demethylation A	$HS—CH_3$	$HS—H$

011	CYP450 Epoxidation 1 A R1=H,C R2=H,C,F,Cl,Br,I R3= H,C,F,Cl,Br,I R4= H,C,F,Cl,Br,I	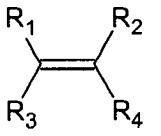	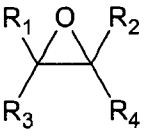
012	CYP450 Epoxidation 2 A R1= C_arR3= C_ar R3= H R3= H,C,F,Cl,Br,I	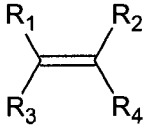	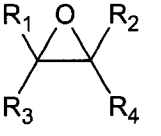
013	CYP450 Acetylene Oxidation A R3= H,C	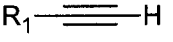	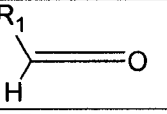
014	CYP450 N-Oxidation A R1= C R3= C R2= C R4= N,P	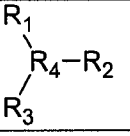	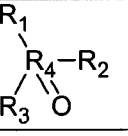
015	CYP450 S-Oxidation A R1= C R2= H,C	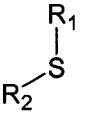	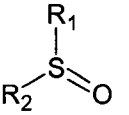
016	CYP450 Sulfoxide Oxidation A R1= C R2= H,C	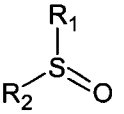	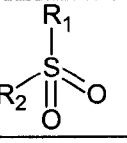
017	CYP450 Phosphine Sulfide A R1= C R3= H,C R2= H,C	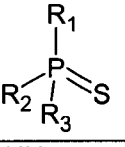	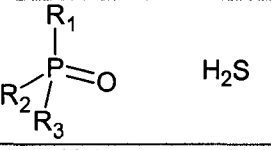
018	Xanthine Oxidase A	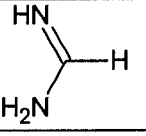	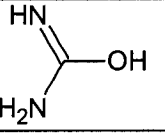
019	Carboxylesterase A R1=H,C R2= C,N X1=O,S X2= O,S	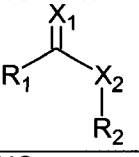	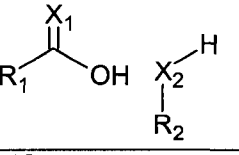
020	Sulfatase Monoester A R1=C	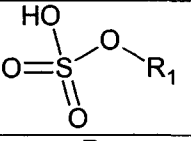	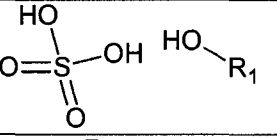
021	Sulfatase Diester A R1= C R2= C	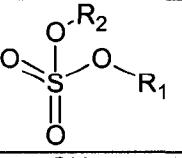	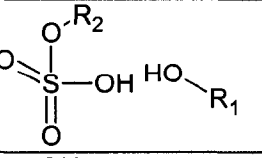
022	Phosphatase Monoester A R1= C	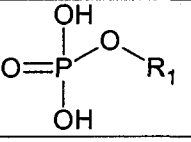	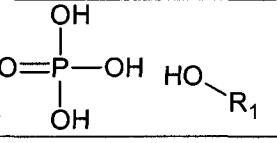

023	Phosphatase Diester A R1= C R2= C	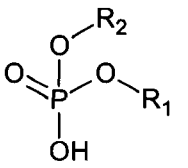	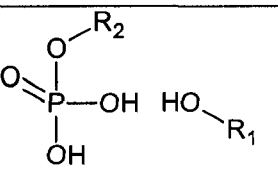
024	Amidase A R1=H,C R3= H,C R2= H,C	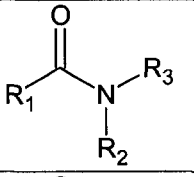	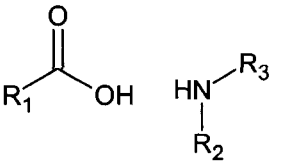
025	Peptidase A R1= C,H R2= C,H	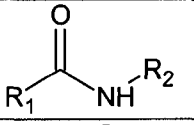	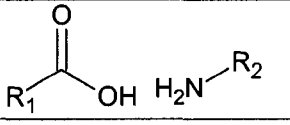
026	Peptidase N-Terminus A R1=H,C R3= C R2= H,C	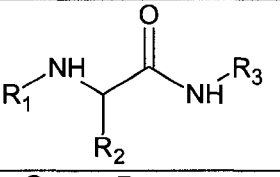	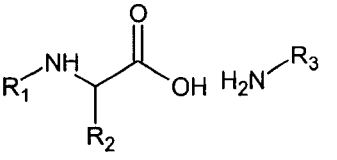
027	Peptidase C-Terminus A R1=H,C R3= C R2= H,C	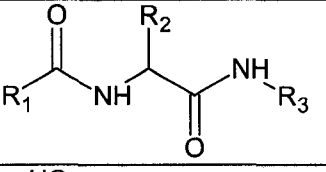	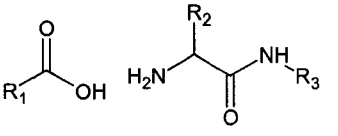
028	Glycosidase A R1= C	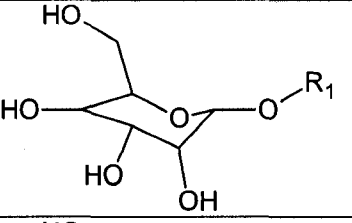	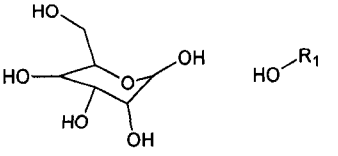
029	S-Glycosidase A R1= C	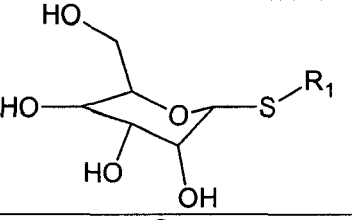	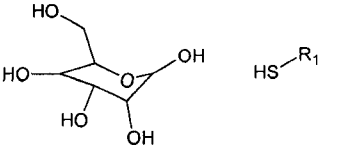
030	Epoxide Hydrolase A R1=H,C R2= H,C R3= H,C R4= H,C	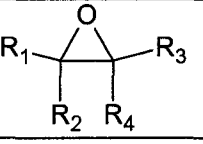	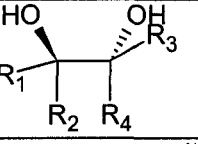
031	GSH Thiol M R1=C R2= H,C R3= H,C	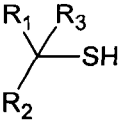	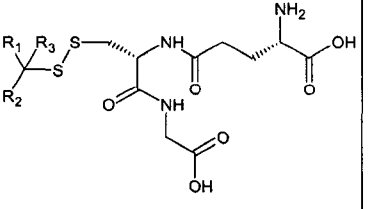

032a	GSH Epoxide M R1=H,C R2= H,C R3= H,C R4= H,C	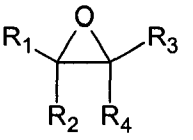	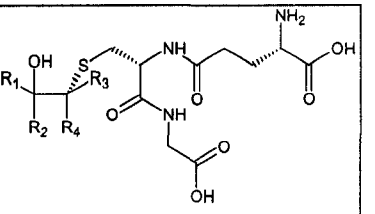
032b	GSH Epoxide M R1=H,C R2= H,C R3= H,C R4= H,C	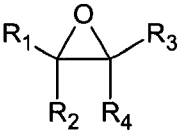	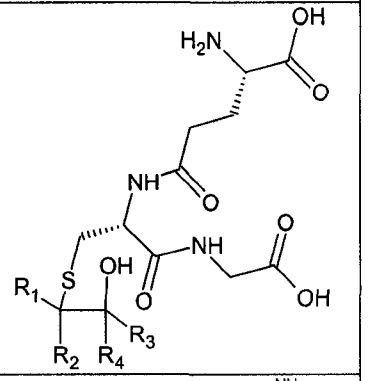
033a	GSH Addition M R1=Cl,Br,-COO,-CN-CF3, CCl3 R2= C,Cl,Br	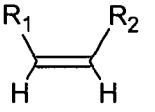	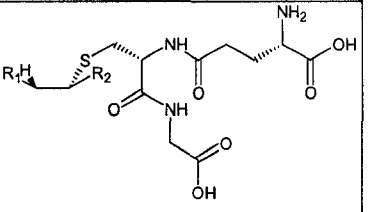
033b	GSH Addition M R1=Cl,Br,-COO,-CN-CF3, CCl3 R2= C,Cl,Br	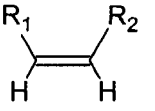	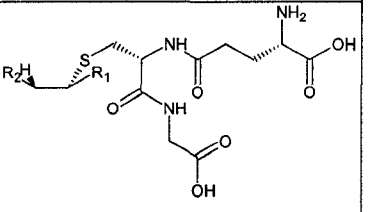
034	GSH Substitution M R1=Cl,Br,-COO,-CN-CF3, CCl3	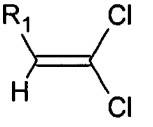	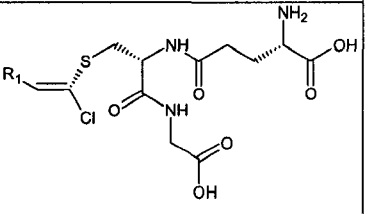
035	GSH Substitution aromatic M R1=C_ar, -C=C, -C=O, -C=S, -C=N	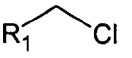	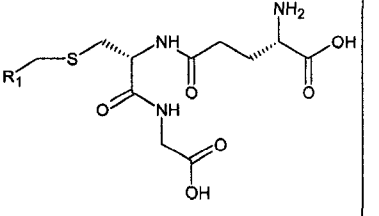

036	Glutathione-gamma-glutamylpeptidase M R1=C,H	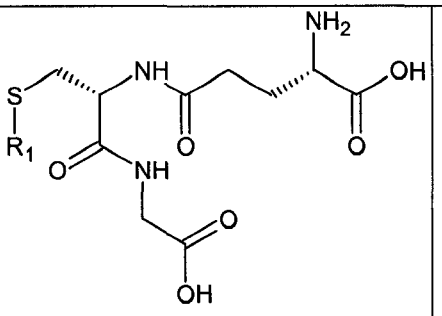	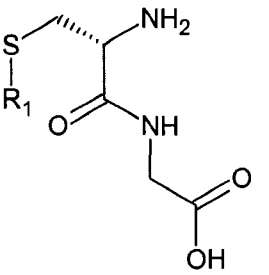
037	Cysteinylglycinase M R1=C	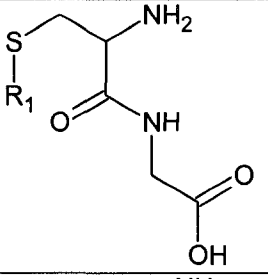	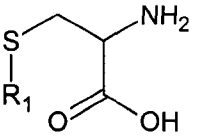
038	N-Acetyltransferase Cystein M R1=C	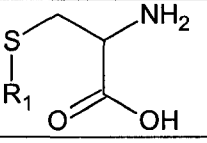	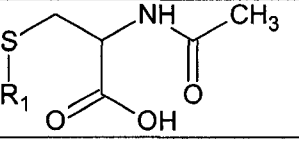
039	S-Methyltransferase B M R1=C_ar		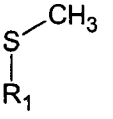
040	O-Methyltransferase P R1=C_ar		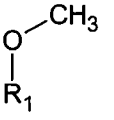
041	O-Methyltransferase M R1=C_ar R2=C_ar	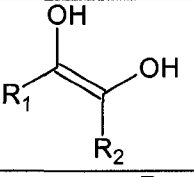	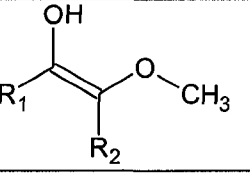
042	Cysteinyl-beta-lyase. M R1=C_ar, -C=C R2=C_ar, -C=C	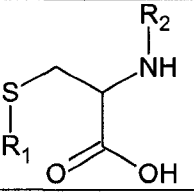	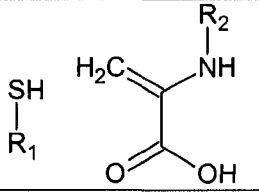
043	Hydrolysis 1 Anhydride H R1=C X2= O,S X1= O,S X3= O,S	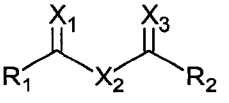	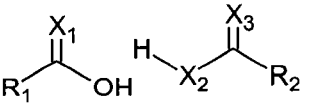
044	Hydrolysis Acylhalogenide H R1=H,C X1=F,Cl,Br,I	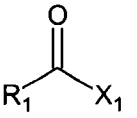	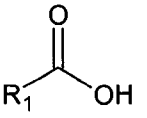

045	Hydrolysis oxidative Dehalogenation H R1=H,C R2= H,C R3= Cl,Br,I	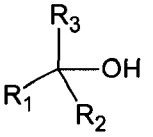	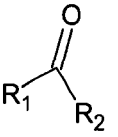
046	Hydrolysis oxidative Deamination H R1=H,C R2= N,O,S	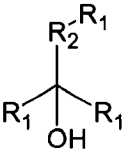	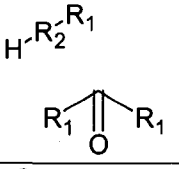
047	Hydrolysis Diol H R1=H,C R2= H,C X1= O,S	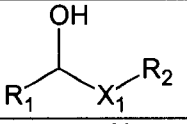	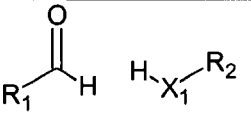
048	oxidative HCN cleavage H R1=H,C R2= H,C	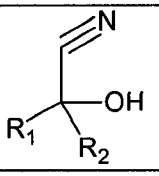	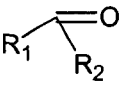
049	Hydrolysis Ketenehydration H R1=H,C	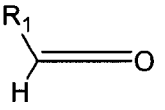	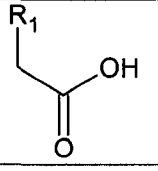
050	Hydrolysis Phenolisomerisation H R1=H,C,Cl	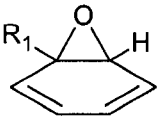	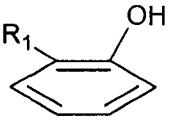
051	Hydrolysis Imine H R1=H,C R3=H,C R2= H,C	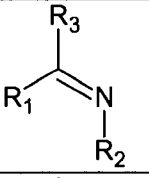	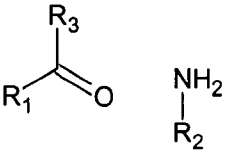
052	Tautomer Iminoalcohol H R1=H,C R2=H,C	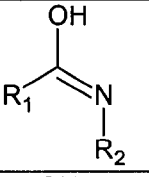	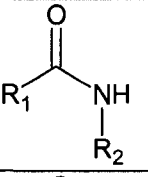
053	Tautomer Enol H R1=H,C R2=H,C	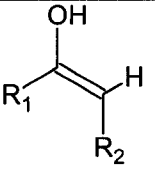	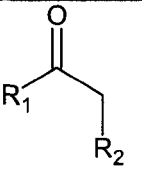
054	Tautomer Oxime H R1=H,C R2=H,C	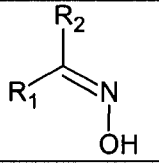	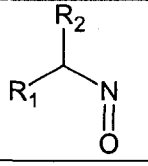

055	Decarboxylation Carbamate A R1=H,C X1=O,S R2=H,C X2=-OH,-SH	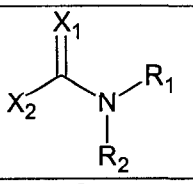	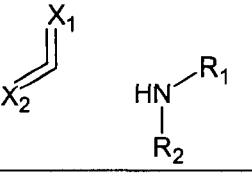
056	Decarboxylase A R1=C_ar	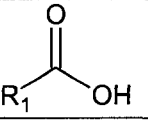	
057	Nitrilreductase B R1=C	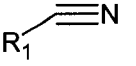	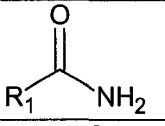
058	Nitroreductase NO2 B R1=C_ar	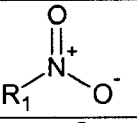	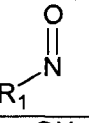
059	Nitroreductase NO B R1=C_ar	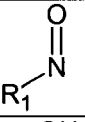	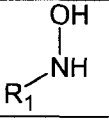
060	Nitroreductase NHOH B R1=C_ar	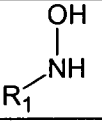	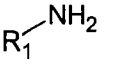
061	Azoreductase B R1=C_ar R2=C_ar	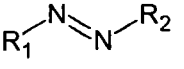	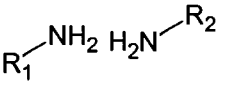
062	N-Acetyltransferase M R1=C_ar R2=C,-OH,-S=O, -S(=O)=O	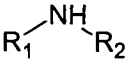	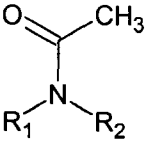
063	Glycine Transferase M R1=C	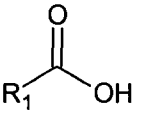	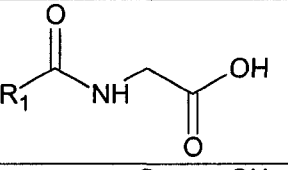
064	Glutamate Transferase M R1=C	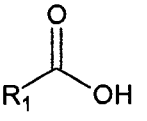	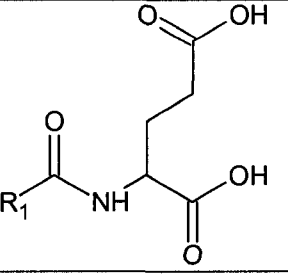

065	Glycosyl Transferase P R1=H,C R2=C R3=H,C	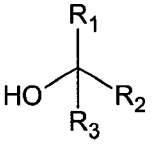	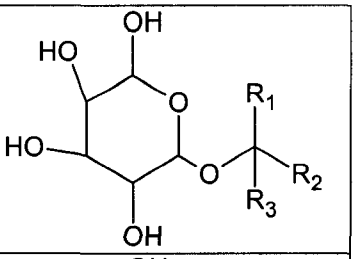
066	Glycosyl Transferase Aromatic Alcohol P R1=C_ar	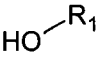	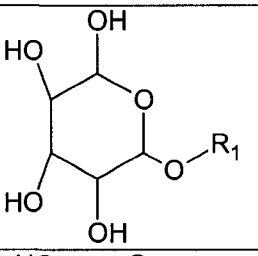
067	Glucuronyl Transferase Alcohol M P R1=H,C R2=C,H R3=H,C	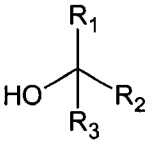	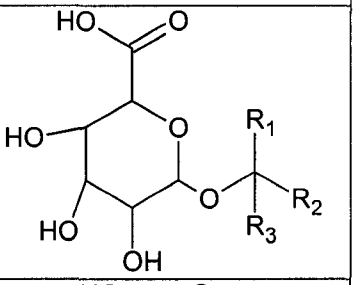
068	Glucuronyl Transferase Aromatic Alcohol M P R1=C_ar	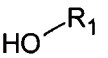	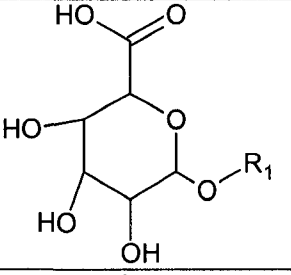
069	Glucuronyl Transferase Aromatic Amine M P R1=C_ar	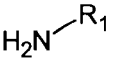	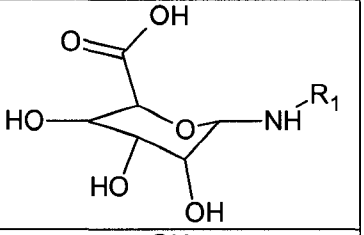
070	Glucuronyl Transferase Aromatic Thiol M P R1=C_ar	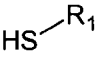	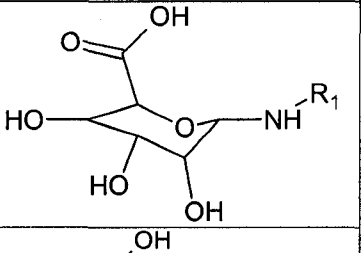
071	Glucuronyl Transferase Carboxylic Acid M P R1=C	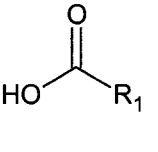	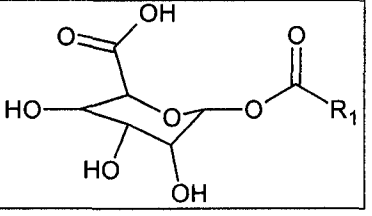

072	Glucuronyl Transferase Thiocarboxylic Acid M P R1=C,N	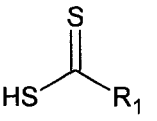	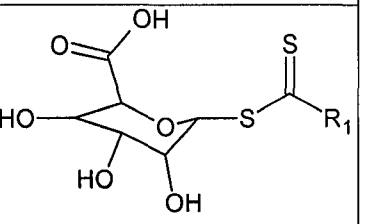
073	Glucuronyl Transferase Aromatic Hydroxylamine M P R1=C_ar	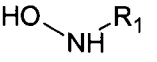	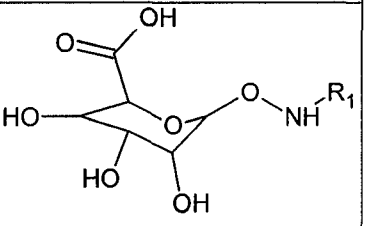
074	Glucuronyl Transferase Tert Amine M P R1=C_ali R2=C_ali R3=C_ali	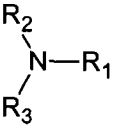	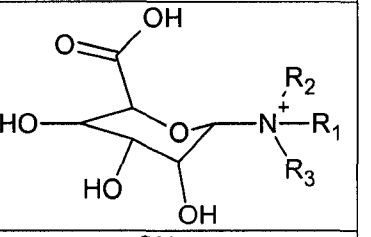
075	Glucuronyl Transferase Sulfonic Acid Aminoester. M P R1=C R2=C	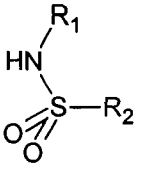	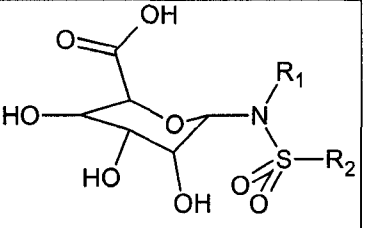
076	Glucuronyl Transferase 1-3-Diketone M P R1=C R2=C	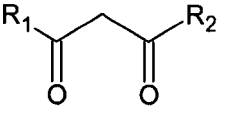	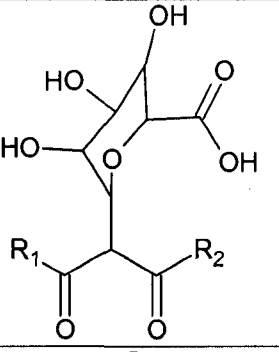
077	Sulfotransferase Alcohol M P R1=C, C_ar	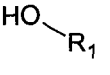	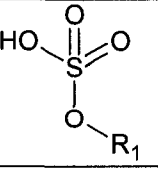
078	Sulfotransferase Aromatic Hydroxylamine M P R1=C_ar	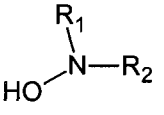	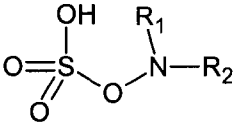

	R2=C,H		
079	Sulfotransferase Aromatic Amine M P R1=C_ar R2=C,H	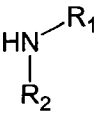	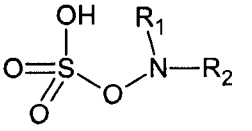

Table 6.2 - Shows which rules are in each of the software defined "List of Rules"

Preset rule lists	Rules is list
Phase 1 Metabolism	1-30, 39, 41-56
Phase 2 Metabolism	31-38, 62-64, 67-79
Acetaminophens	24, 68, 69, 77, 79
All Rules Mammals	1-39, 41-56, 62-64, 67-79
Cytochrome P450	7-18, 46, 47

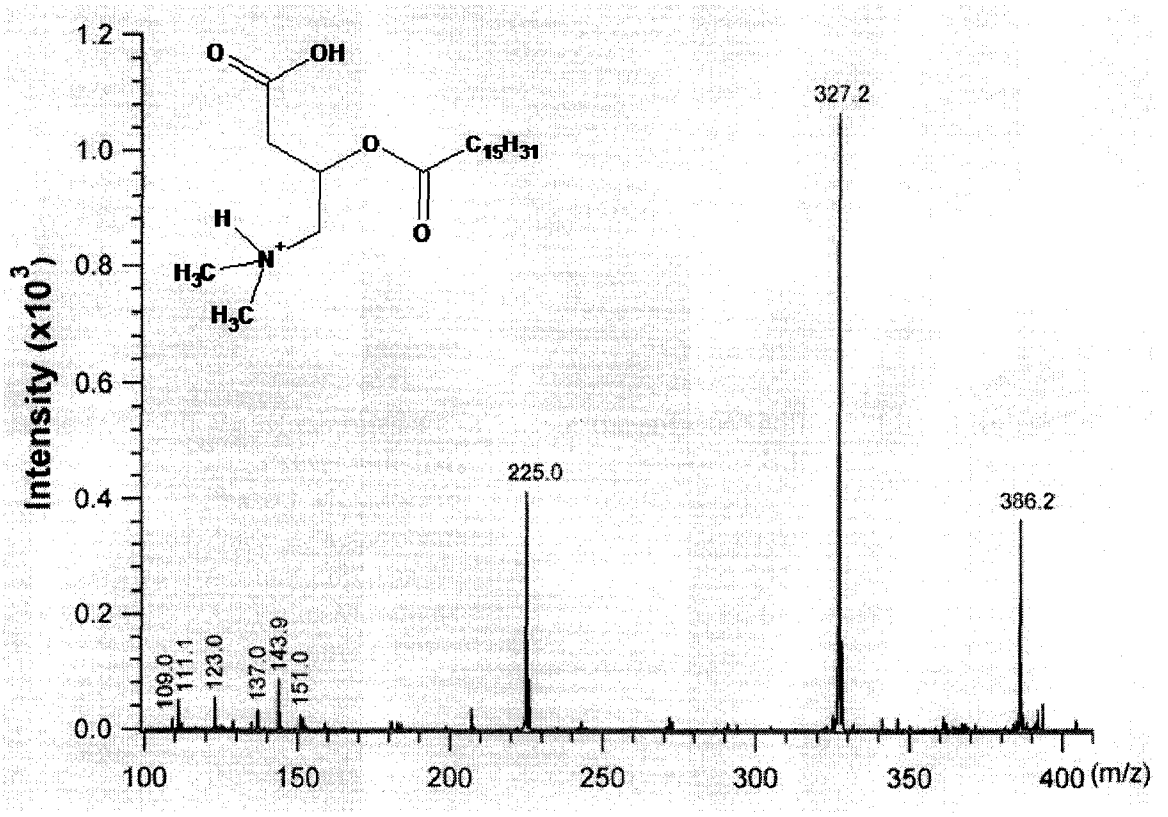

Figure 6.1 - MS/MS spectrum for palmitoylcarnitine metabolite m/z 386

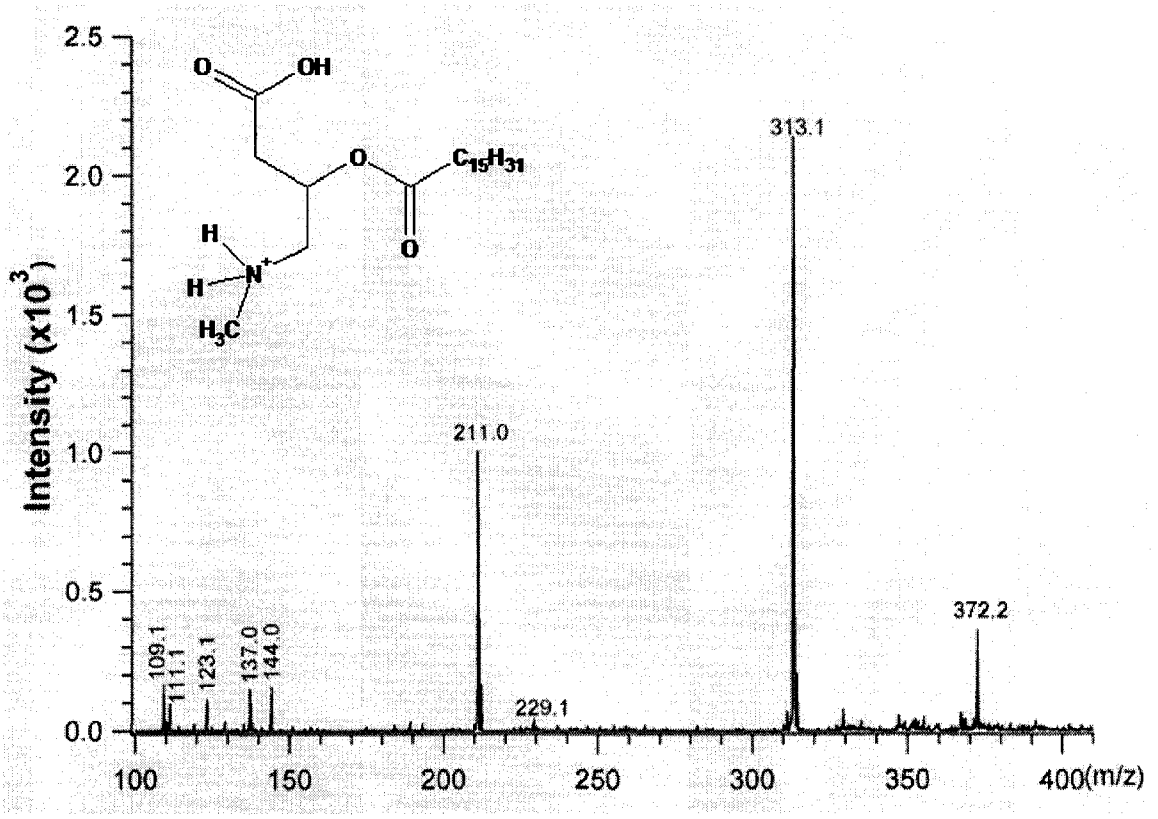

Figure 6.2 - MS/MS spectrum for palmitoylcarnitine metabolite m/z 372

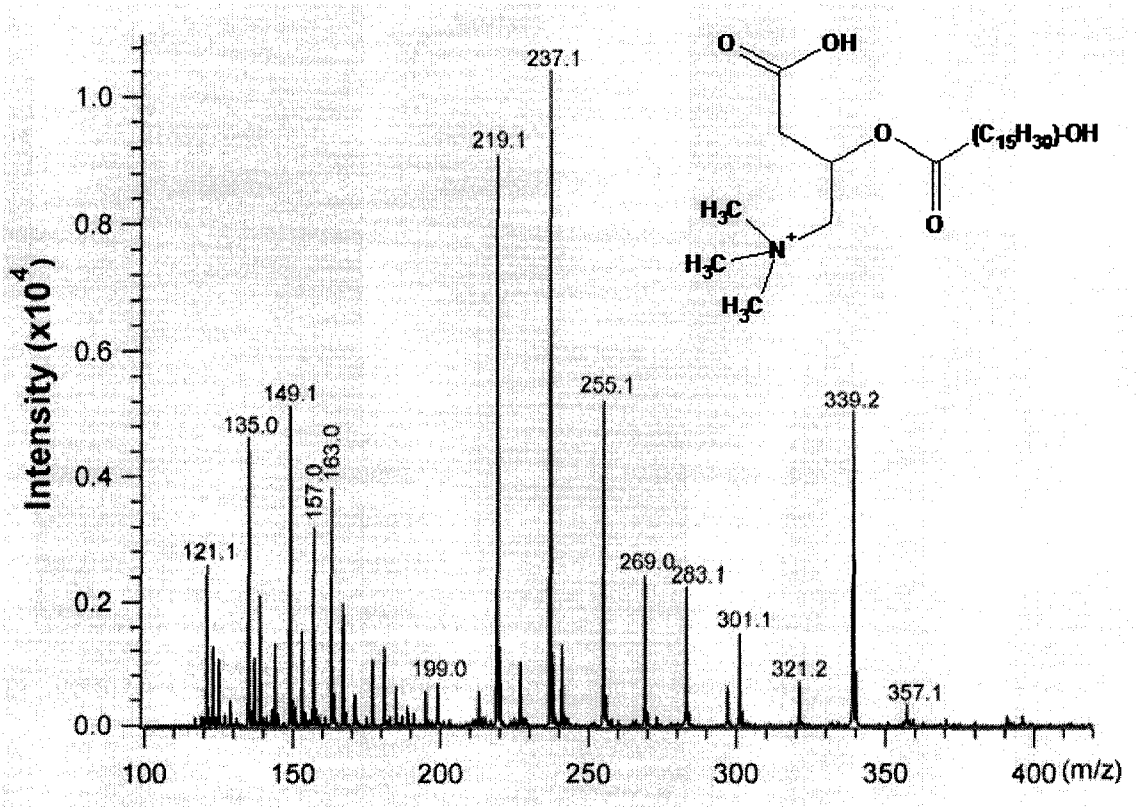

Figure 6.3 - MS/MS spectrum for palmitoylcarnitine metabolite m/z 416a

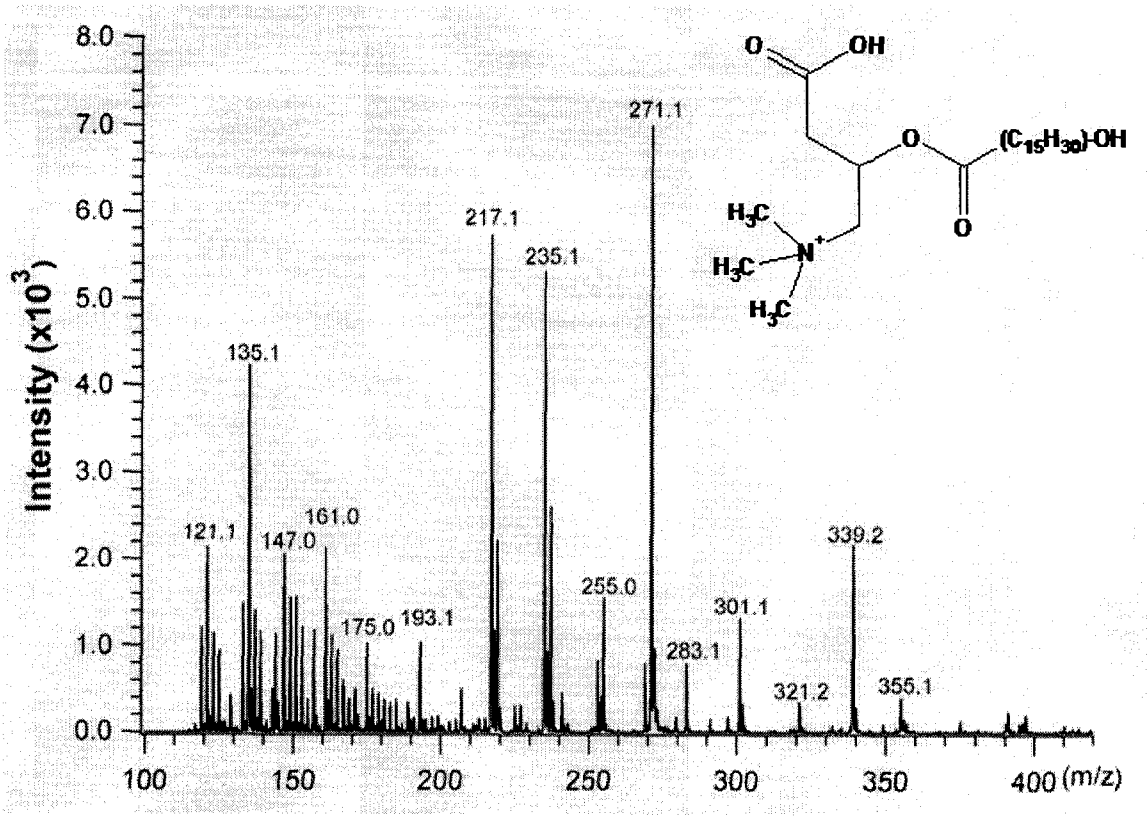

Figure 6.4 - MS/MS spectrum for palmitoylcarnitine metabolite m/z 416b

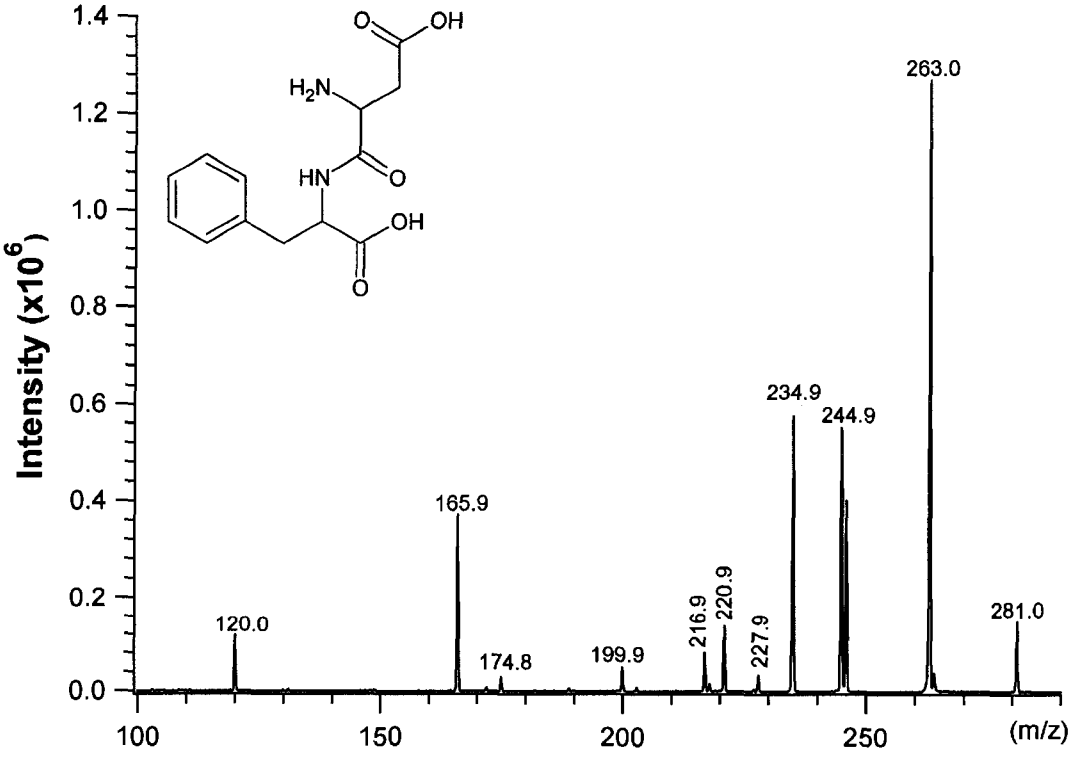

Figure 6.5 - MS/MS spectrum for aspartylphenylalanine (positive mode)

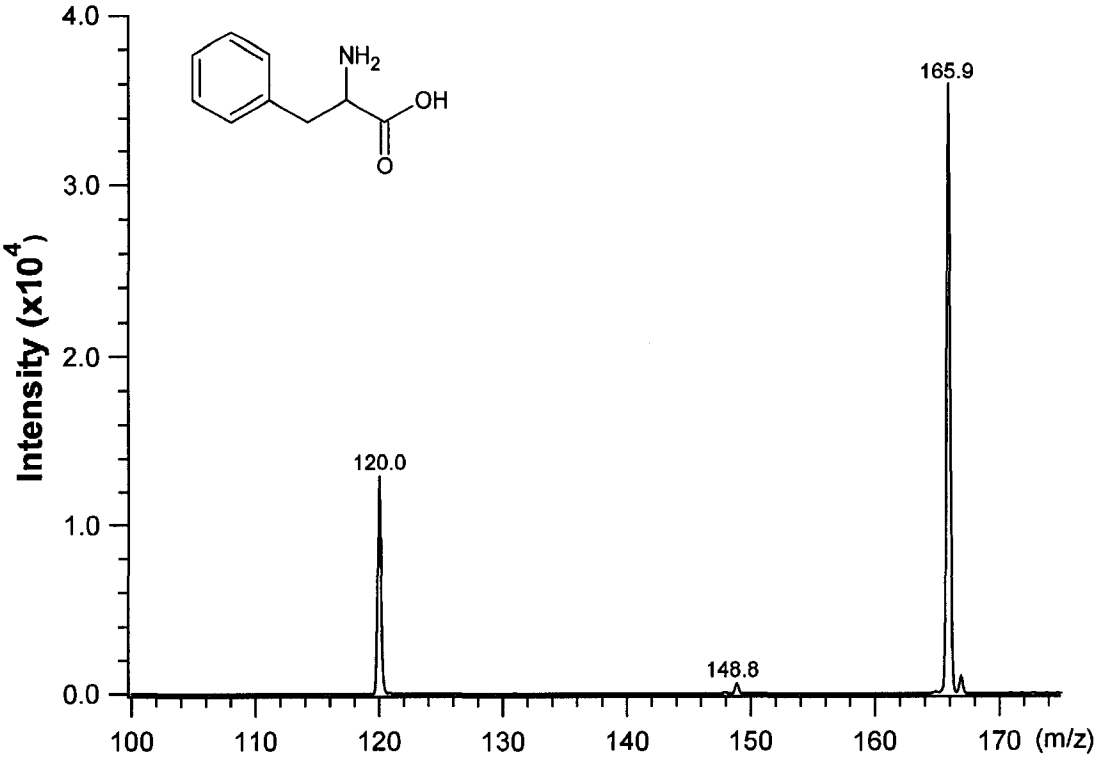

Figure 6.6 - MS/MS spectrum for aspartylphenylalanine metabolite m/z 166 (positive mode)

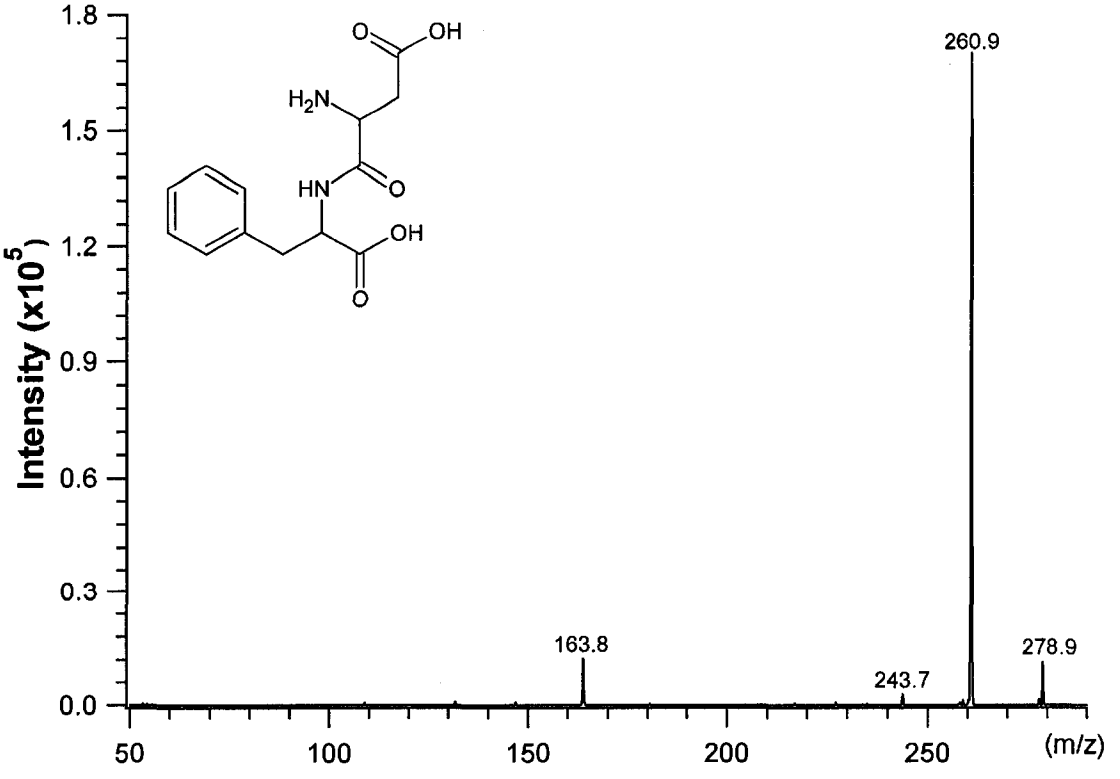

Figure 6.7 - MS/MS spectrum for aspartylphenylalanine (negative mode)

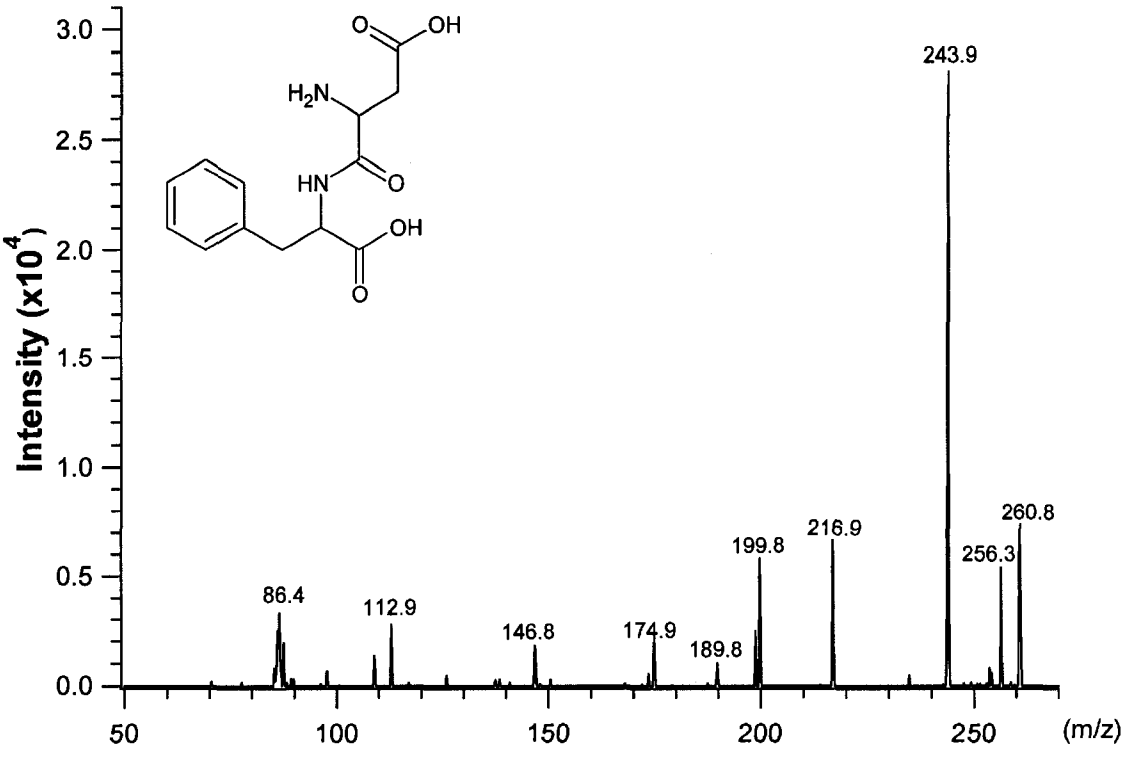

Figure 6.8 - MSn spectrum for aspartylphenylalanine (negative mode)

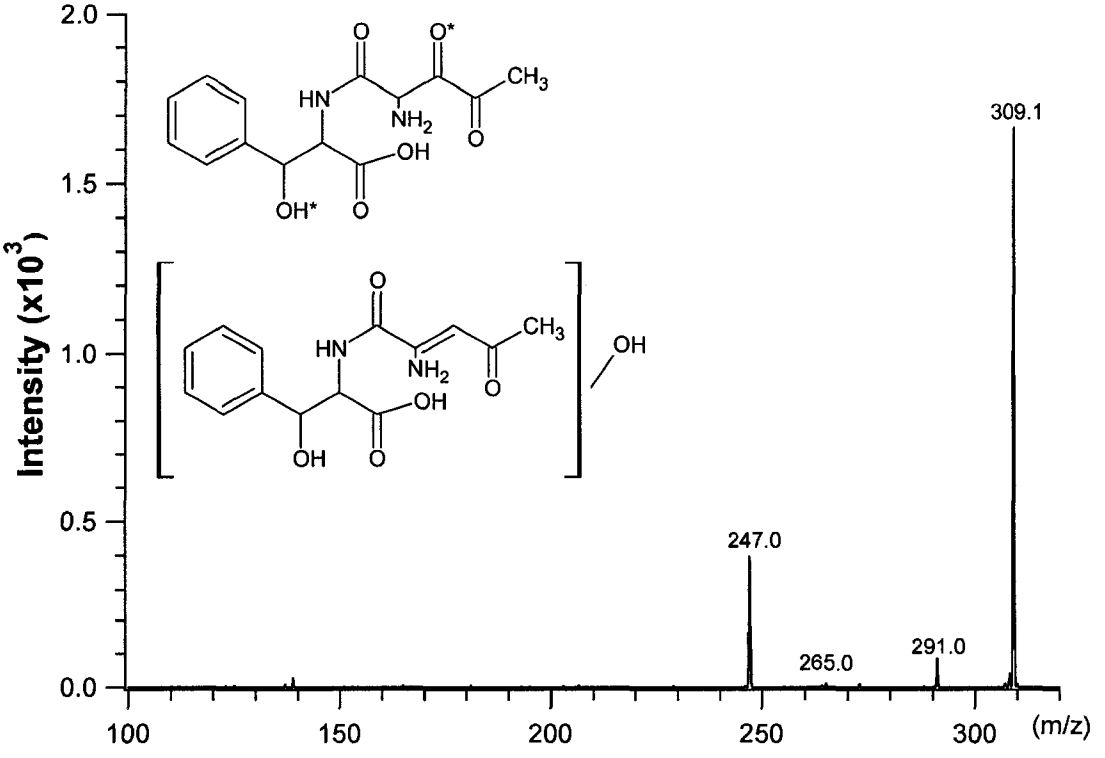

Figure 6.9 - MS/MS spectrum for aspartylphenylalanine metabolite m/z 309, the *'s in the top structure indicate that these two functional groups could be switched

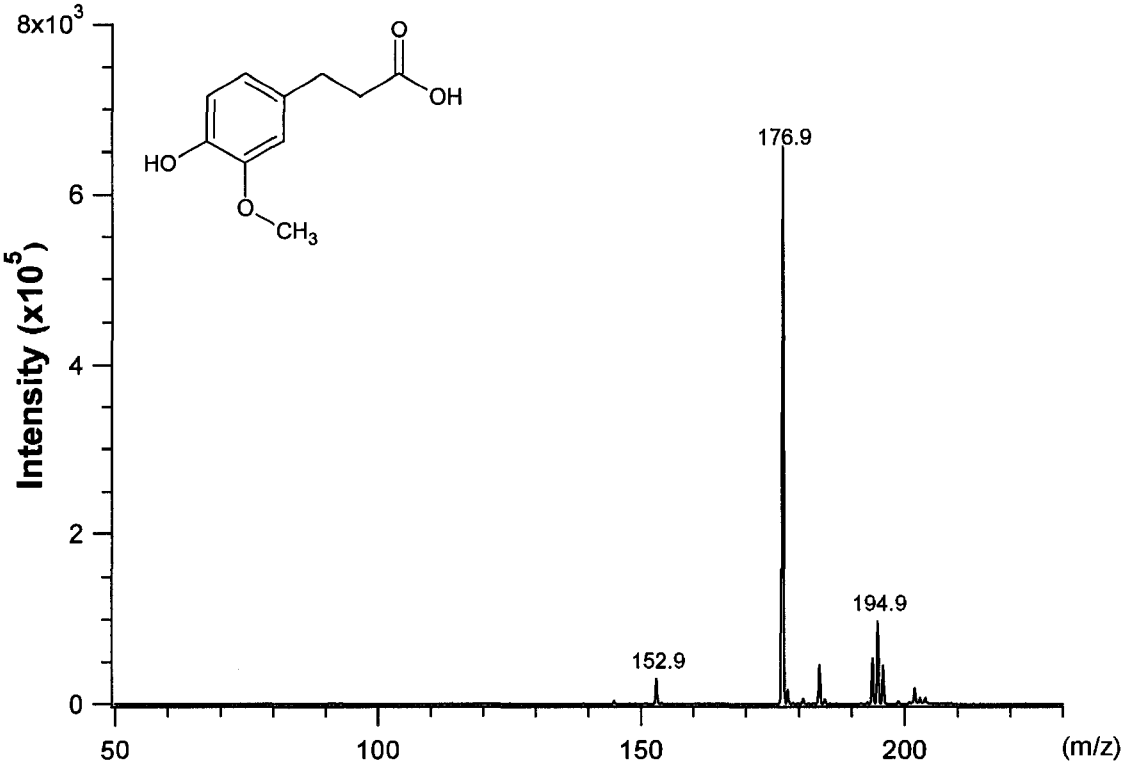

Figure 6.10 - MS/MS spectrum for ferulic acid

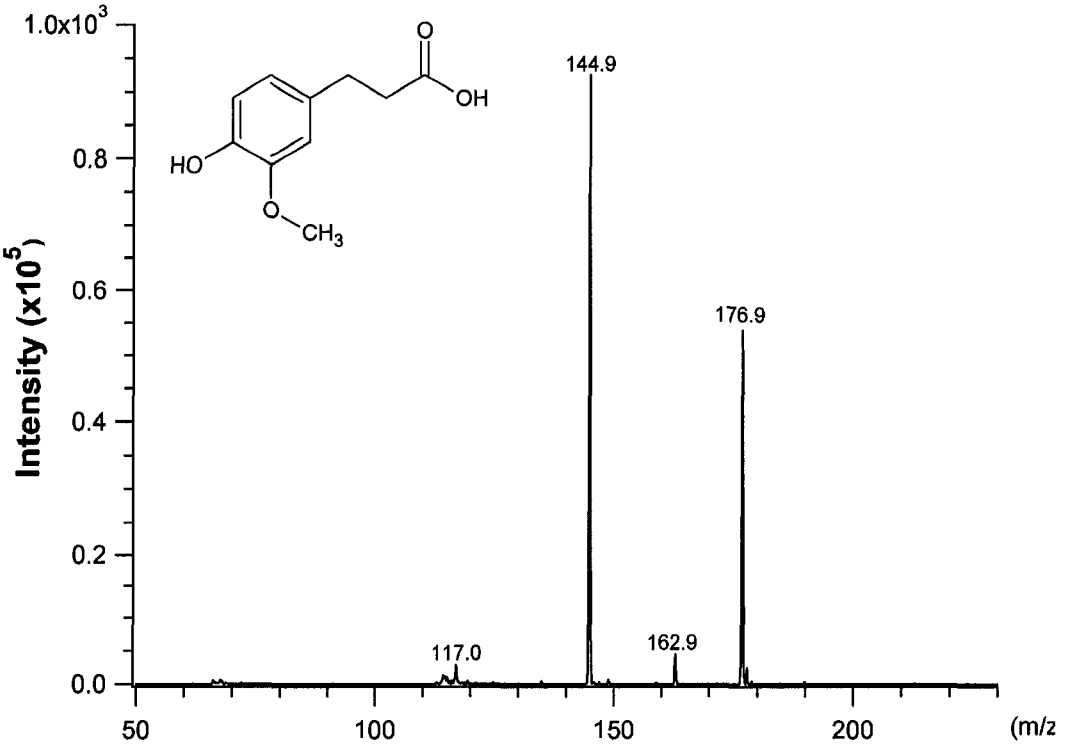

Figure 6.11 - MSn spectrum for ferulic acid

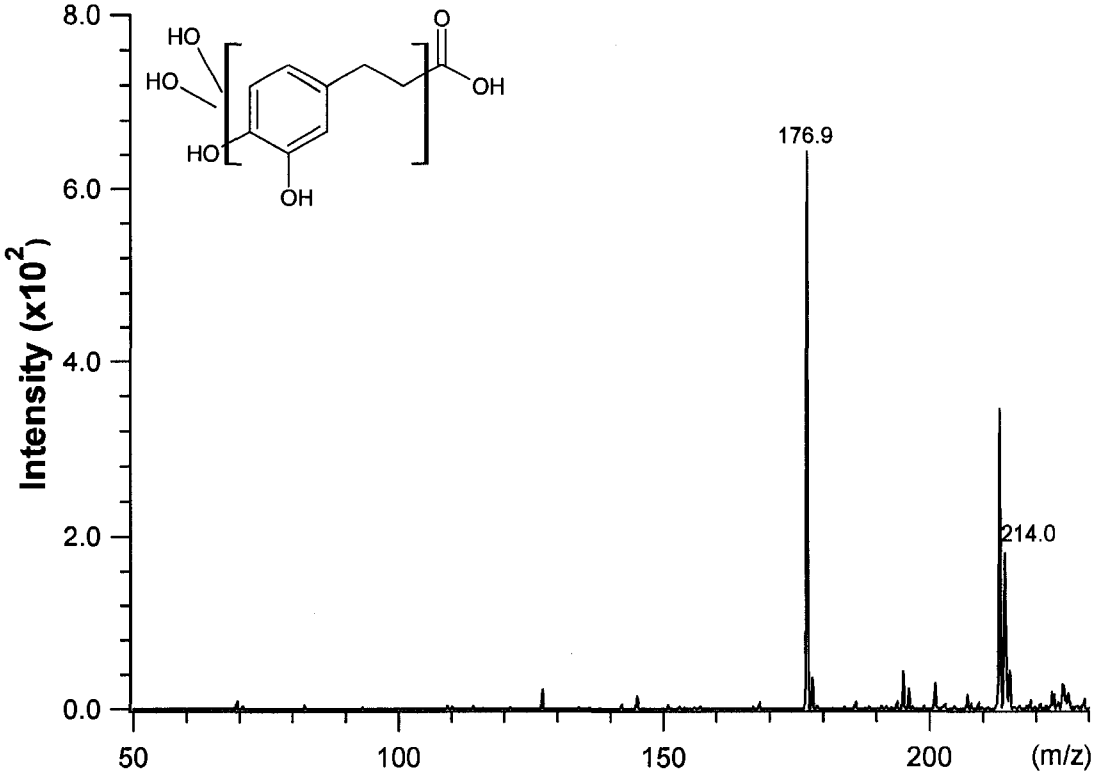

Figure 6.12 - MS/MS spectrum for ferulic acid metabolite m/z 214

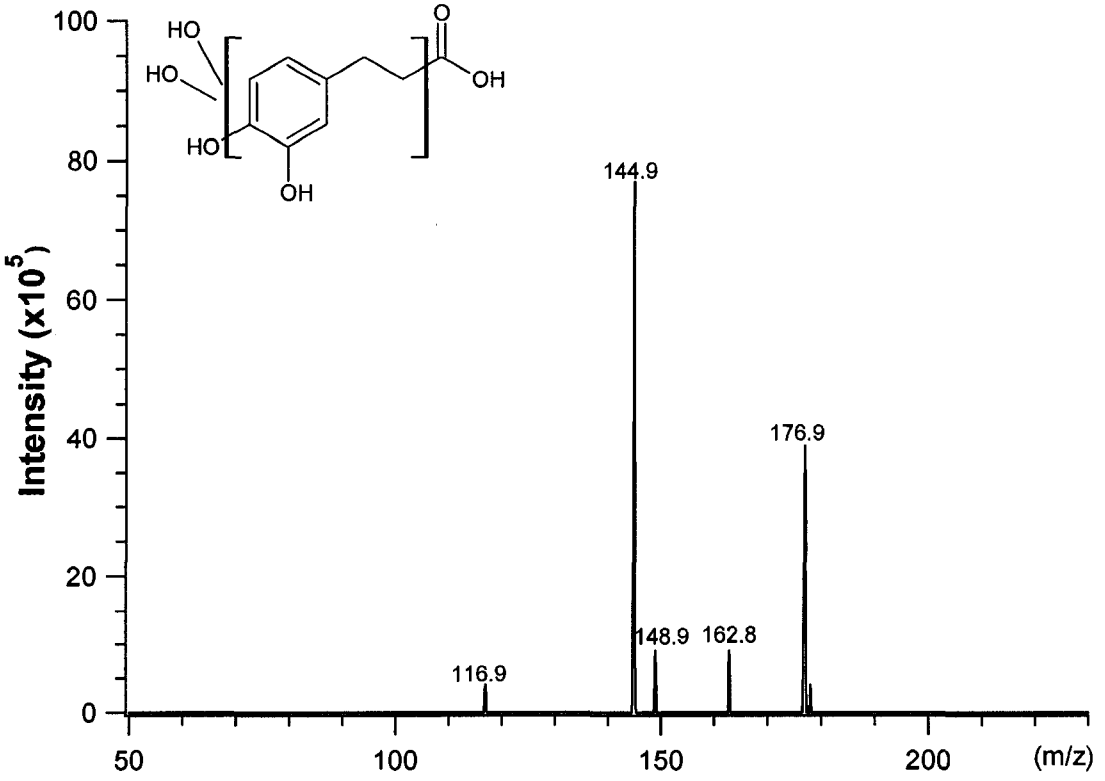

Figure 6.13 - MSn spectrum for ferulic acid metabolite m/z 214

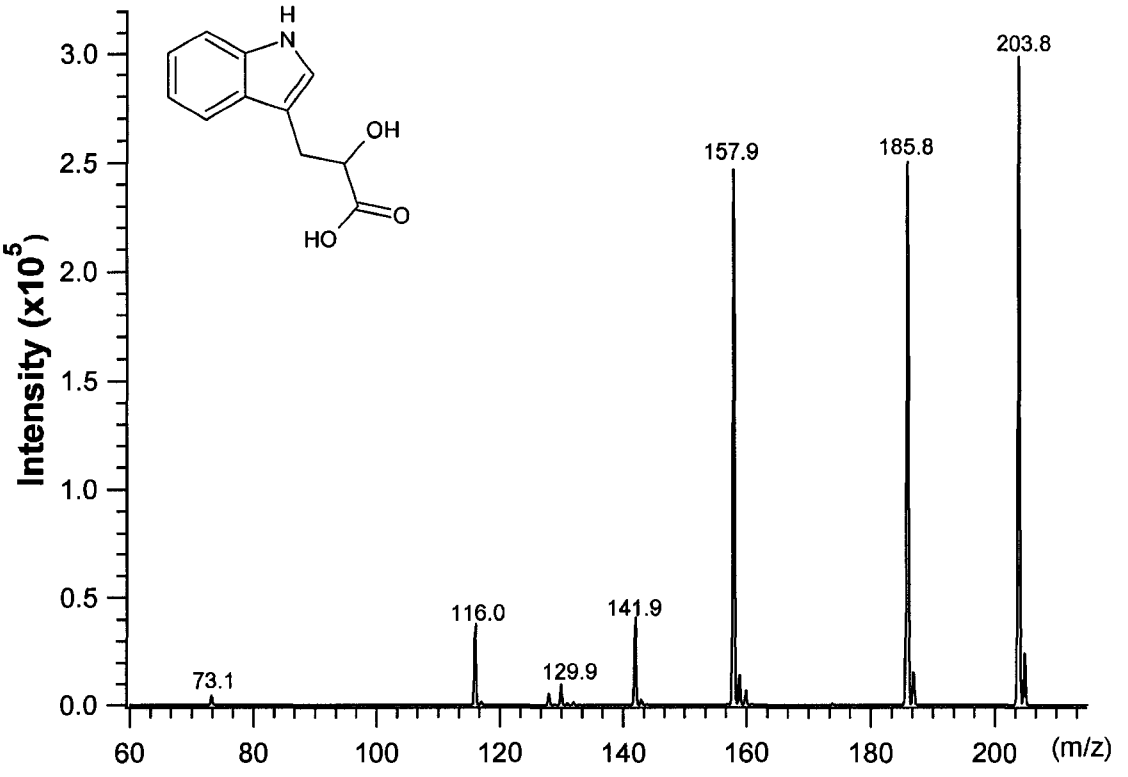

Figure 6.14 - MS/MS spectrum for indolelactic acid (negative mode)

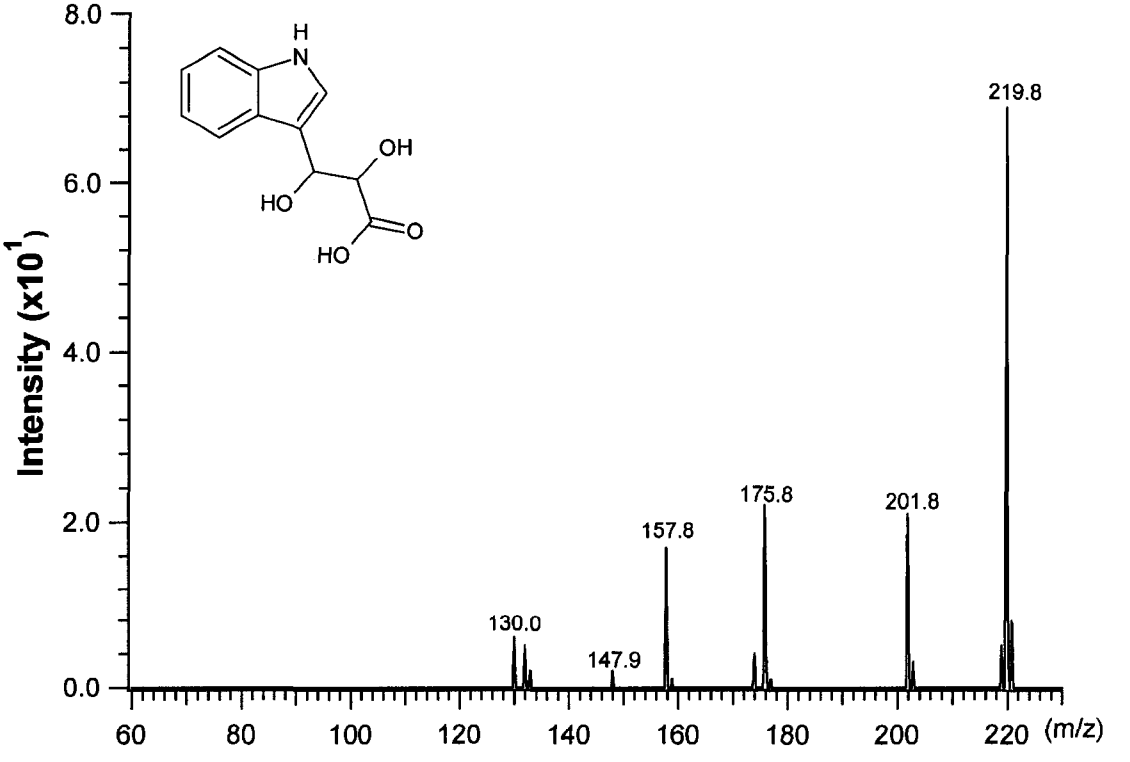

Figure 6.15 - MS/MS spectrum for indolelactic acid metabolite m/z 220 (negative mode)

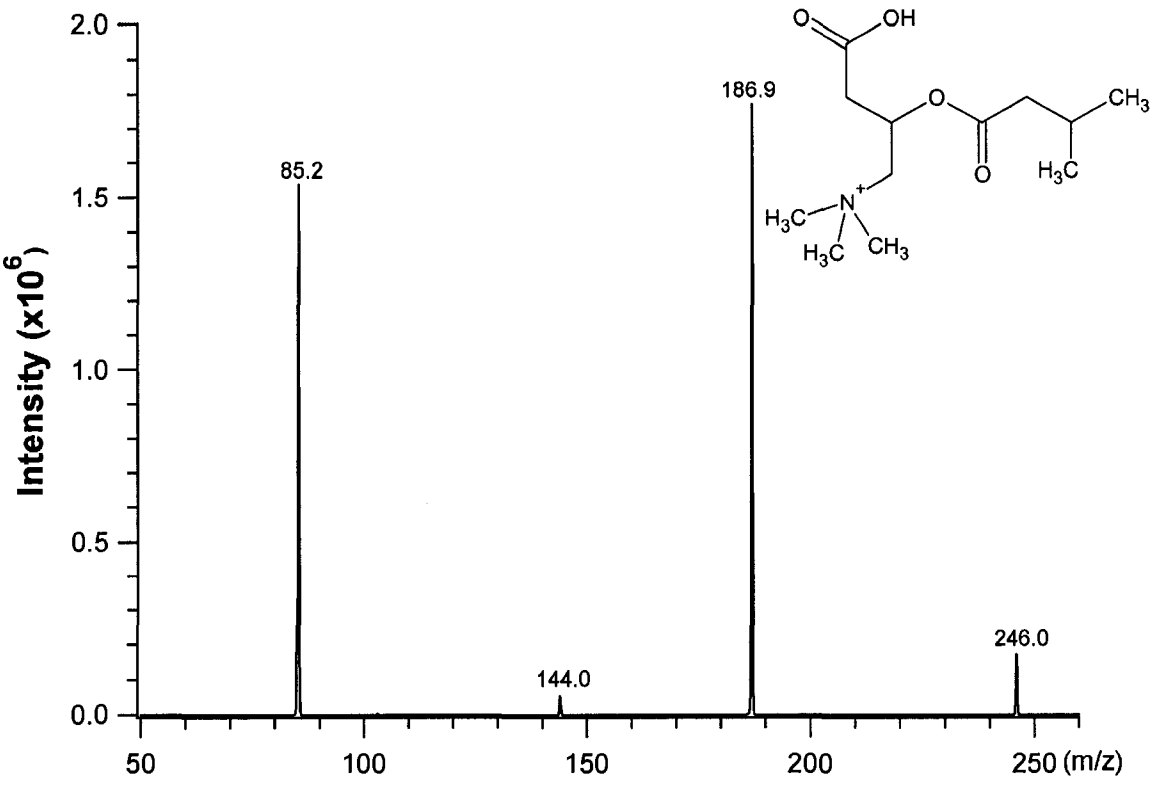

Figure 6.16 - MS/MS spectrum for Isovarylcarnitine

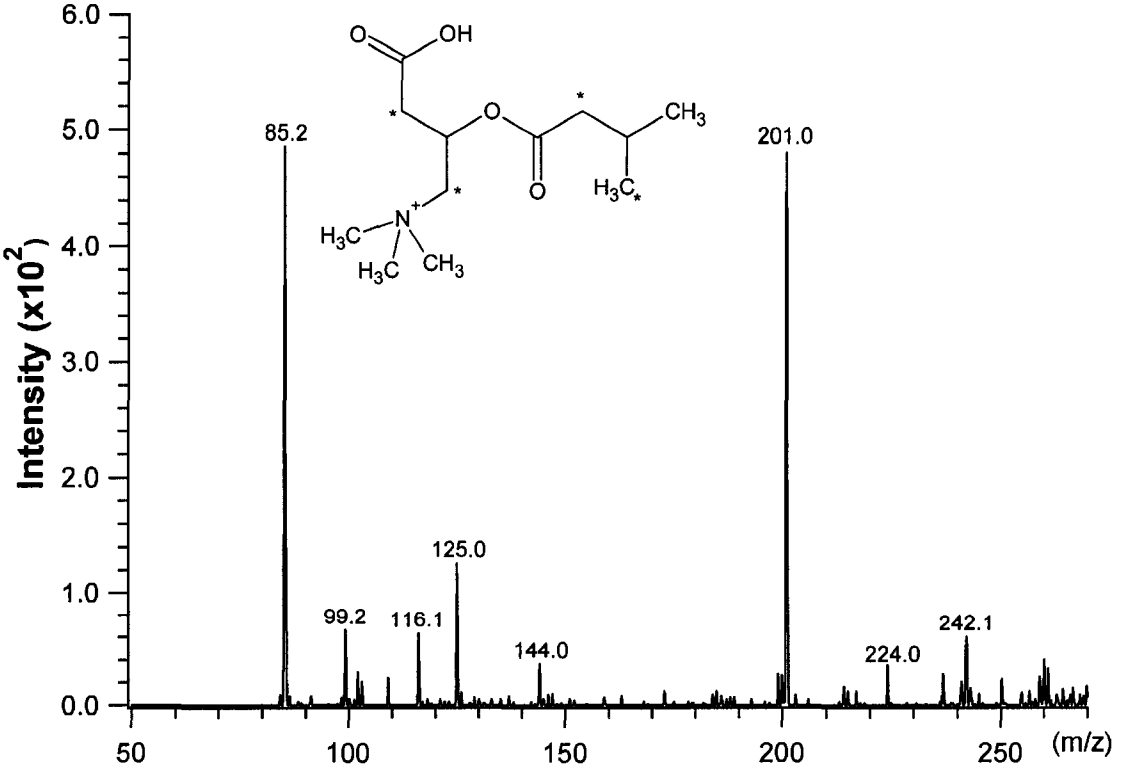

Figure 6.17 - MS/MS spectrum for Isovarylcarnitine metabolite m/z 260

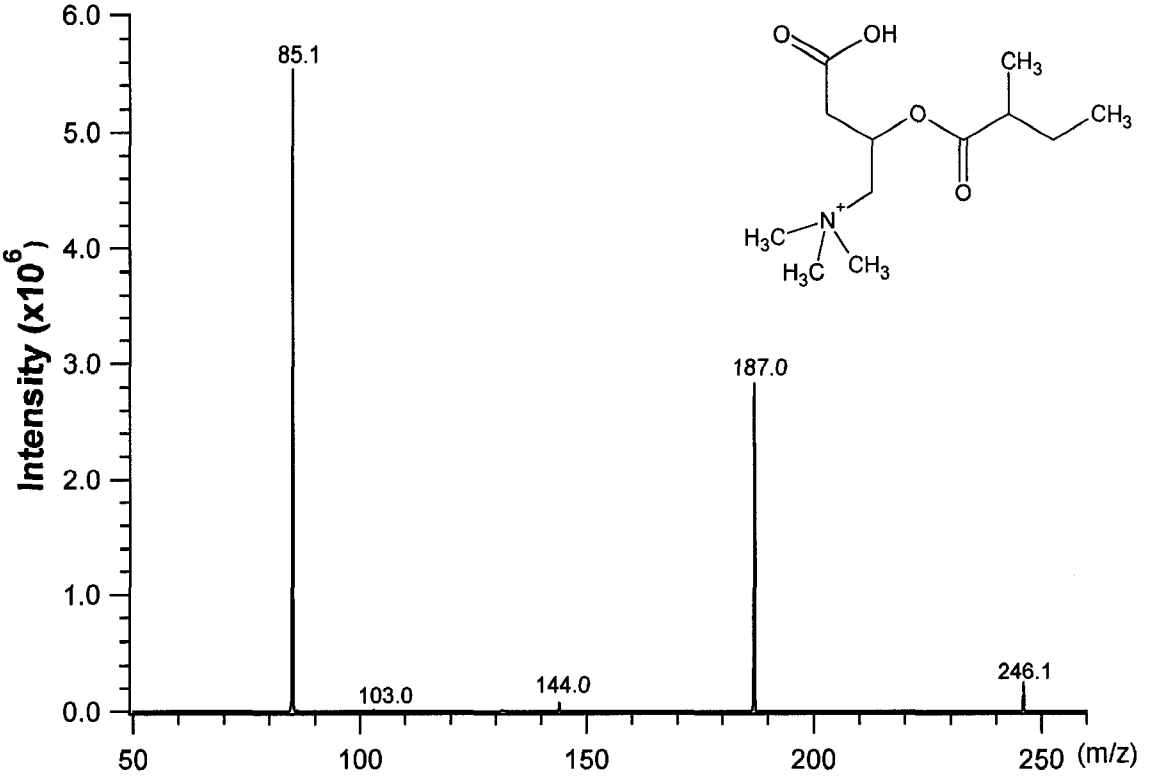

Figure 6.18 - MS/MS spectrum for 2-methylbutyroylcarnitine

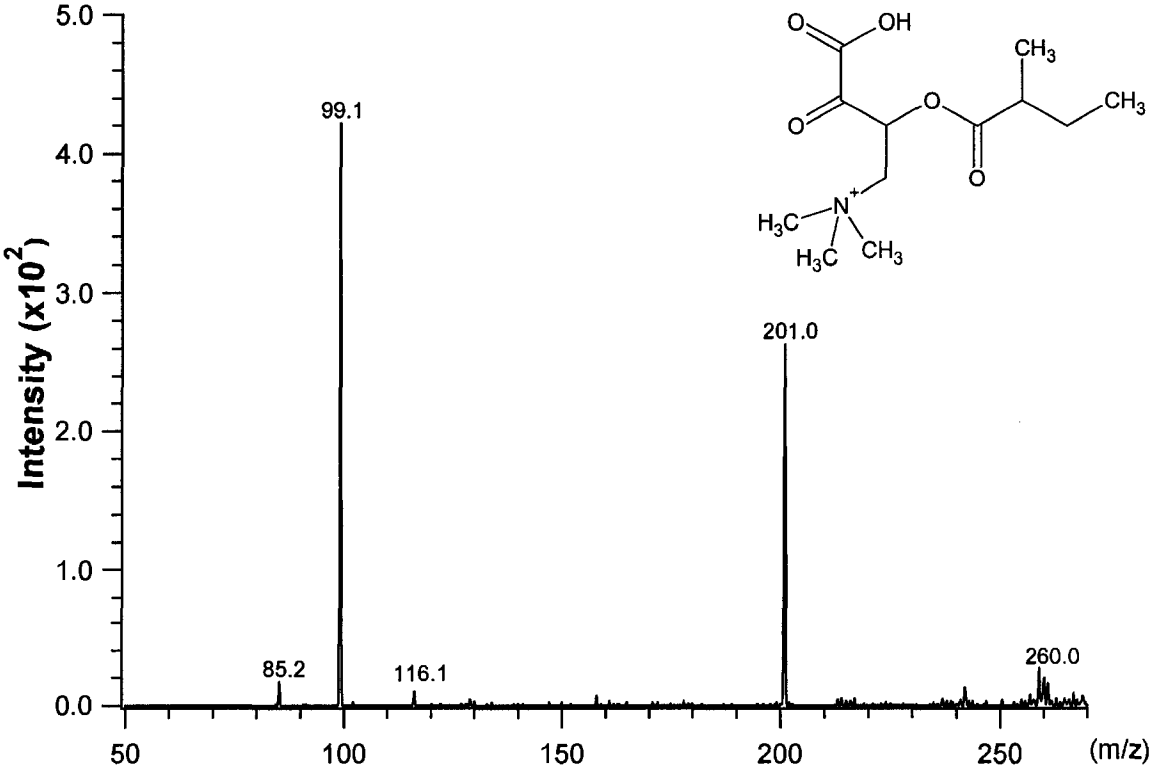

Figure 6.19 - MS/MS spectrum for 2-methylbutyroylcarnitine metabolite m/z 260

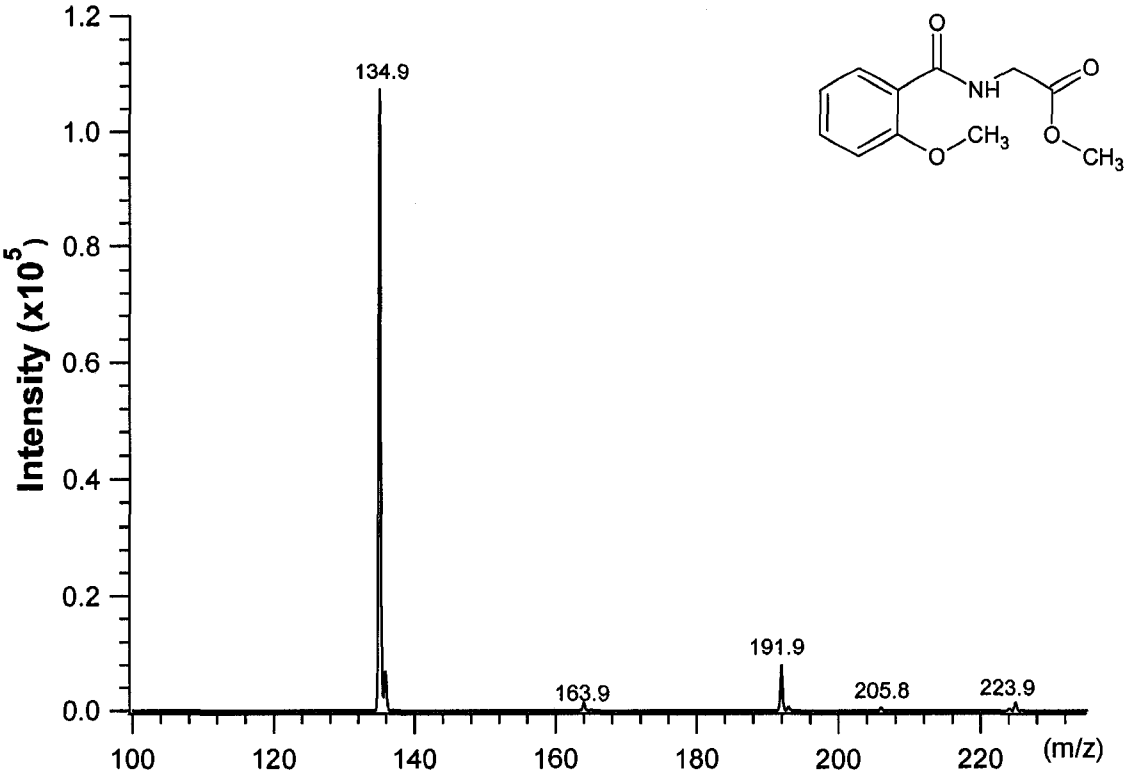

Figure 6.20 - MS/MS spectrum for methyl o-methoxyhippuric acid

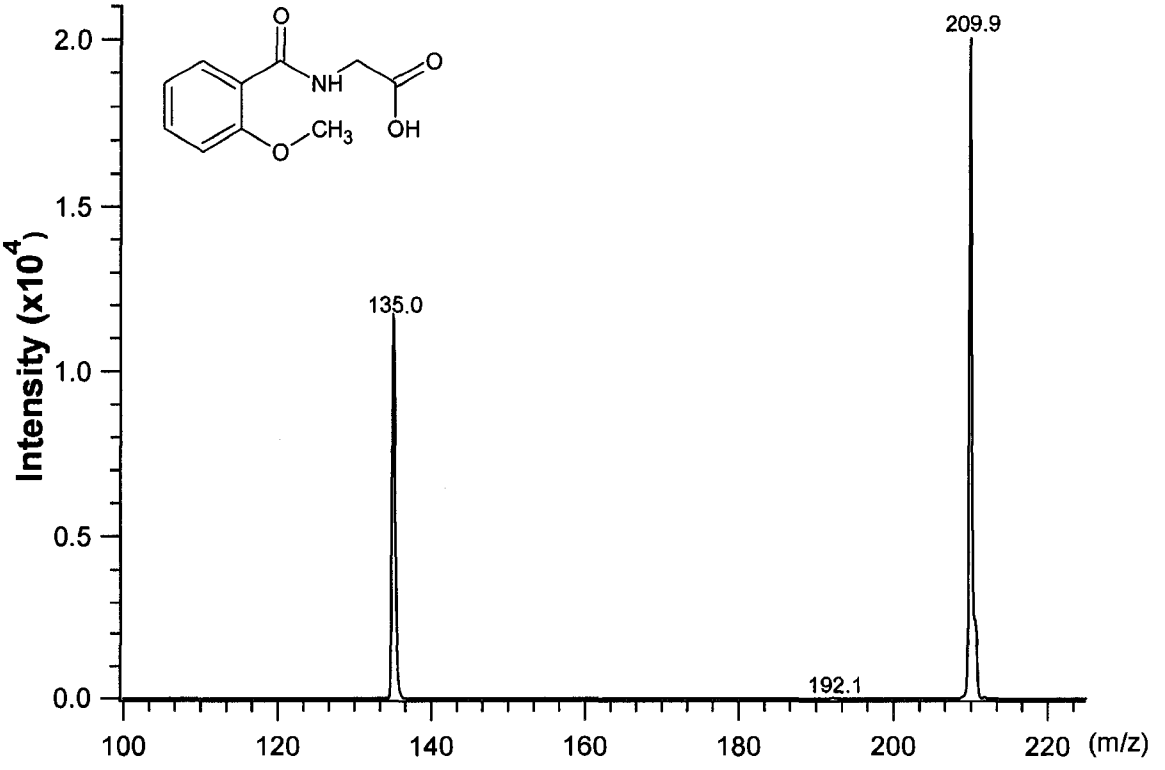

Figure 6.21 - MS/MS spectrum for methyl o-methoxyhippuric acid metabolite m/z 210

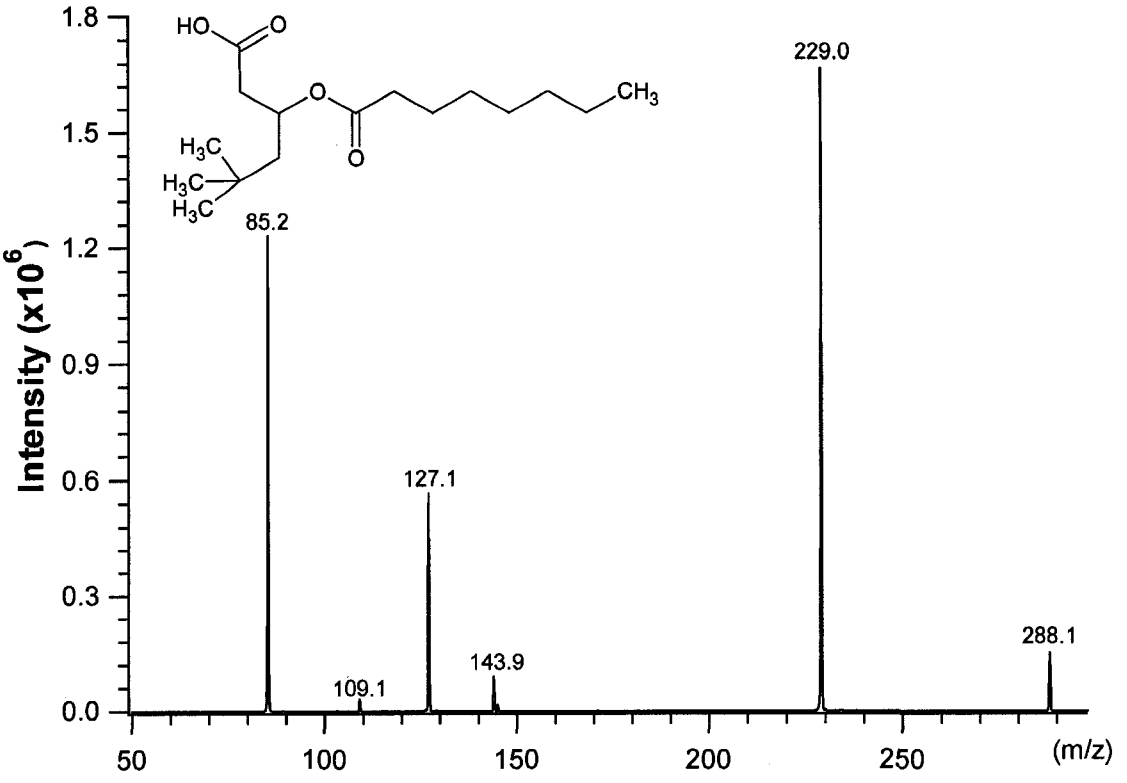

Figure 6.22 - MS/MS spectrum for octanoylcarnitine

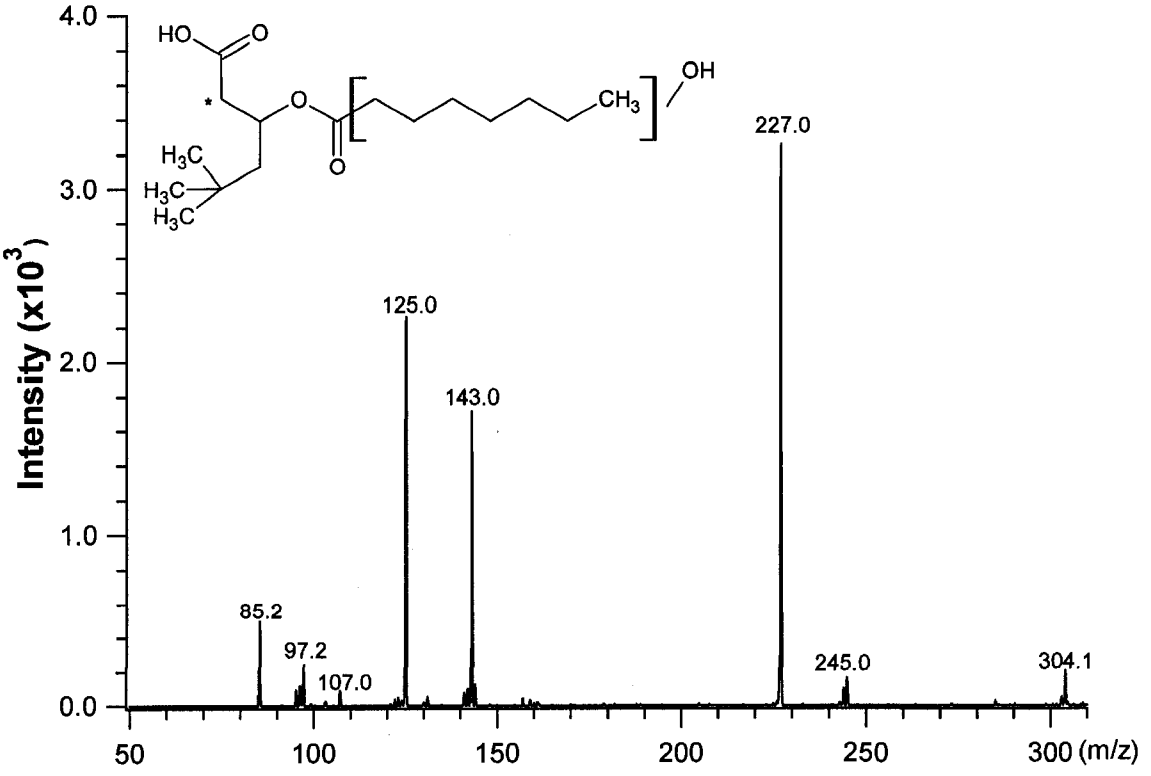

Figure 6.23 - MS/MS spectrum for octanoylcarnitine metabolite m/z 304

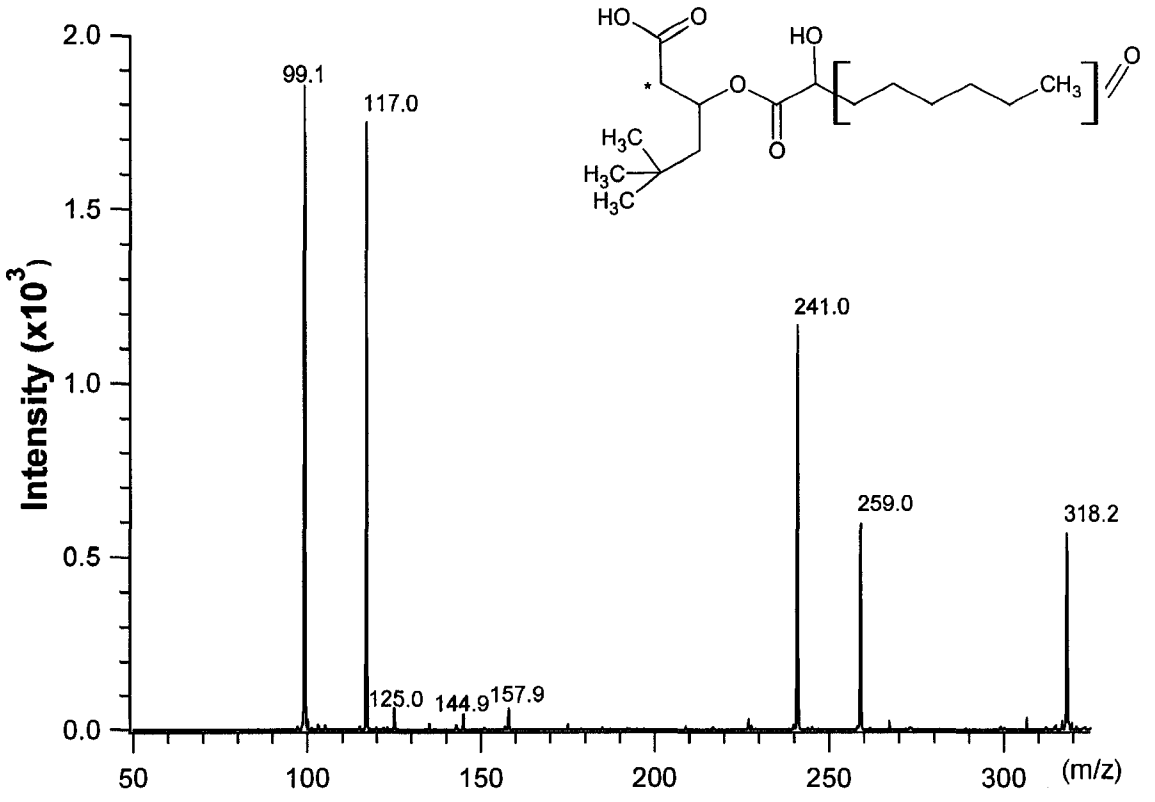

Figure 6.24 - MS/MS spectrum for octanoylcarnitine metabolite m/z 318

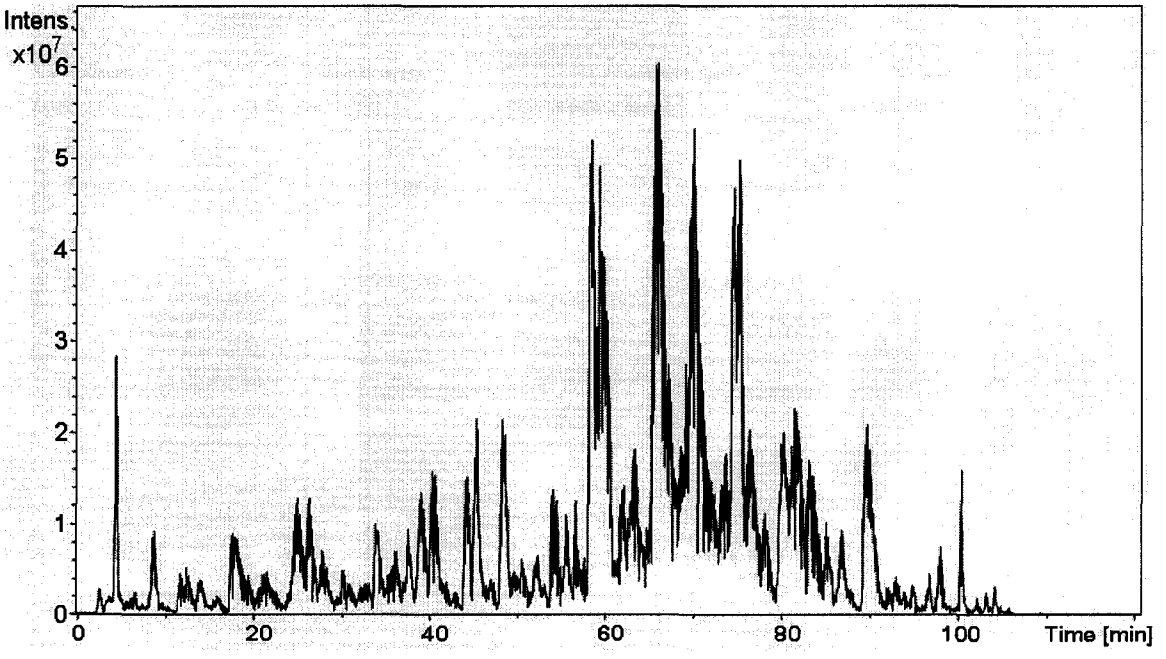

Figure 6.25 - FT-ICR-MS BPC 90 - 370 m/z, urine prepared using SPE

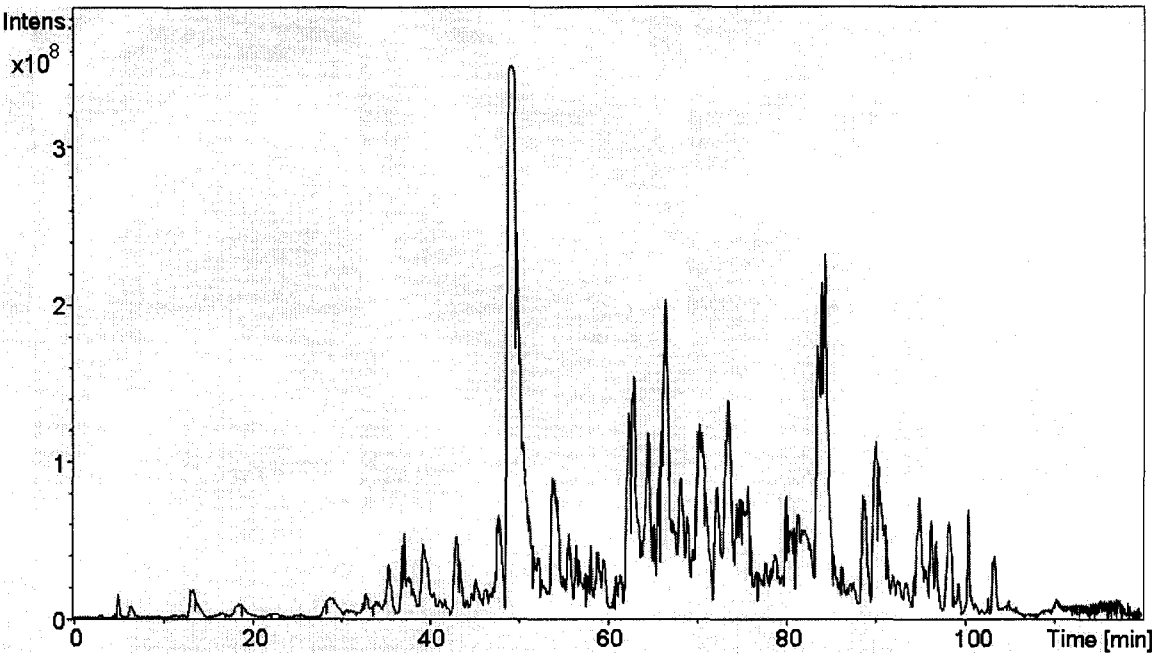

Figure 6.26 - FT-ICR-MS BPC 300 - 650 m/z, urine prepared using SPE

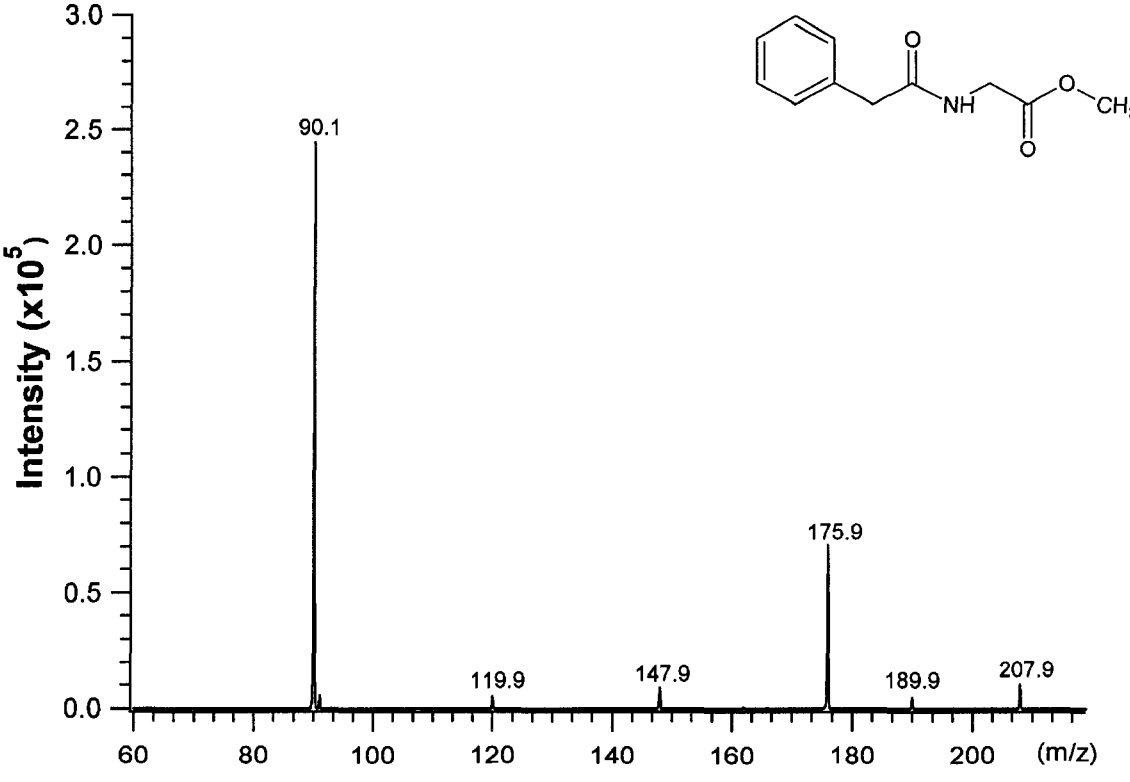

Figure 6.27 - MS/MS spectrum for phenylacetylglycine methyl ester

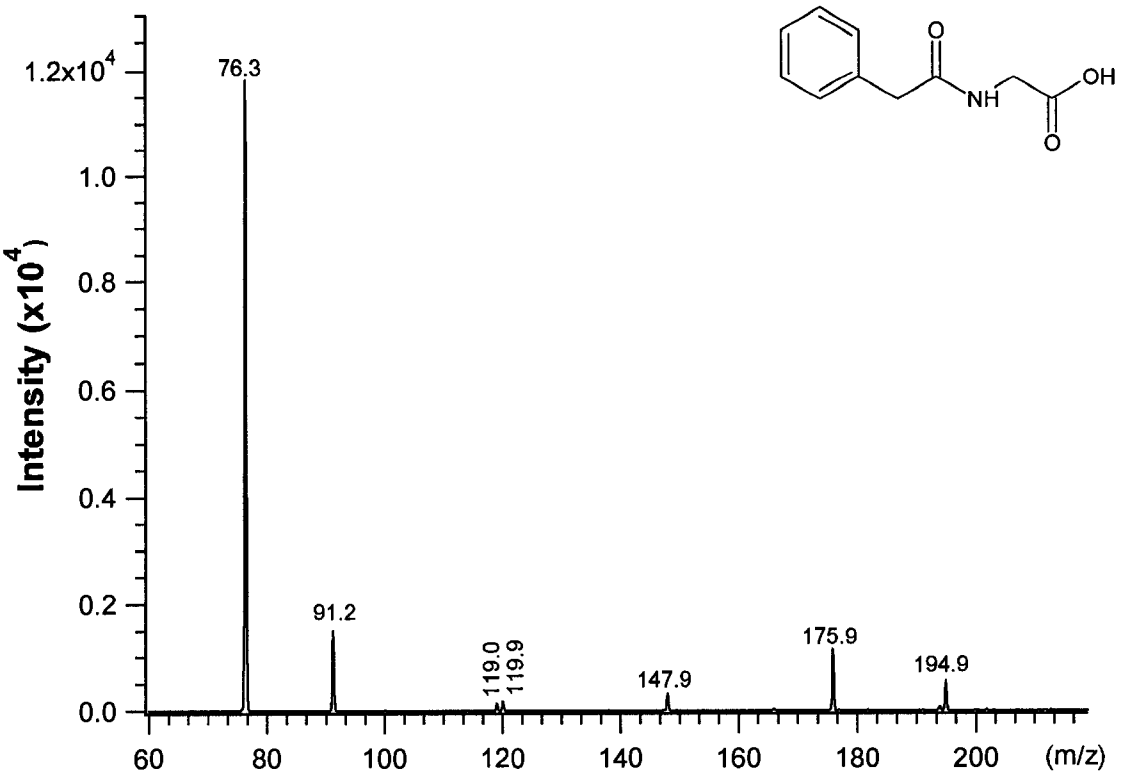

Figure 6.28 - MS/MS spectrum for phenylacetylglycine methyl ester metabolite m/z 194

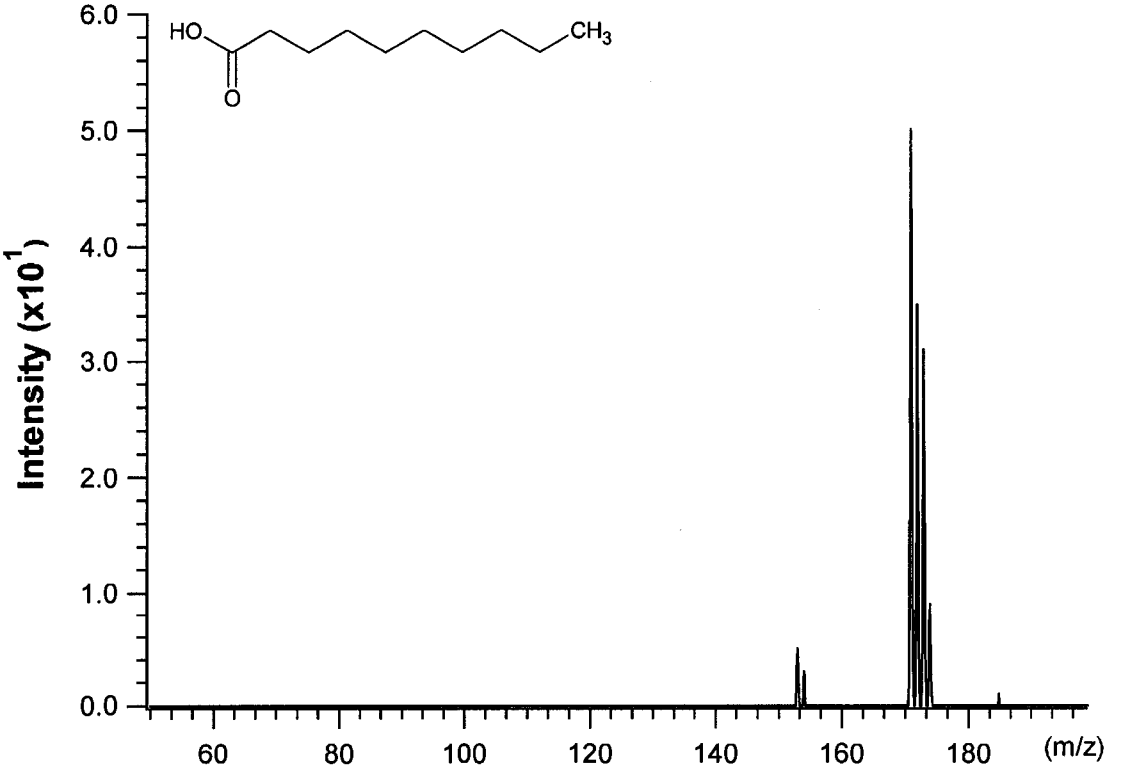

Figure 6.29 - MS/MS spectrum for capric acid

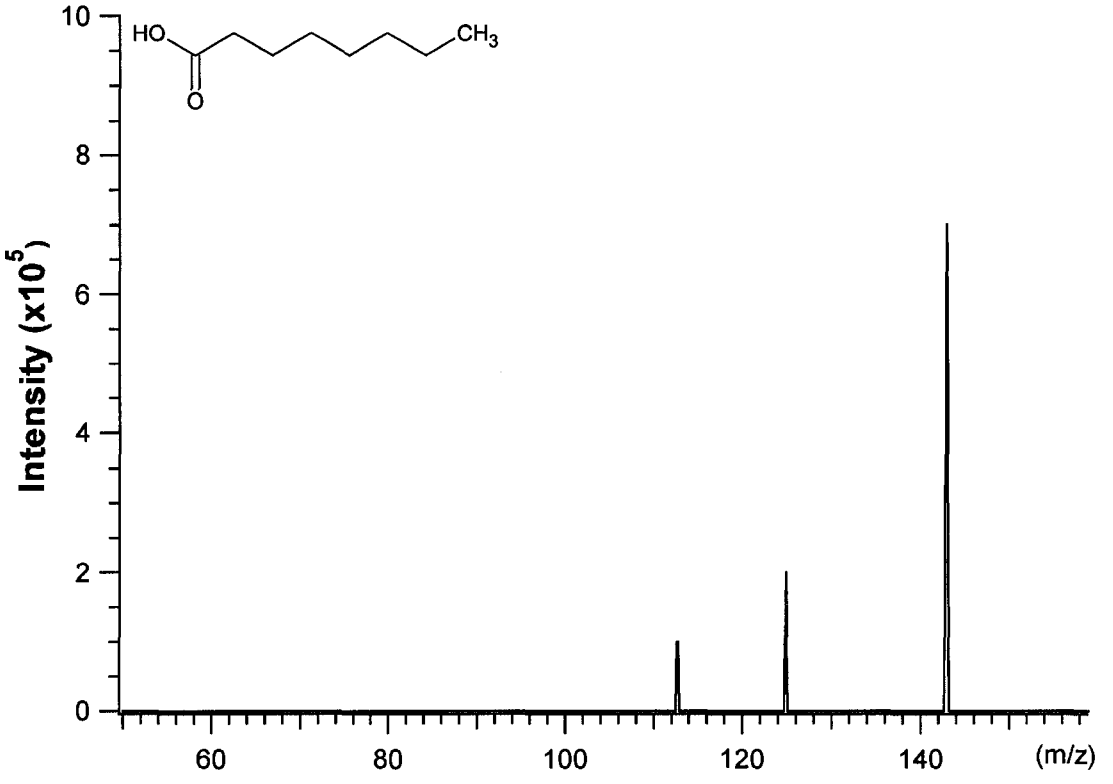

Figure 6.30 - MS/MS spectrum for caprylic acid

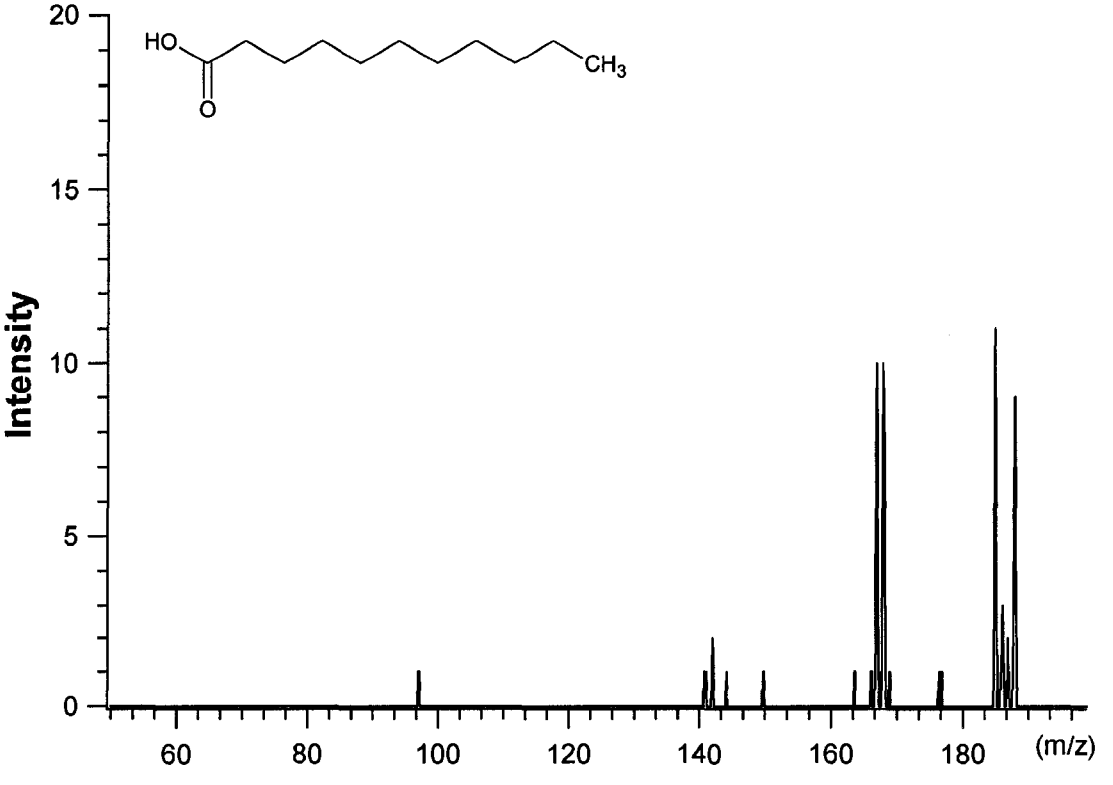

Figure 6.31 - MS/MS spectrum for undecanoic acid

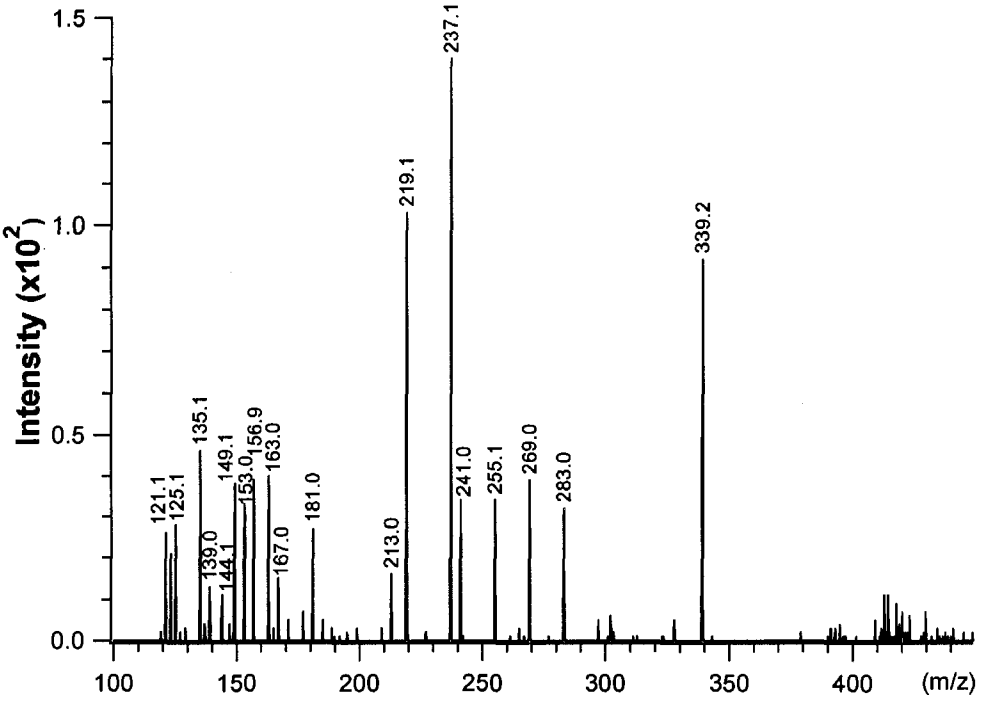

Figure 6.32 - MS/MS spectrum for palmitoylcarnitine metabolite m/z 416, UPLC separation 12.6 to 12.9 minutes

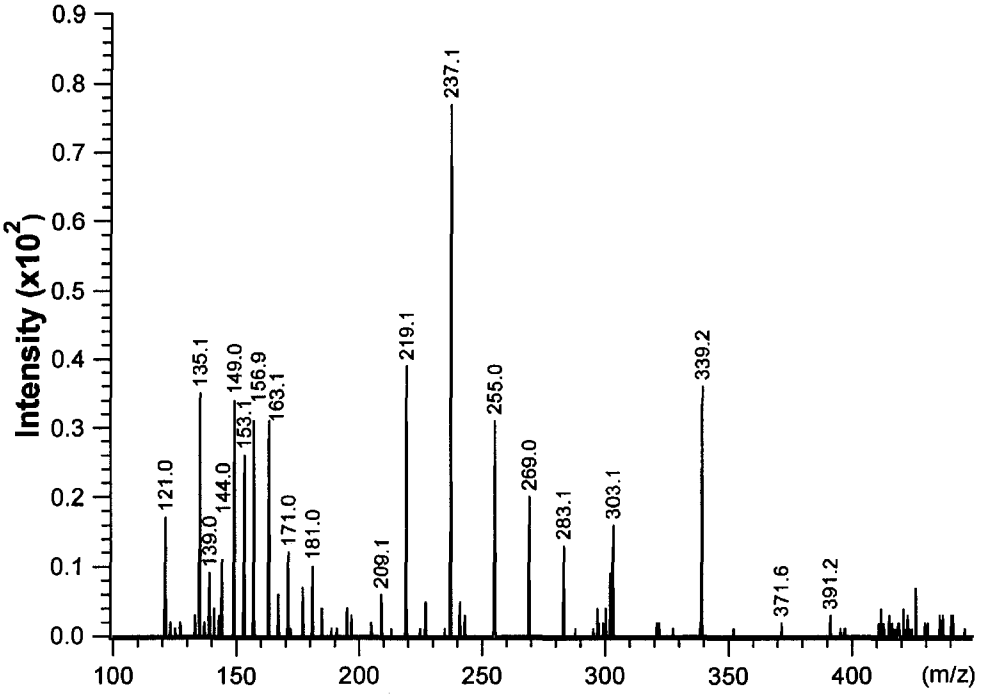

Figure 6.33 - MS/MS spectrum for palmitoylcarnitine metabolite m/z 416, UPLC separation 13.4 to 13.6 minutes

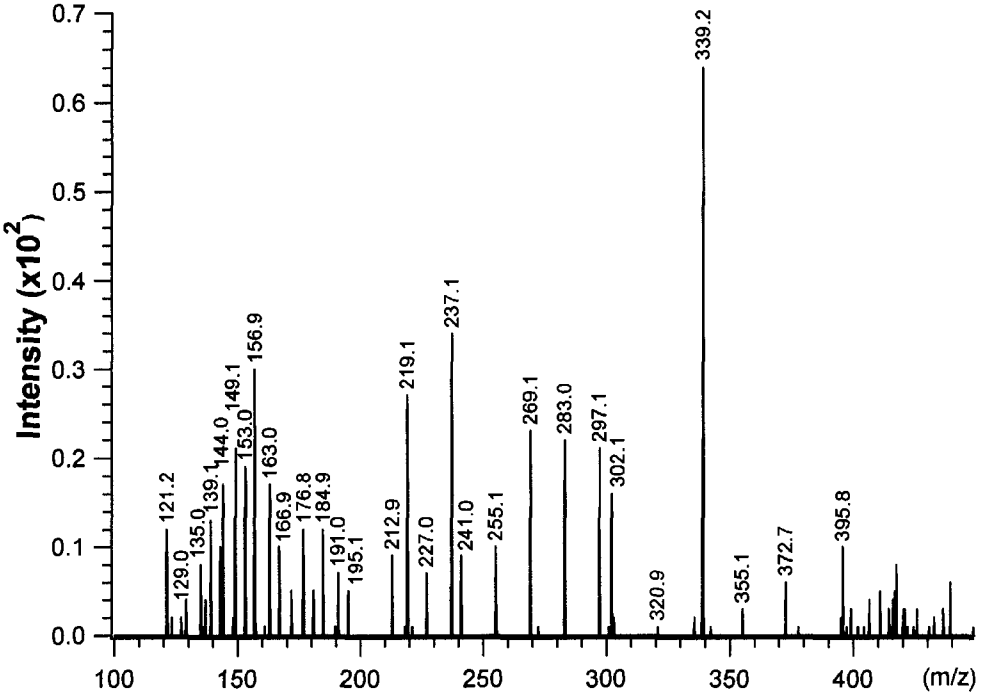

Figure 6.34 - MS/MS spectrum for palmitoylcarnitine metabolite m/z 416, UPLC separation 14.0 to 14.5 minutes

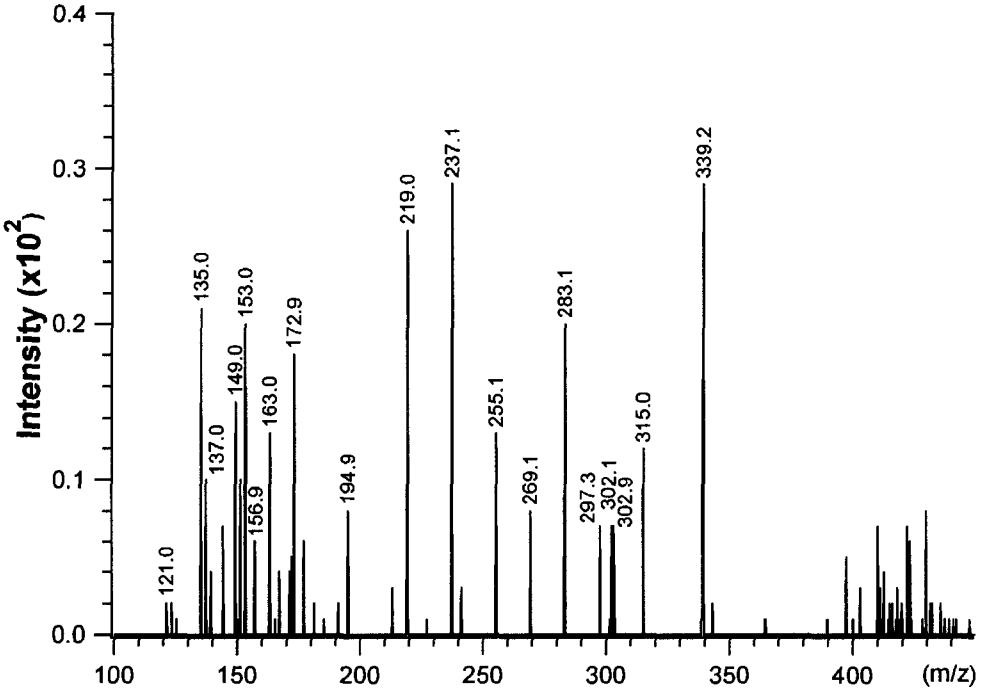

Figure 6.35 - MS/MS spectrum for palmitoylcarnitine metabolite m/z 416, UPLC separation 14.8 to 15.1 minutes

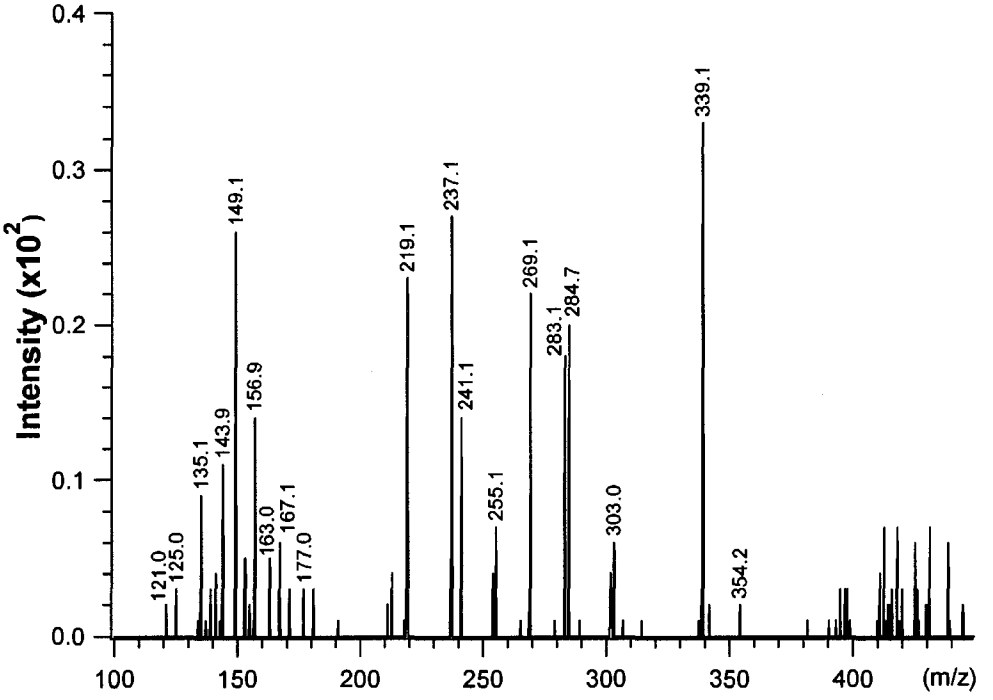

Figure 6.36 - MS/MS spectrum for palmitoylcarnitine metabolite m/z 416, UPLC separation 16.0 to 16.3 minutes

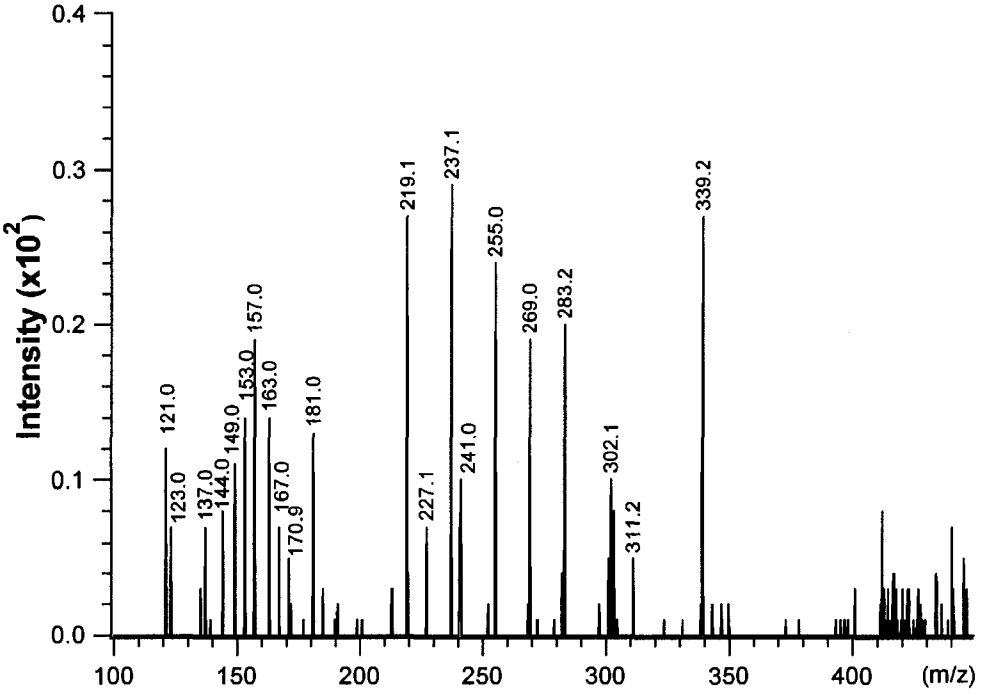

Figure 6.37 - MS/MS spectrum for palmitoylcarnitine metabolite m/z 416, UPLC separation 17.2 to 17.8 minutes

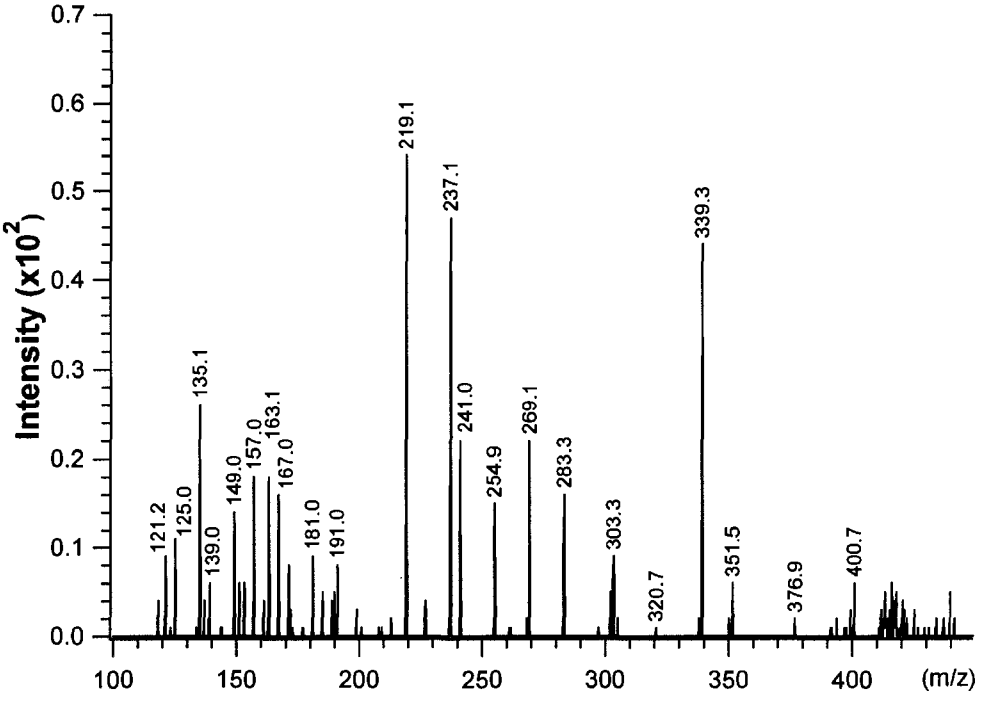

Figure 6.38 - MS/MS spectrum for palmitoylcarnitine metabolite m/z 416, UPLC separation 19.0 to 19.5 minutes

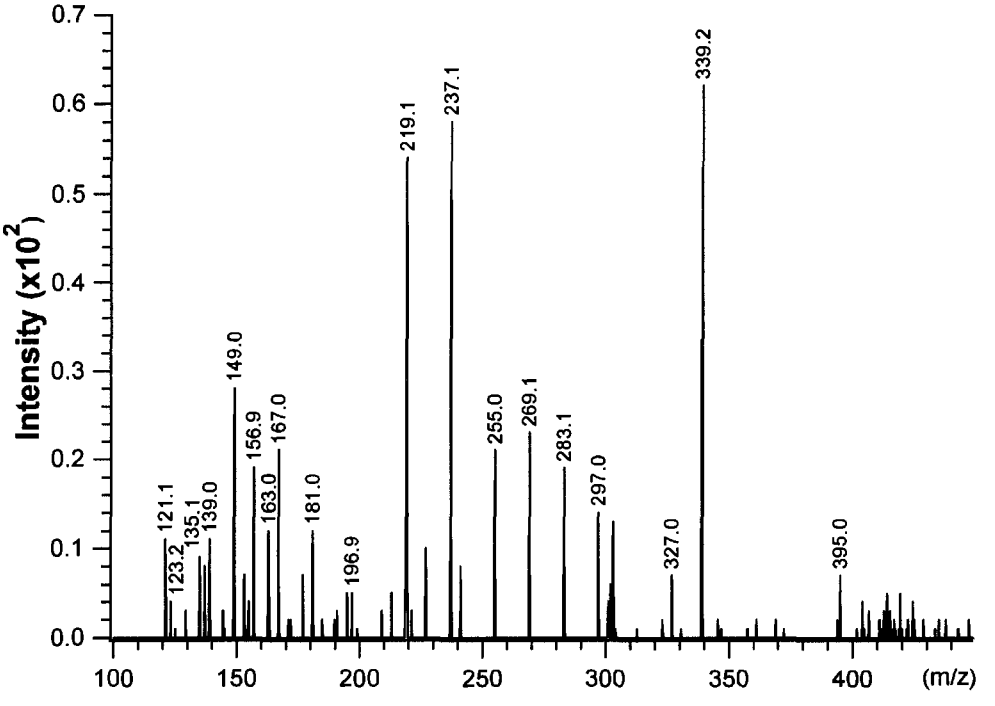

Figure 6.39 - MS/MS spectrum for palmitoylcarnitine metabolite m/z 416, UPLC separation 20.9 to 21.4 minutes

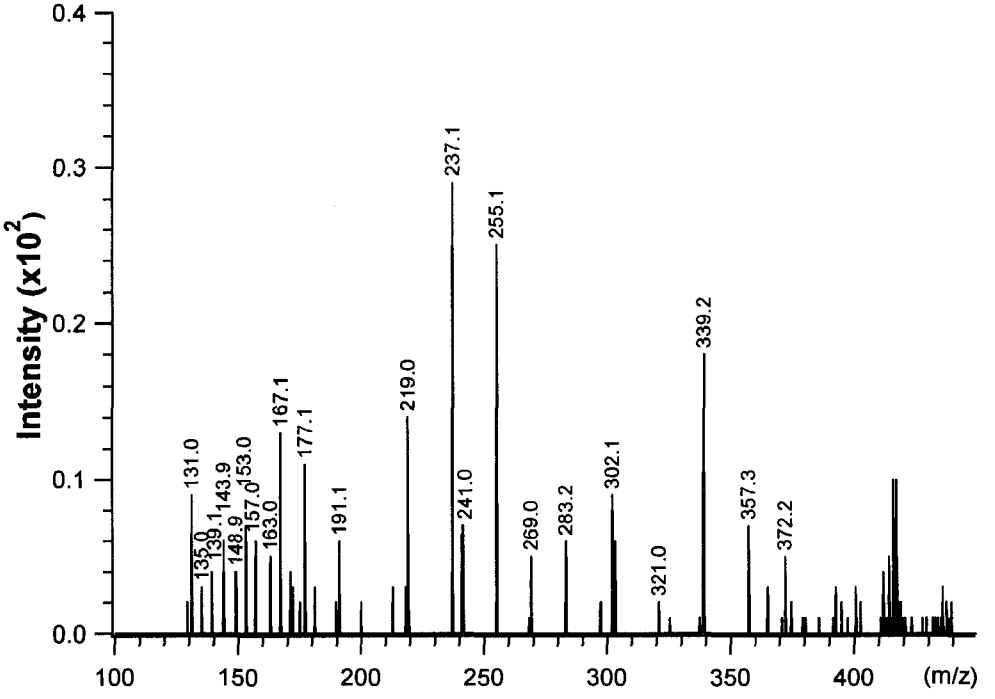

Figure 6.40 - MS/MS spectrum for palmitoylcarnitine metabolite m/z 416, UPLC separation 23.3 to 23.6 minutes

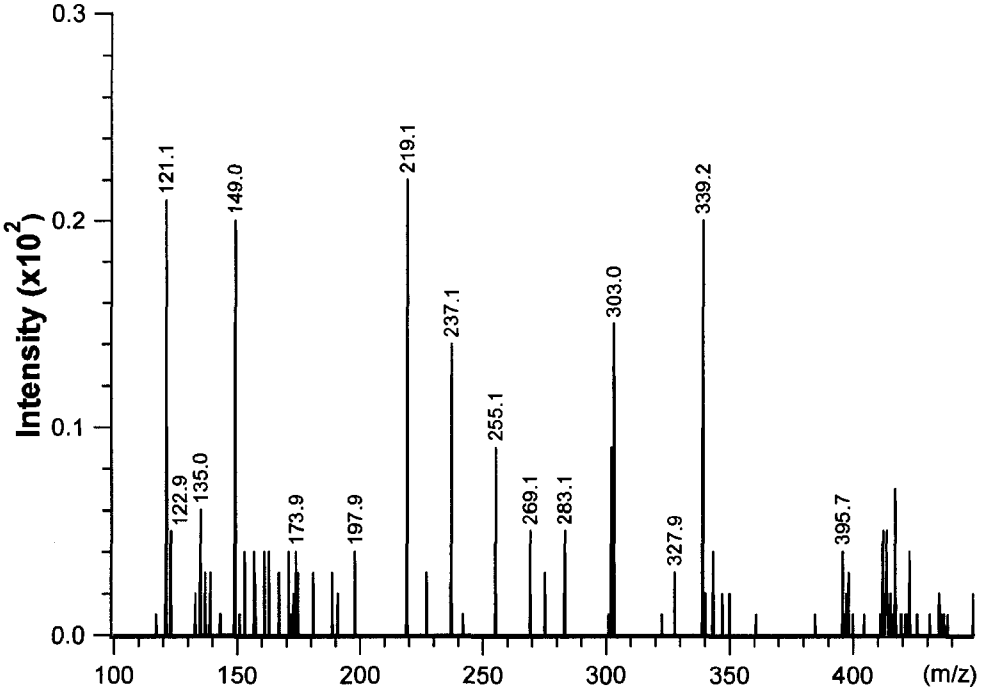

Figure 6.41 - MS/MS spectrum for palmitoylcarnitine metabolite m/z 416, UPLC separation 26.4 to 26.7 minutes

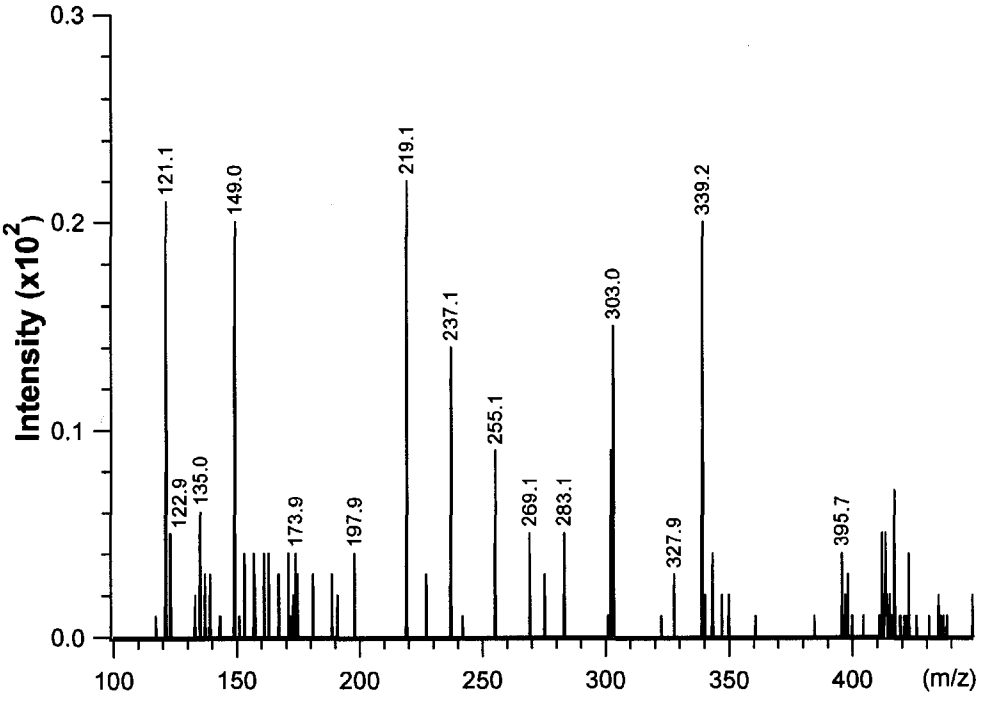

Figure 6.42 - MS/MS spectrum for palmitoylcarnitine metabolite m/z 416, UPLC separation 30.4 to 30.6 minutes

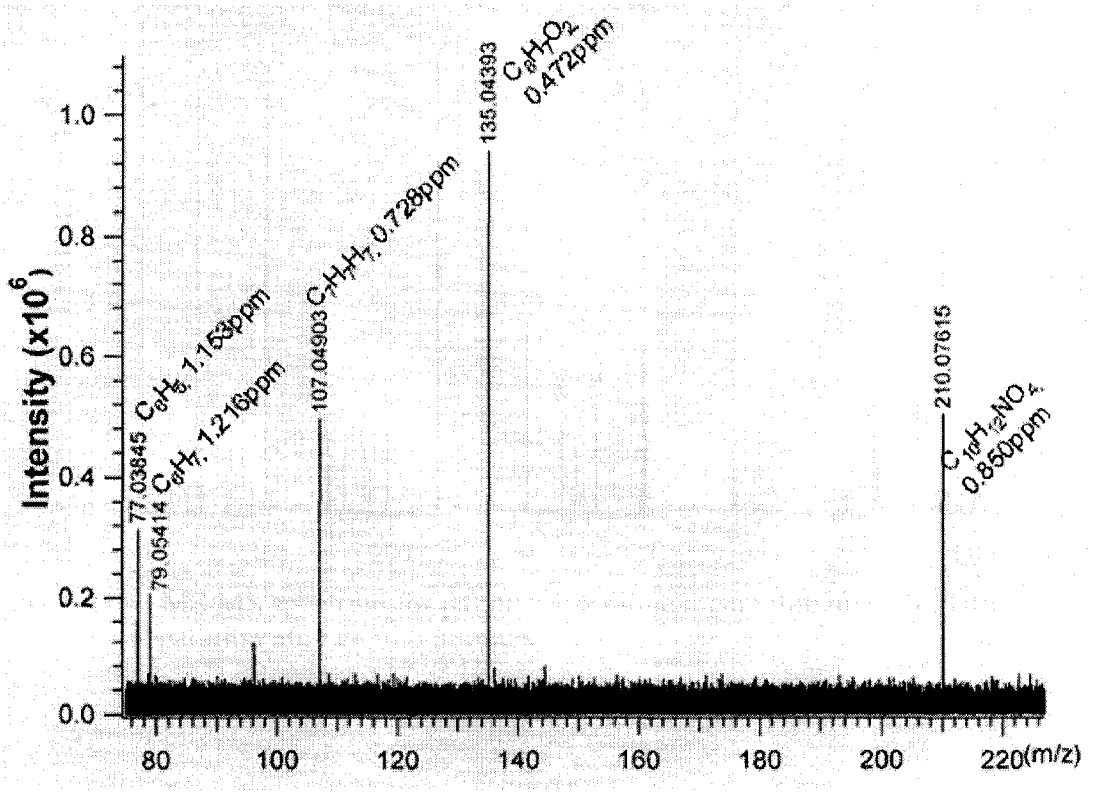

Figure 6.43 - FT-MS/MS of o-methoxyhippuric acid standard

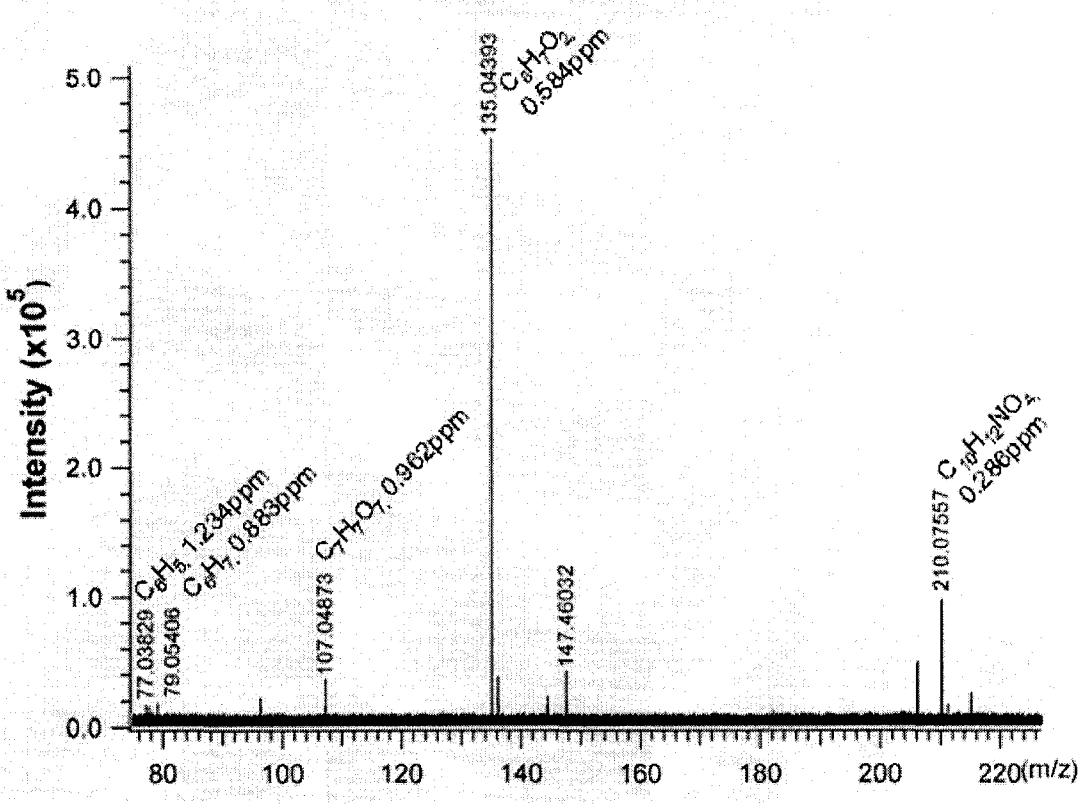

Figure 6.44 - FT-MS/MS analysis of p or m-methyoxyhippuric acid found in a urine sample

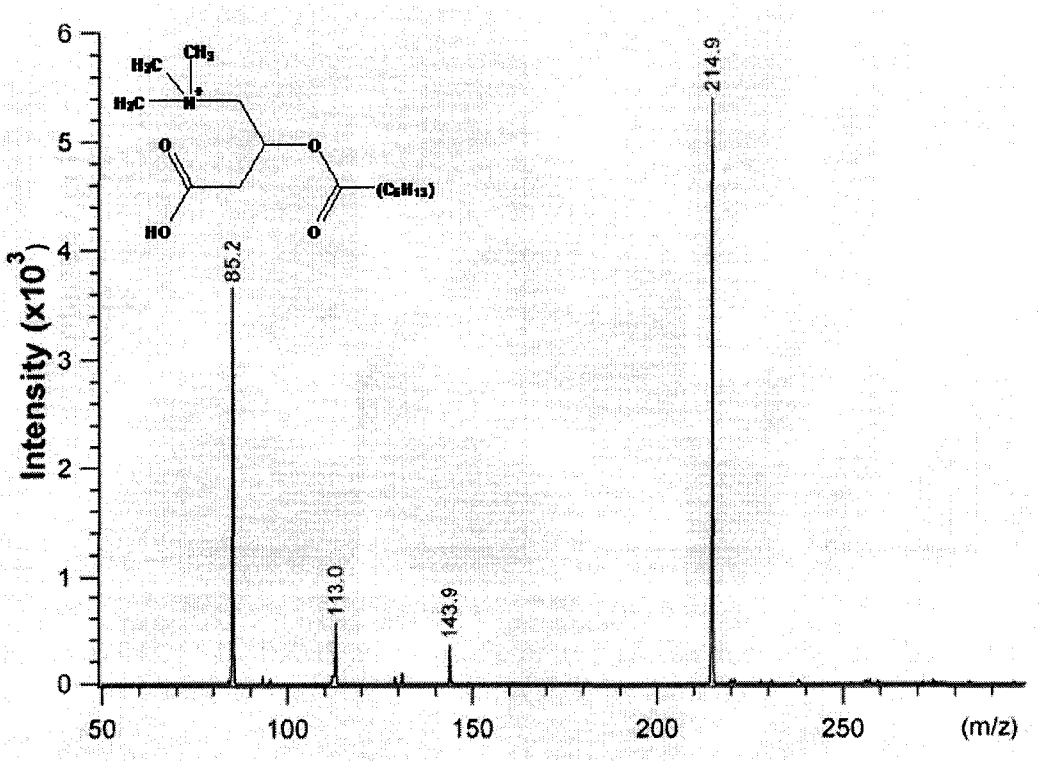

Figure 6.45 - Esquire MS/MS analysis of m/z 274 at 5.9 min and proposed structure

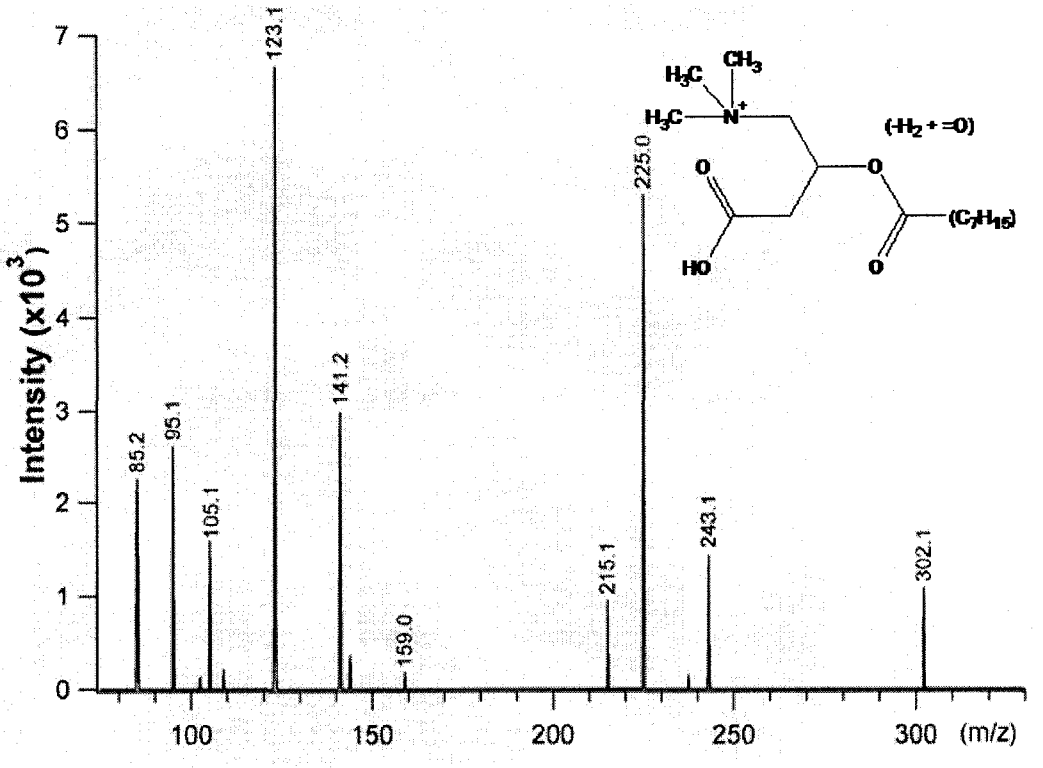

Figure 6.46 - Esquire MS/MS analysis of m/z 302 at 24.1 min and proposed structure

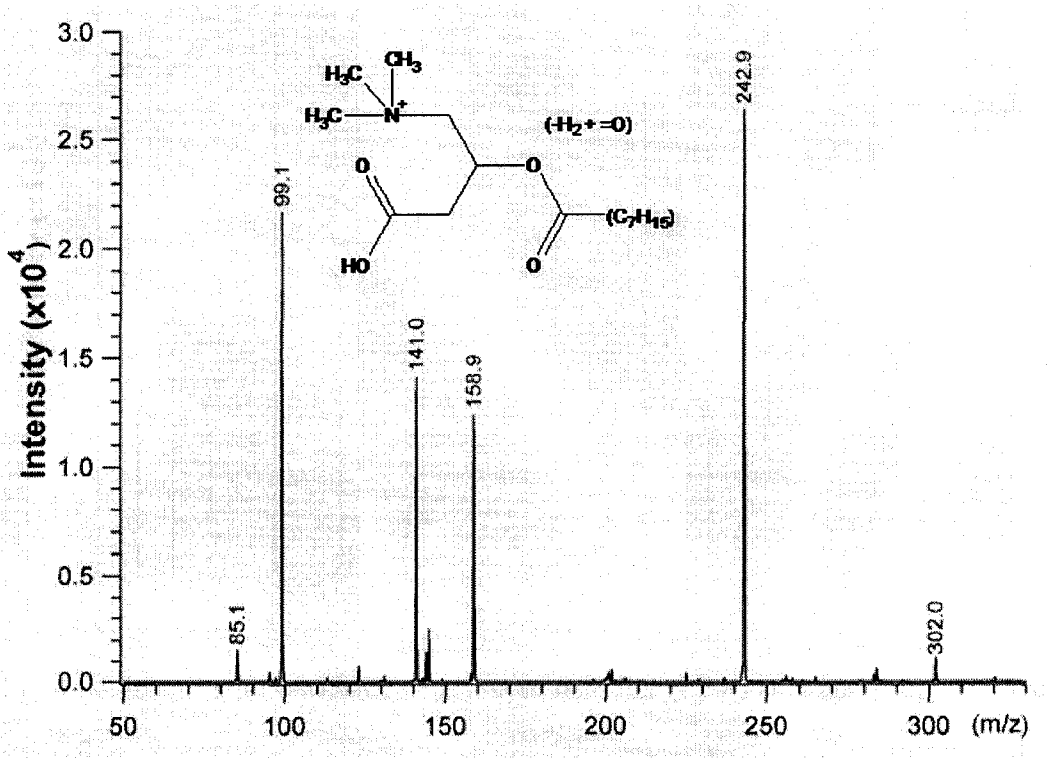

Figure 6.47 - Esquire MS/MS analysis of m/z 302 at 38.3 min and proposed structure

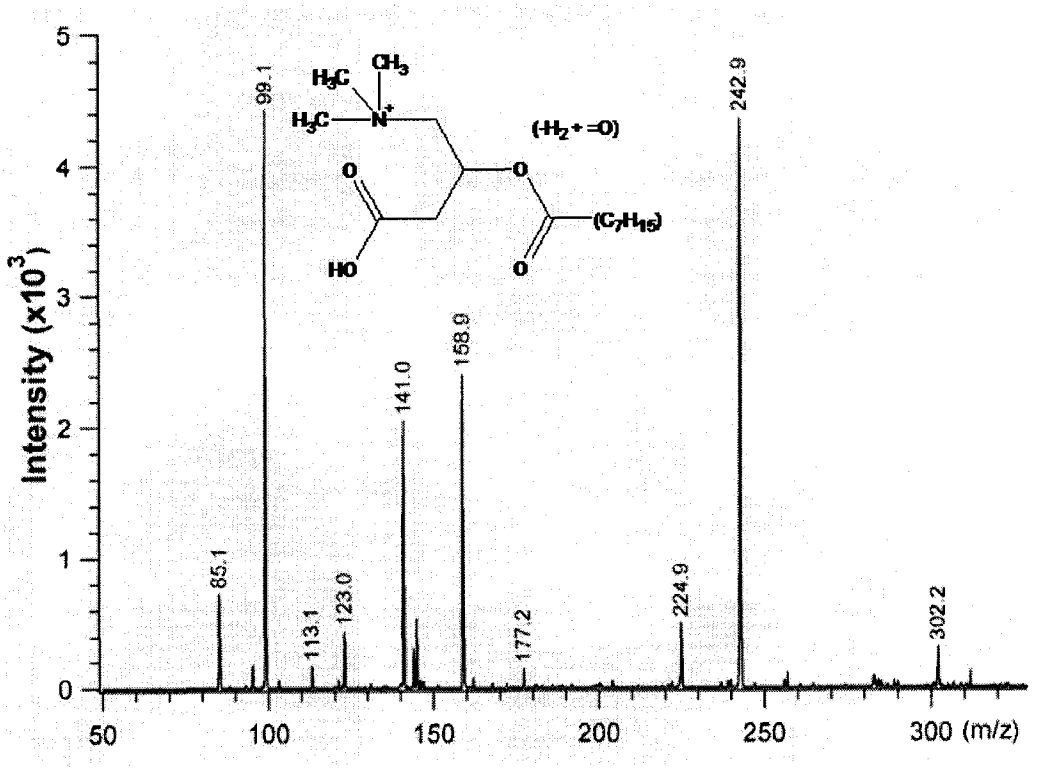

Figure 6.48 - Esquire MS/MS analysis of m/z 302 at 39.4 min and proposed structure

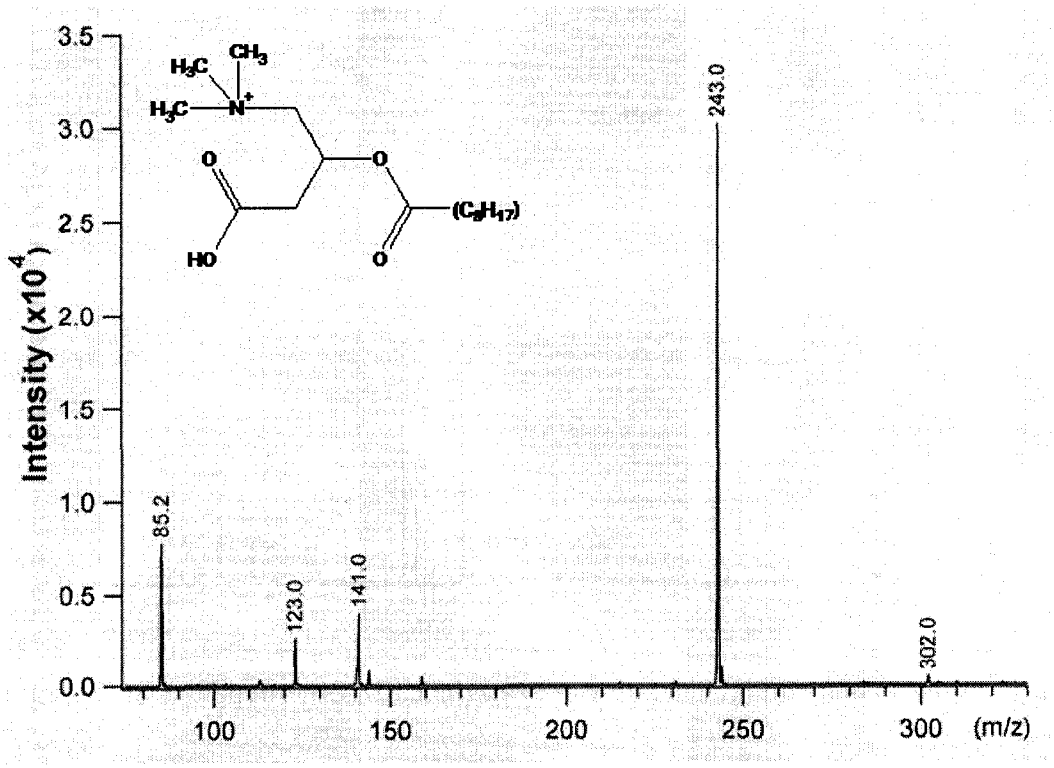

Figure 6.49 - Esquire MS/MS analysis of m/z 302b at 75.5 min and proposed structure

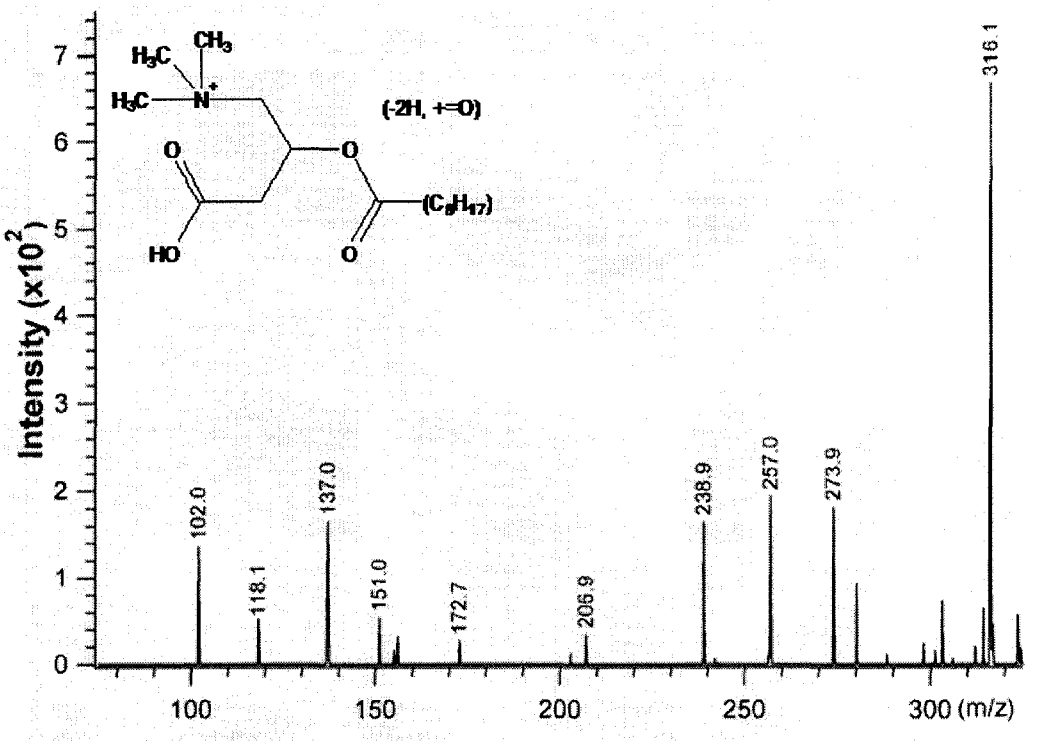

Figure 6.50 - Esquire MS/MS analysis of m/z 316 at 32.1 min and proposed structure

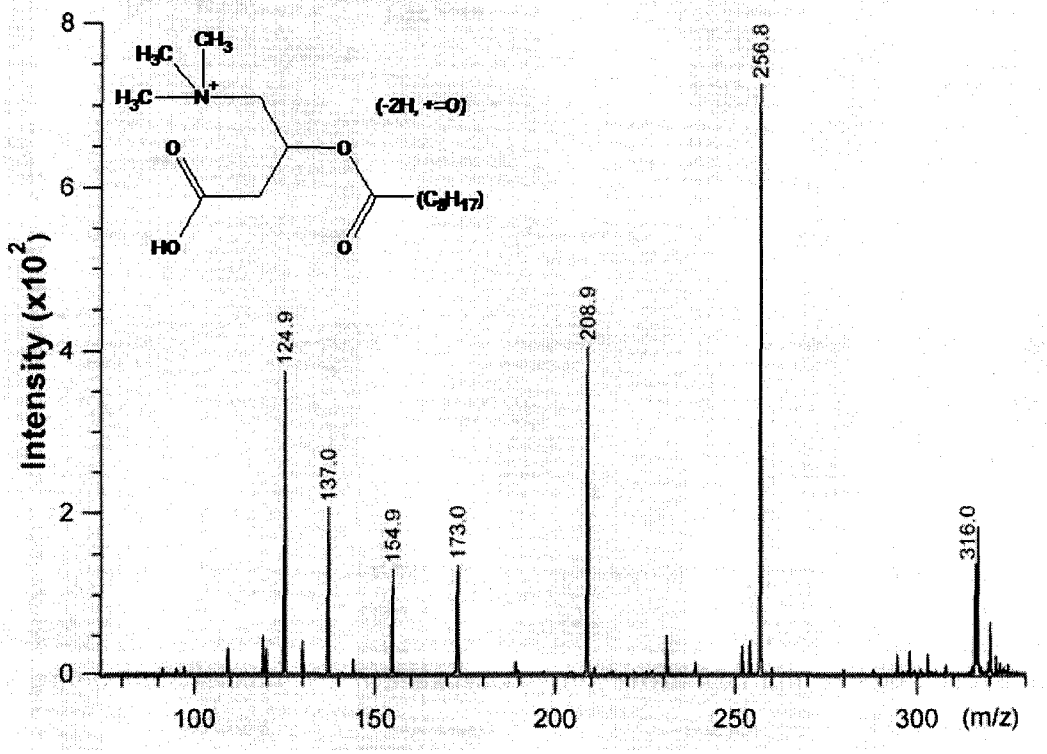

Figure 6.51 - Esquire MS/MS analysis of m/z 316 at 36.6 min and proposed structure

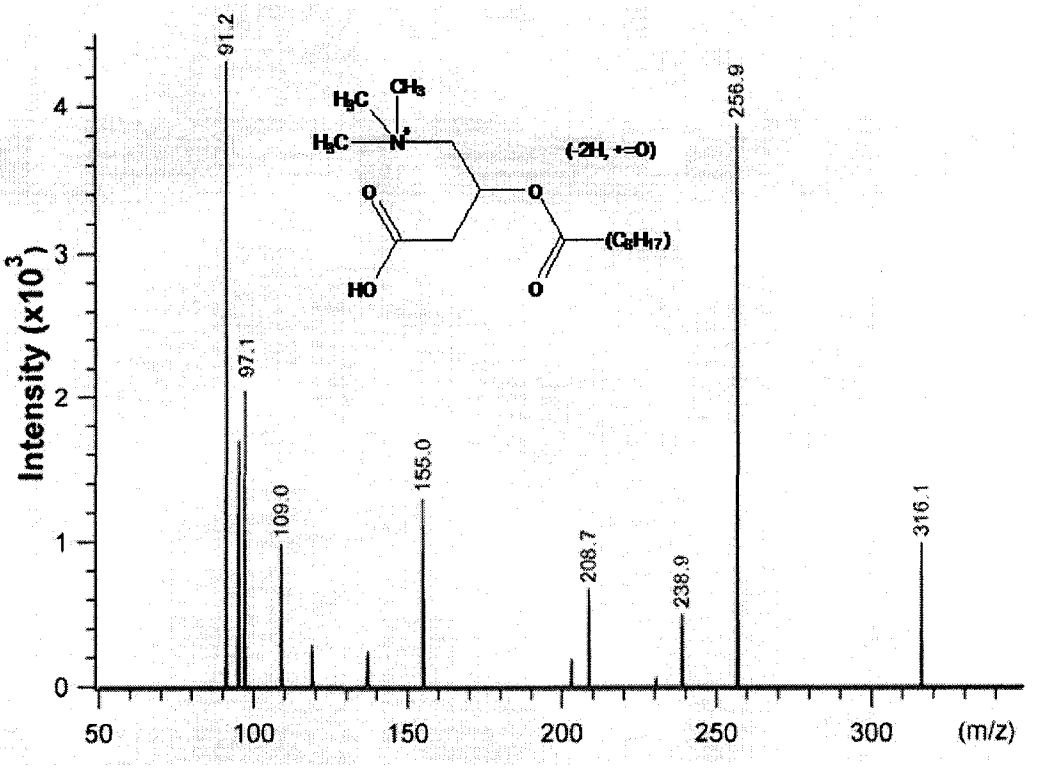

Figure 6.52 - Esquire MS/MS analysis of m/z 316 at 40.0 min and proposed structure

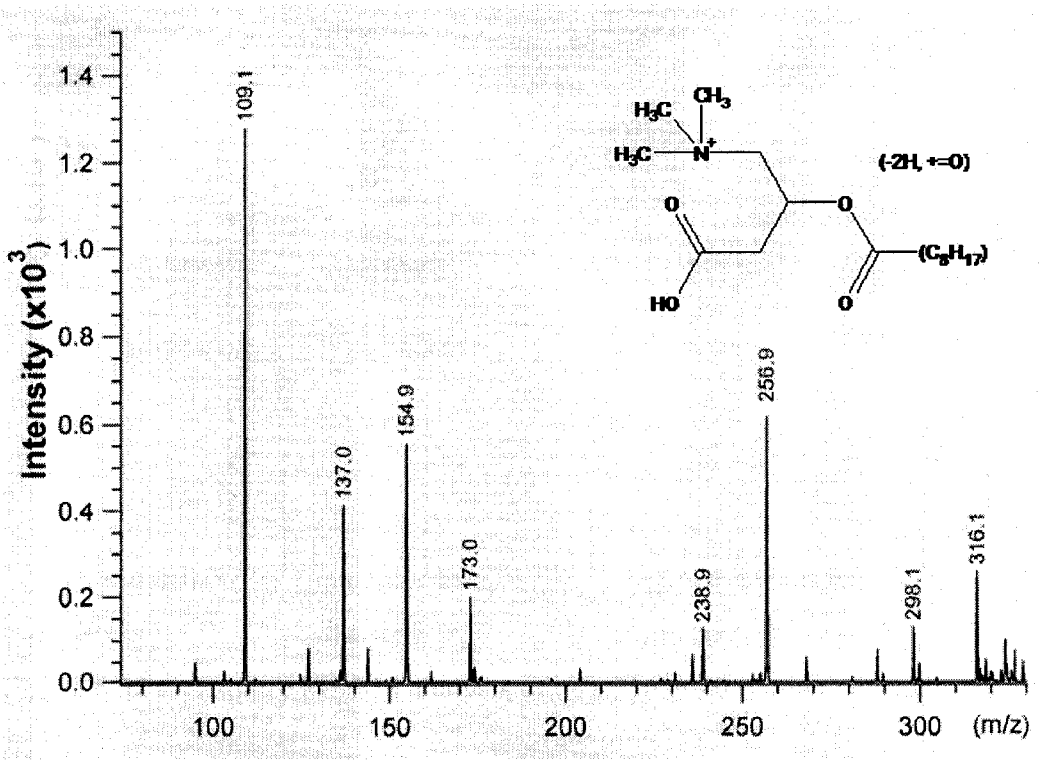

Figure 6.53 - Esquire MS/MS analysis of m/z 316 at 40.8 min and proposed structure

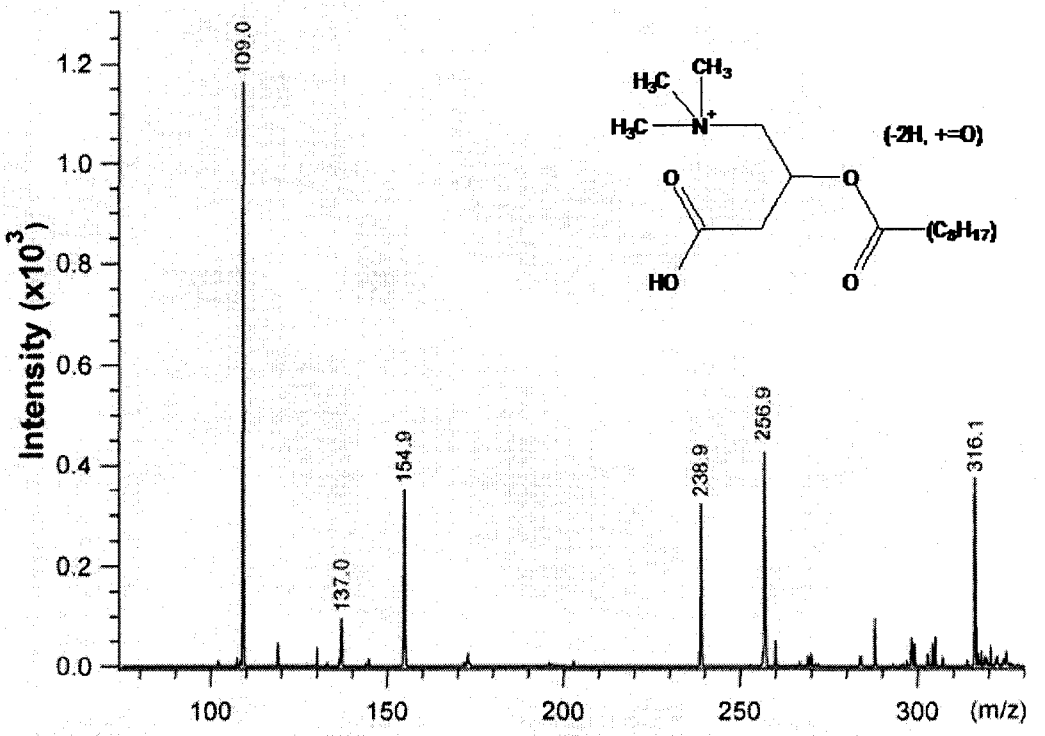

Figure 6.54 - Esquire MS/MS analysis of m/z 316 at 42.7 min and proposed structure

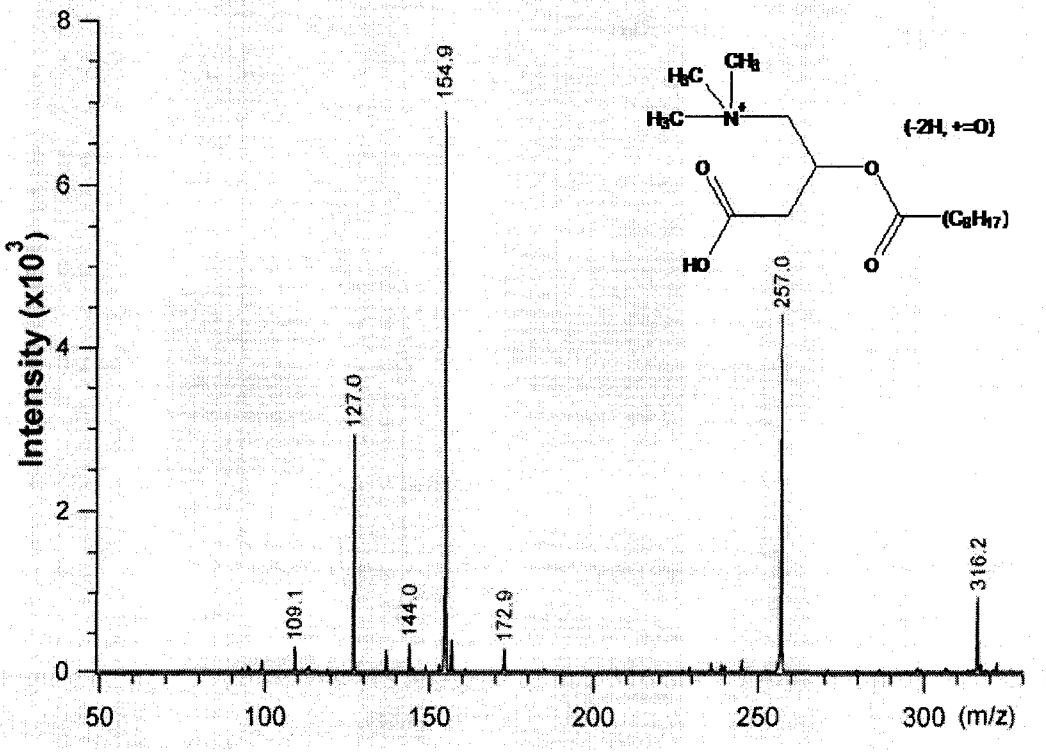

Figure 6.55 - Esquire MS/MS analysis of m/z 316 at 46.1 min and proposed structure

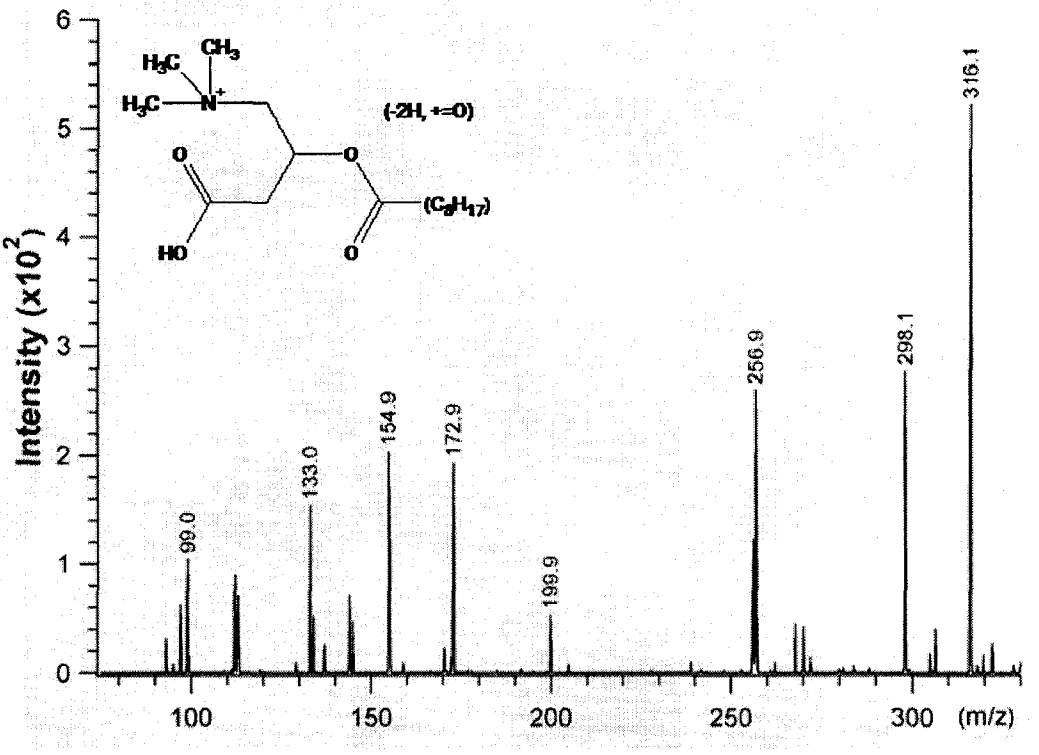

Figure 6.56 - Esquire MS/MS analysis of m/z 316 at 58.0 min and proposed structure

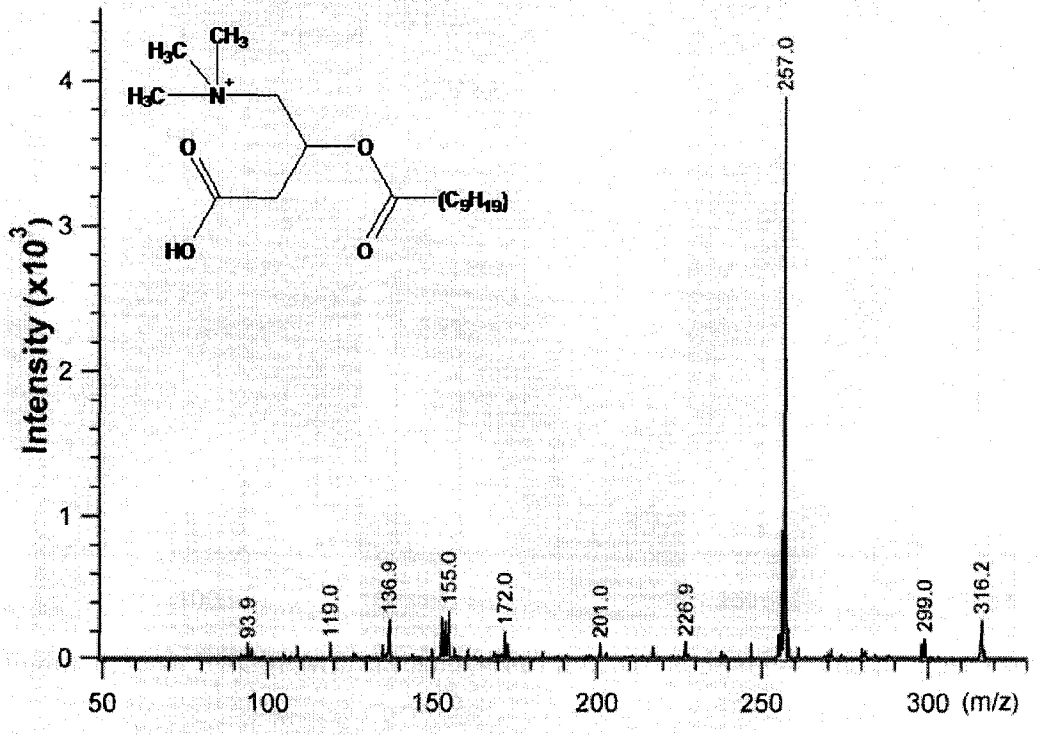

Figure 6.57 - Esquire MS/MS analysis of m/z 316b at 82.3 min and proposed structure

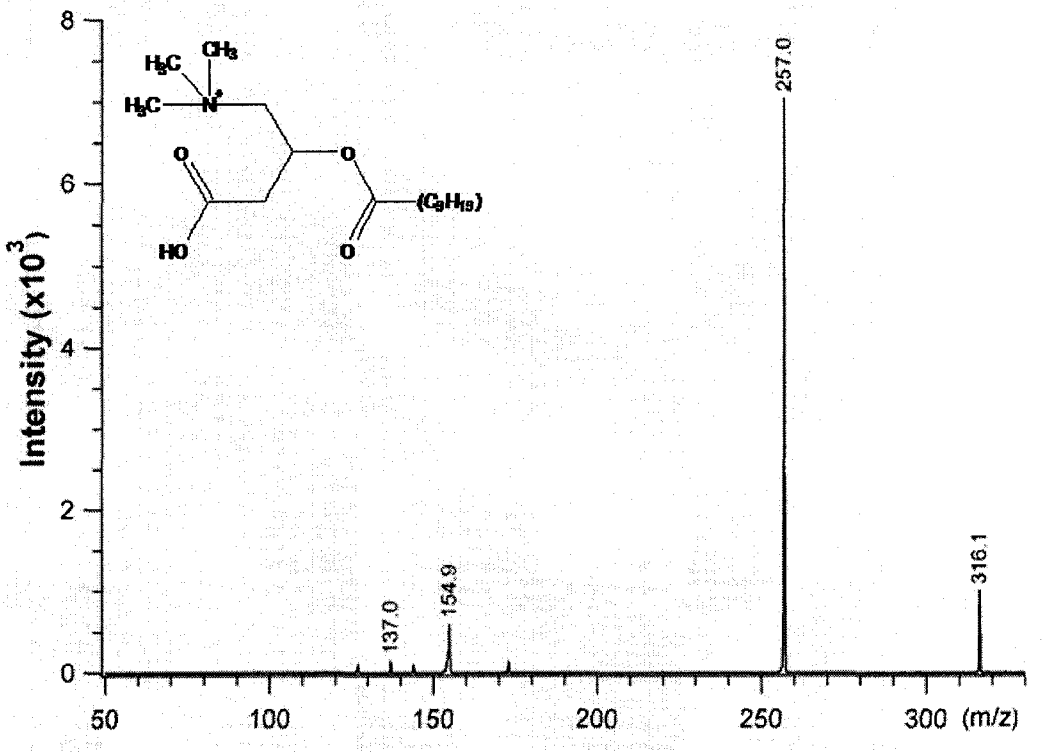

Figure 6.58 - Esquire MS/MS analysis of m/z 316b at 86.7 min and proposed structure

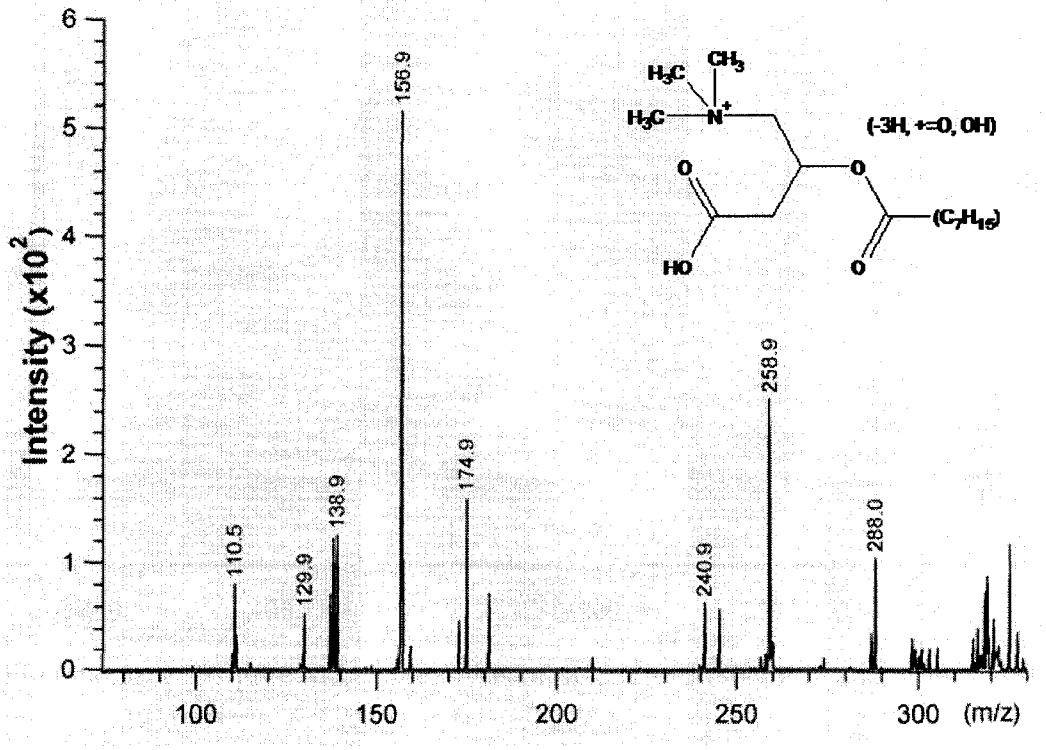

Figure 6.59 - Esquire MS/MS analysis of m/z 318 at 37.5 min and proposed structure

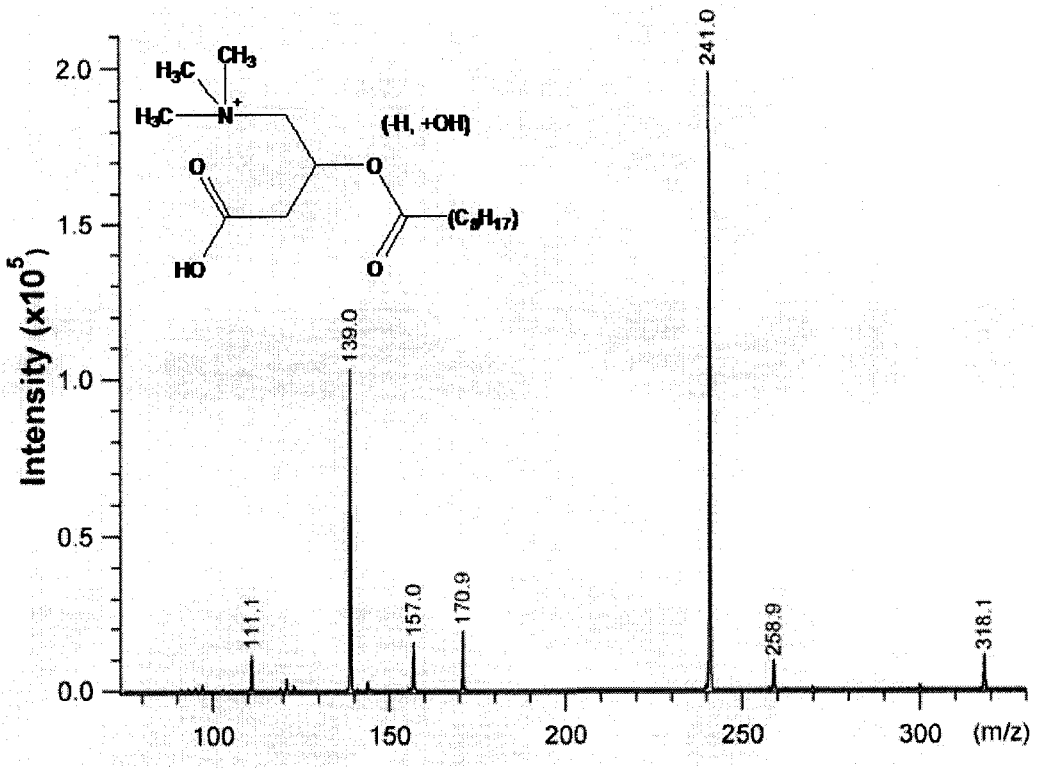

Figure 6.60 - Esquire MS/MS analysis of m/z 318b at 40.5 min and proposed structure

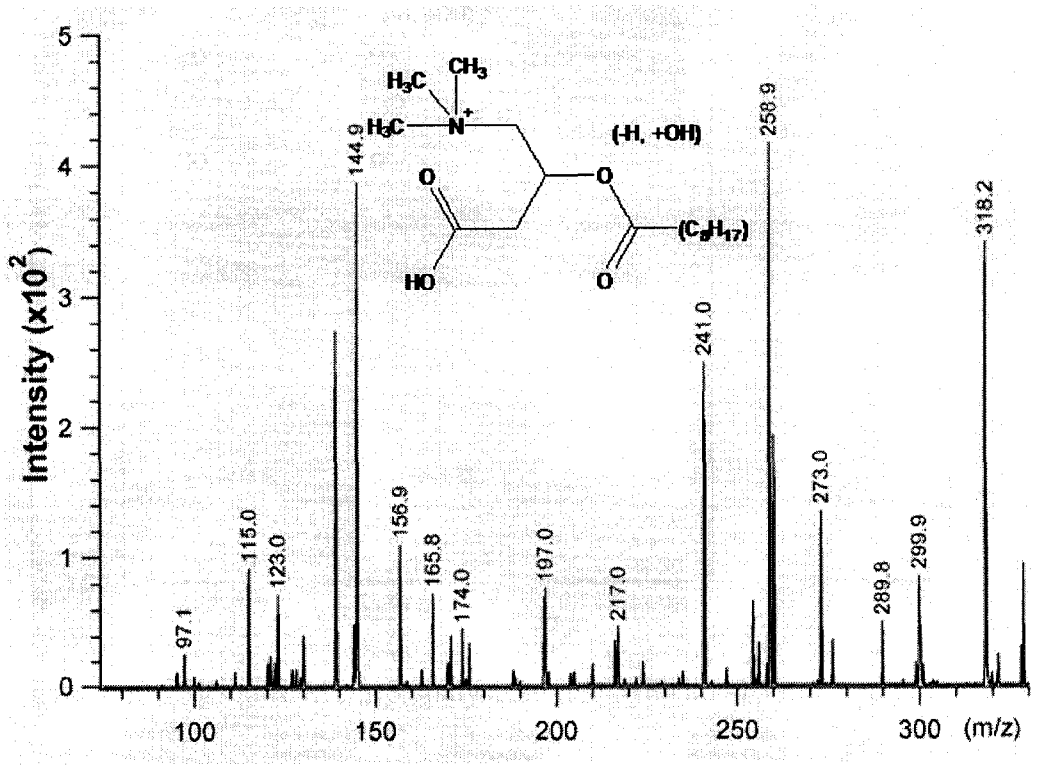

Figure 6.61 - Esquire MS/MS analysis of m/z 318b at 57.0 min and proposed structure

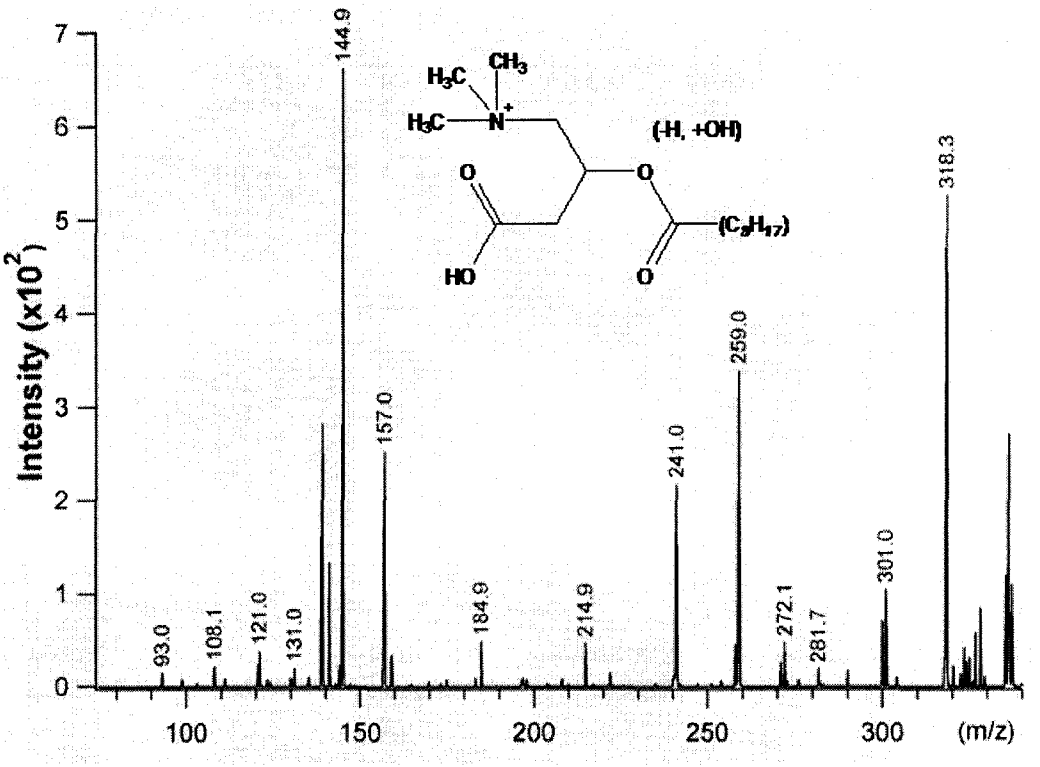

Figure 6.62 - Esquire MS/MS analysis of m/z 318 at 57.9 min and proposed structure

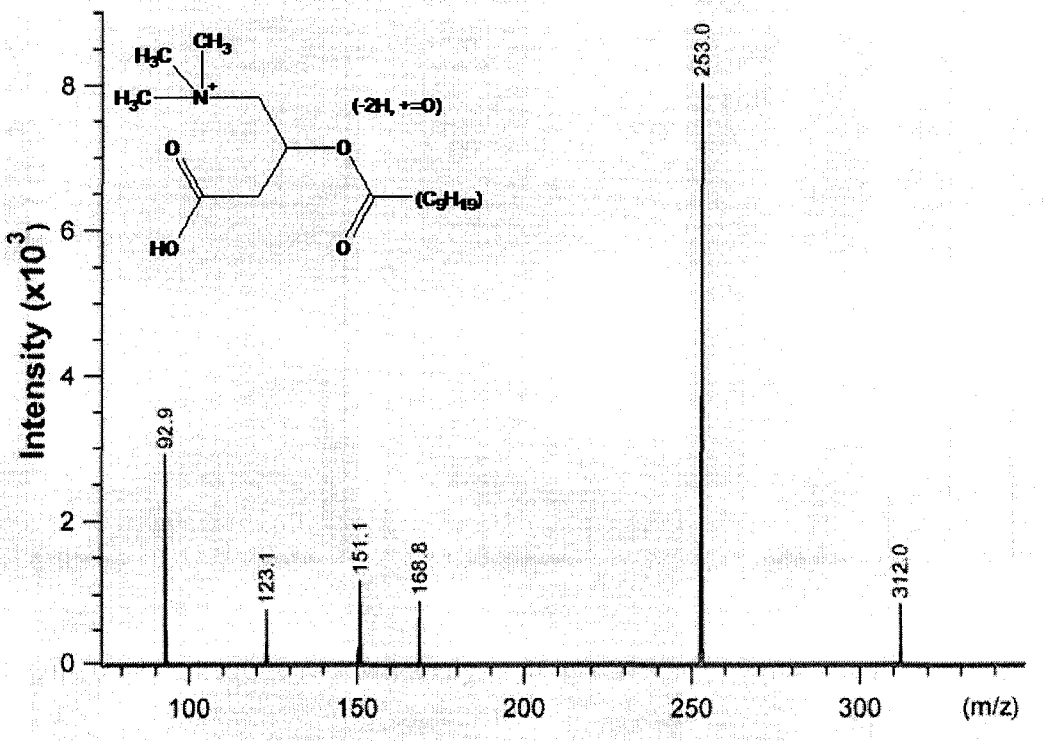

Figure 6.63 - Esquire MS/MS analysis of m/z 330 at 35.6 min and proposed structure

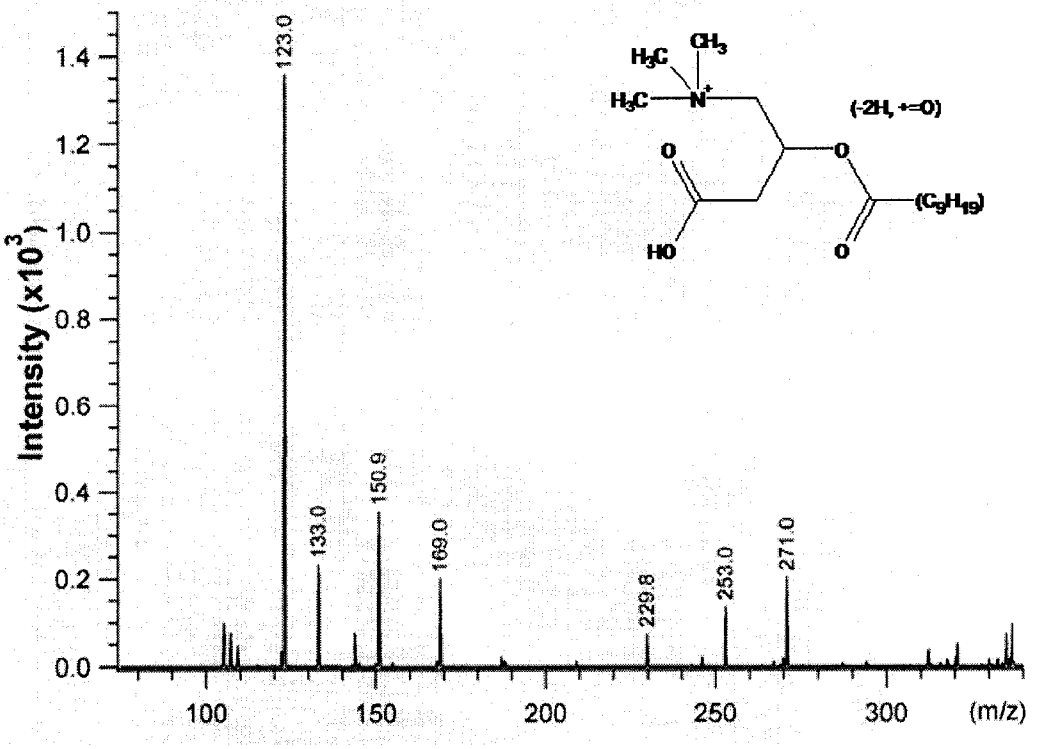

Figure 6.64 - Esquire MS/MS analysis of m/z 330 at 52.9 min and proposed structure

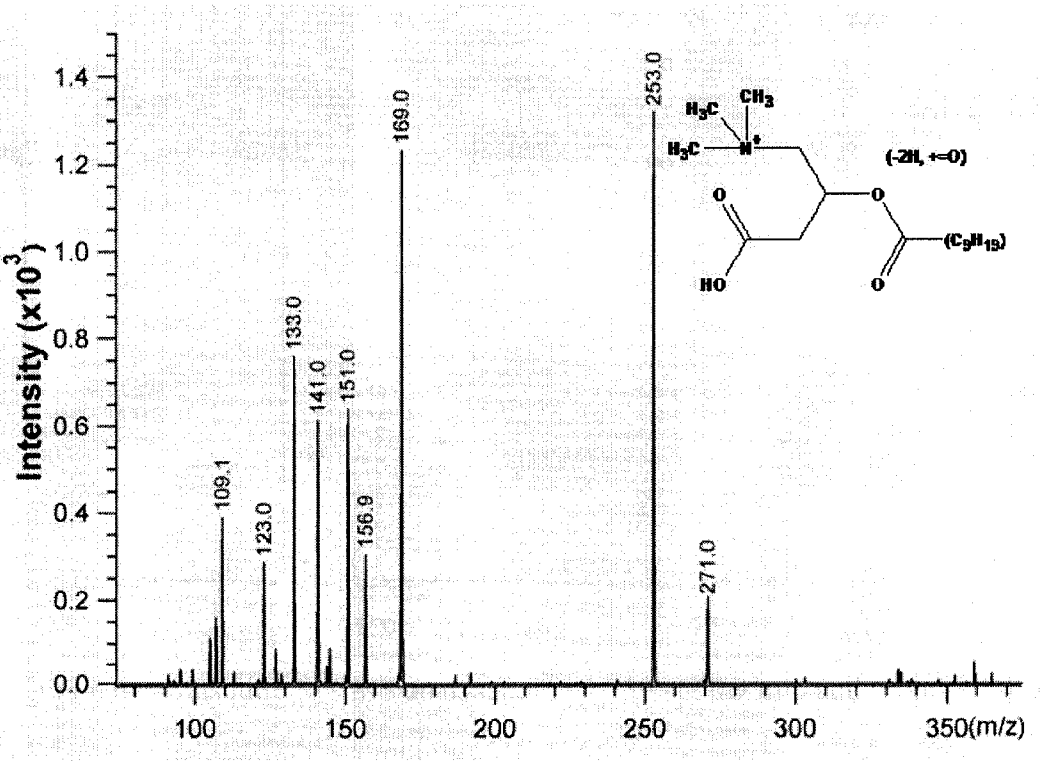

Figure 6.65 - Esquire MS/MS analysis of m/z 330 at 56.9 min and proposed structure

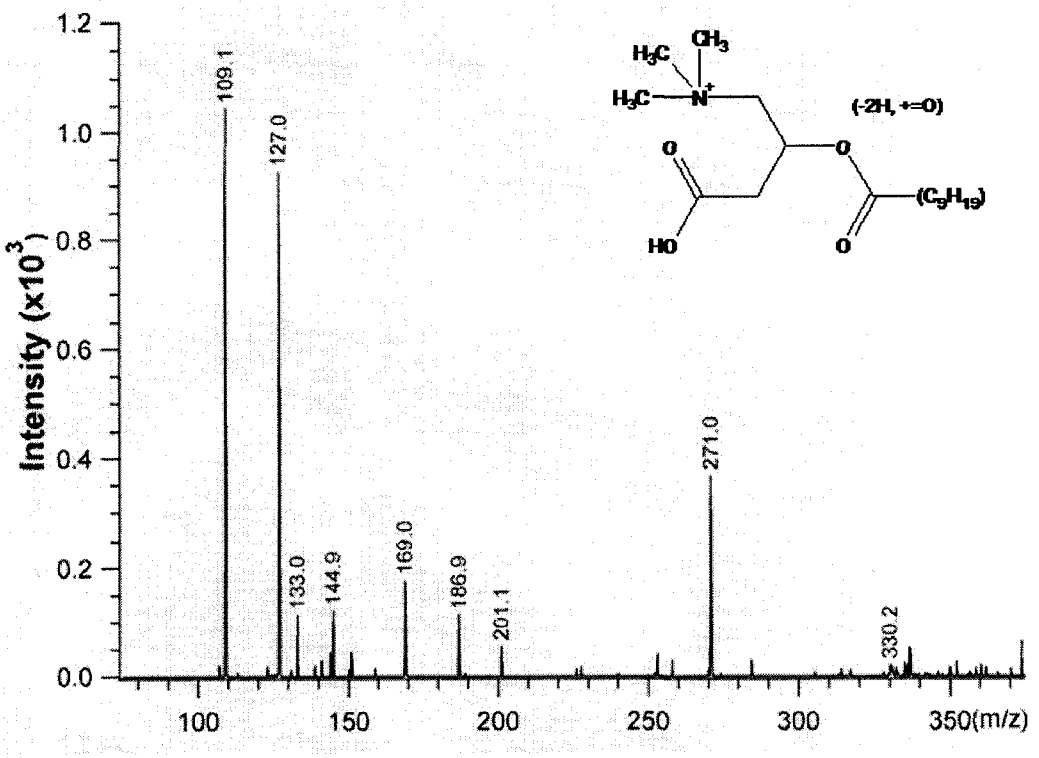

Figure 6.66 - Esquire MS/MS analysis of m/z 330 at 60.5 min and proposed structure

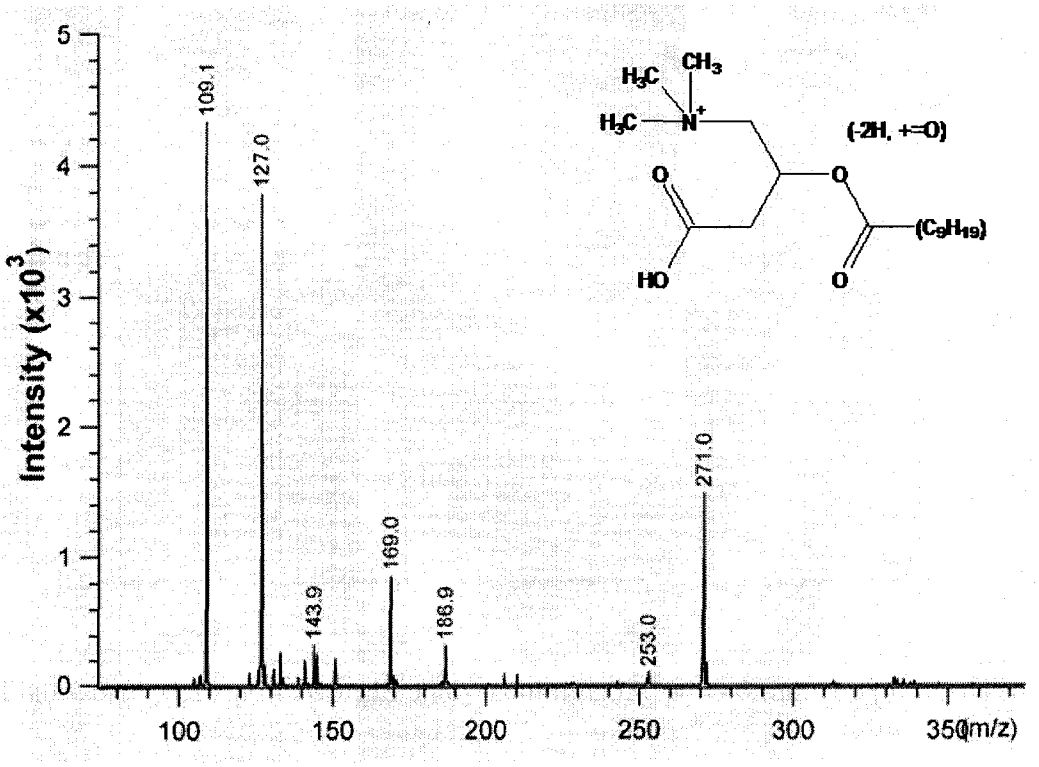

Figure 6.67 - Esquire MS/MS analysis of m/z 330 at 62.2 min and proposed structure

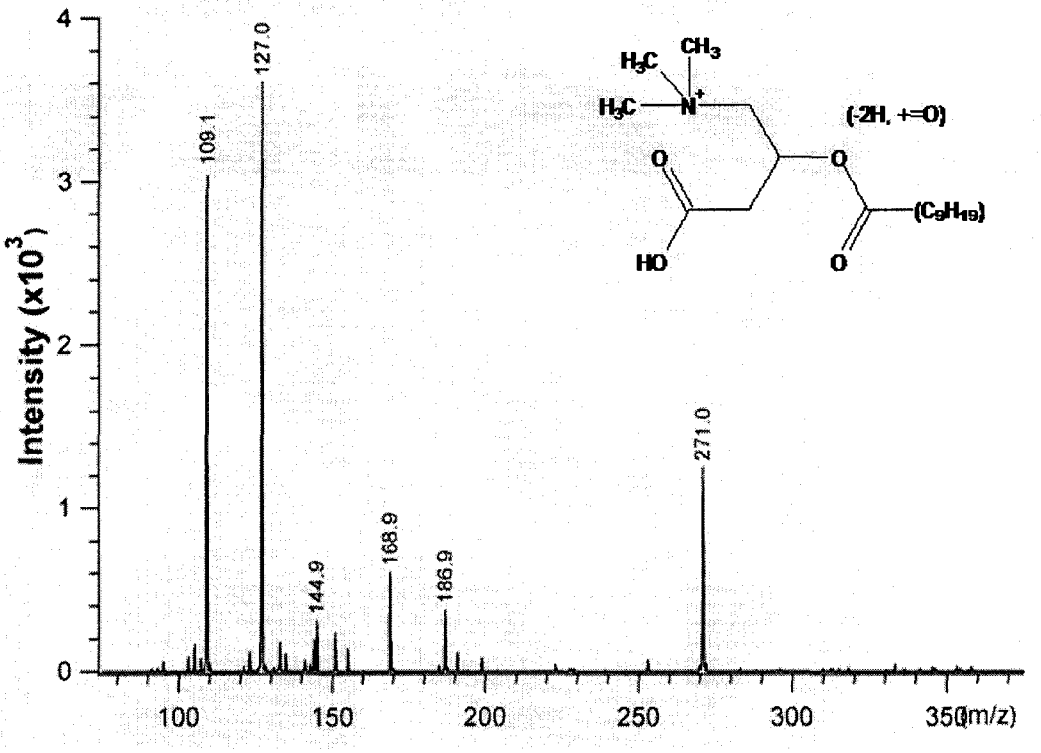

Figure 6.68 - Esquire MS/MS analysis of m/z 330 at 63.4 min and proposed structure

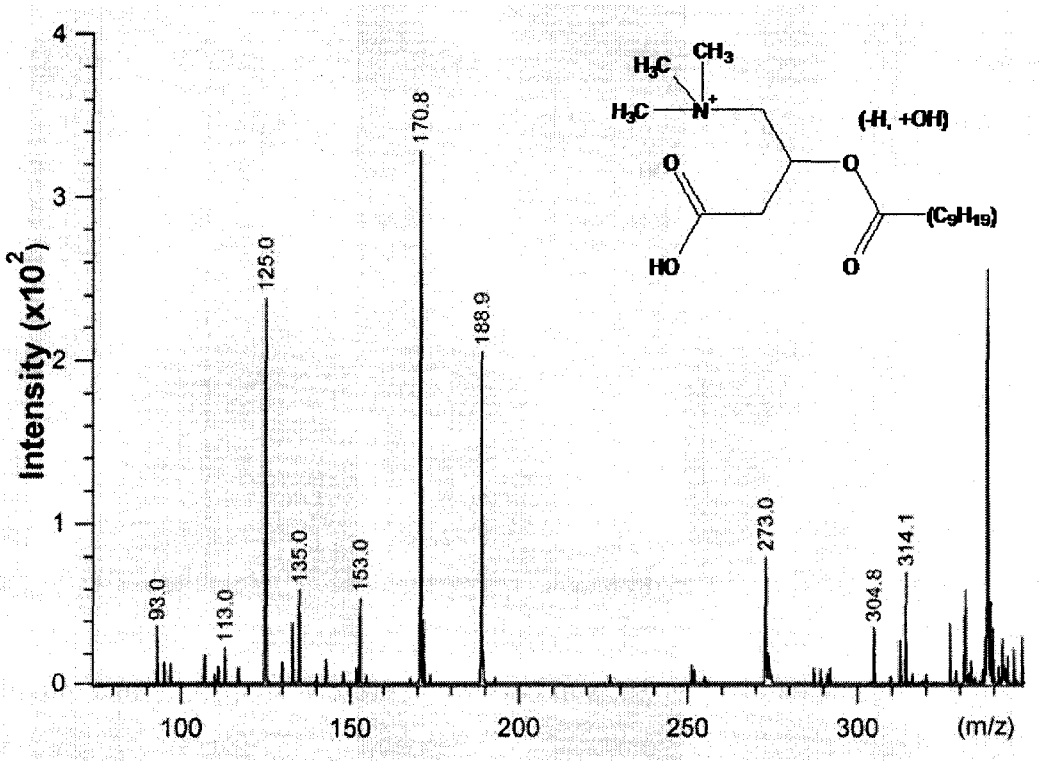

Figure 6.69 - Esquire MS/MS analysis of m/z 332 at 45.5 min and proposed structure

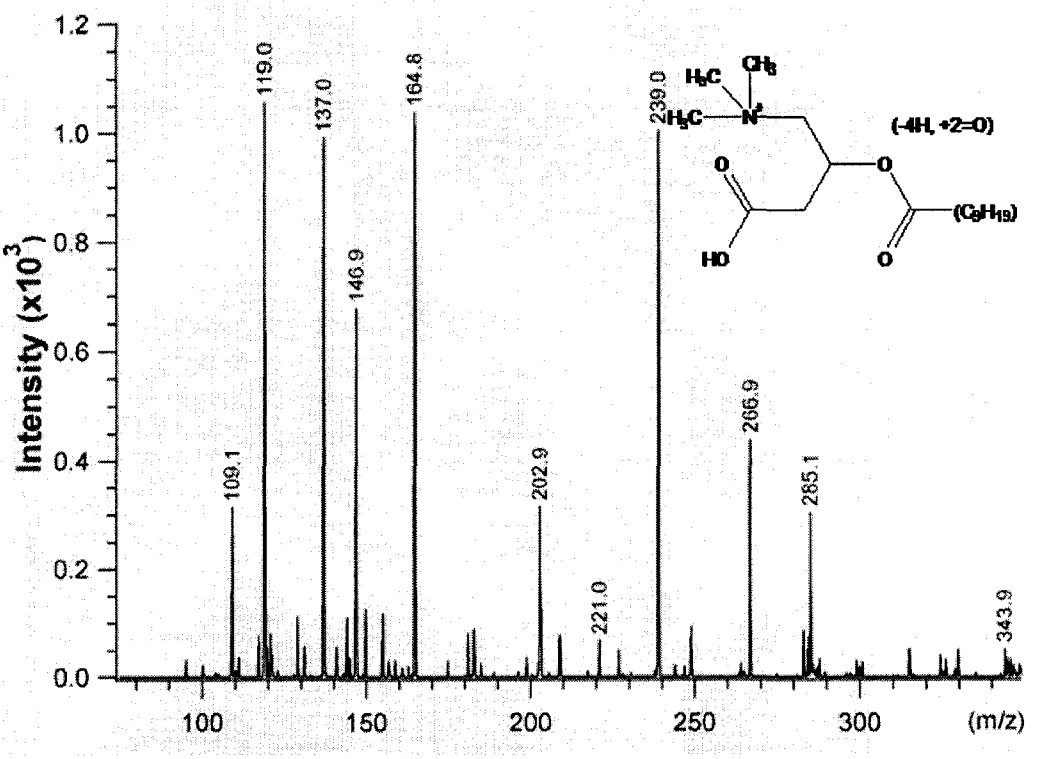

Figure 6.70 - Esquire MS/MS analysis of m/z 344 at 50.8 min and proposed structure

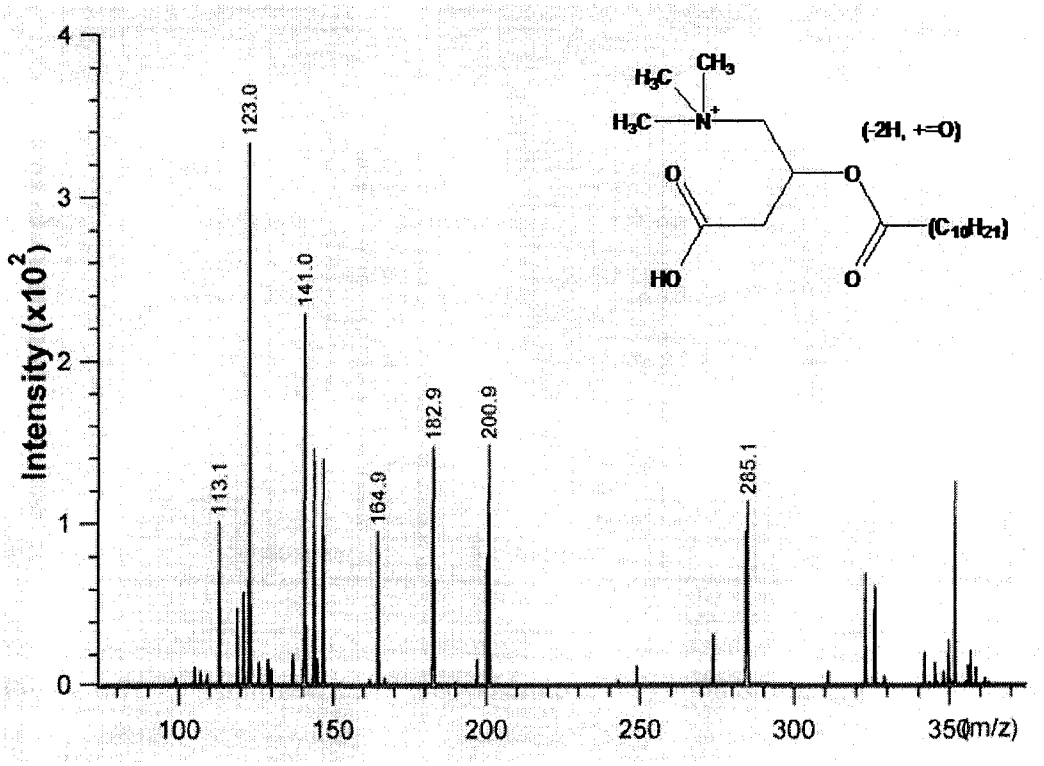

Figure 6.71 - Esquire MS/MS analysis of m/z 344b at 79.5 min and proposed structure

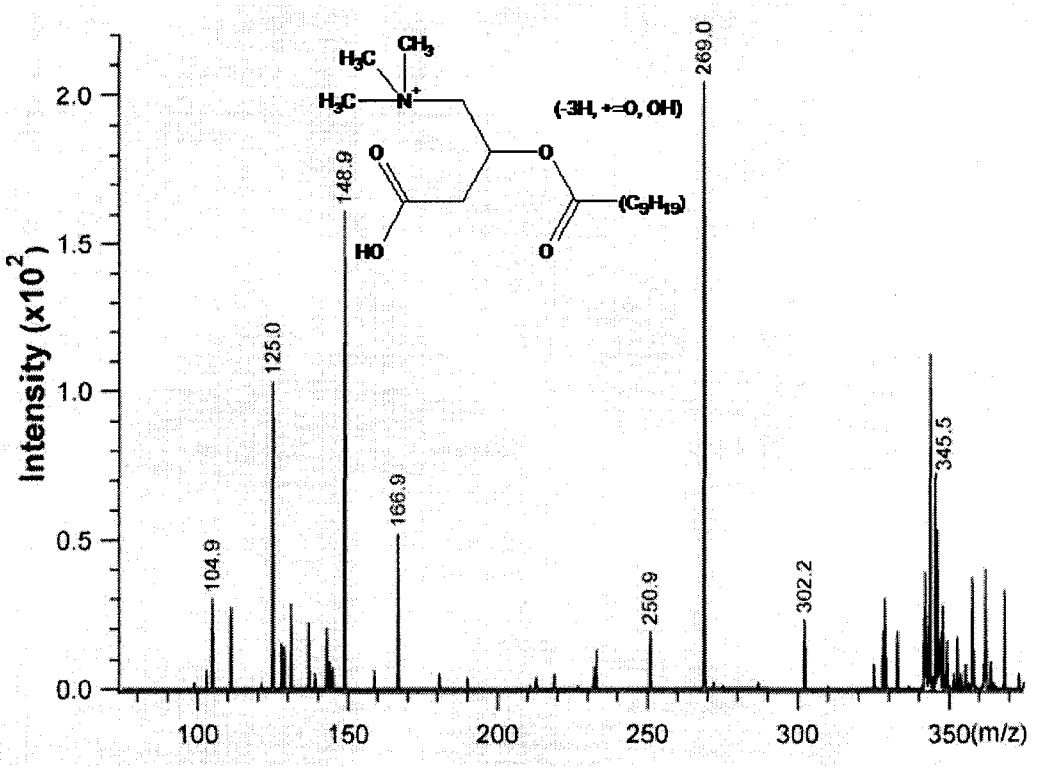

Figure 6.72 - Esquire MS/MS analysis of m/z 346 at 37.9 min and proposed structure

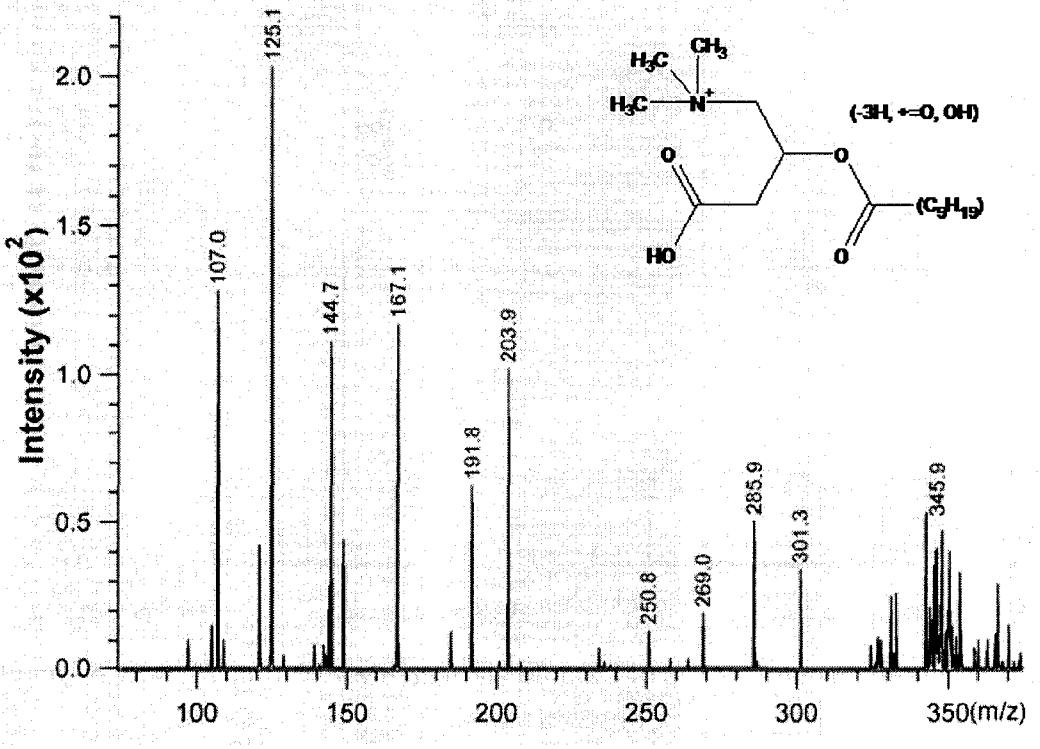

Figure 6.73 - Esquire MS/MS analysis of m/z 346 at 39.4 min and proposed structure

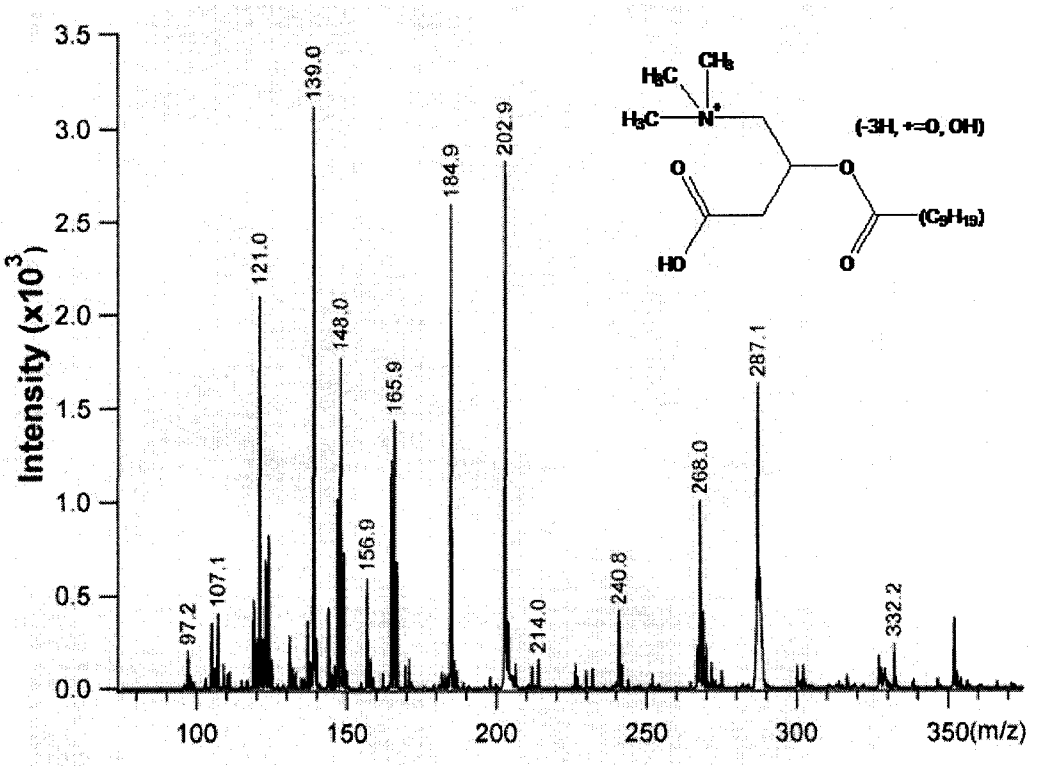

Figure 6.74 - Esquire MS/MS analysis of m/z 346 at 54.2 min and proposed structure

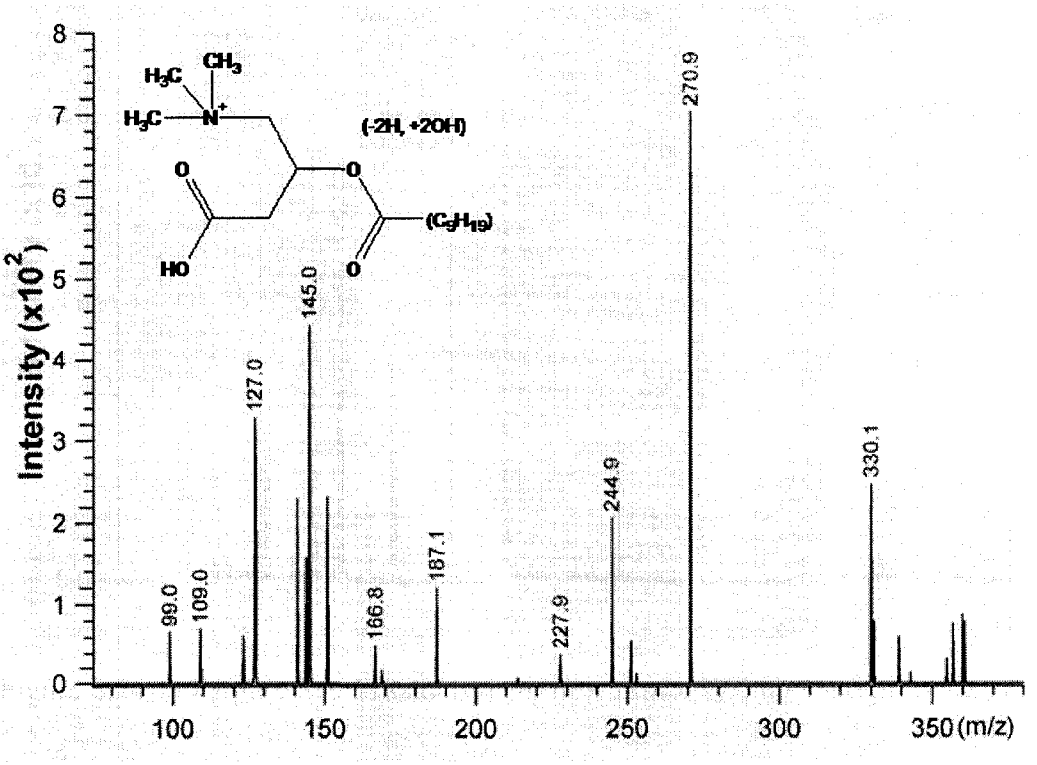

Figure 6.75 - Esquire MS/MS analysis of m/z 348 at 35.1 min and proposed structure

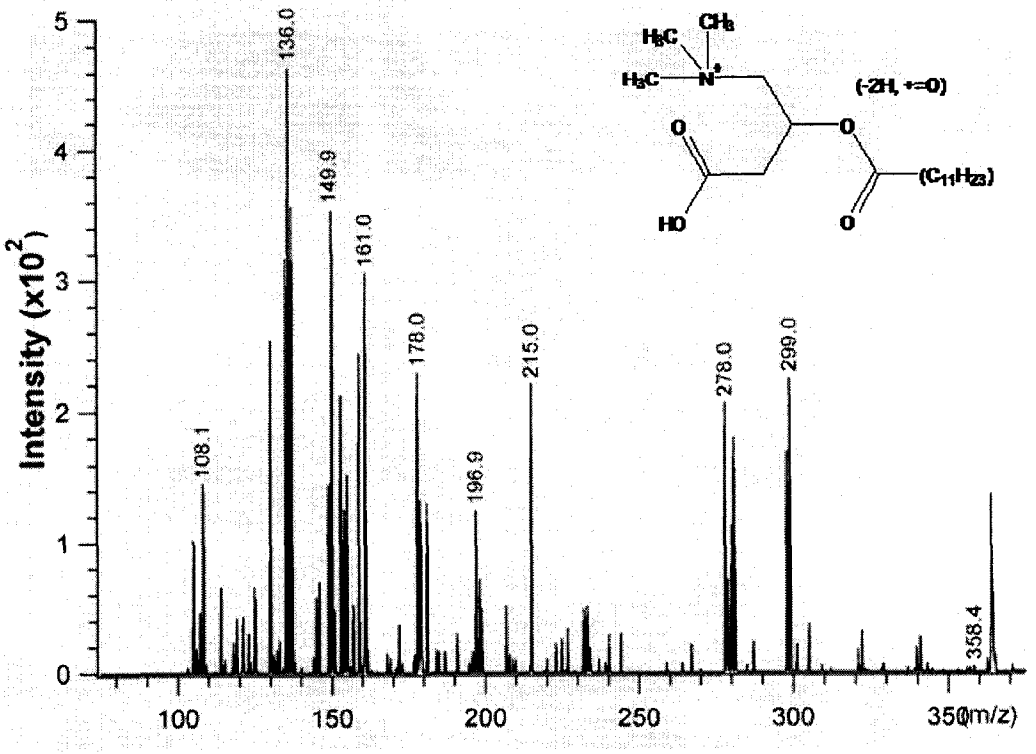

Figure 6.76 - Esquire MS/MS analysis of m/z 358 at 79.8 min and proposed structure

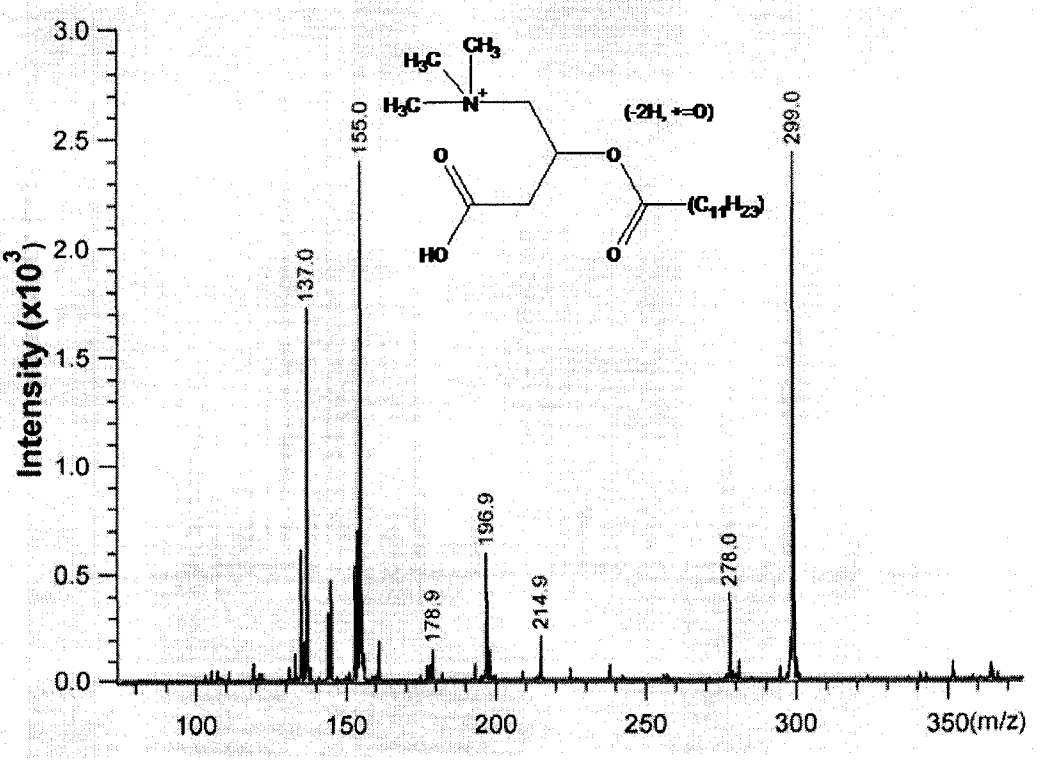

Figure 6.77 - Esquire MS/MS analysis of m/z 358 at 80.4 min and proposed structure

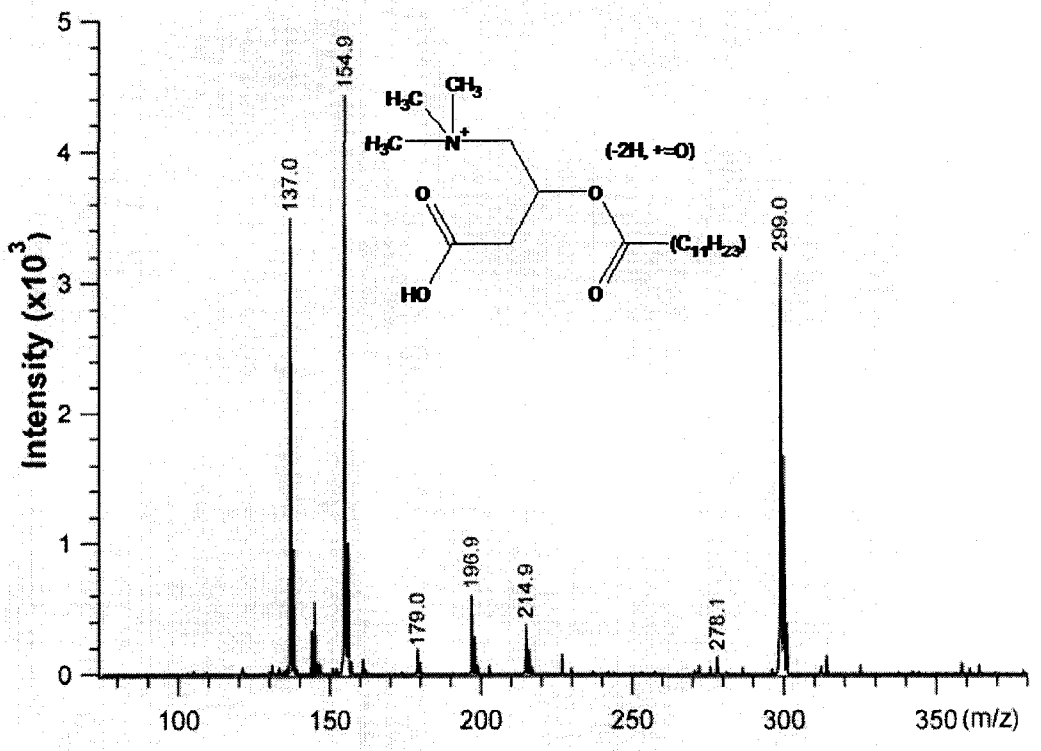

Figure 6.78 - Esquire MS/MS analysis of m/z 358 at 80.8 min and proposed structure

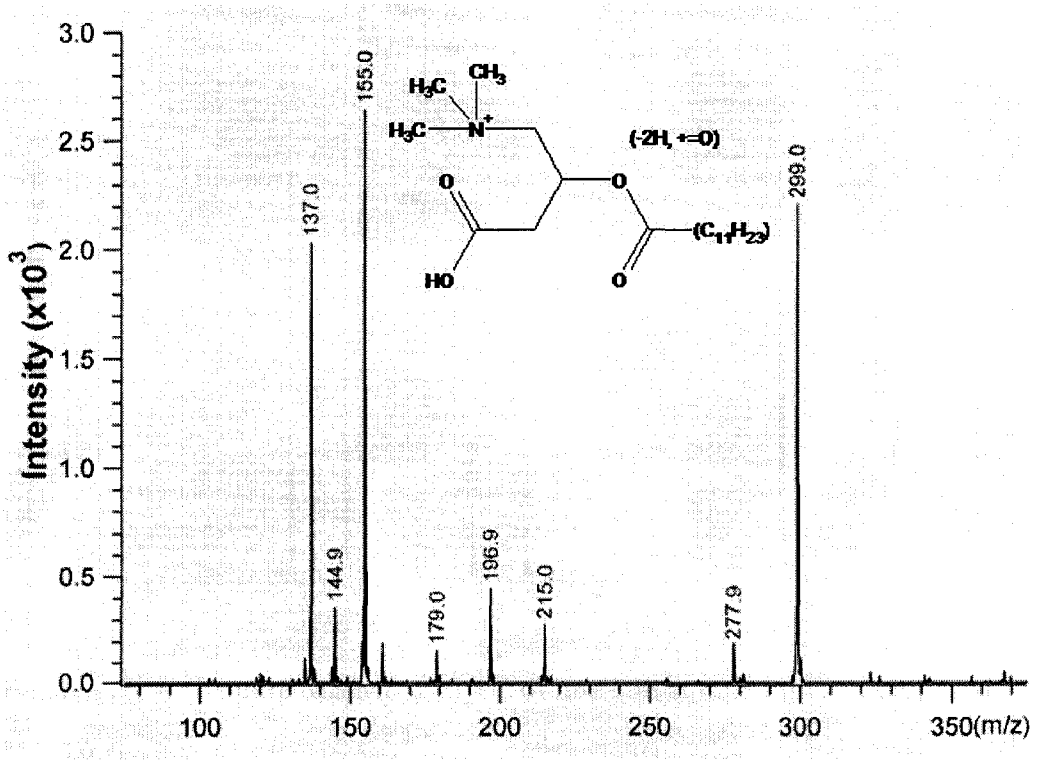

Figure 6.79 - Esquire MS/MS analysis of m/z 358 at 81.5 min and proposed structure

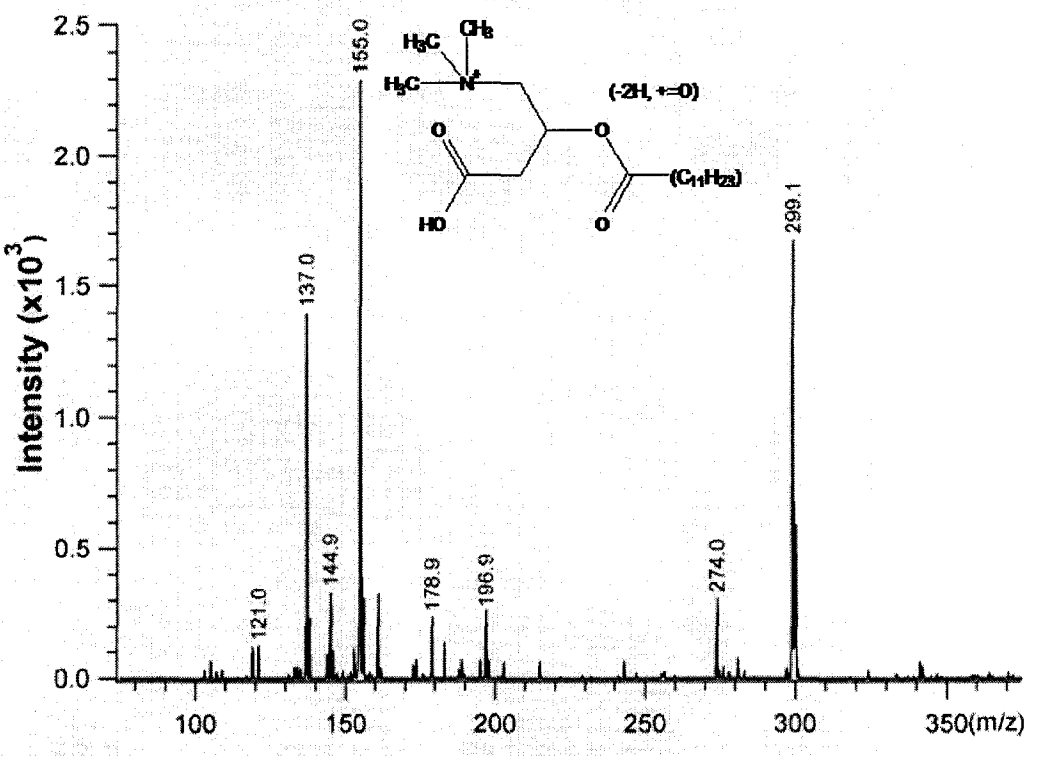

Figure 6.80 - Esquire MS/MS analysis of m/z 358 at 82.7 min and proposed structure

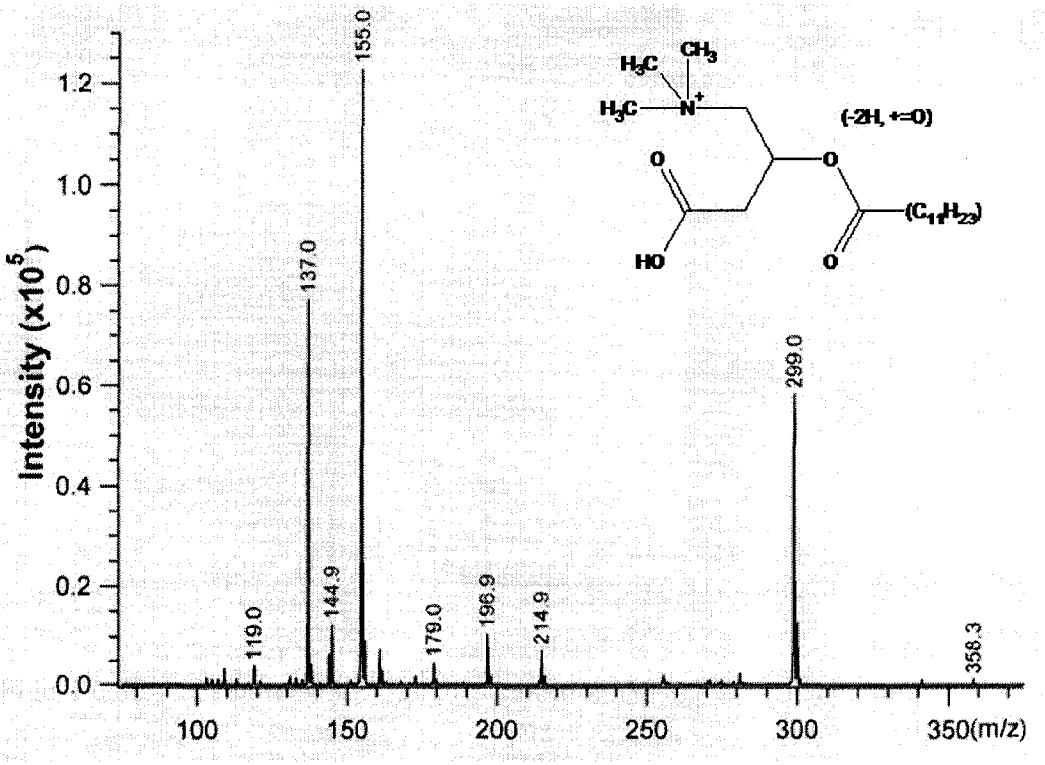

Figure 6.81 - Esquire MS/MS analysis of m/z 358 at 83.2 min and proposed structure

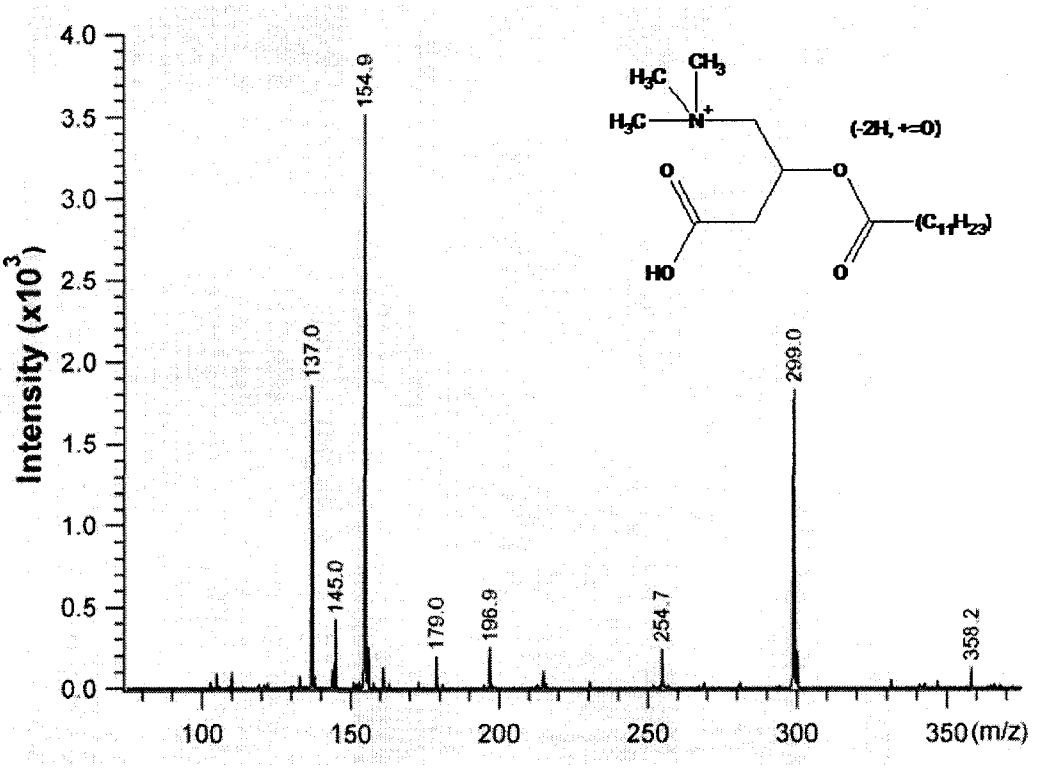

Figure 6.82 - Esquire MS/MS analysis of m/z 358 at 84.9 min and proposed structure

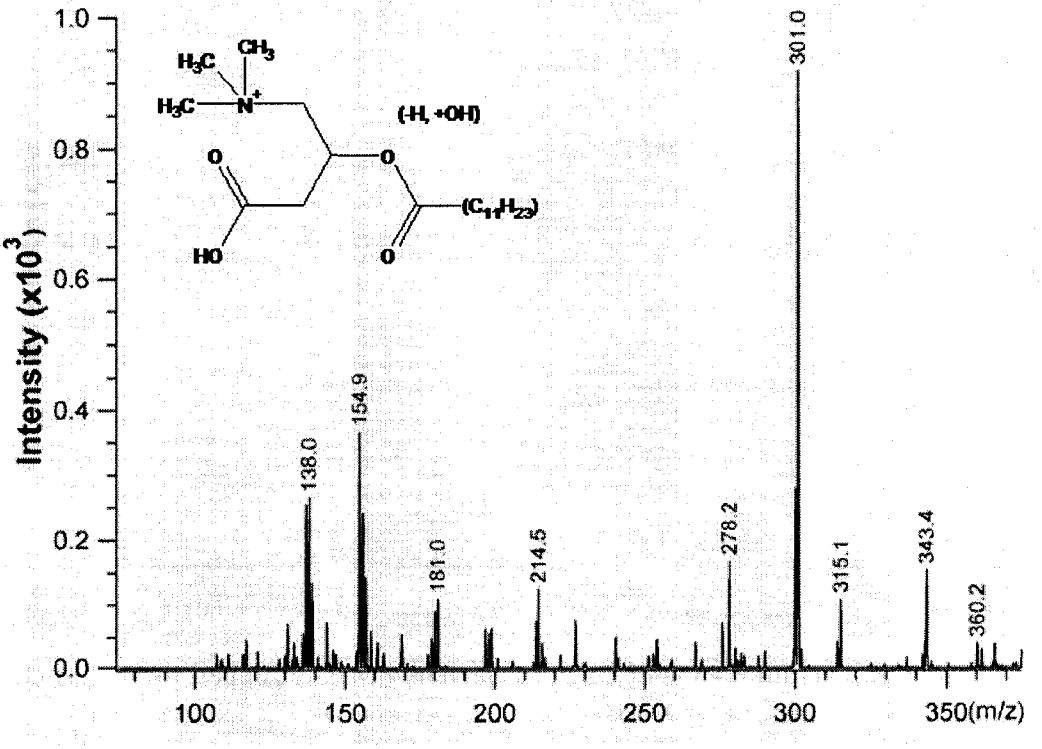

Figure 6.83 - Esquire MS/MS analysis of m/z 360 at 80.5 min and proposed structure

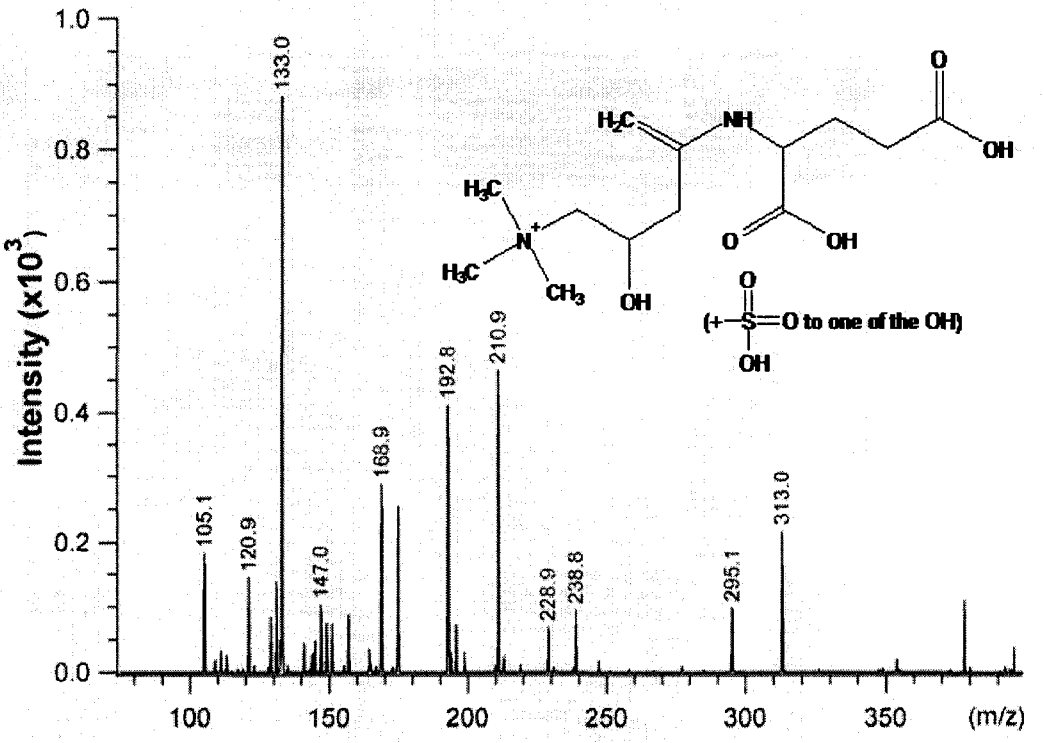

Figure 6.84 - Esquire MS/MS analysis of m/z 372 at 62.6 min and proposed structure

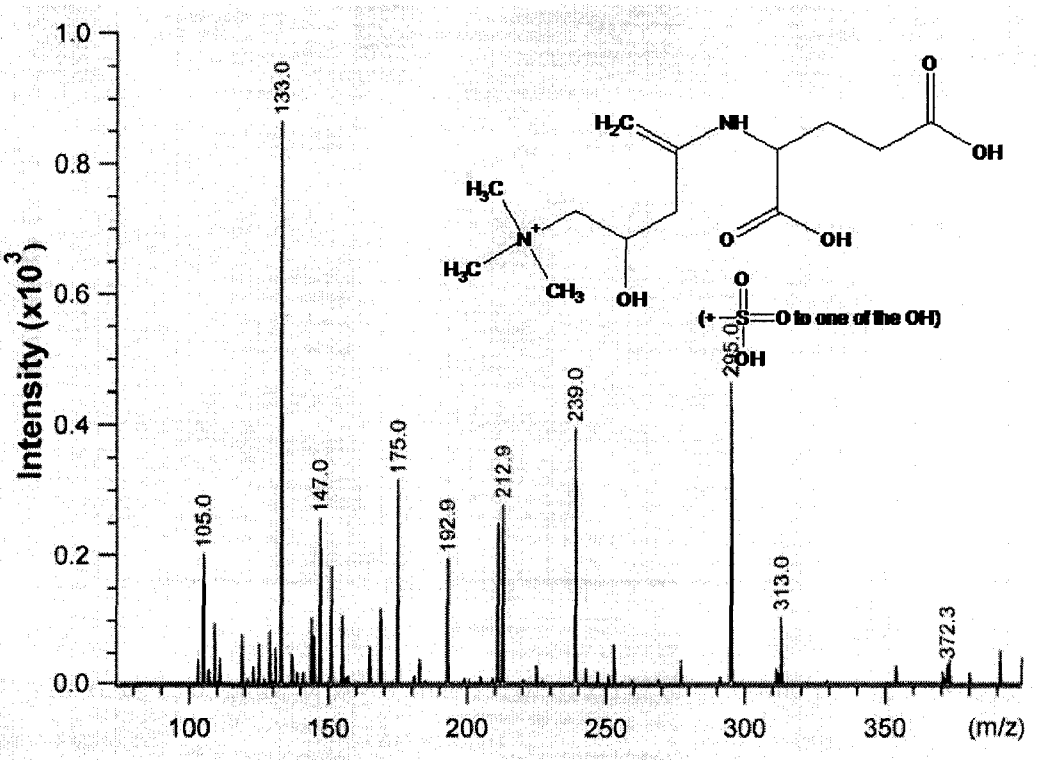

Figure 6.85 - Esquire MS/MS analysis of m/z 372 at 66.4 min and proposed structure

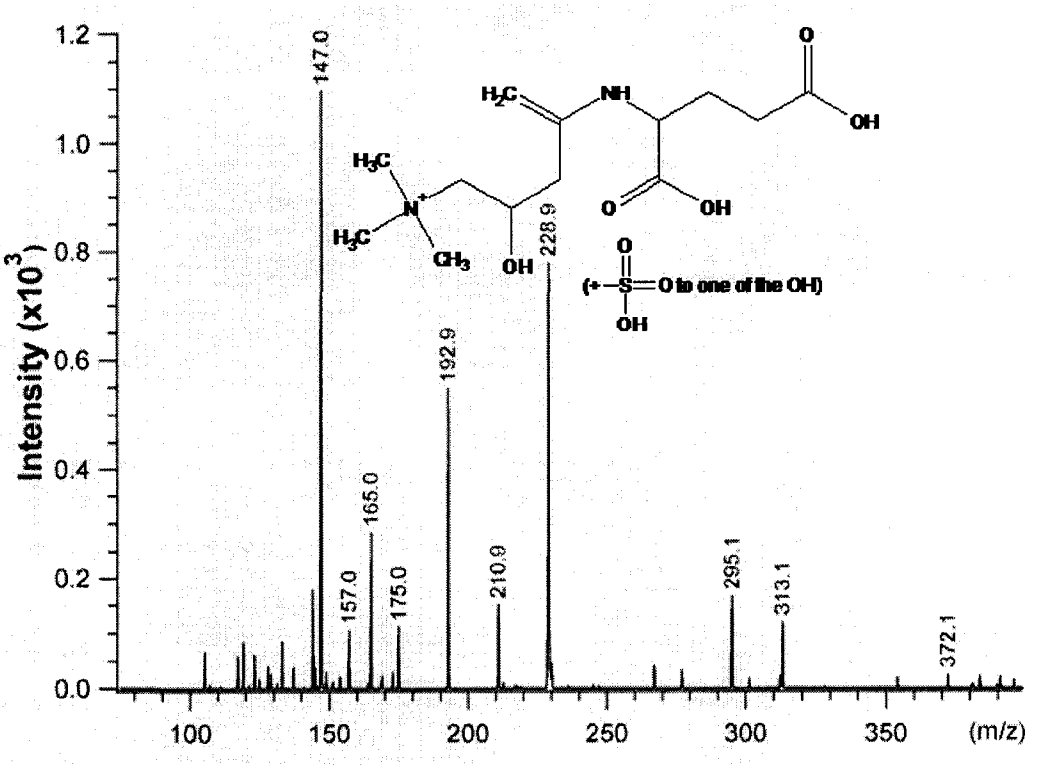

Figure 6.86 - Esquire MS/MS analysis of m/z 372 at 71.5 min and proposed structure

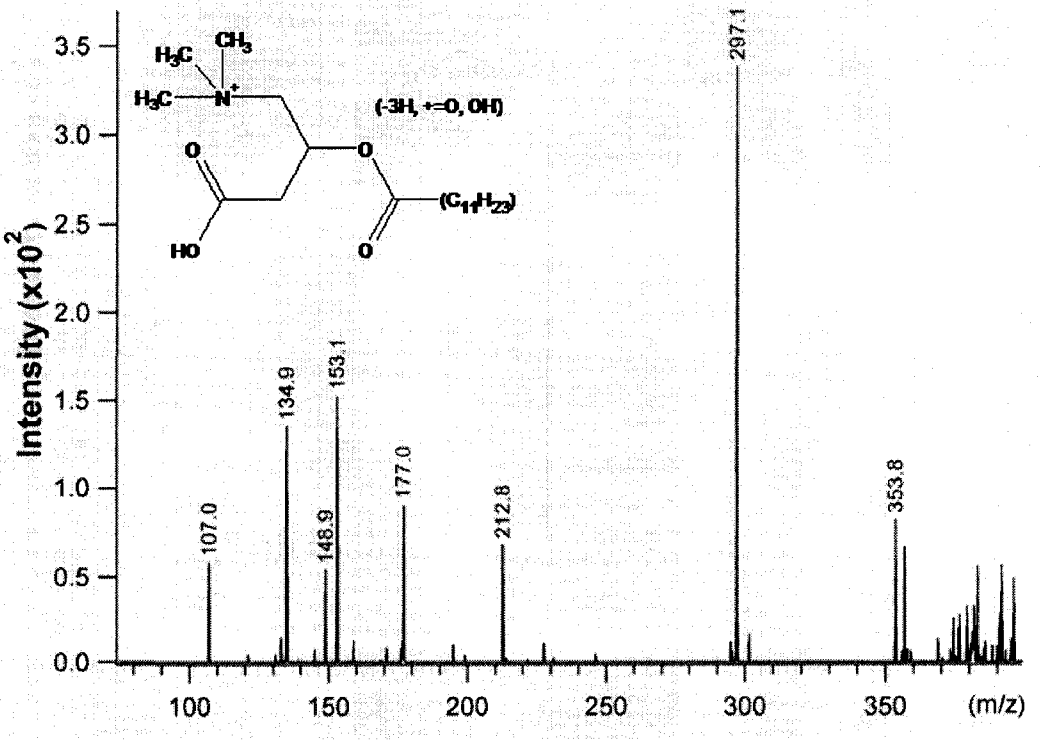

Figure 6.87 - Esquire MS/MS analysis of m/z 374 at 49.9 min and proposed structure

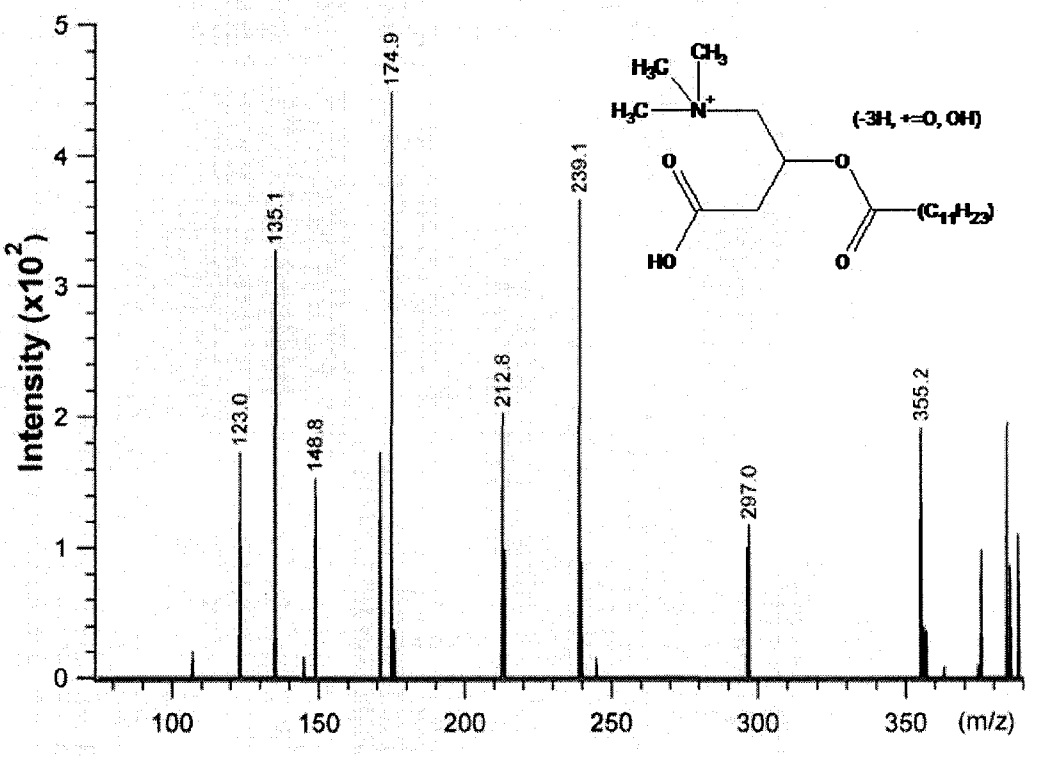

Figure 6.88 - Esquire MS/MS analysis of m/z 374 at 52.1 min and proposed structure

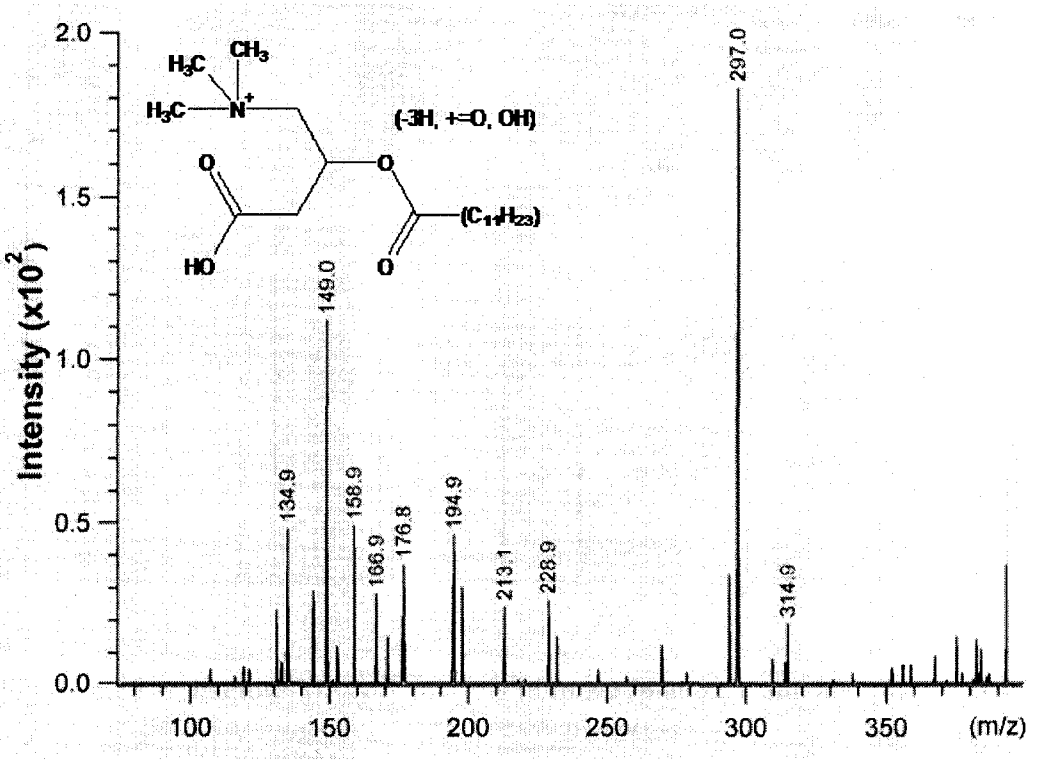

Figure 6.89 - Esquire MS/MS analysis of m/z 374 at 54.3 min and proposed structure

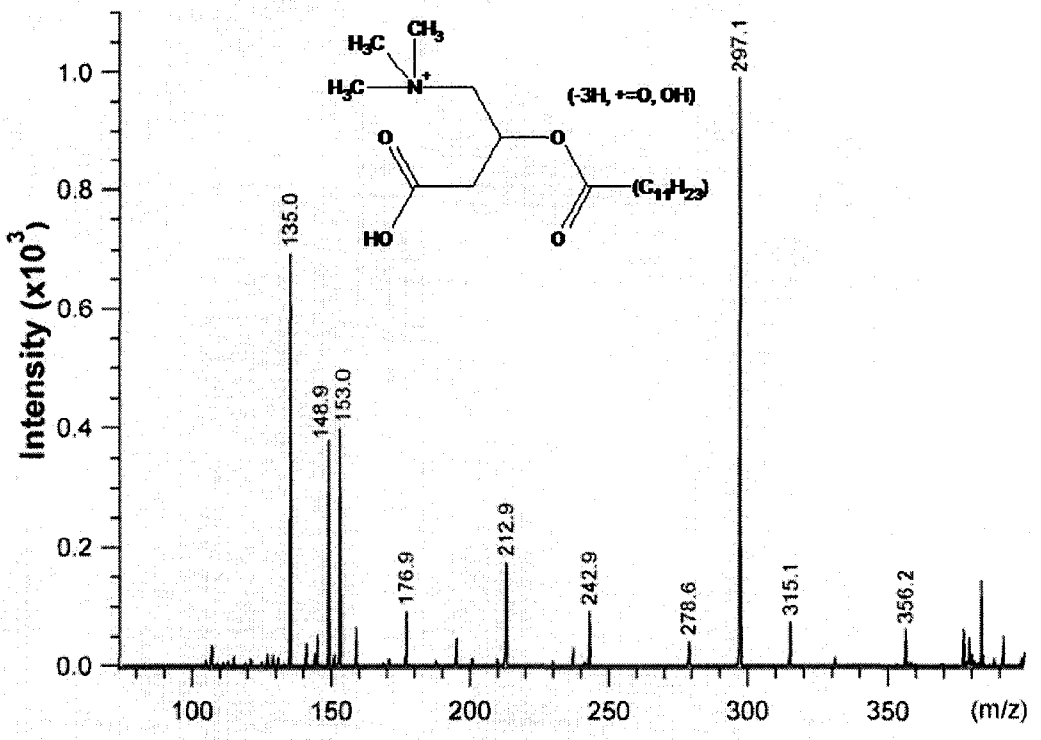

Figure 6.90 - Esquire MS/MS analysis of m/z 374 at 58.9 min and proposed structure

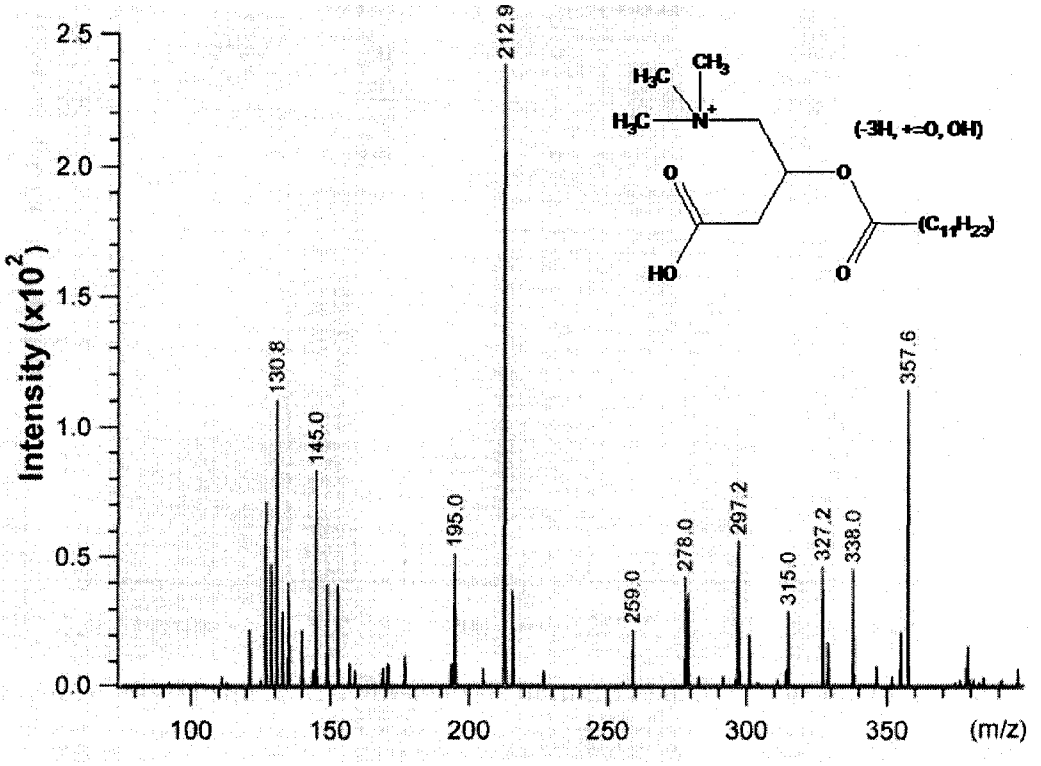

Figure 6.91 - Esquire MS/MS analysis of m/z 374 at 60.8 min and proposed structure

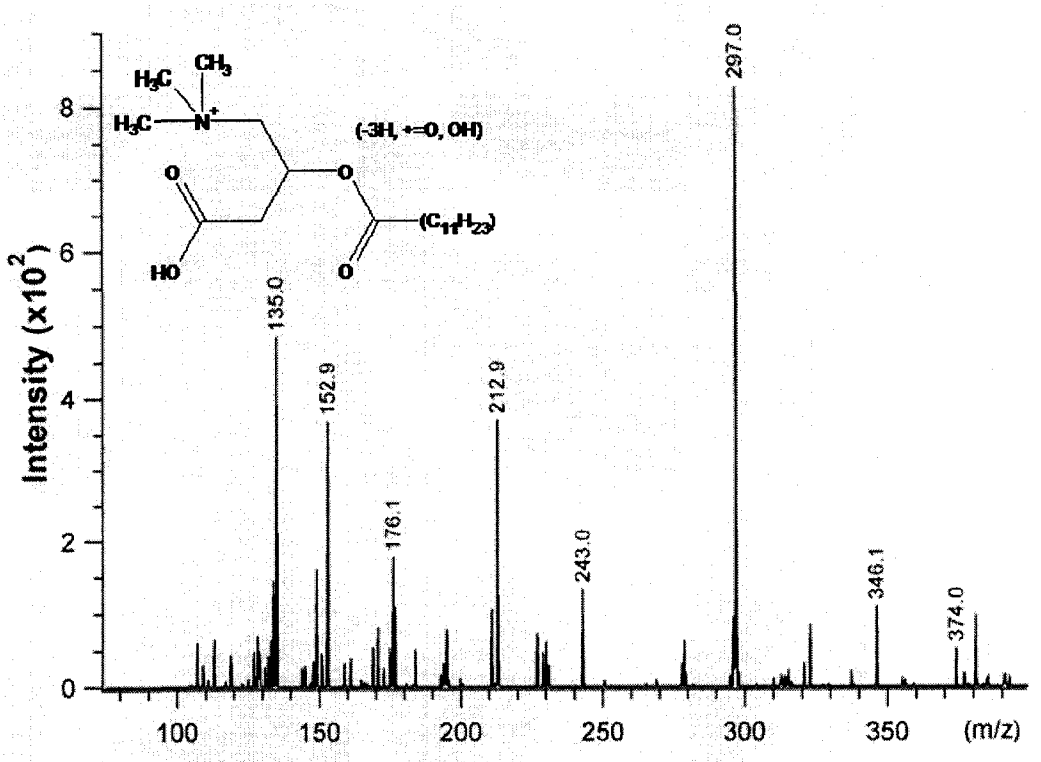

Figure 6.92 - Esquire MS/MS analysis of m/z 374 at 62.0 min and proposed structure

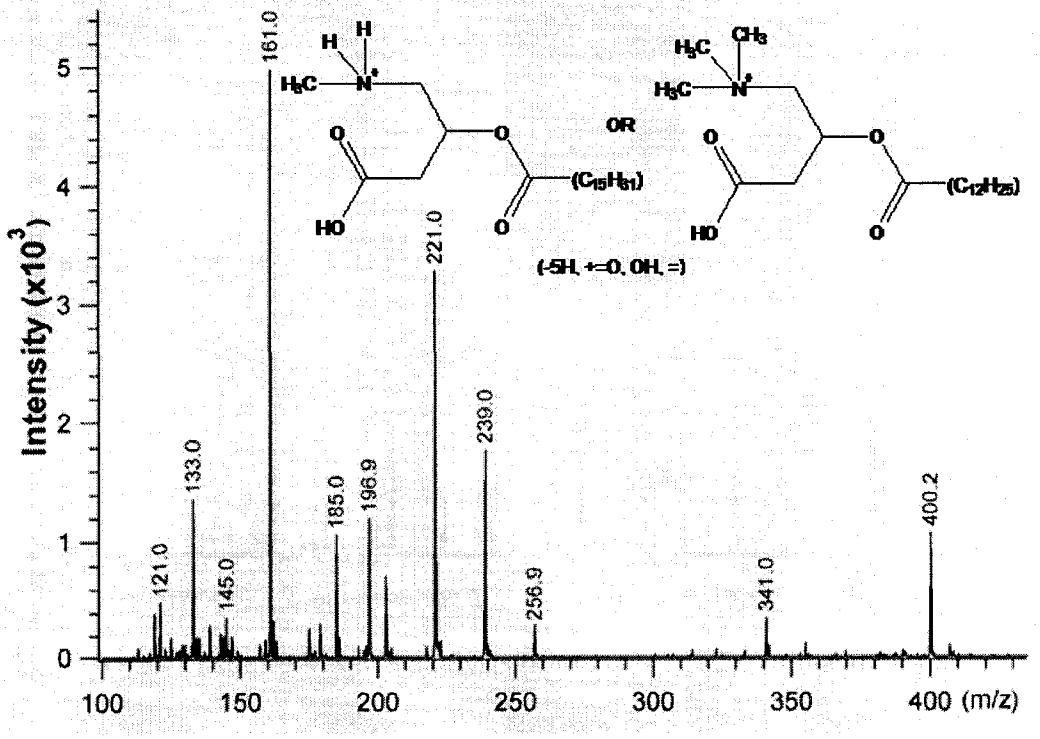

Figure 6.93 - Esquire MS/MS analysis of m/z 400 at 64.3 min and proposed structure

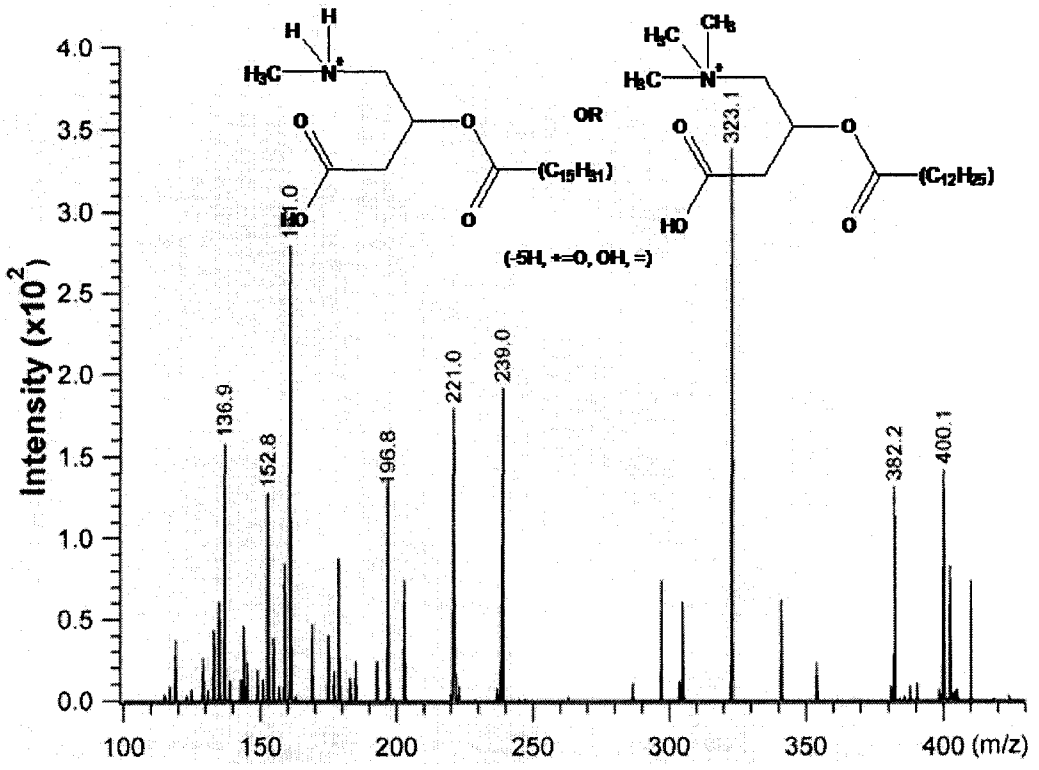

Figure 6.94 - Esquire MS/MS analysis of m/z 400 at 73.4 min and proposed structure

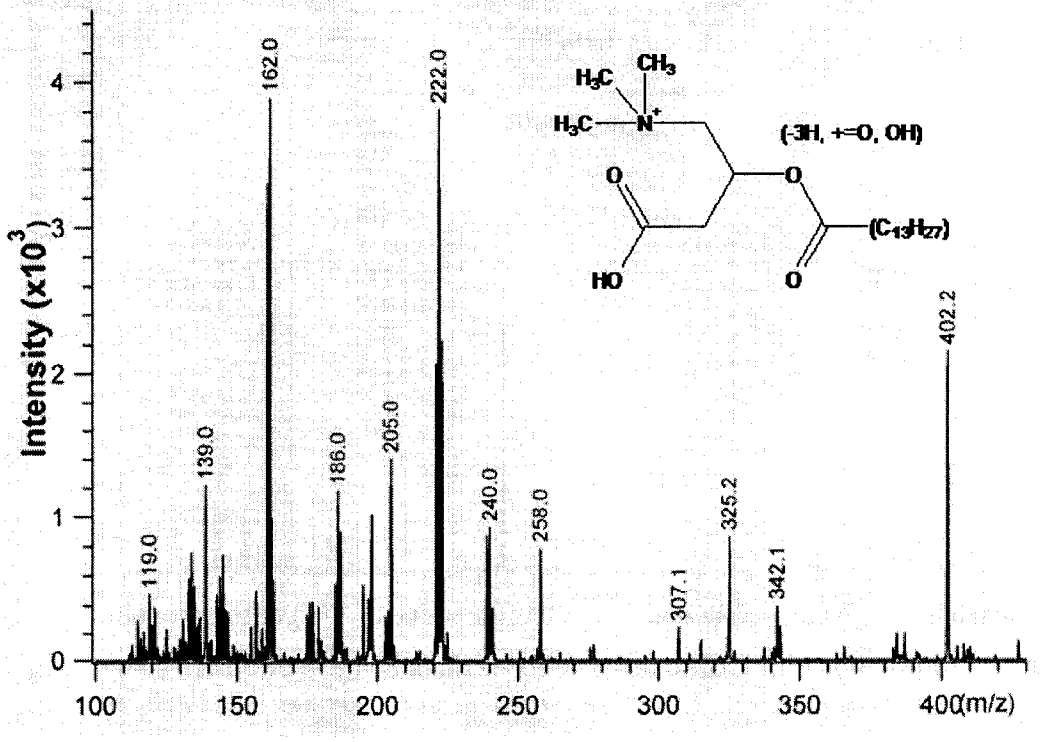

Figure 6.95 - Esquire MS/MS analysis of m/z 402 at 64.9 min and proposed structure

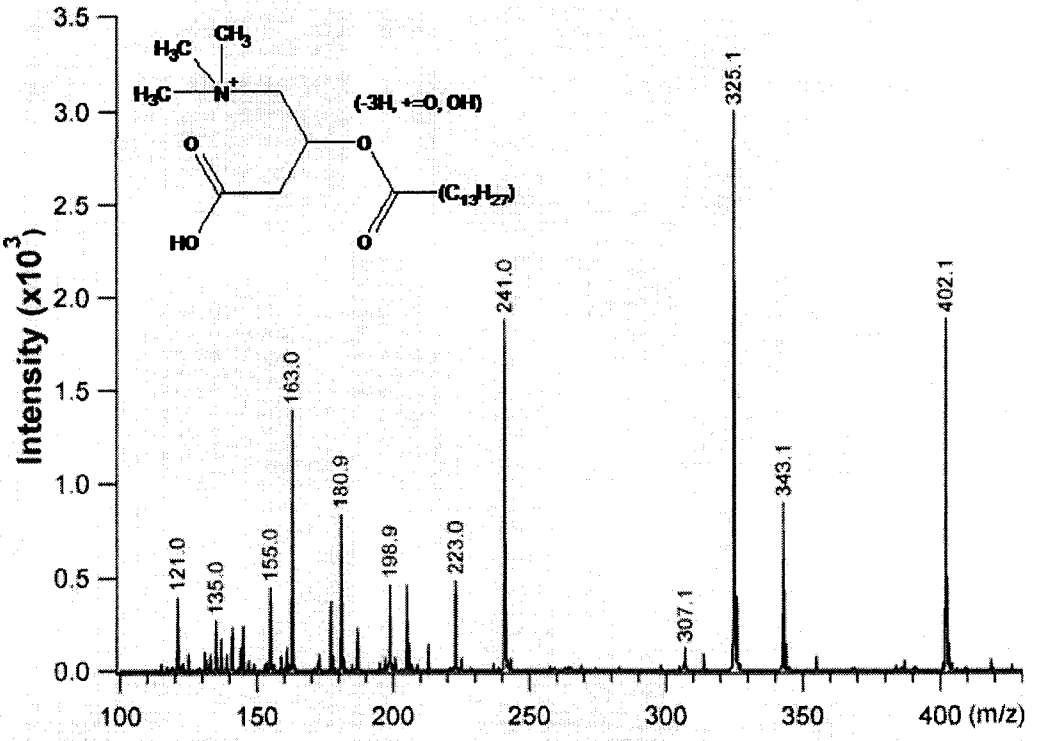

Figure 6.96 - Esquire MS/MS analysis of m/z 402 at 79.1 min and proposed structure

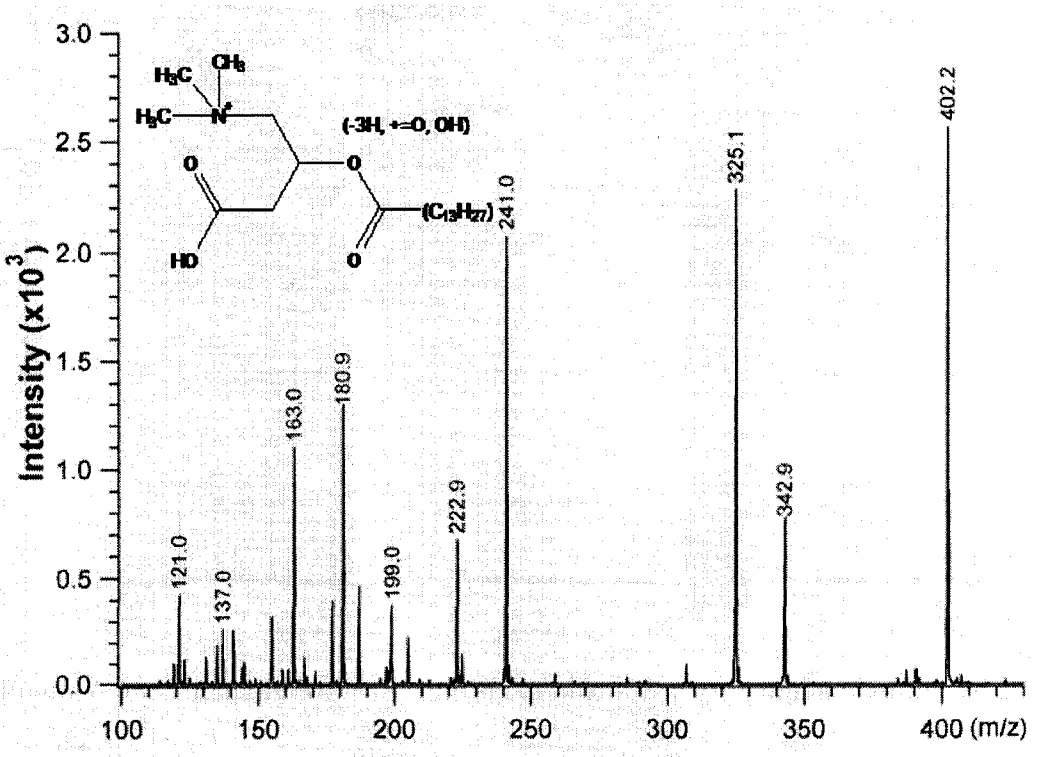

Figure 6.97 - Esquire MS/MS analysis of m/z 402 at 79.7 min and proposed structure

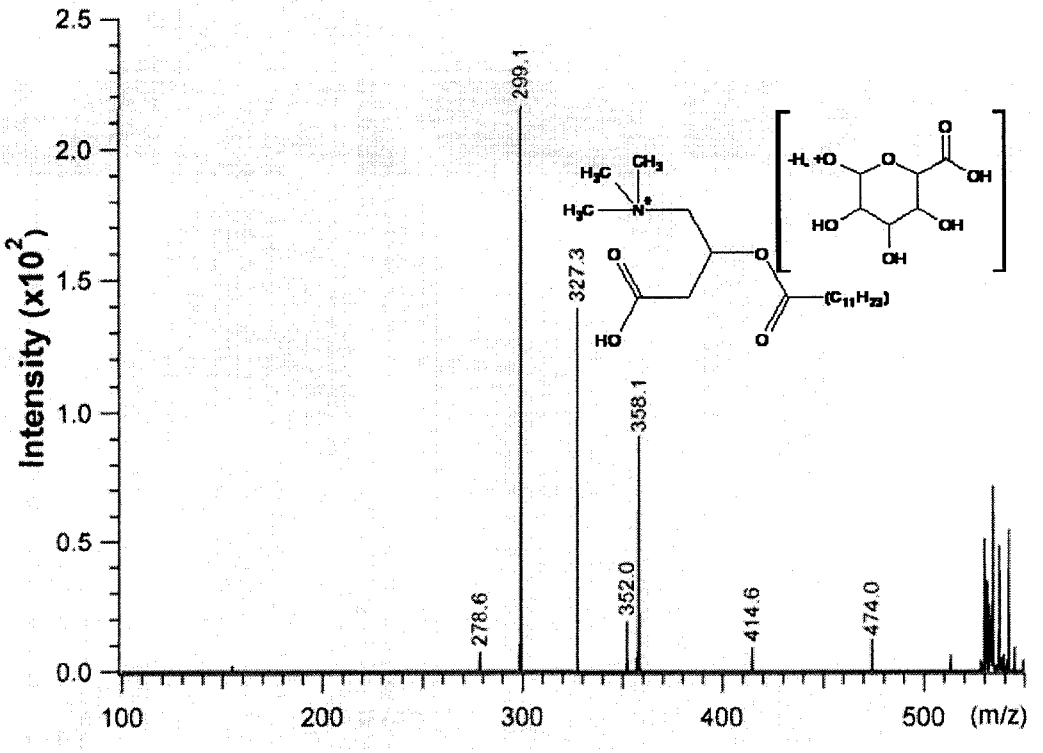

Figure 6.98 - Esquire MS/MS analysis of m/z 534 at 72.6 min and proposed structure

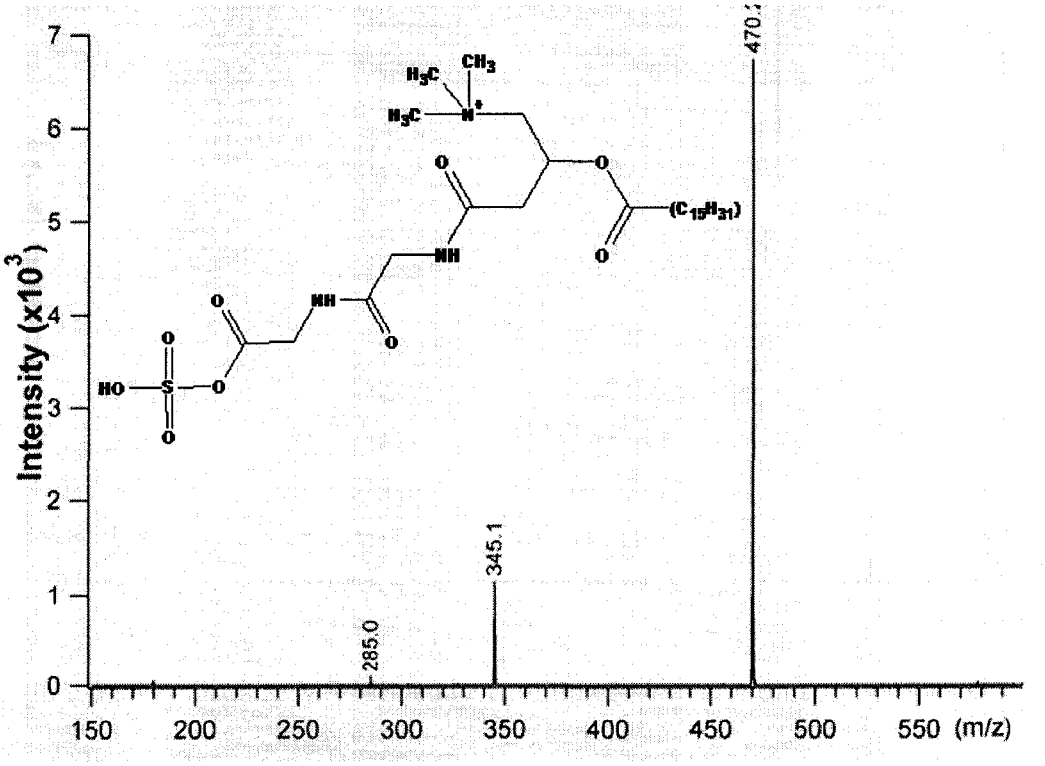

Figure 6.99 - Esquire MS/MS analysis of m/z 595 at 71.0 min and proposed structure

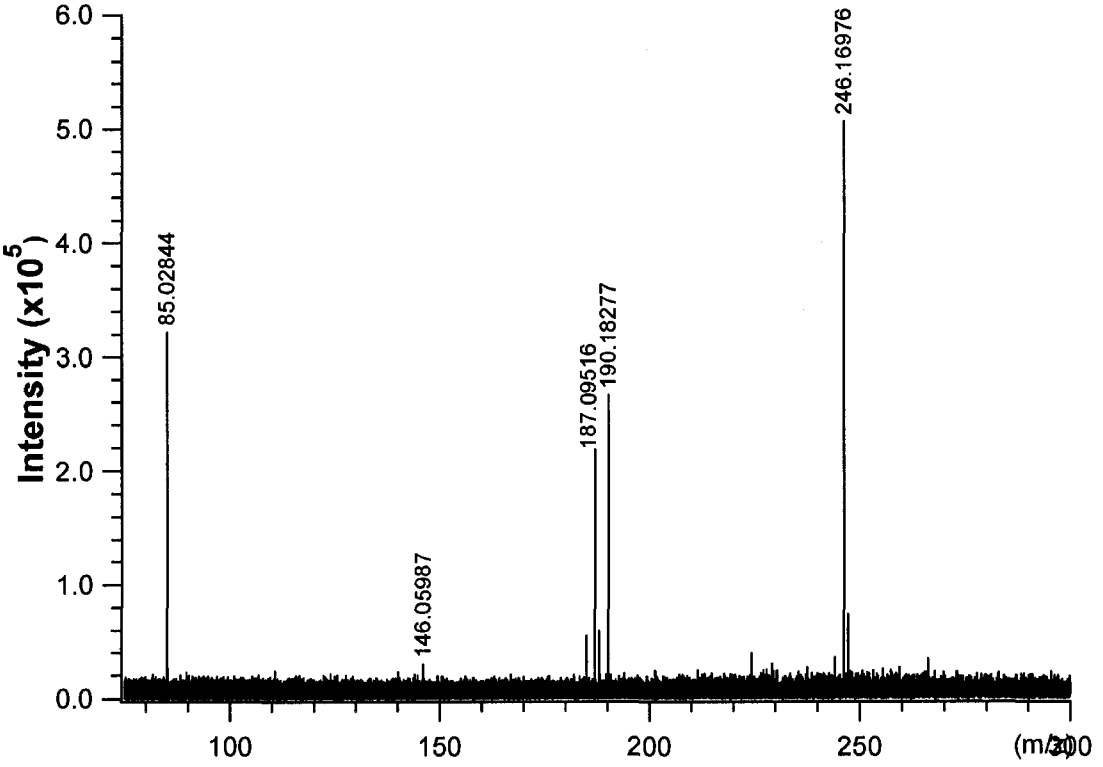

Figure 6.100 - Auto FT MS/MS analysis of m/z 246.17023 at 4.6 min

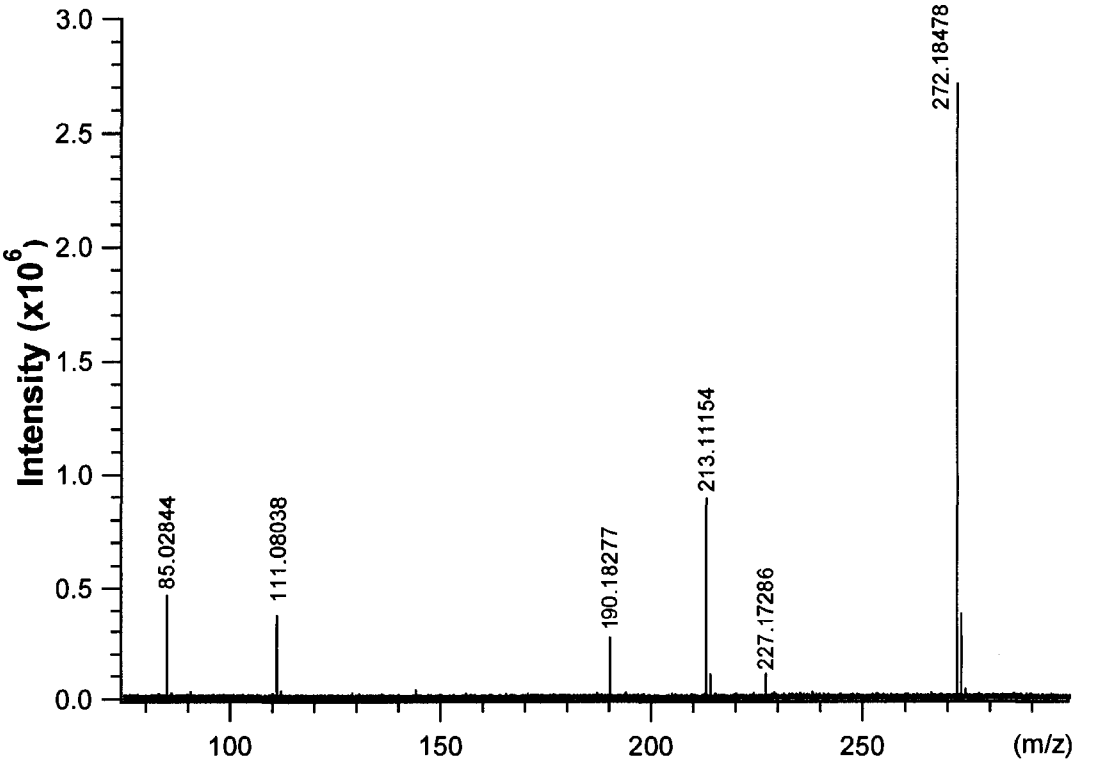

Figure 6.101 - Auto FT MS/MS analysis of m/z 272.18564 at 4.9 min

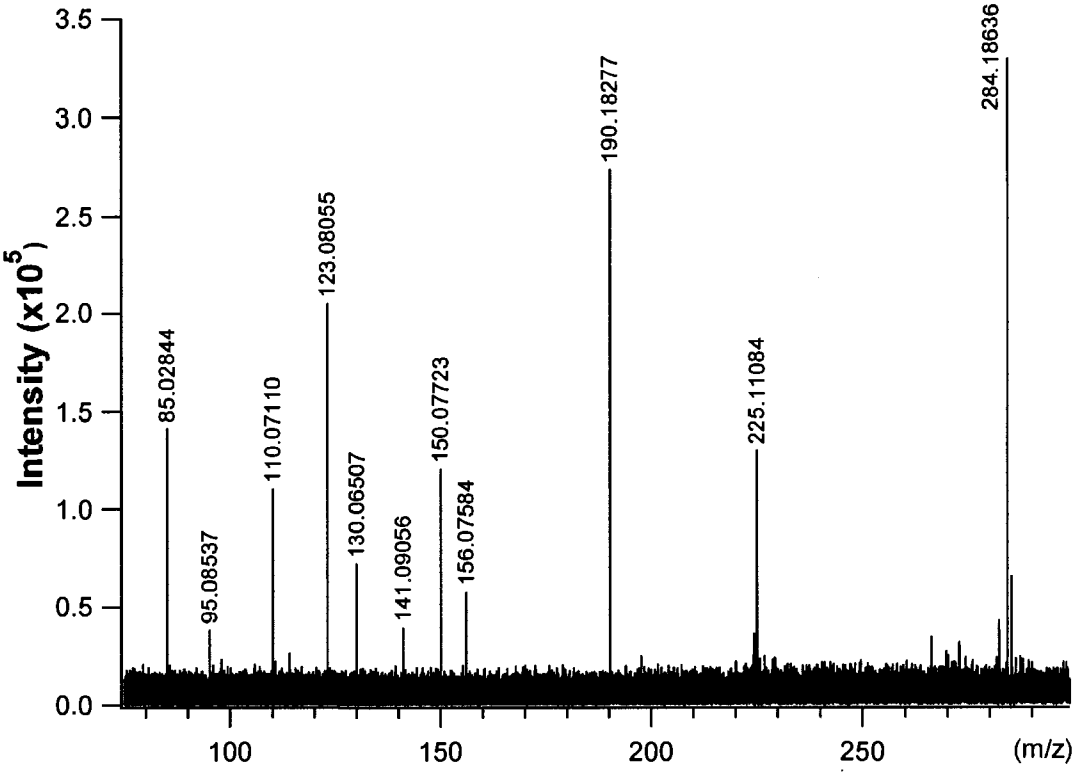

Figure 6.102 - Auto FT MS/MS analysis of m/z 284.18567 at 5.1 min

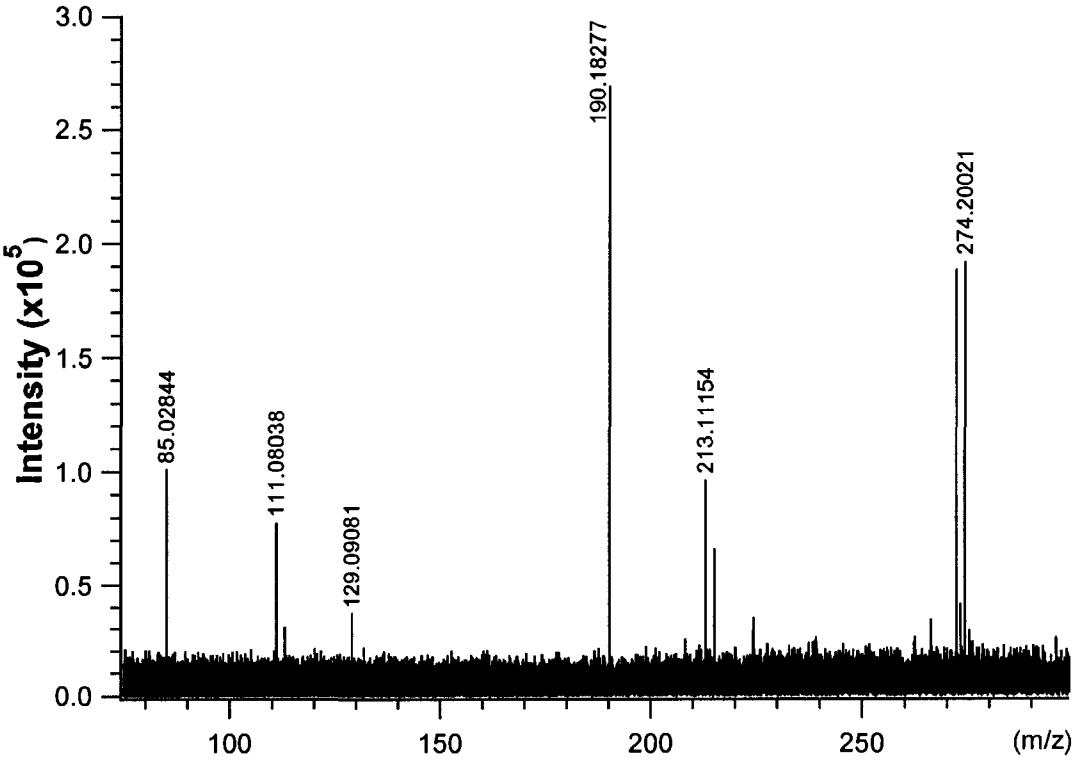

Figure 6.103 - Auto FT MS/MS analysis of m/z 274.20132 at 5.8 min

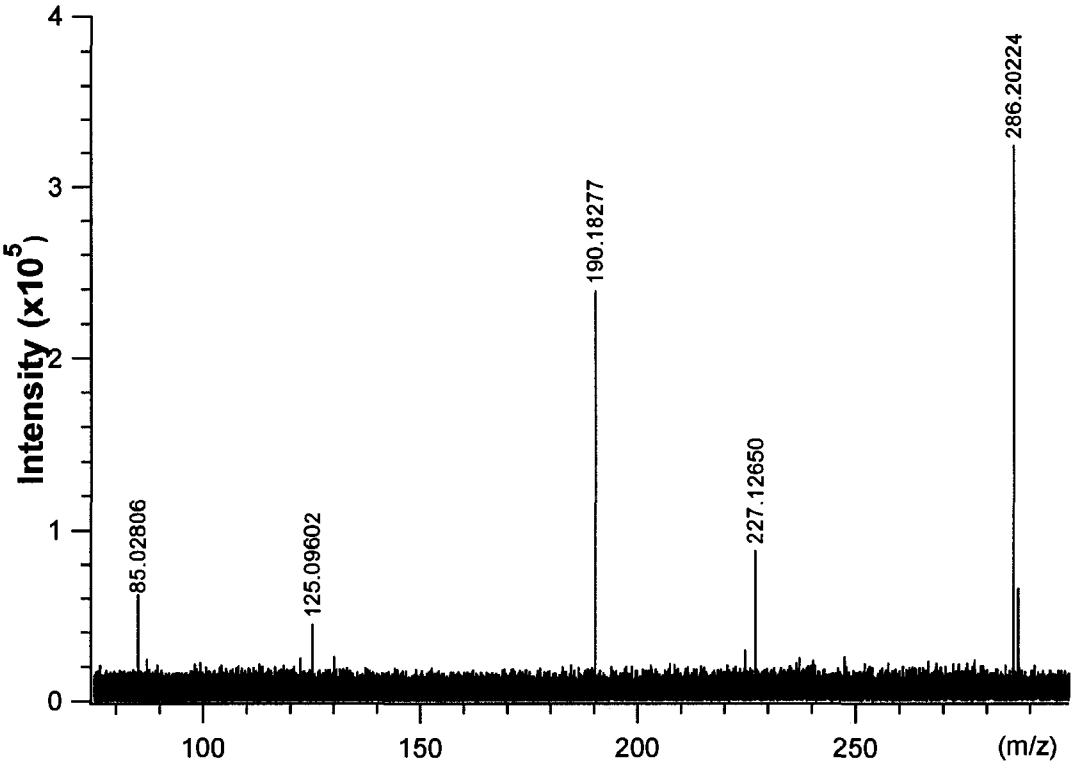

Figure 6.104 - Auto FT MS/MS analysis of m/z 286.20114 at 36.3 min

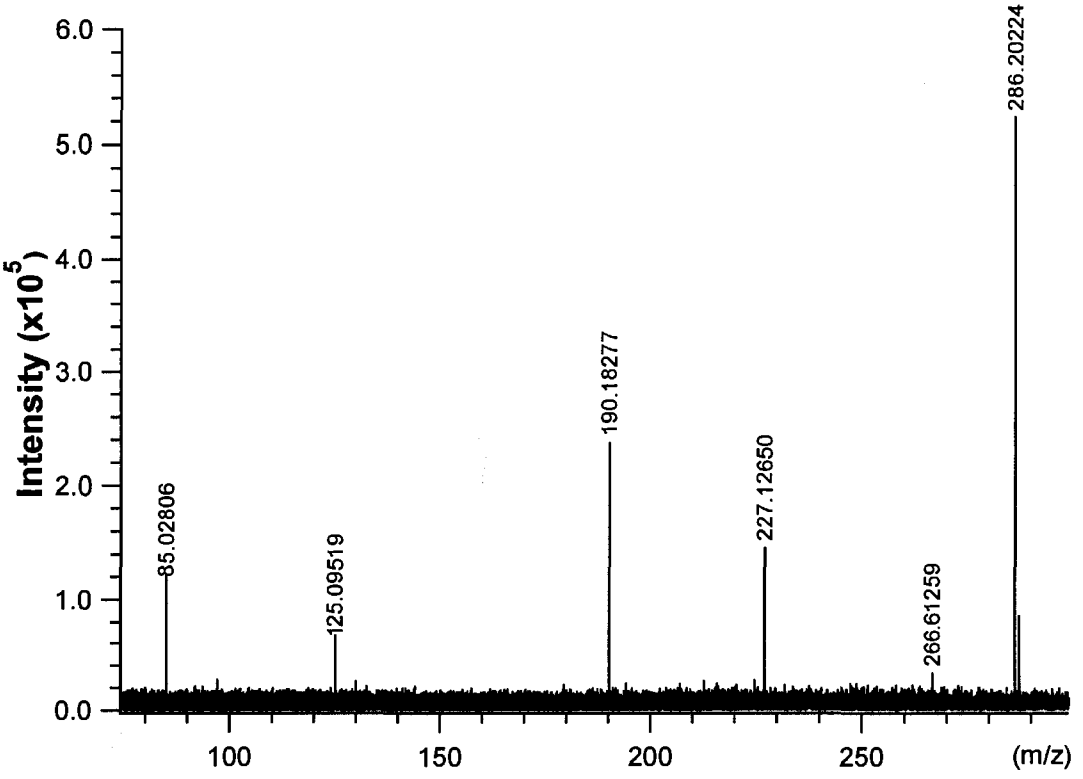

Figure 6.105 - Auto FT MS/MS analysis of m/z 286.20114 at 37.6 min

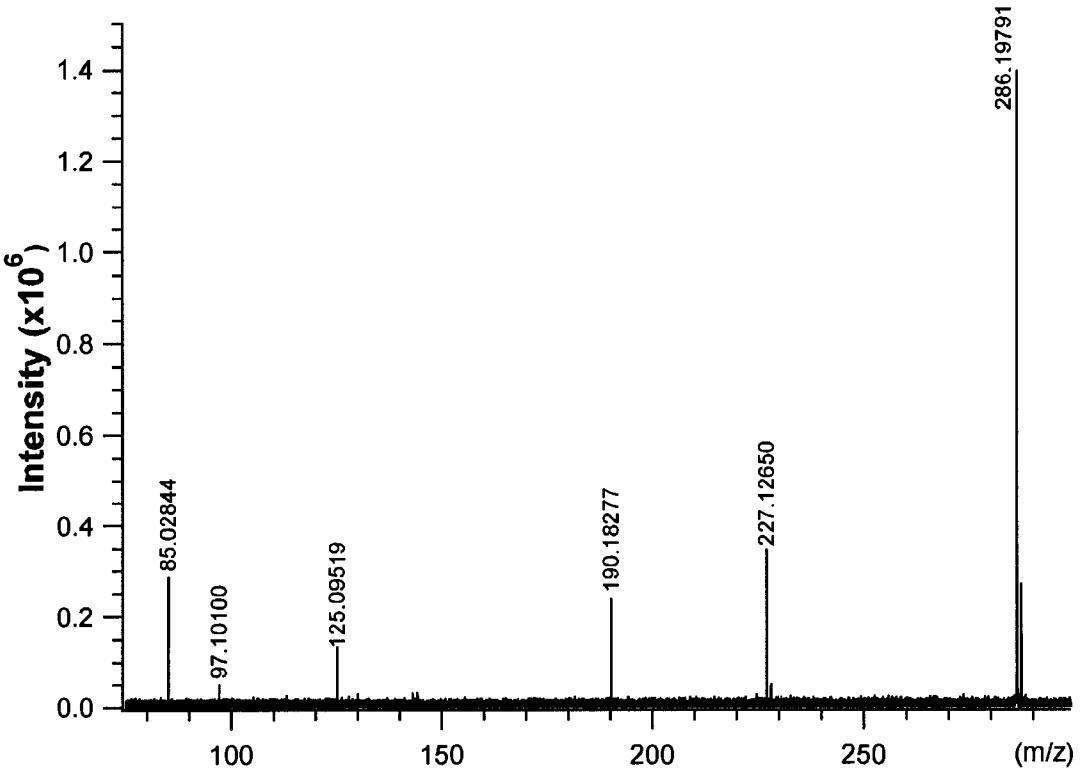

Figure 6.106 - Auto FT MS/MS analysis of m/z 286.20114 at 38.9 min

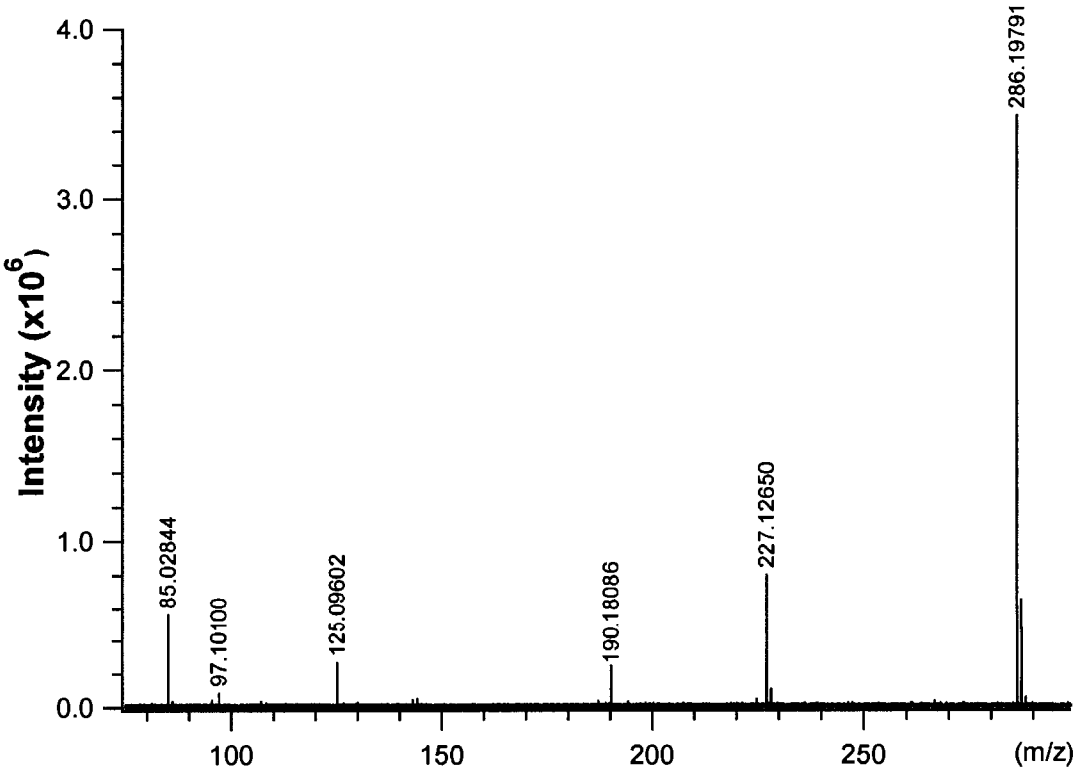

Figure 6.107 - Auto FT MS/MS analysis of m/z 286.20114 at 40.2 min

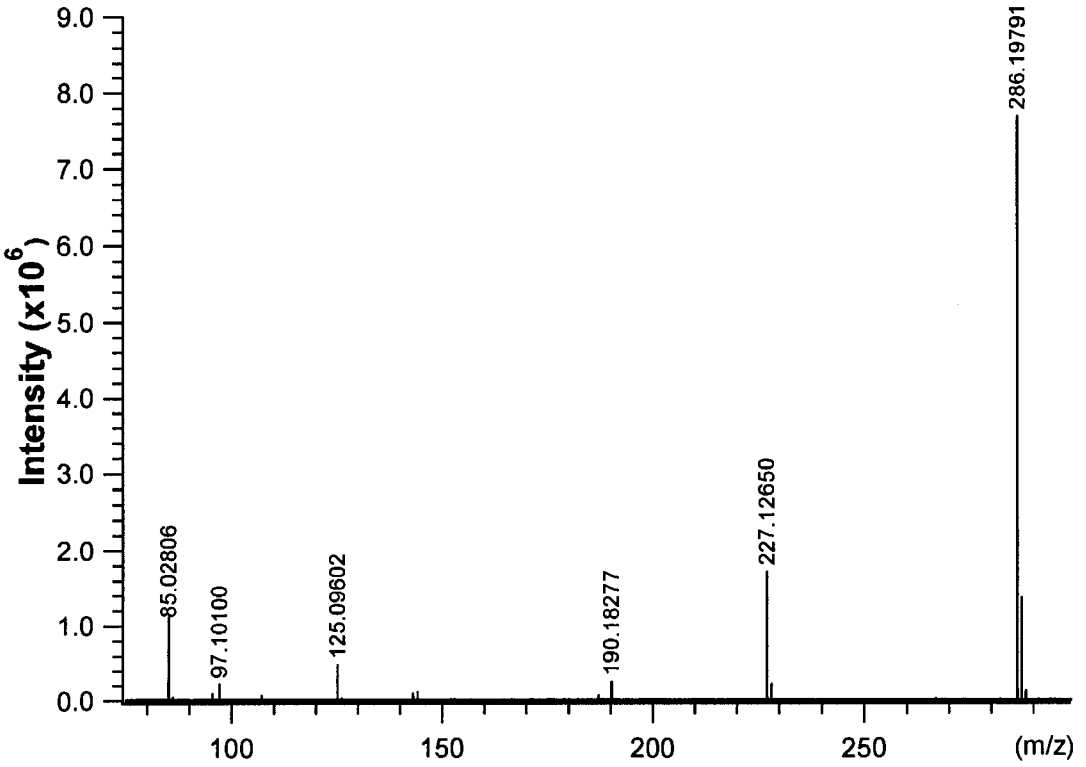

Figure 6.108 - Auto FT MS/MS analysis of m/z 286.20114 at 42.6 min

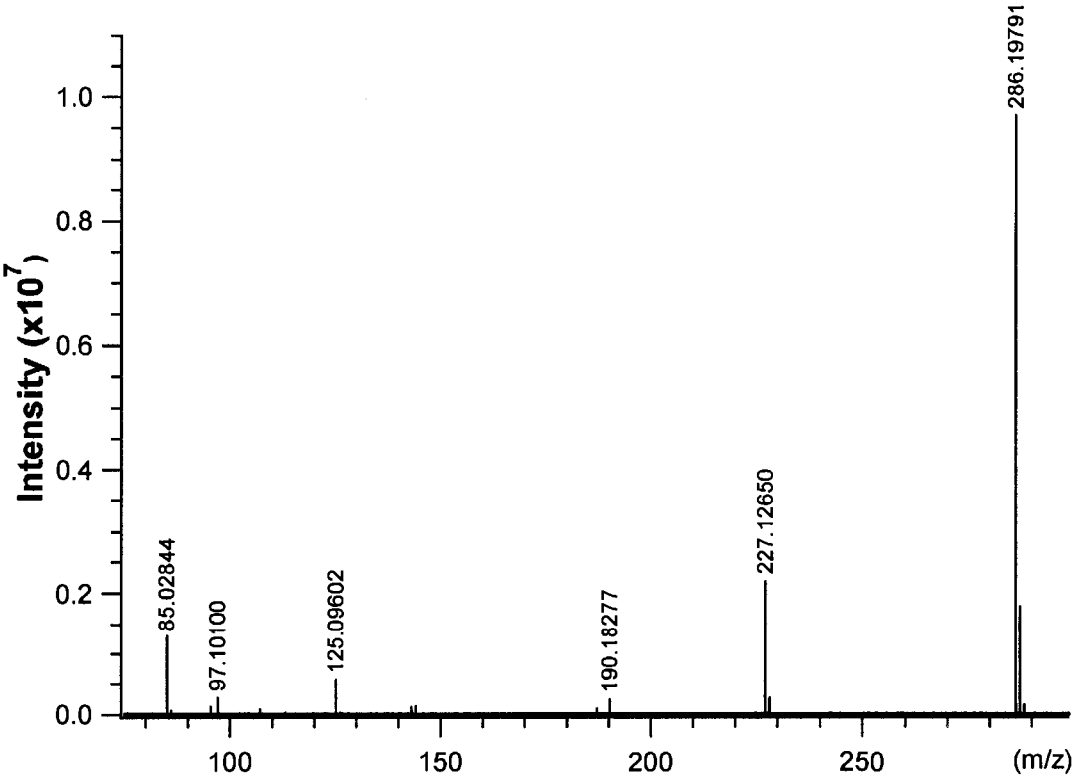

Figure 6.109 - Auto FT MS/MS analysis of m/z 286.20114 at 43.9 min

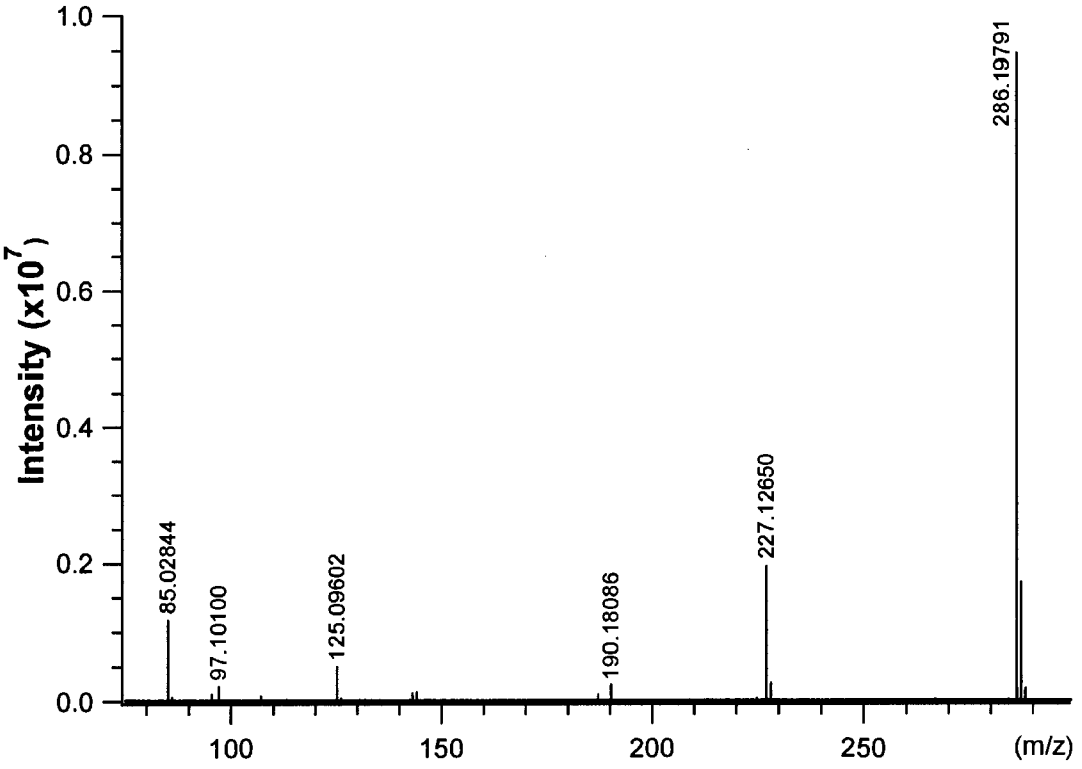

Figure 6.110 - Auto FT MS/MS analysis of m/z 286.20114 at 45.2 min

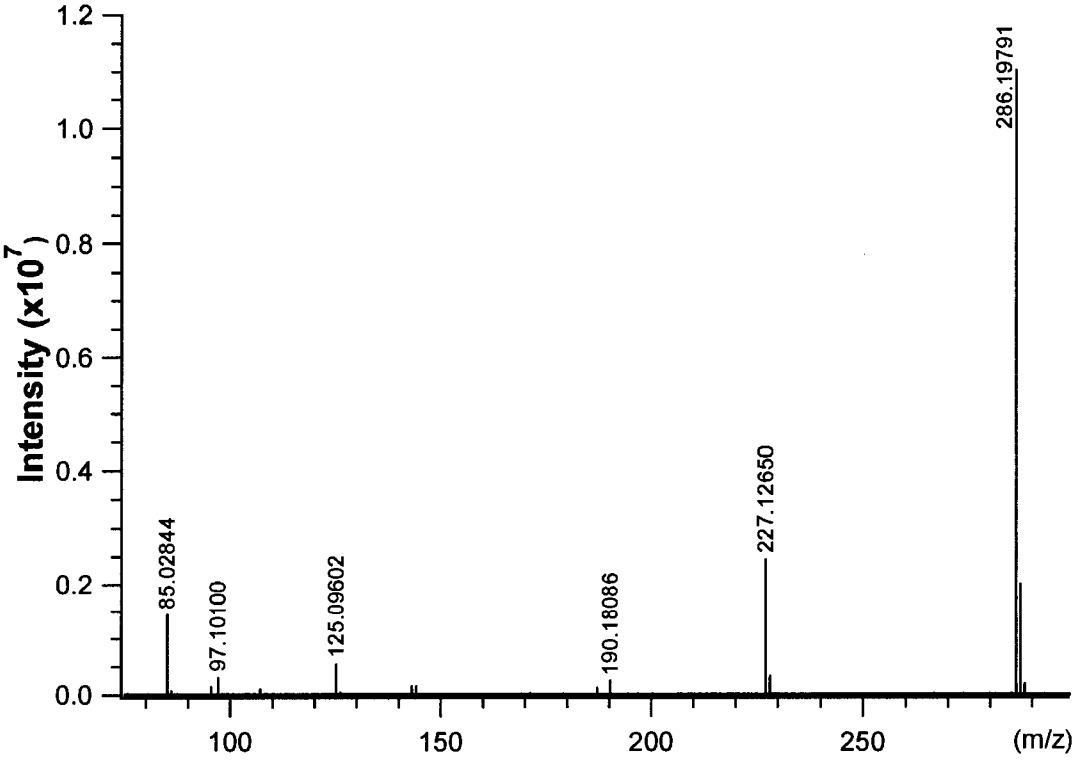

Figure 6.111 - Auto FT MS/MS analysis of m/z 286.20114 at 46.5 min

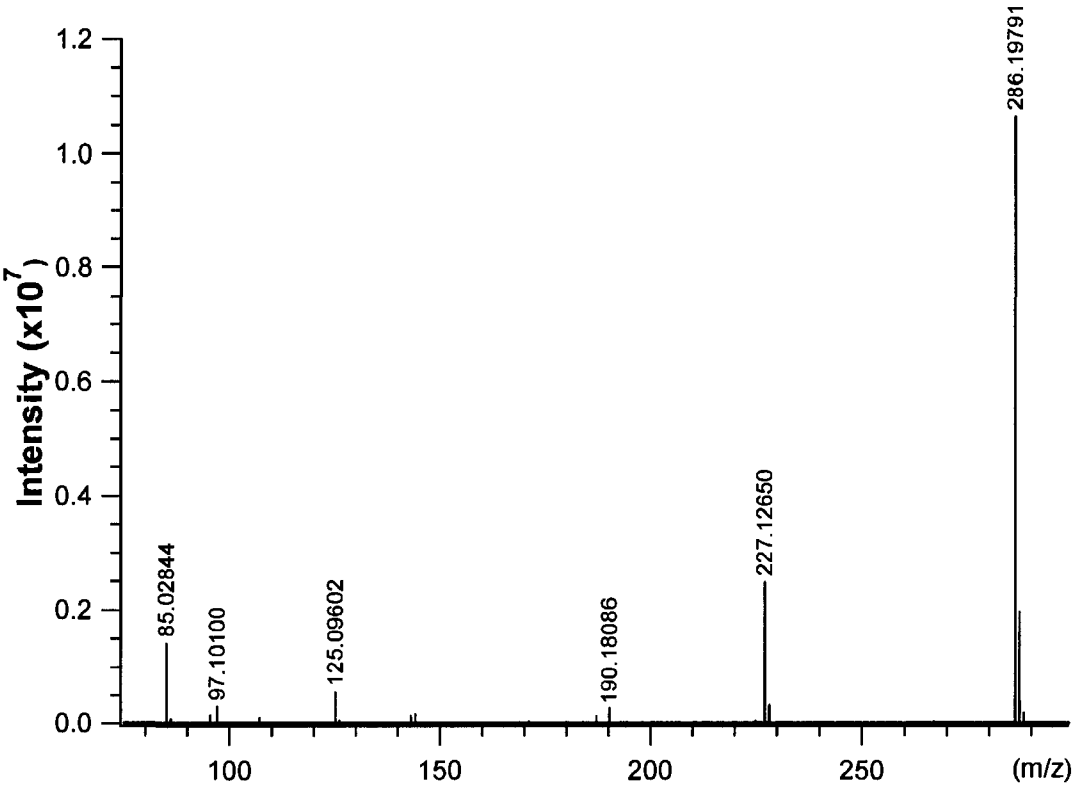

Figure 6.112 - Auto FT MS/MS analysis of m/z 286.20114 at 47.8 min

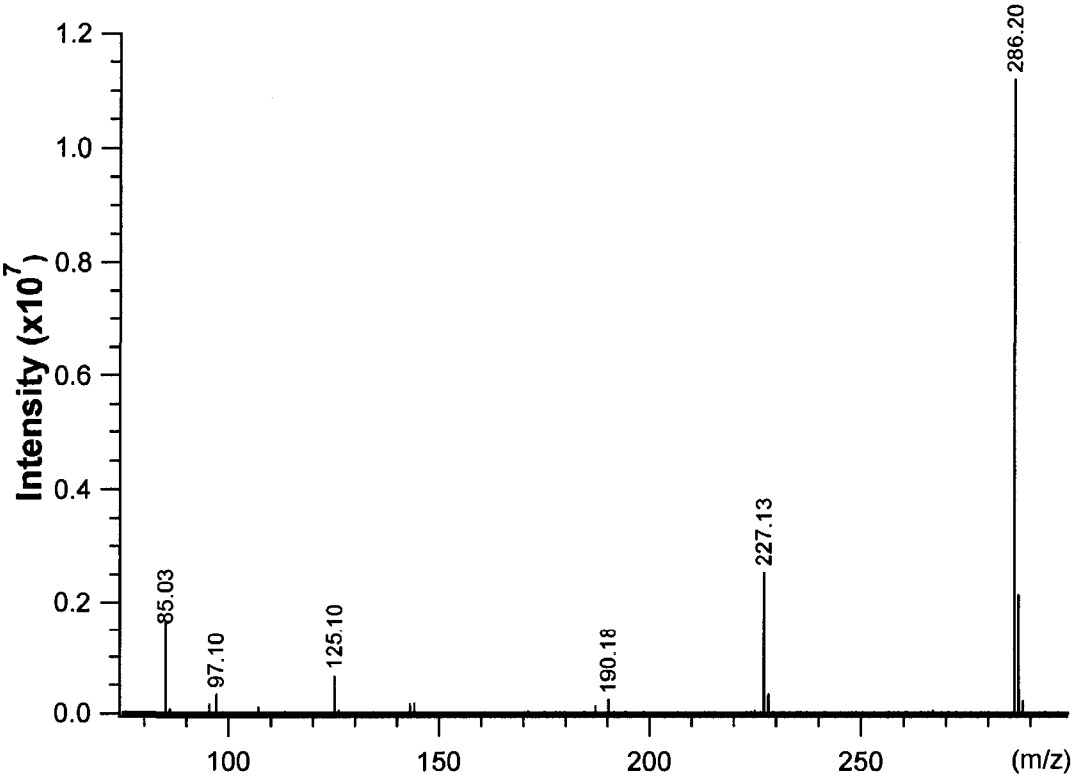

Figure 6.113 - Auto FT MS/MS analysis of m/z 286.20114 at 49.1 min

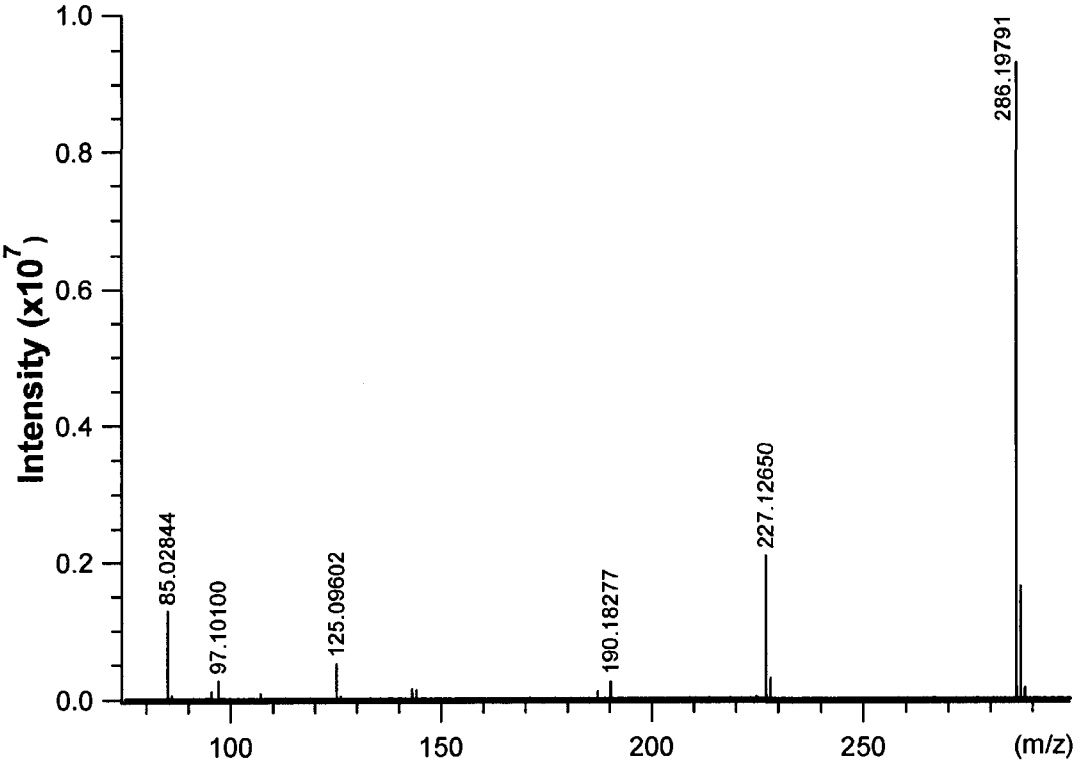

Figure 6.114 - Auto FT MS/MS analysis of m/z 286.20114 at 50.3 min

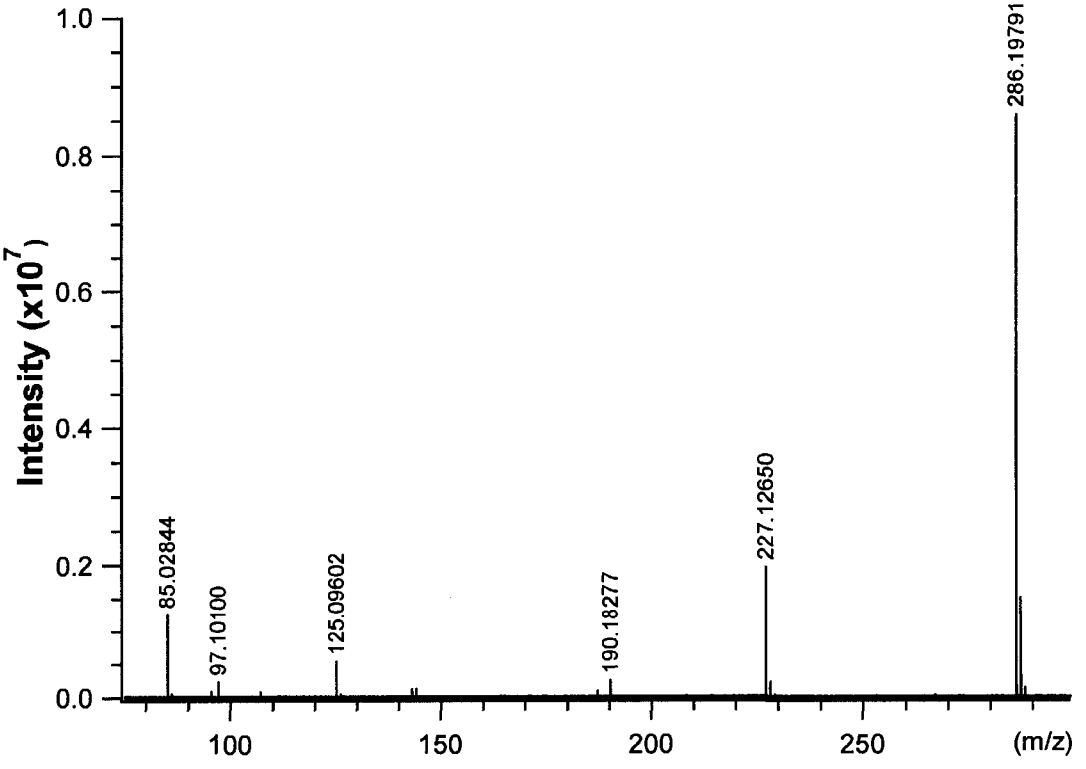

Figure 6.115 - Auto FT MS/MS analysis of m/z 286.20114 at 51.6 min

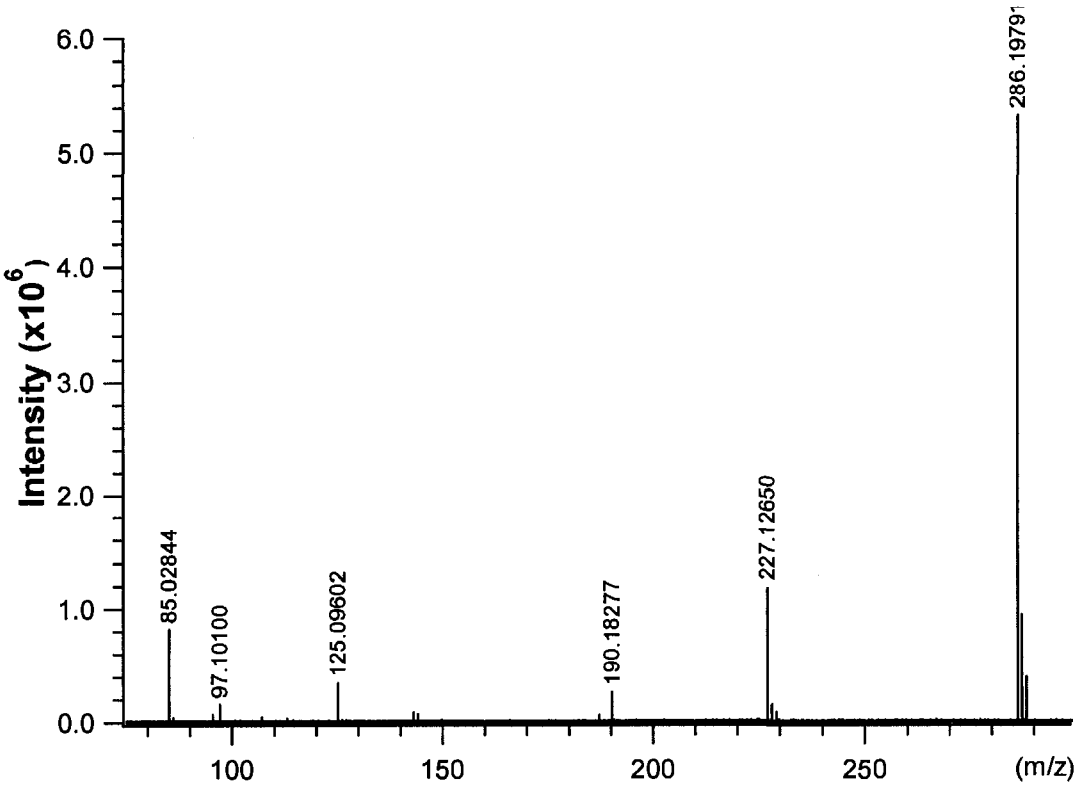

Figure 6.116 - Auto FT MS/MS analysis of m/z 286.20114 at 52.9 min

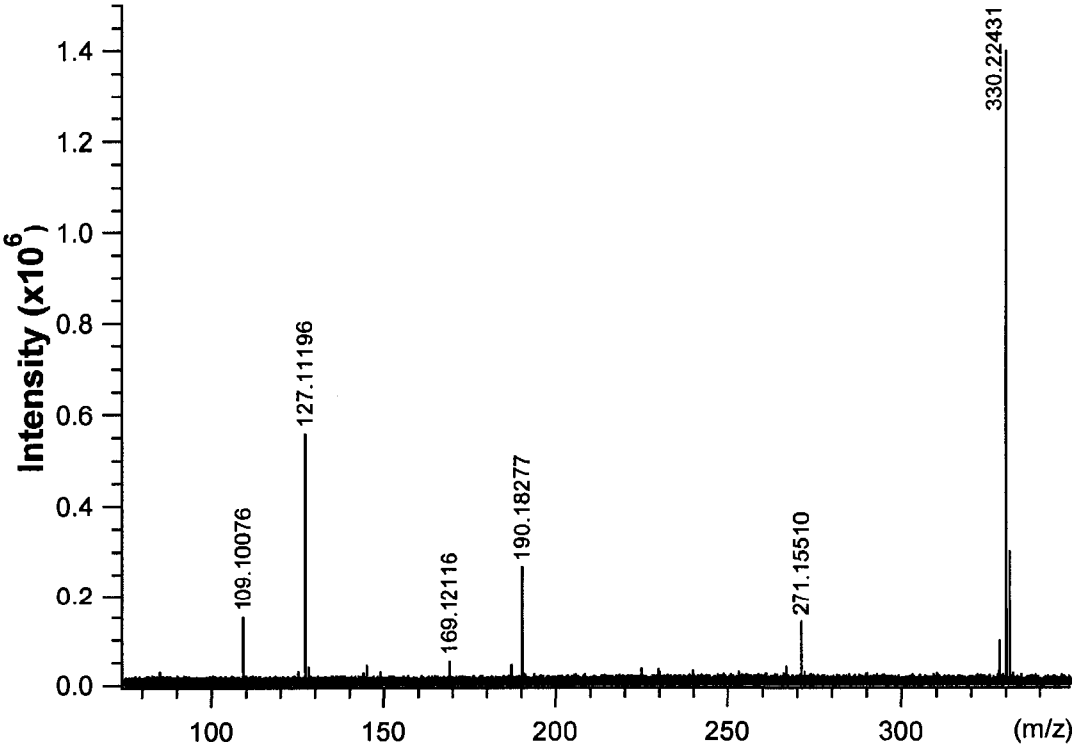

Figure 6.117 - Auto FT MS/MS analysis of m/z 330.22449 at 53.3 min

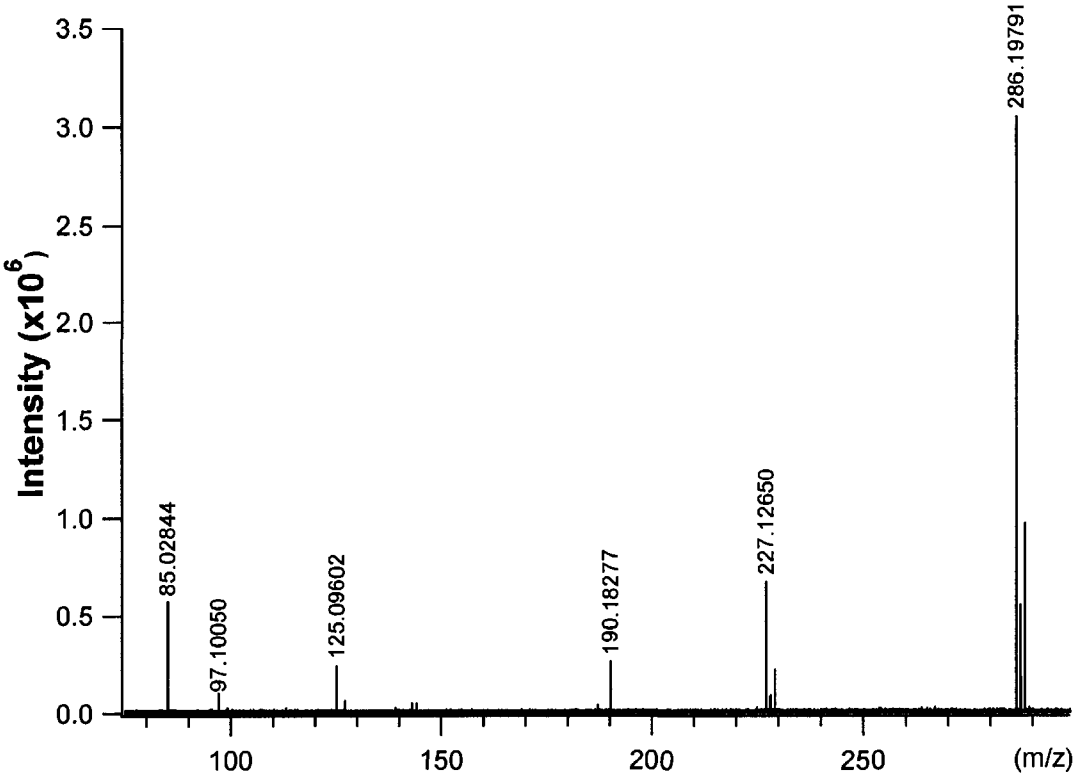

Figure 6.118 - Auto FT MS/MS analysis of m/z 286.20114 at 54.2 min

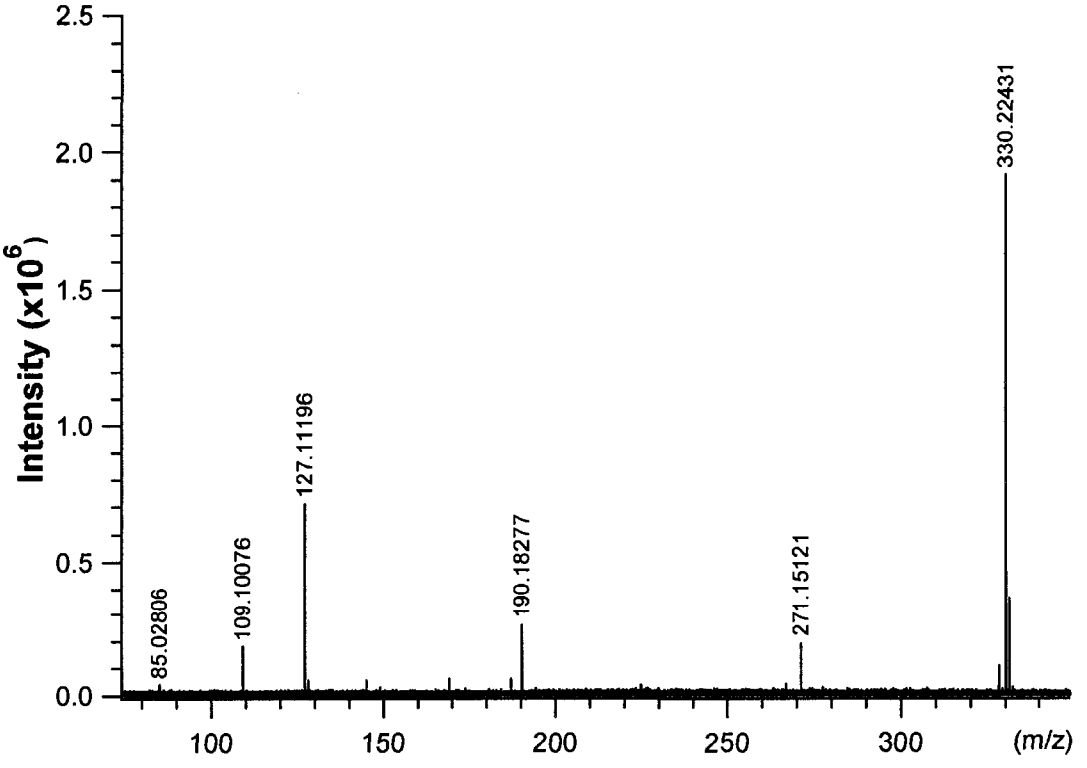

Figure 6.119 - Auto FT MS/MS analysis of m/z 330.22449 at 54.6 min

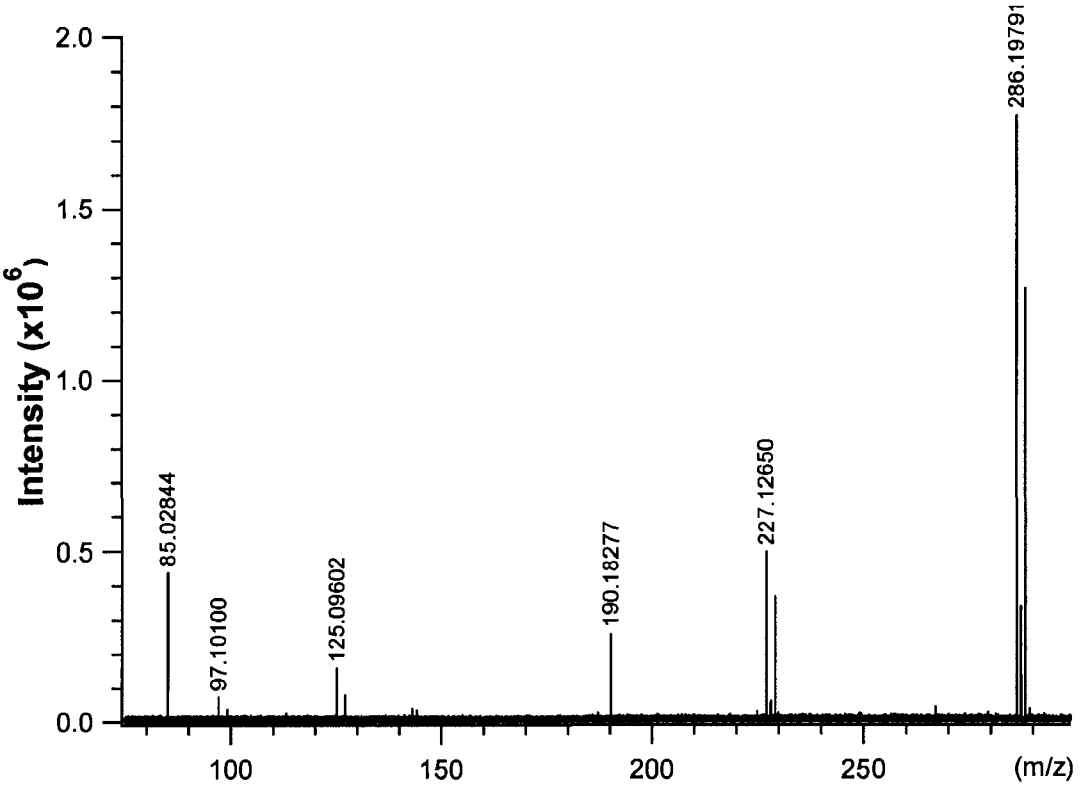

Figure 6.120 - Auto FT MS/MS analysis of m/z 286.20114 at 55.5 min

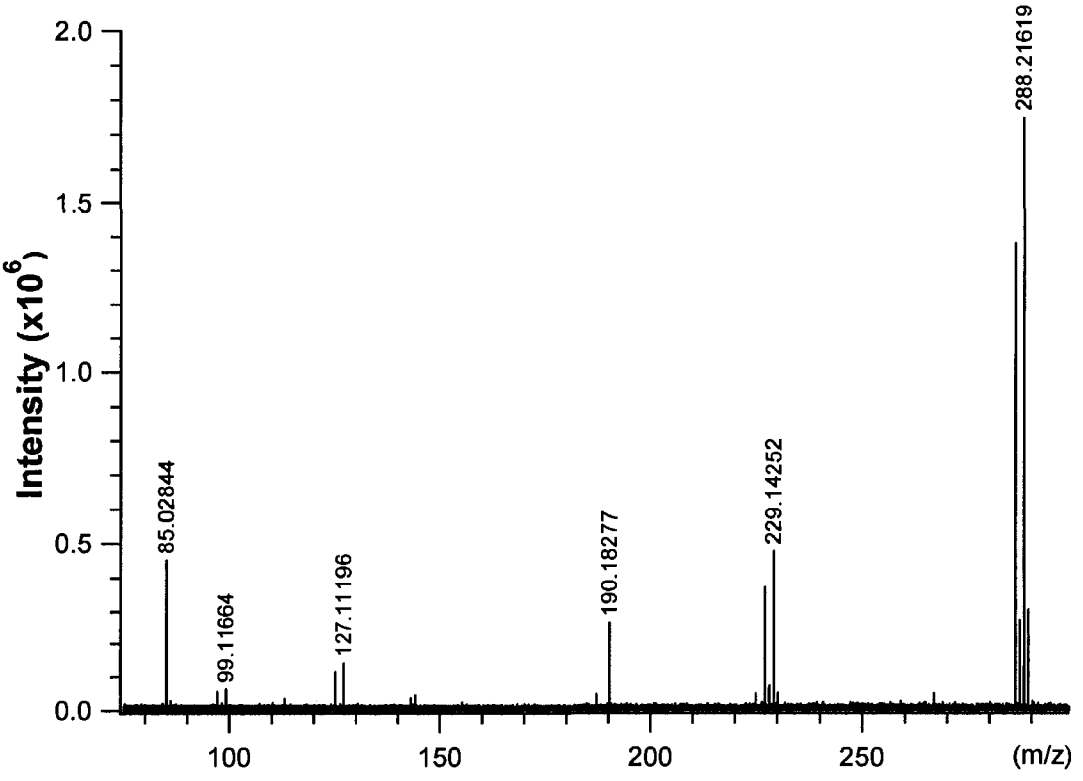

Figure 6.121 - Auto FT MS/MS analysis of m/z 288.21591 at 55.7 min

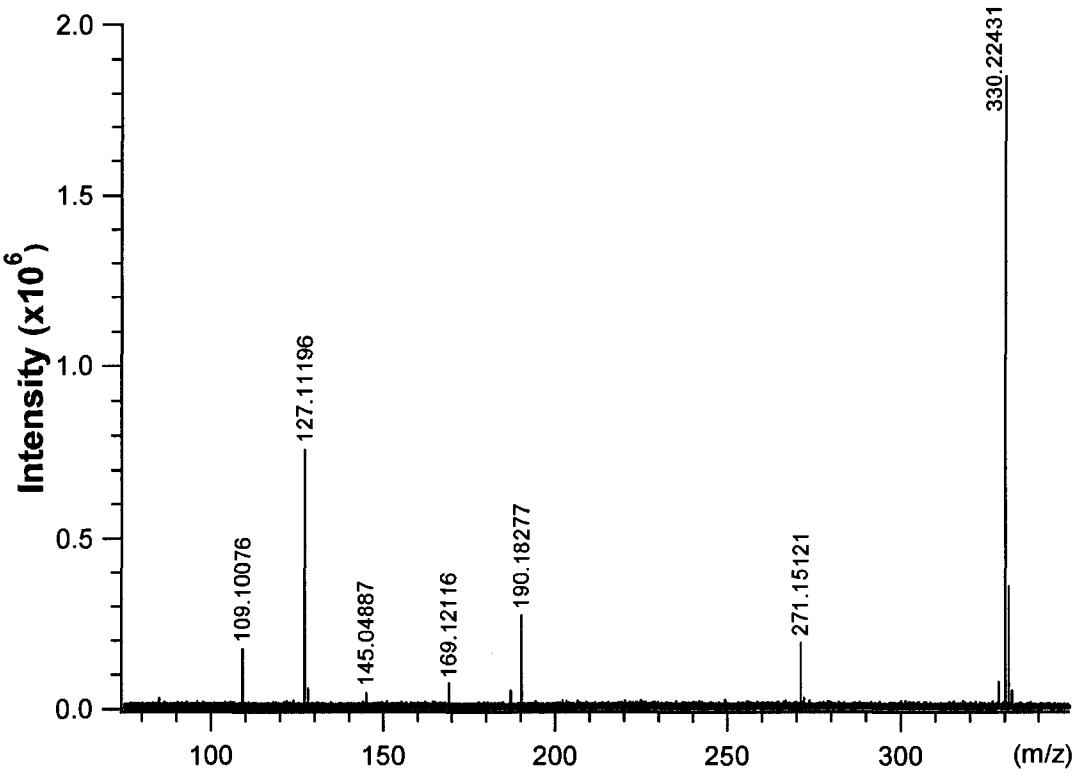

Figure 6.122 - Auto FT MS/MS analysis of m/z 330.22449 at 55.9 min

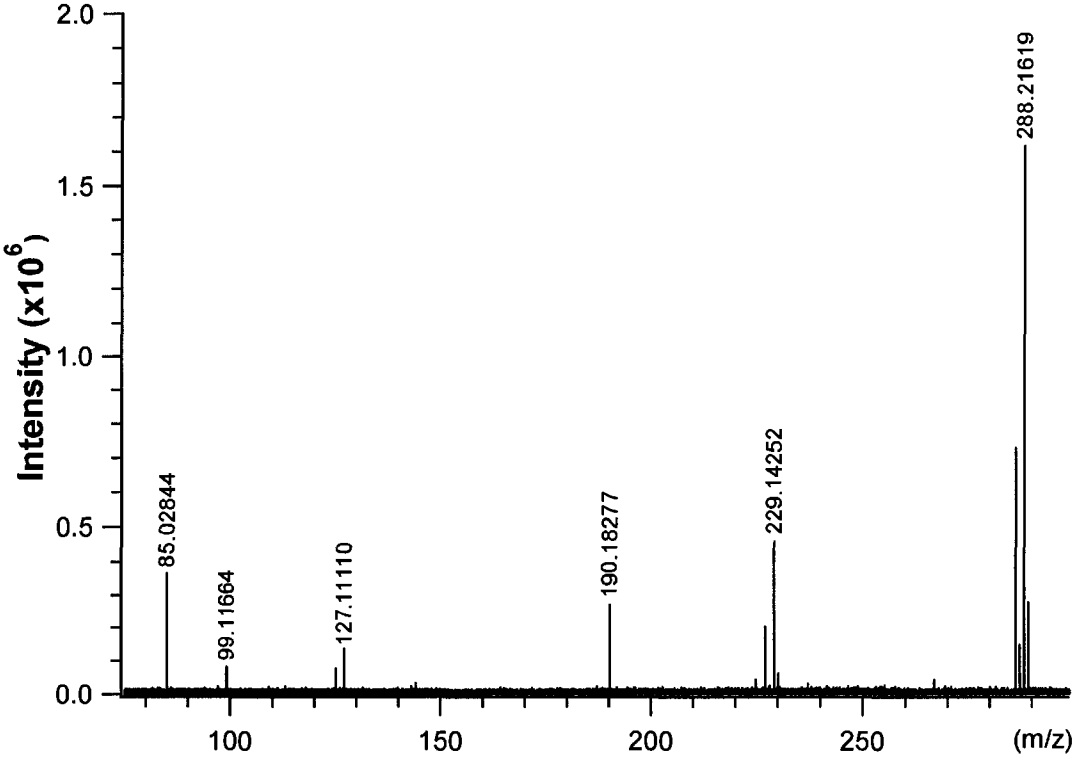

Figure 6.123 - Auto FT MS/MS analysis of m/z 288.21591 at 57.1 min

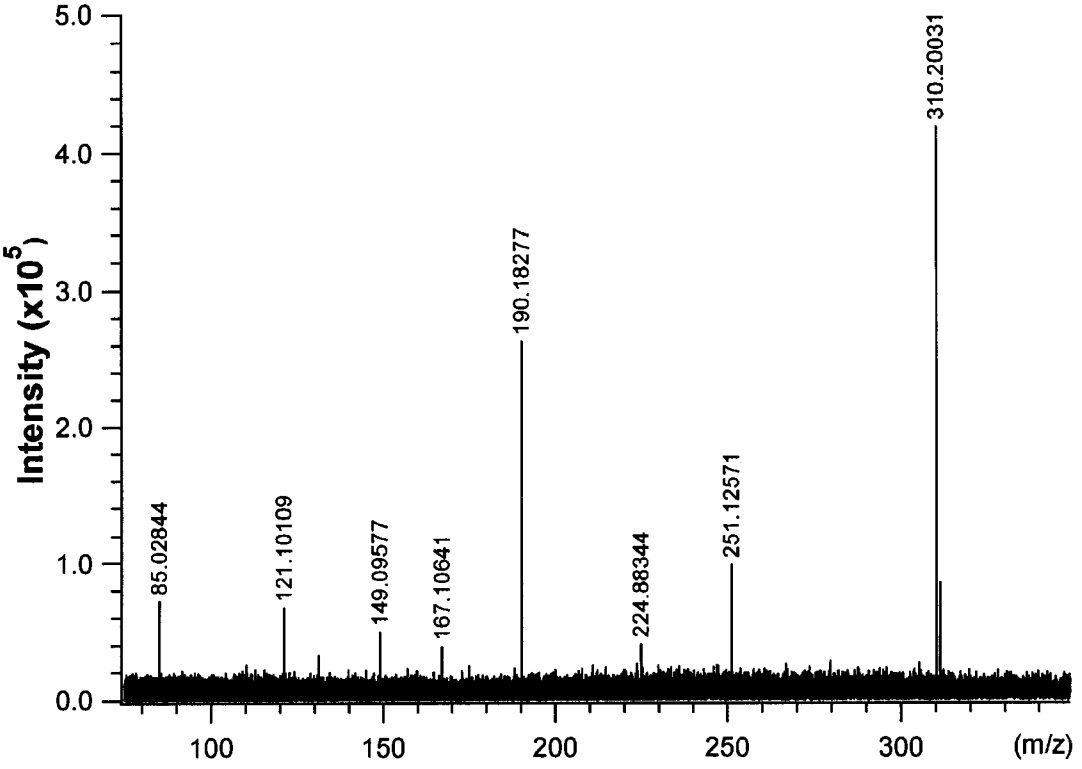

Figure 6.124 - Auto FT MS/MS analysis of m/z 310.19992 at 57.3 min

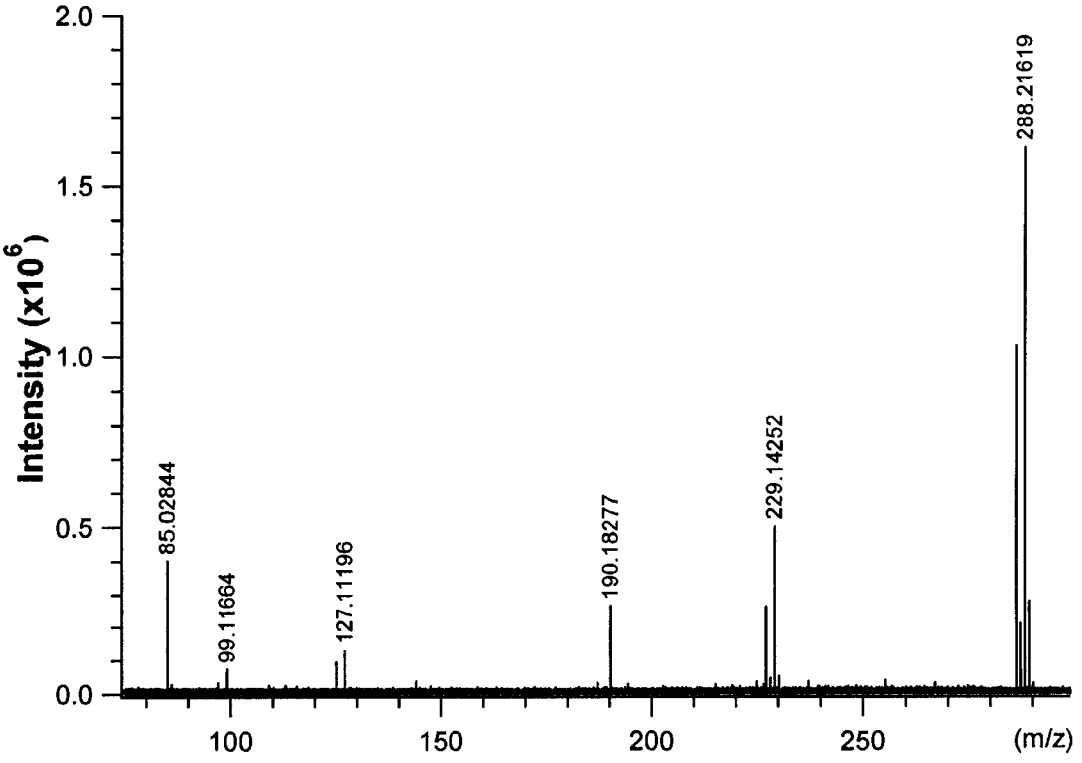

Figure 6.125 - Auto FT MS/MS analysis of m/z 288.21591 at 58.4 min

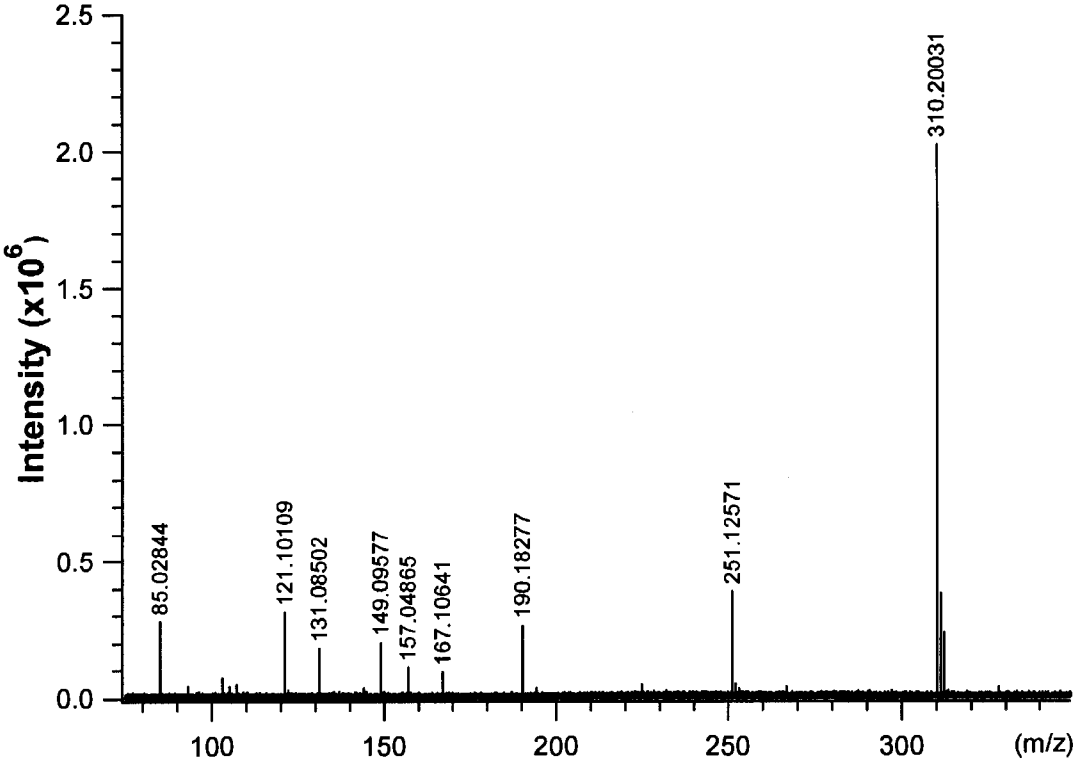

Figure 6.126 - Auto FT MS/MS analysis of m/z 310.19992 at 58.6 min

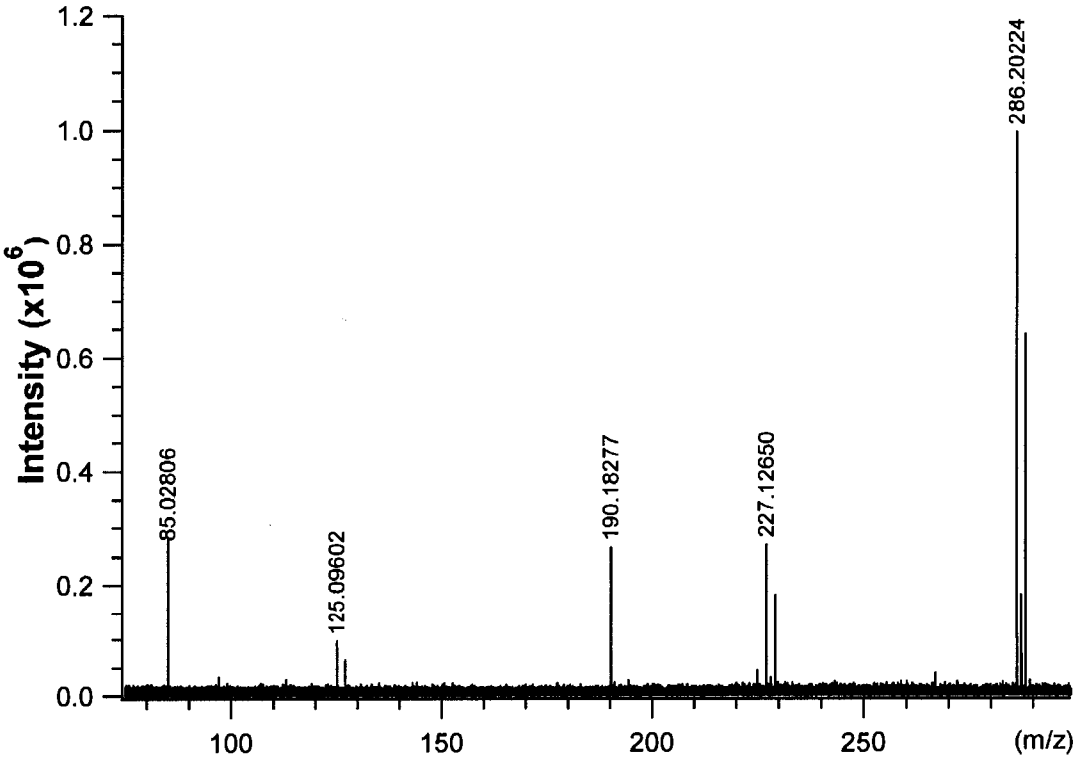

Figure 6.127 - Auto FT MS/MS analysis of m/z 286.20114 at 59.4 min

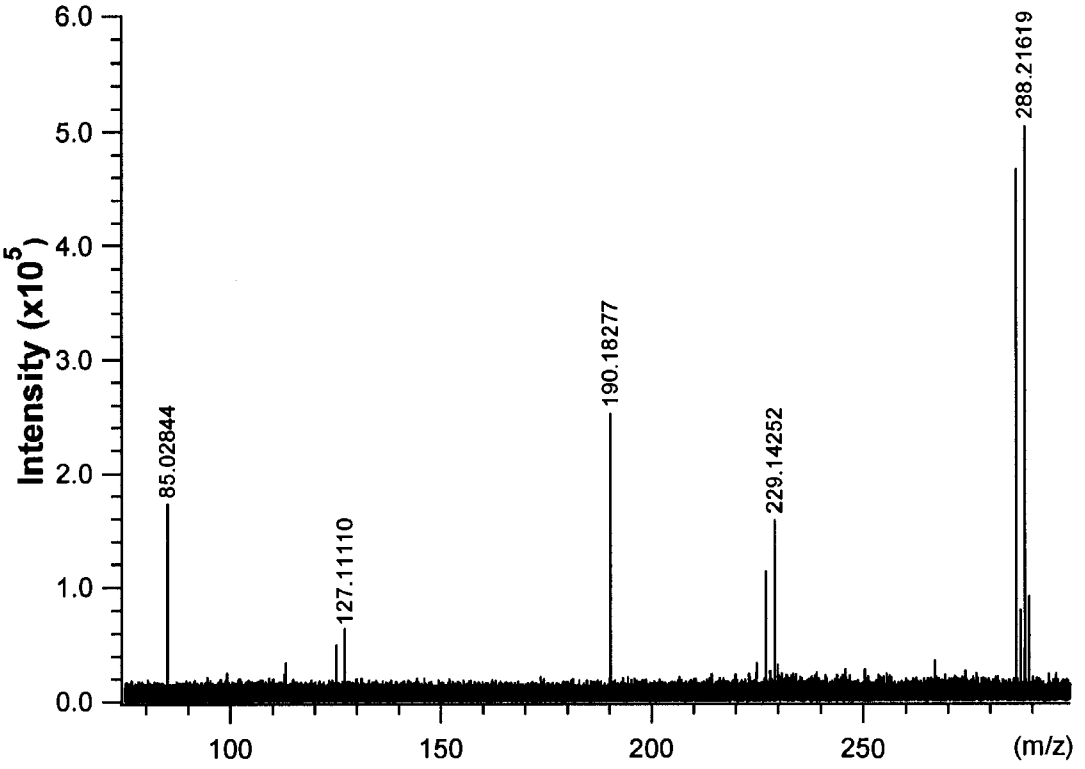

Figure 6.128 - Auto FT MS/MS analysis of m/z 288.21591 at 59.6 min

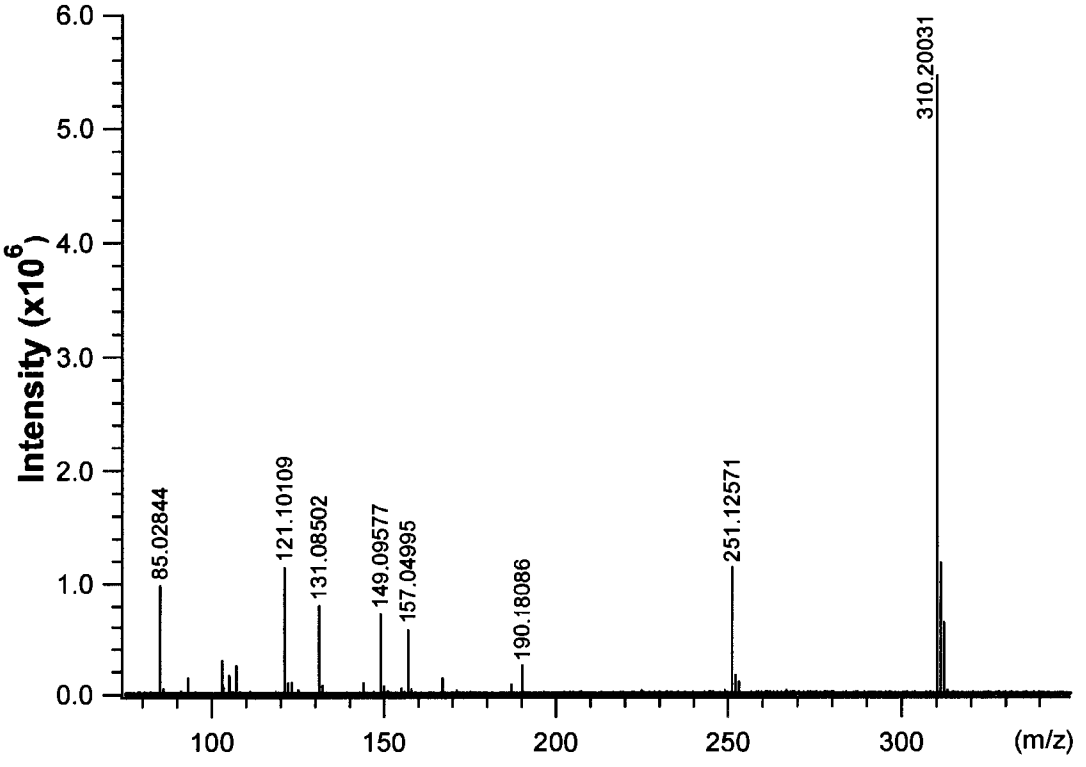

Figure 6.129 - Auto FT MS/MS analysis of m/z 310.19992 at 59.9 min

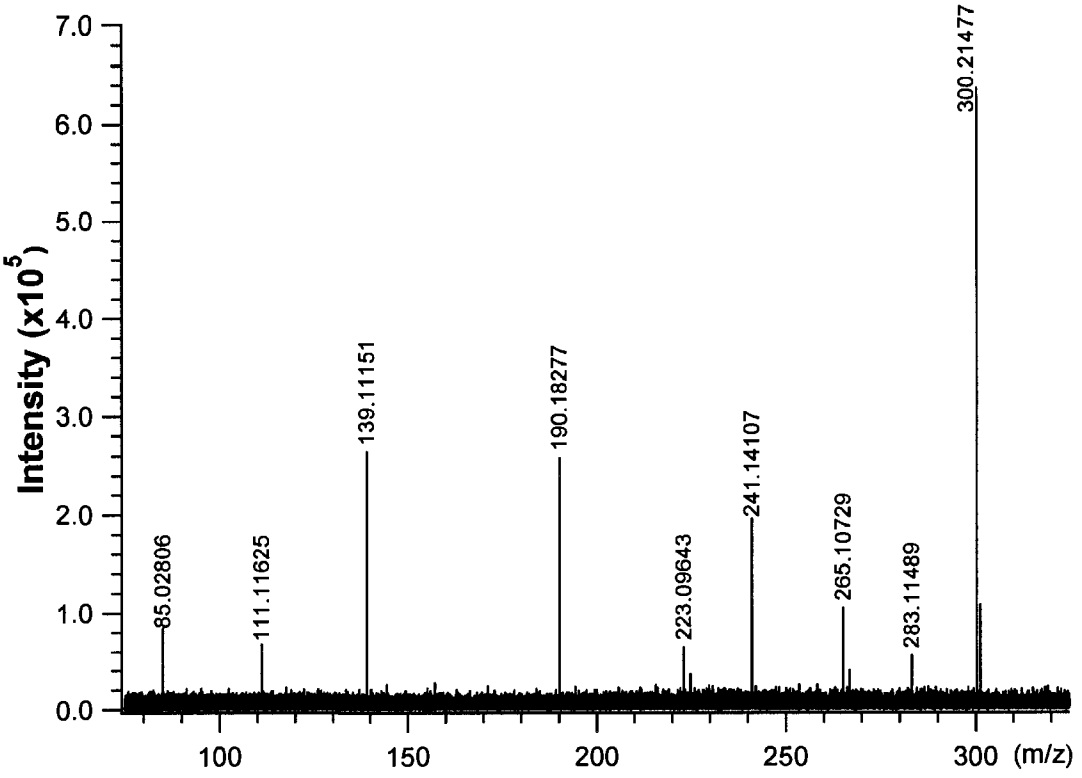

Figure 6.130 - Auto FT MS/MS analysis of m/z 300.21768 at 60.3 min

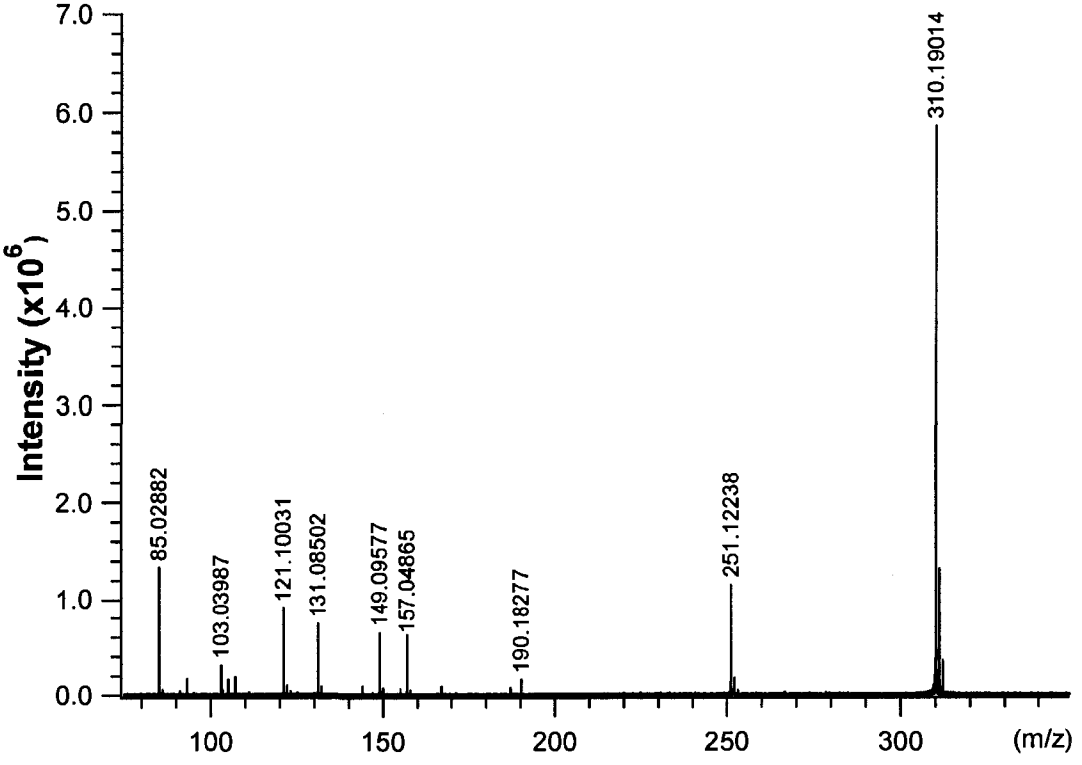

Figure 6.131 - Auto FT MS/MS analysis of m/z 310.19992at 61.1 min

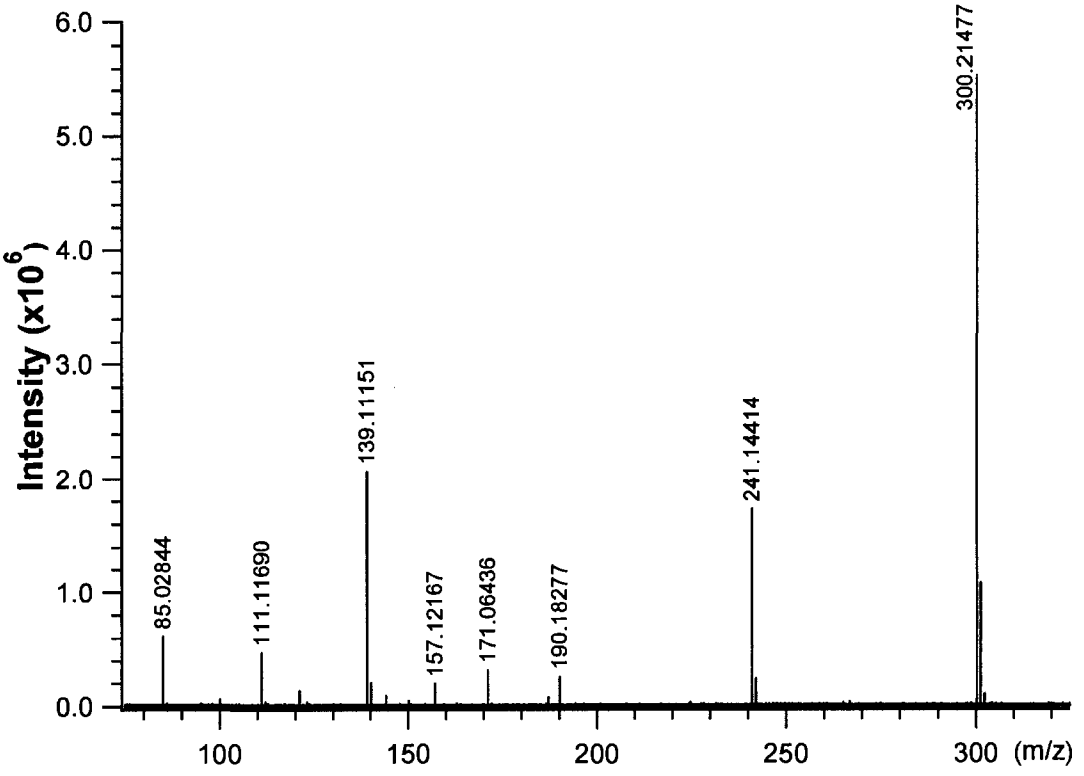

Figure 6.132 - Auto FT MS/MS analysis of m/z 300.21768 at 61.5 min

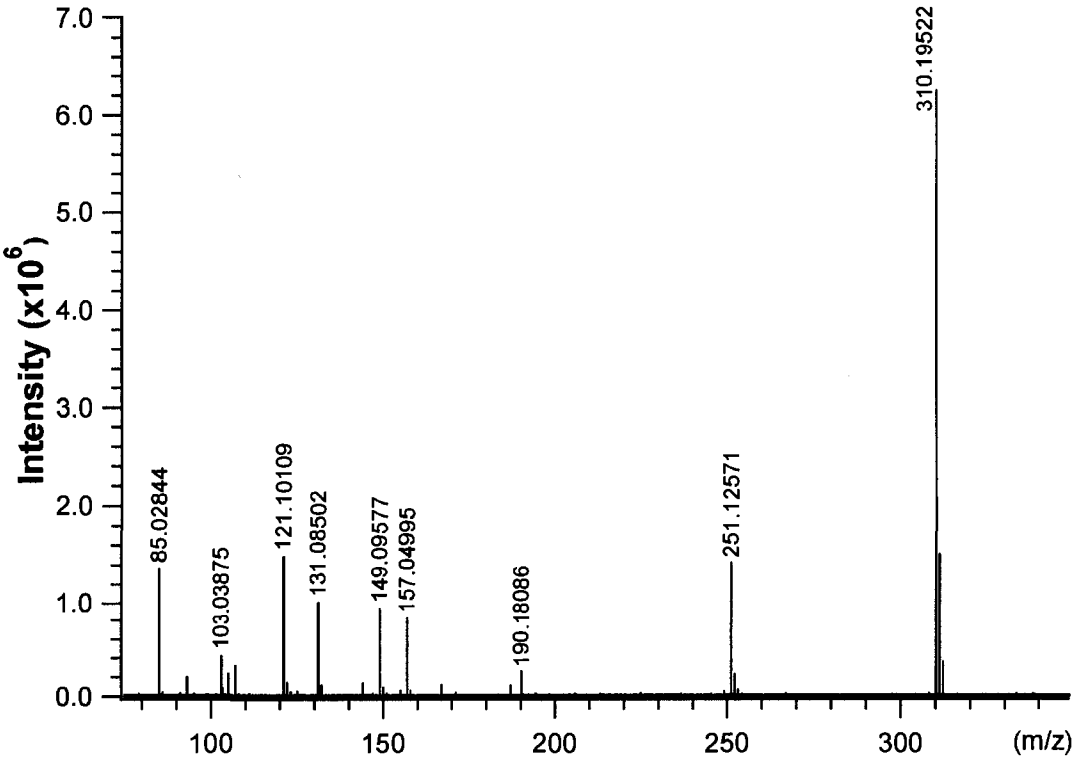

Figure 6.133 - Auto FT MS/MS analysis of m/z 310.19992 at 62.4 min

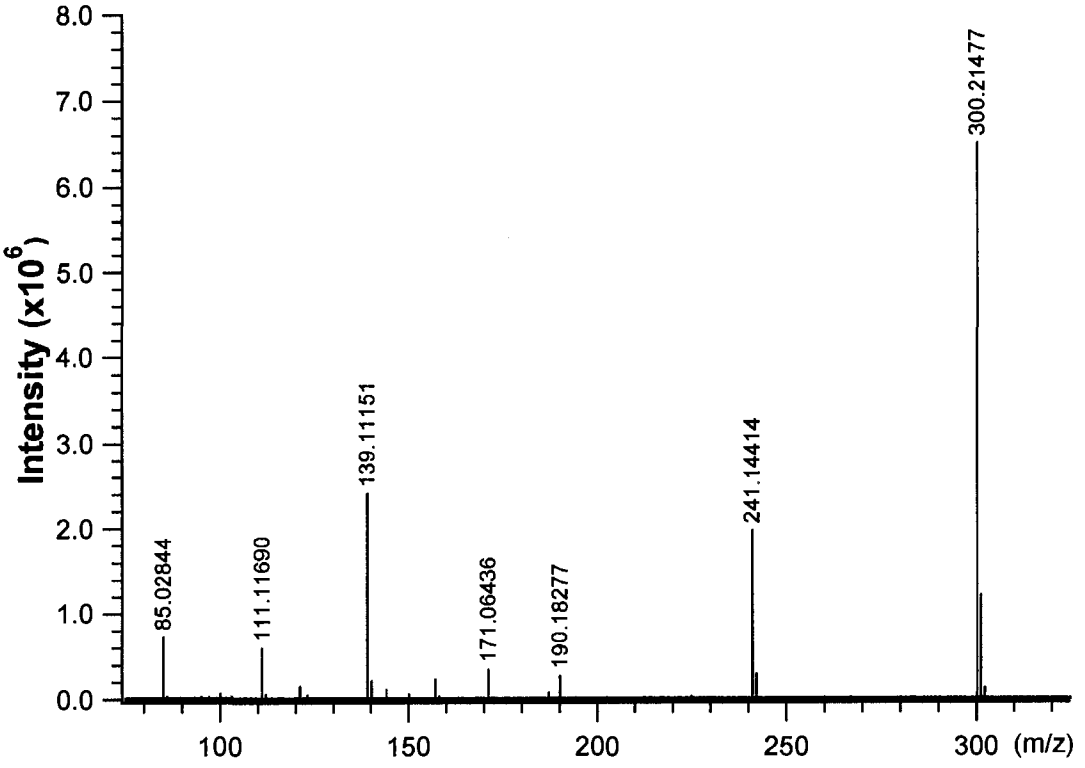

Figure 6.134 - Auto FT MS/MS analysis of m/z 300.21768 at 62.8 min

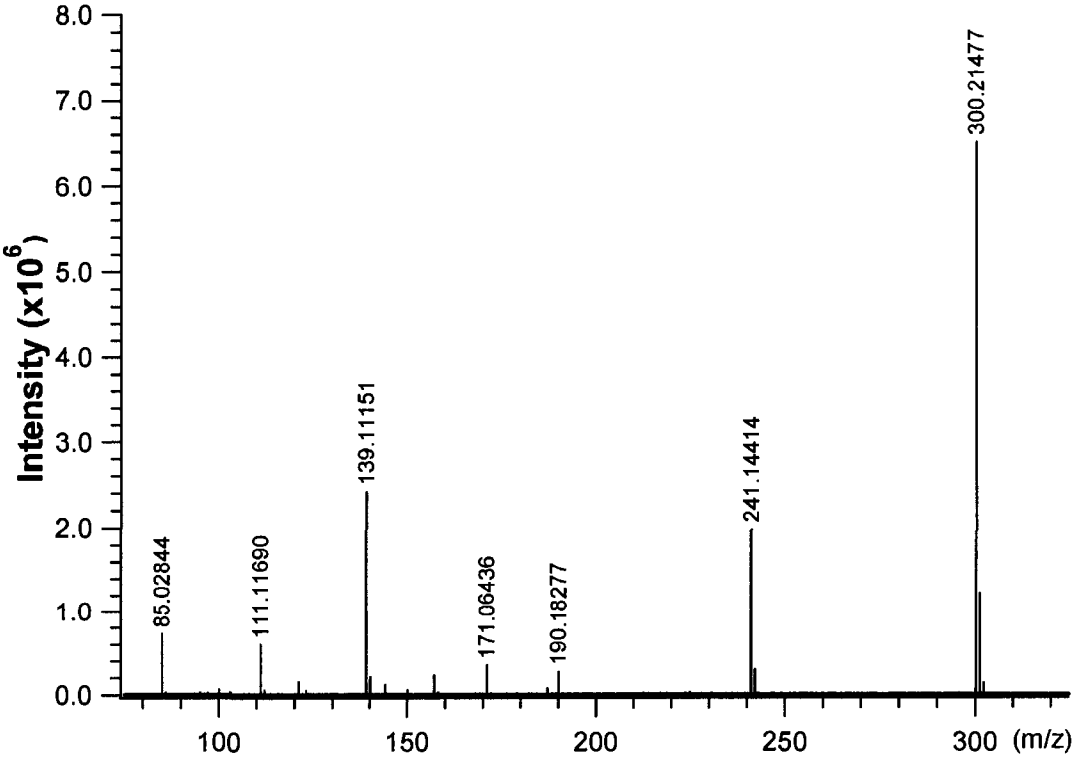

Figure 6.135 - Auto FT MS/MS analysis of m/z 310.19992 at 63.7 min

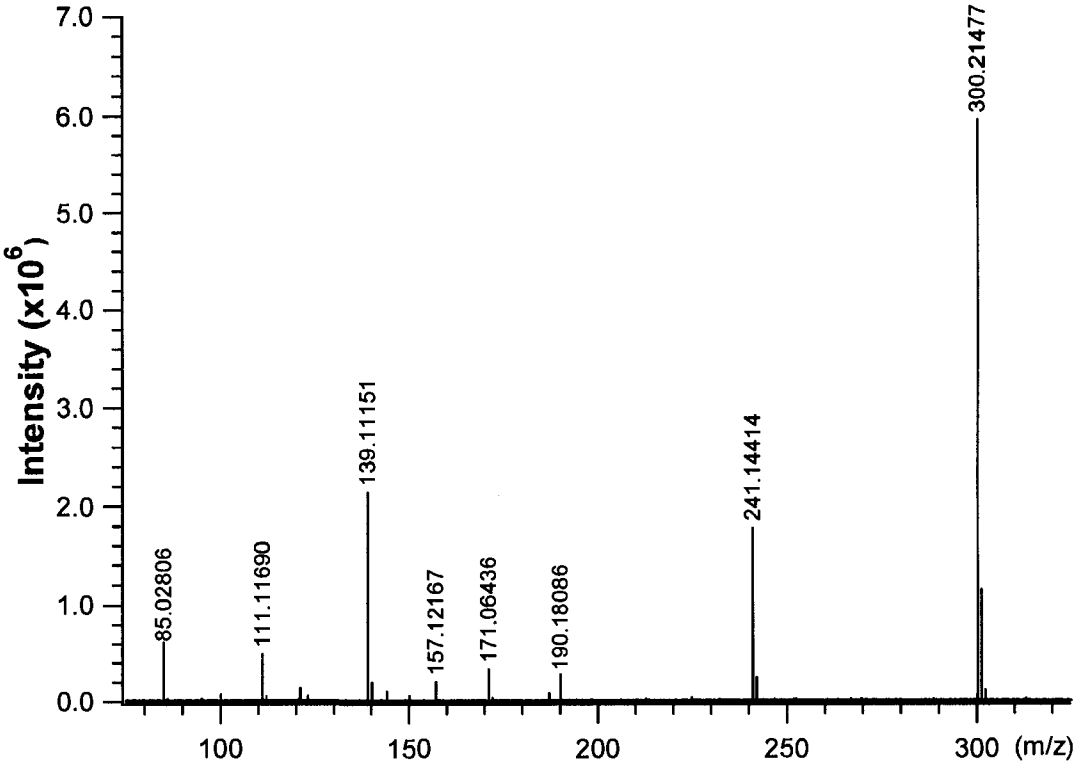

Figure 6.136 - Auto FT MS/MS analysis of m/z 300.21768 at 64.1 min

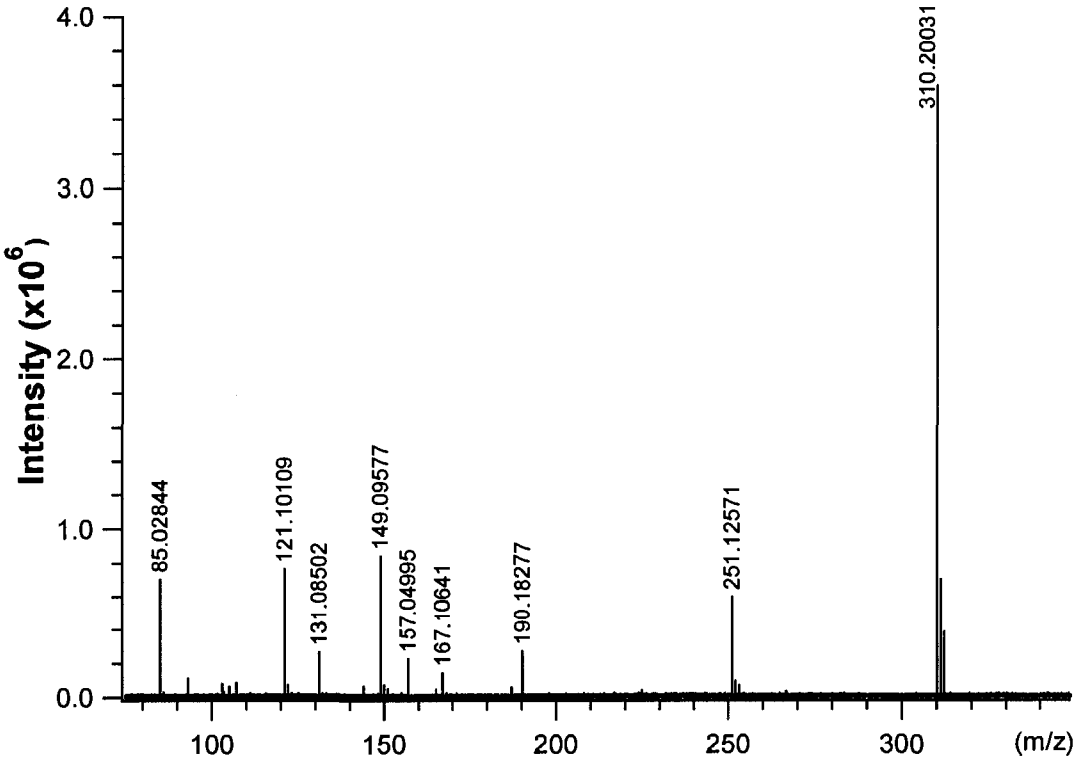

Figure 6.137 - Auto FT MS/MS analysis of m/z 310.19992 at 65.0 min

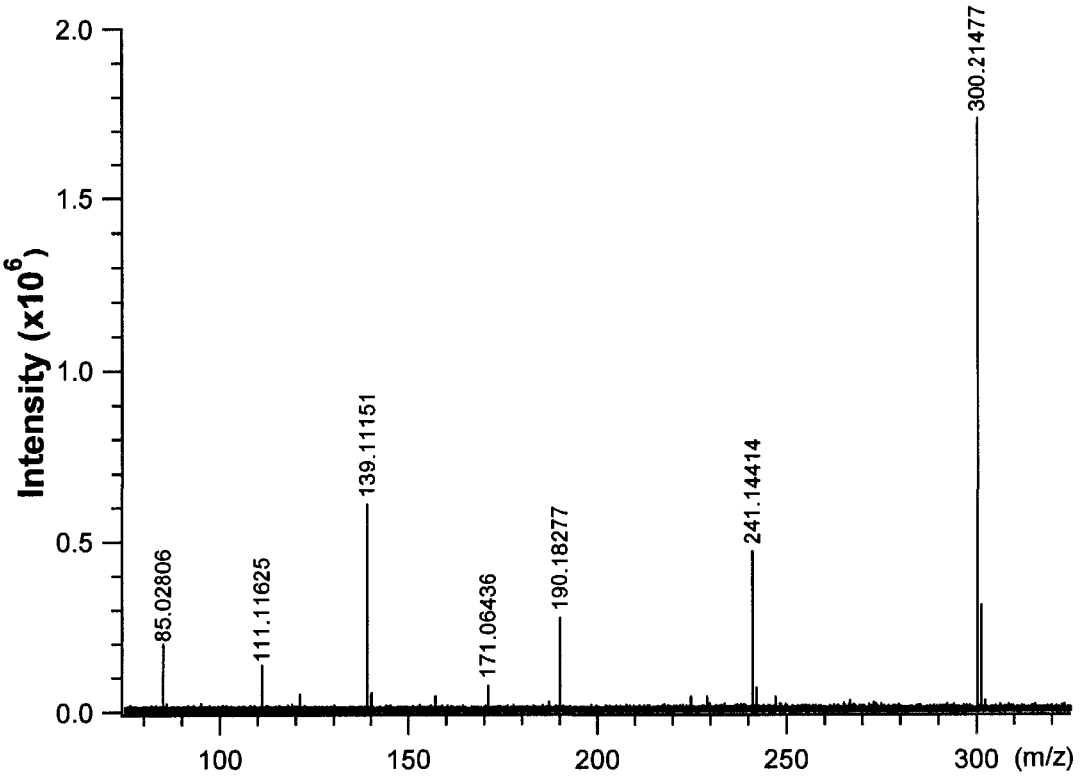

Figure 6.138 - Auto FT MS/MS analysis of m/z 300.21768 at 65.4 min

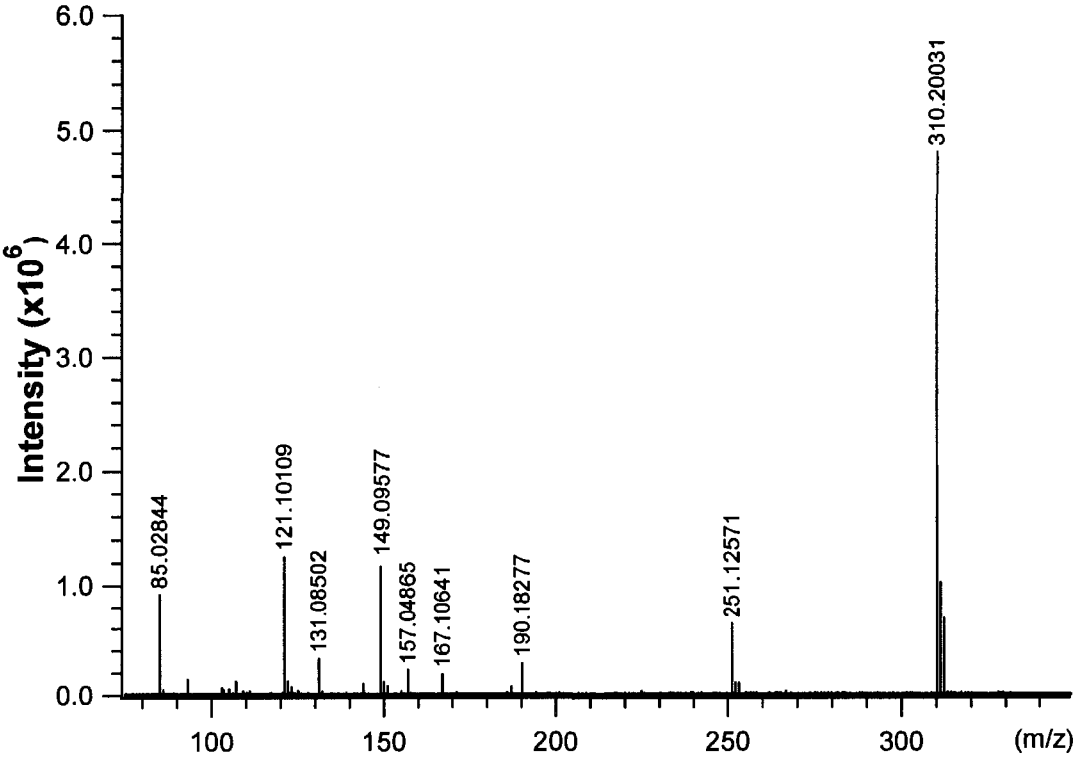

Figure 6.139 - Auto FT MS/MS analysis of m/z 310.19992 at 66.3 min

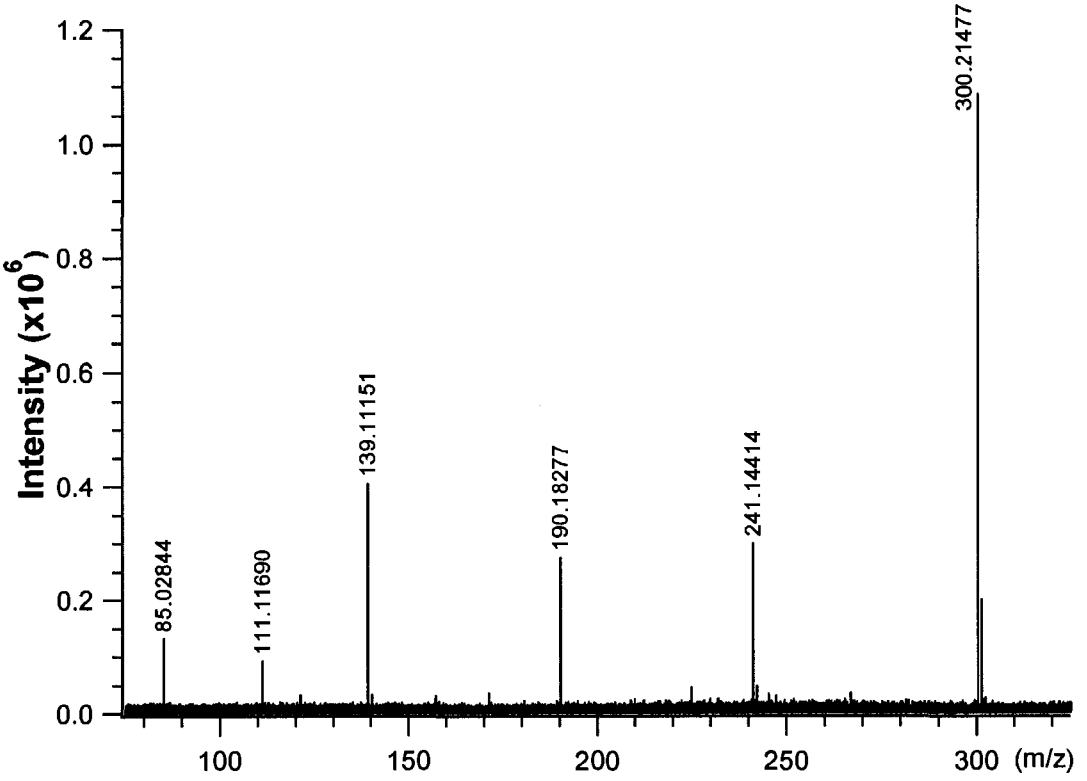

Figure 6.140 - Auto FT MS/MS analysis of m/z 300.21768 at 66.6 min

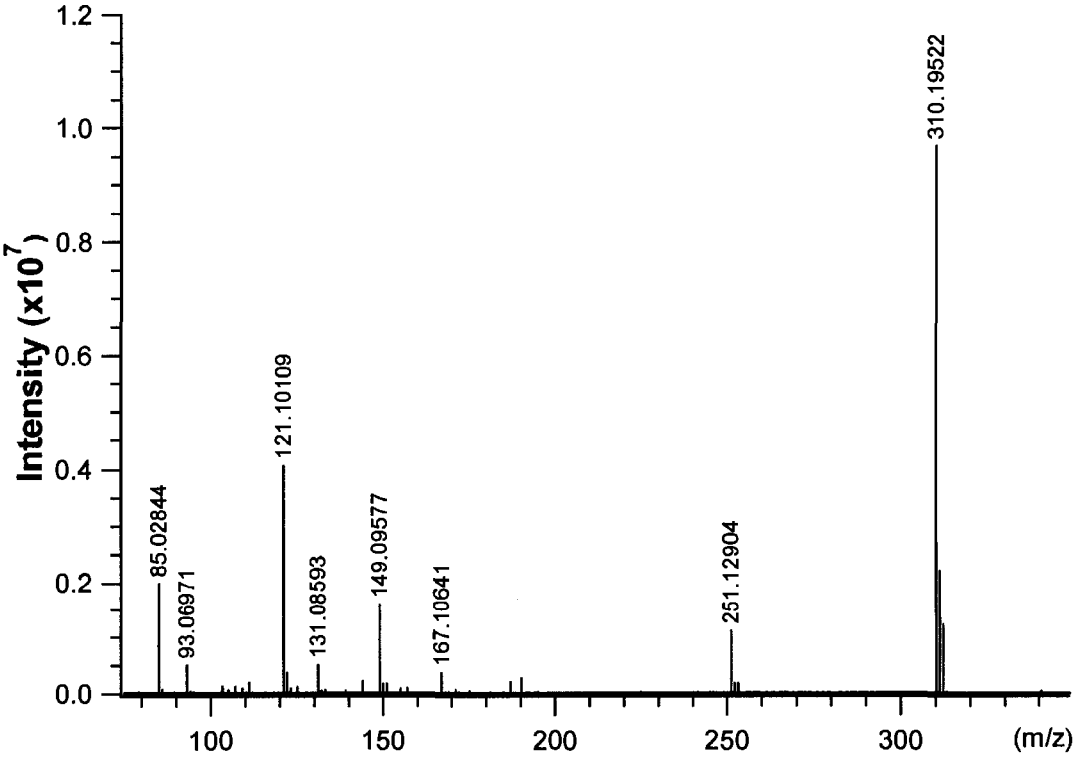

Figure 6.141 - Auto FT MS/MS analysis of m/z 310.19992 at 67.5 min

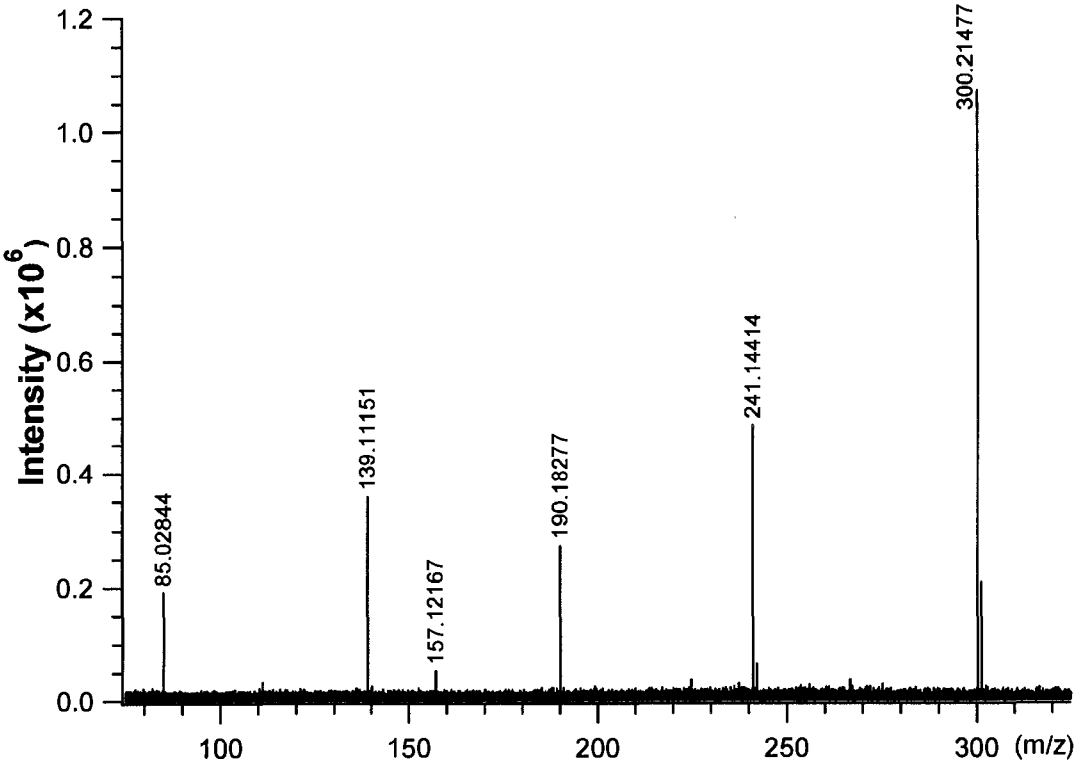

Figure 6.142 - Auto FT MS/MS analysis of m/z 300.21768 at 67.9 min

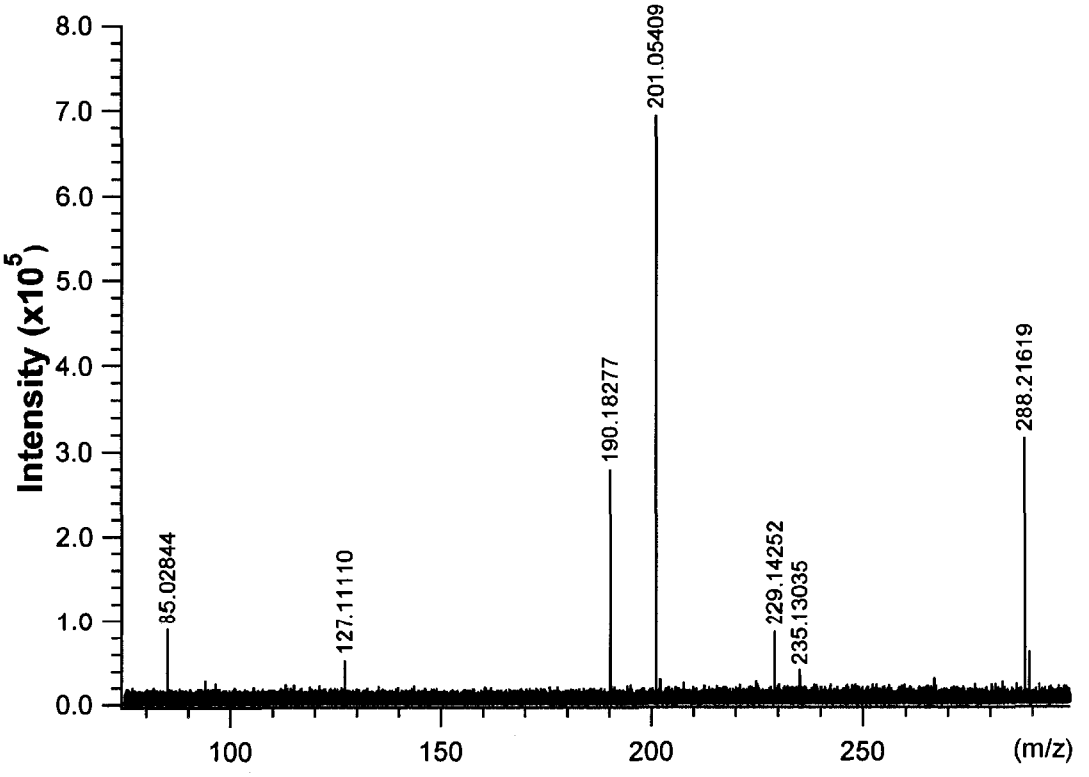

Figure 6.143 - Auto FT MS/MS analysis of m/z 288.21591 at 68.4 min

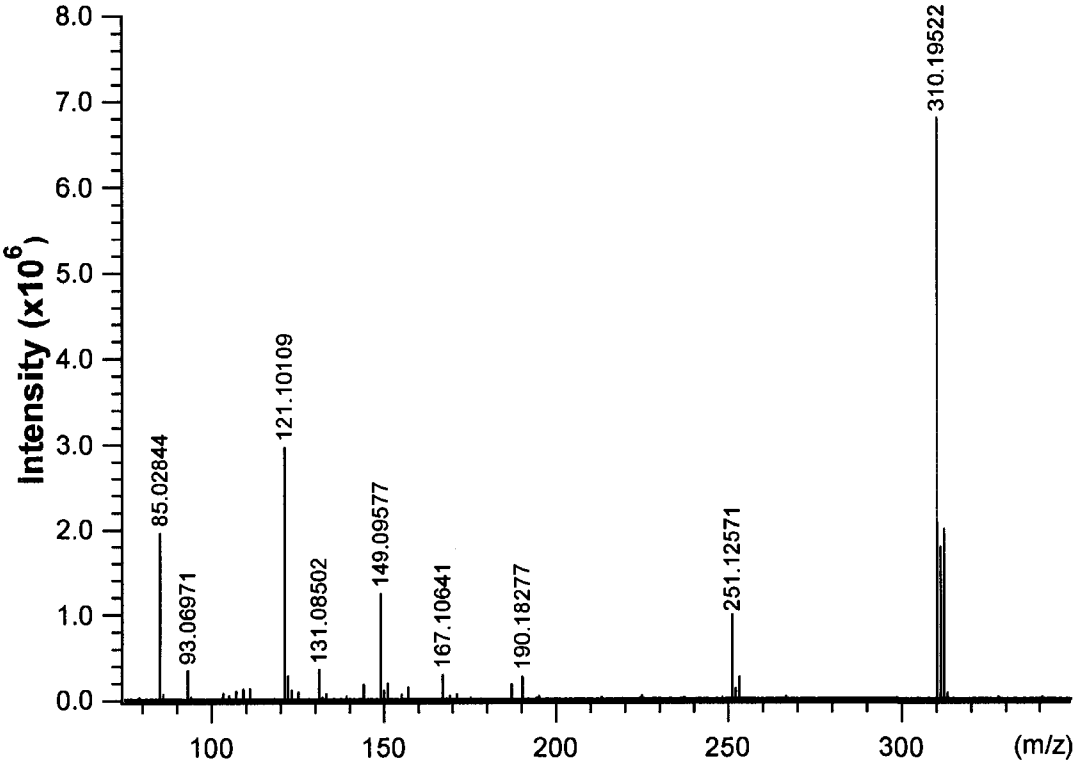

Figure 6.144 - Auto FT MS/MS analysis of m/z 310.19992 at 68.8 min

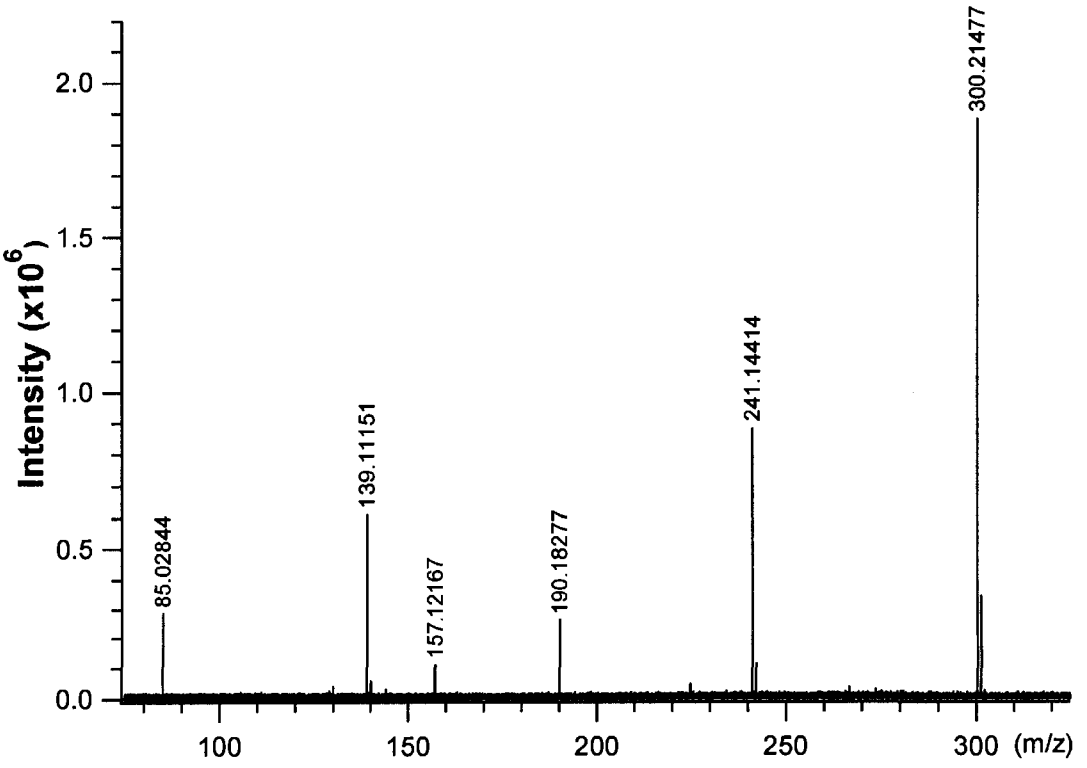

Figure 6.145 - Auto FT MS/MS analysis of m/z 300.21768 at 69.2 min

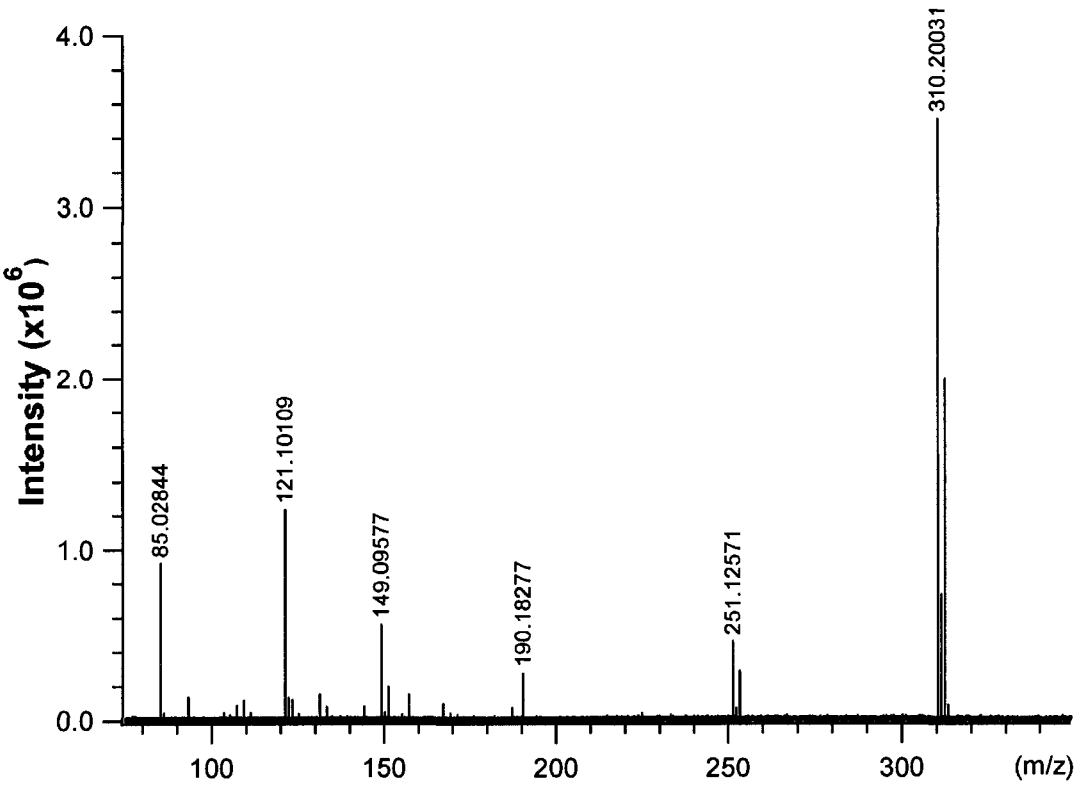

Figure 6.146 - Auto FT MS/MS analysis of m/z 310.19992 at 70.1 min

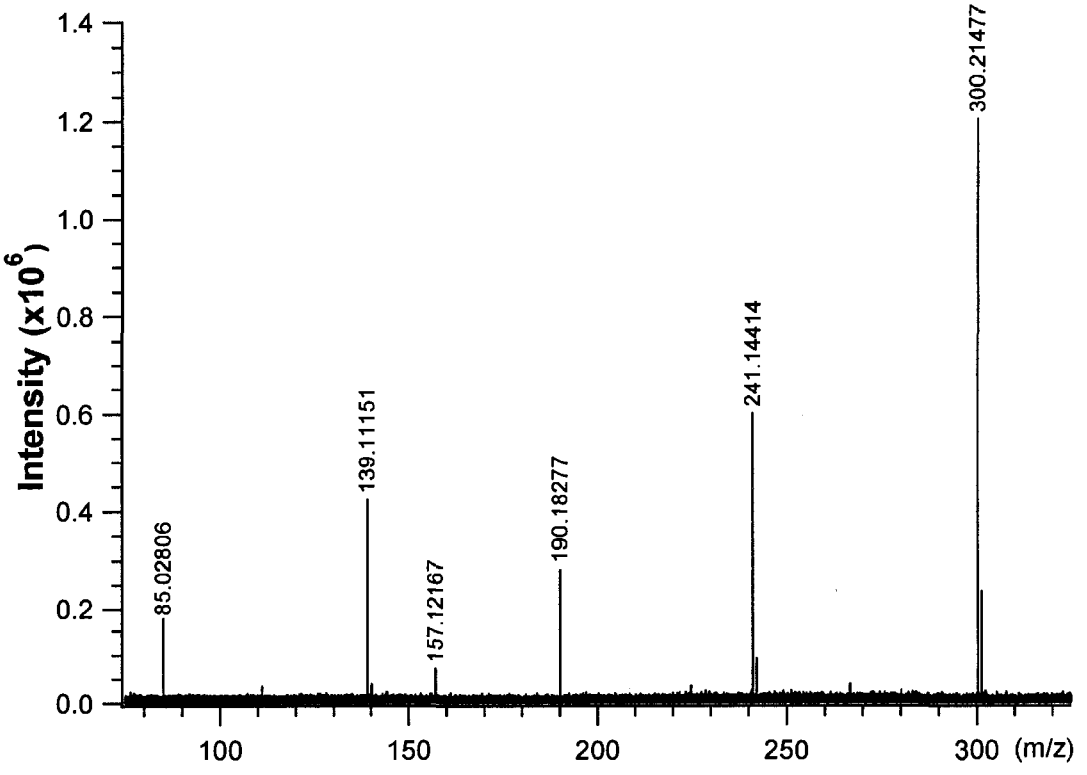

Figure 6.147 - Auto FT MS/MS analysis of m/z 300.21768 at 70.5 min

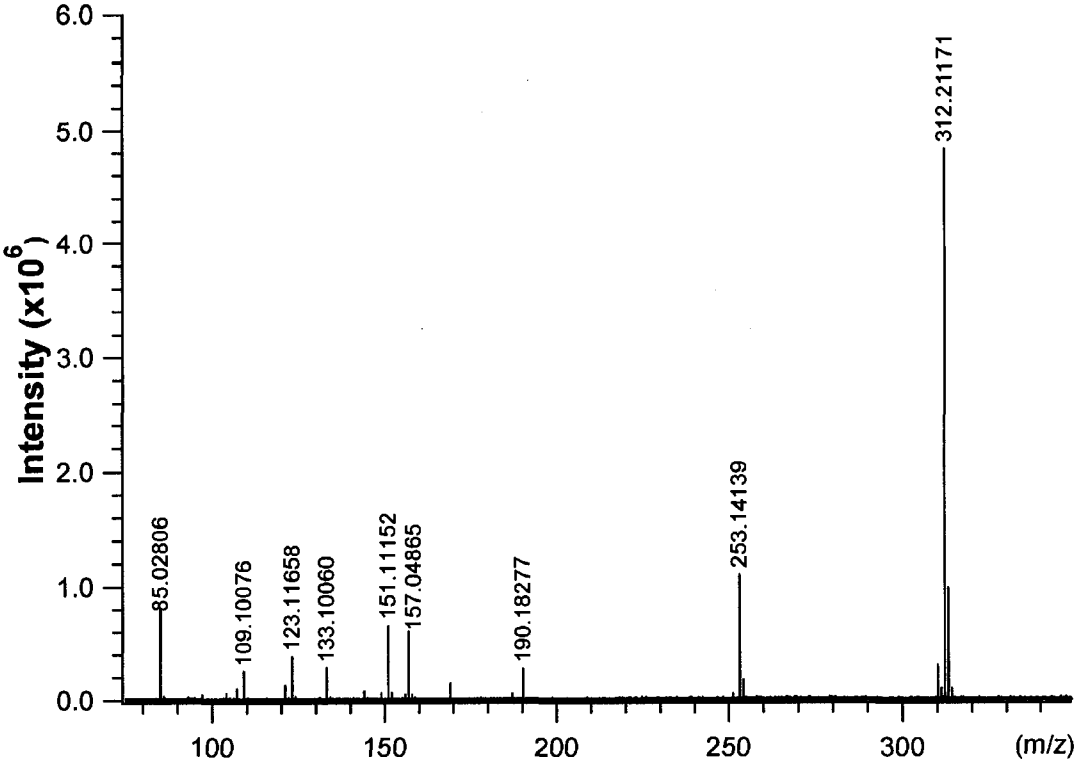

Figure 6.148 - Auto FT MS/MS analysis of m/z 312.26553 at 71.7 min

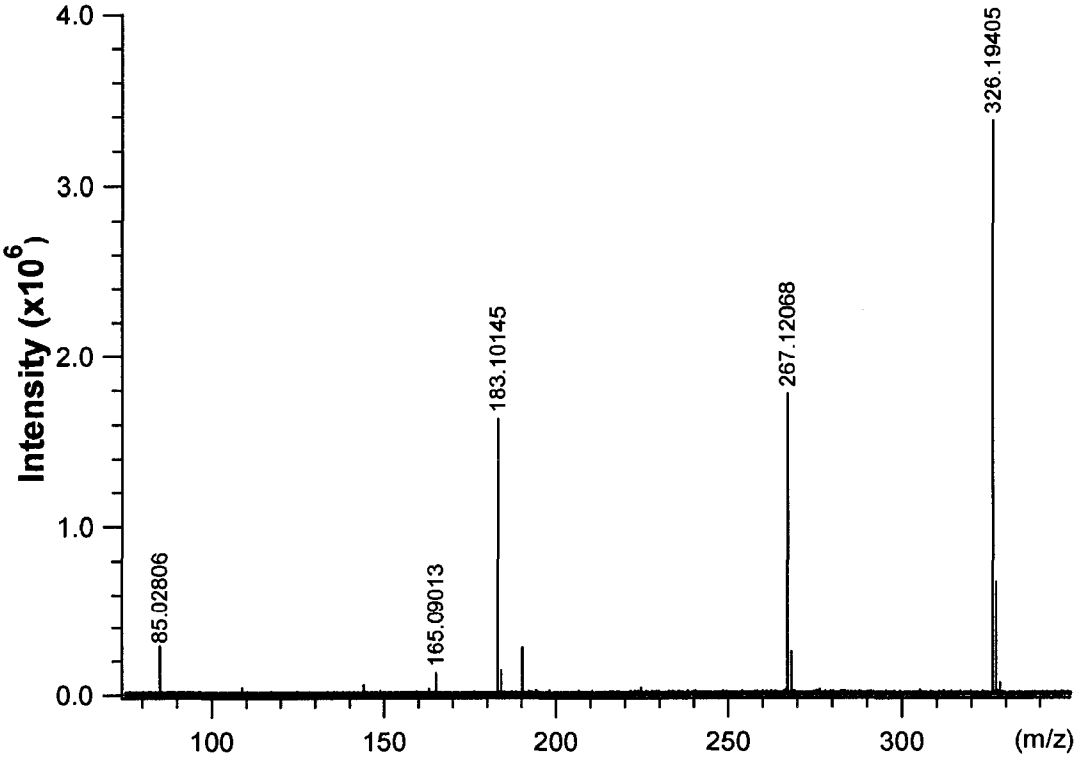

Figure 6.149 - Auto FT MS/MS analysis of m/z 326.14459 at 72.1 min

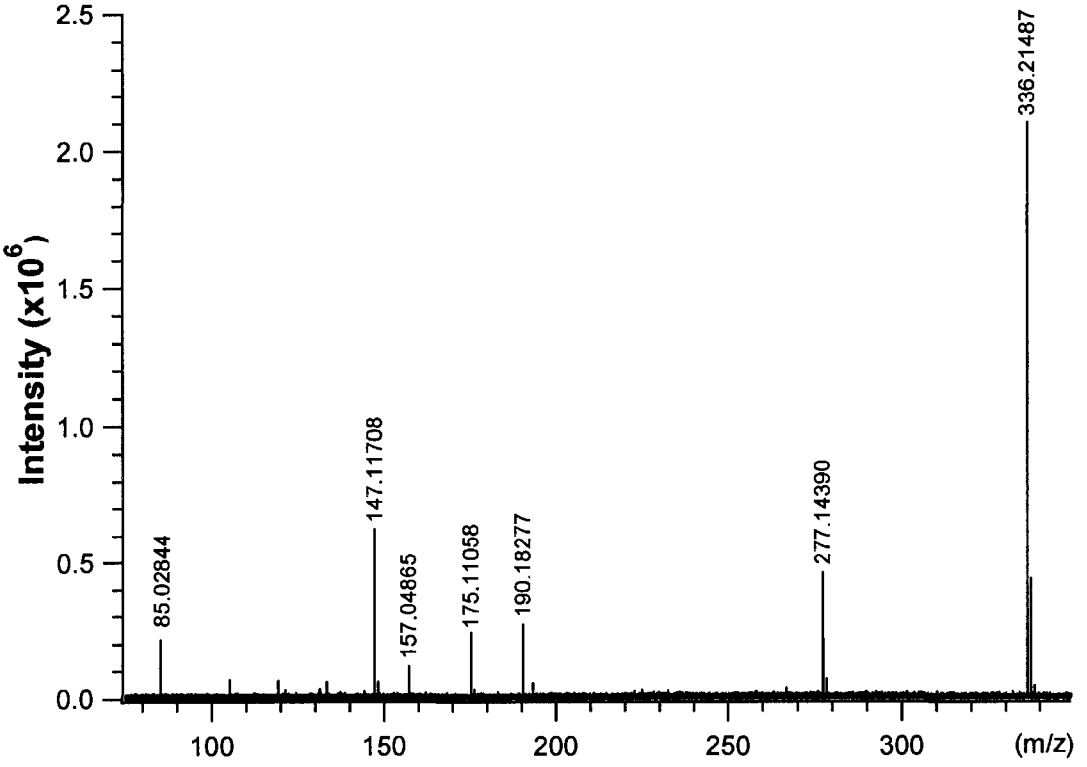

Figure 6.150 - Auto FT MS/MS analysis of m/z 336.21396 at 72.4 min

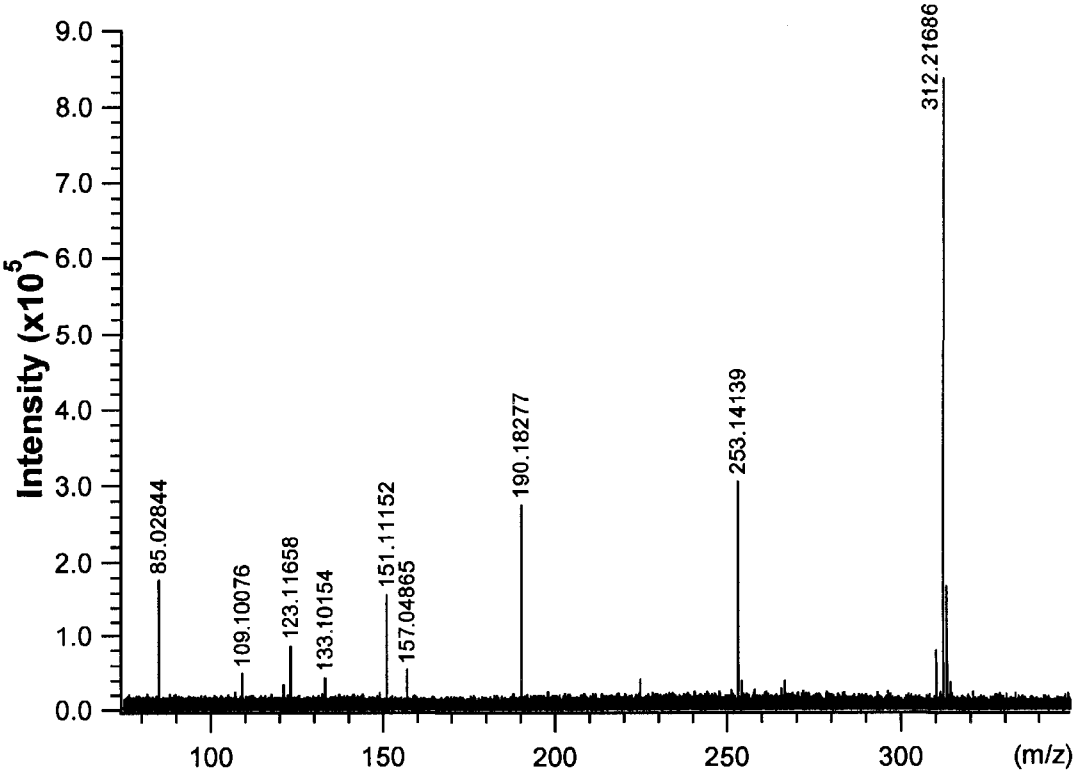

Figure 6.151 - Auto FT MS/MS analysis of m/z 312.26553 at 73.0 min

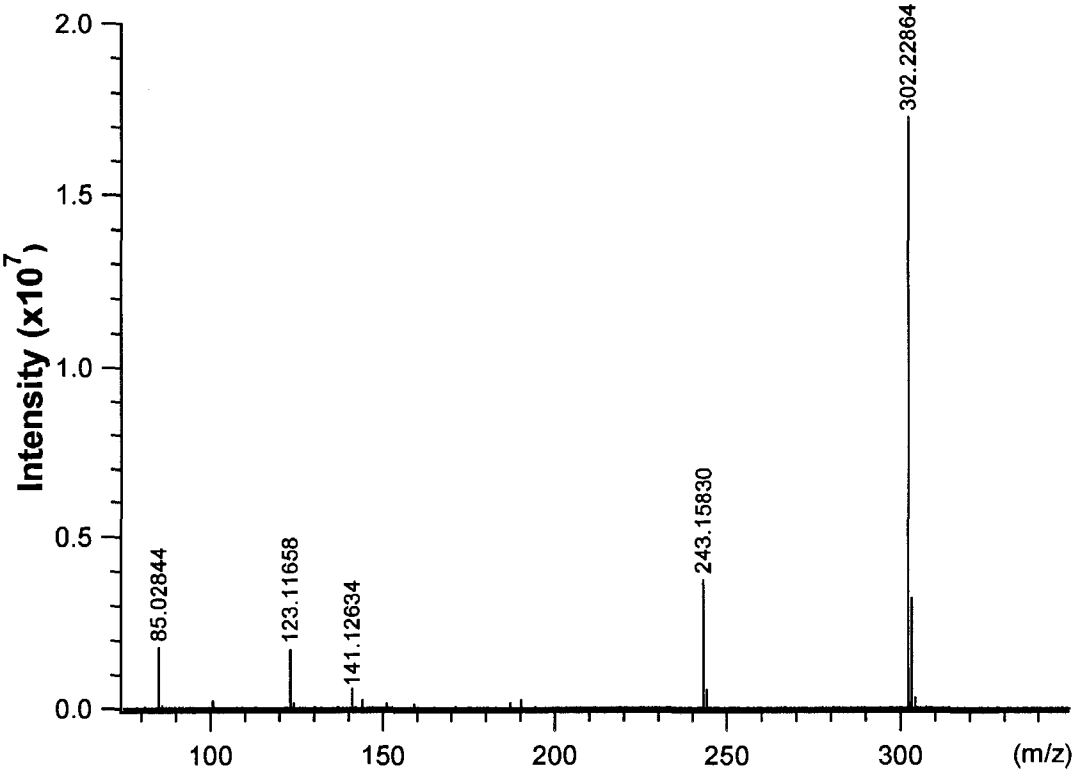

Figure 6.152 - Auto FT MS/MS analysis of m/z 302.19608 at 73.6 min

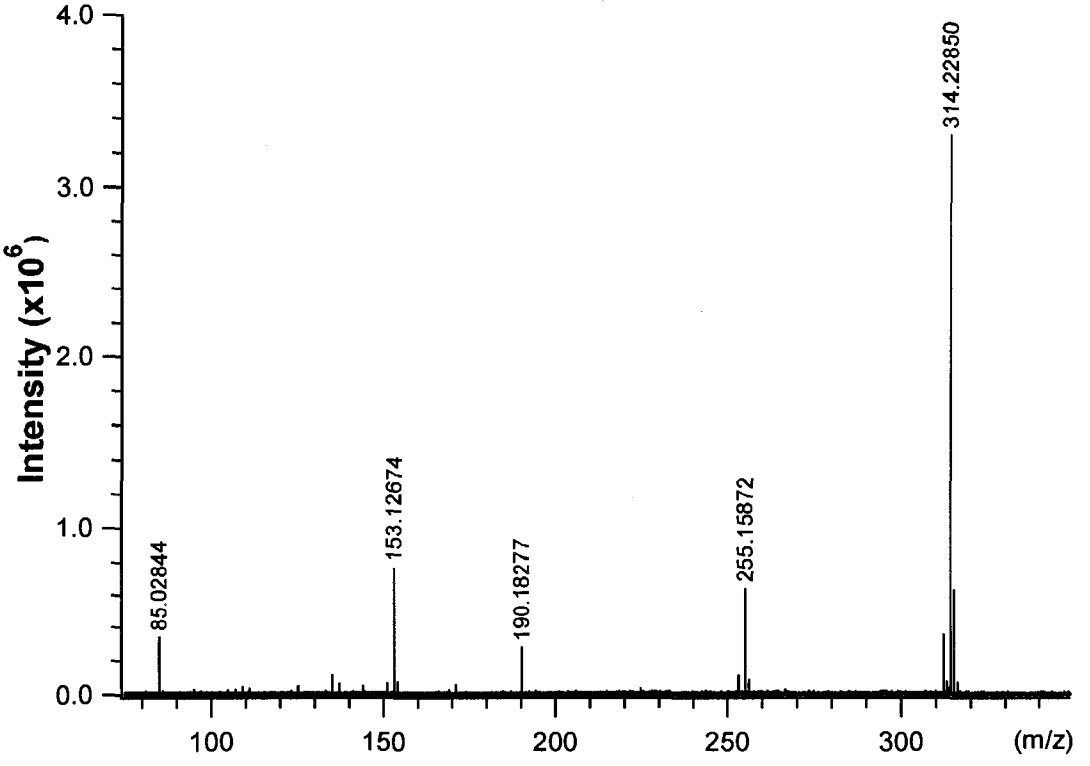

Figure 6.153 - Auto FT MS/MS analysis of m/z 314.22919 at 75.0 min

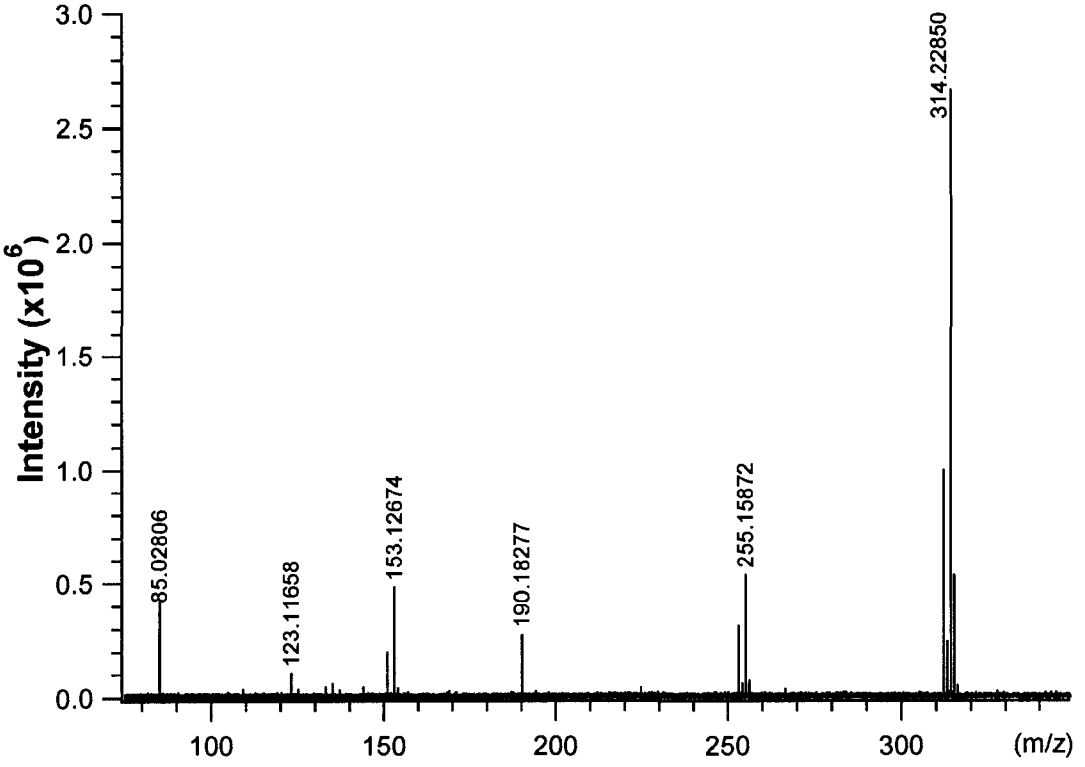

Figure 6.154 - Auto FT MS/MS analysis of m/z 314.22919 at 76.3 min

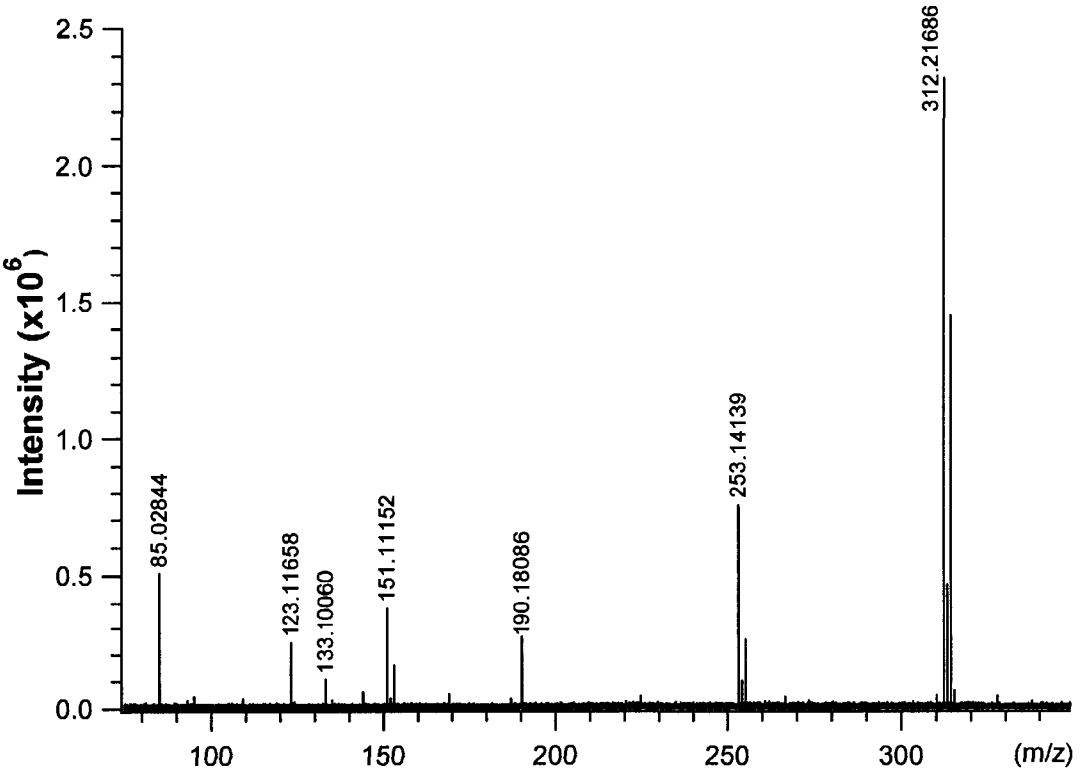

Figure 6.155 - Auto FT MS/MS analysis of m/z 312.26553 at 76.9 min

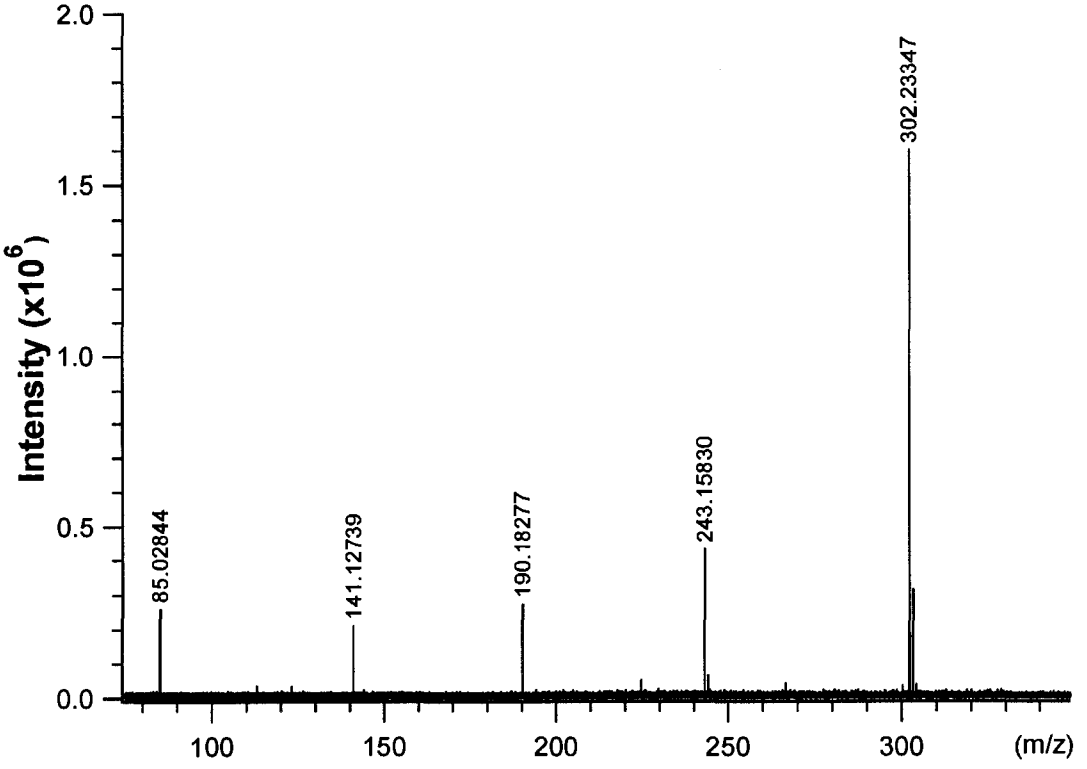

Figure 6.156 - Auto FT MS/MS analysis of m/z 302.19608 at 77.5 min

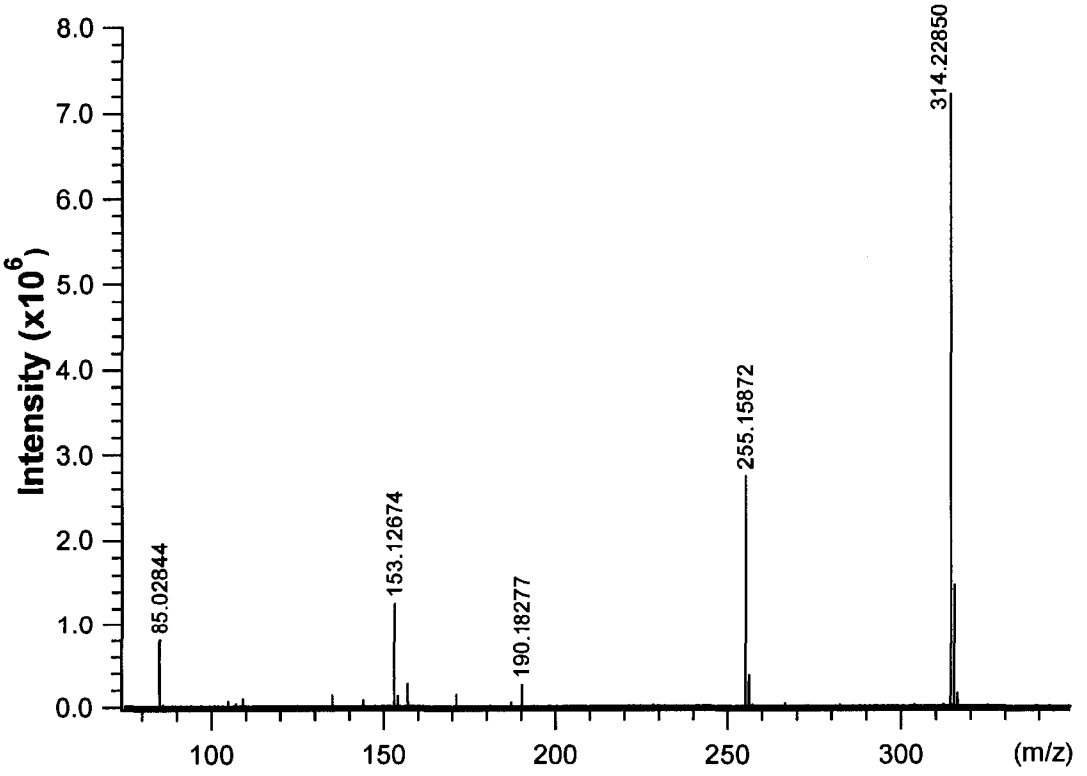

Figure 6.157 - Auto FT MS/MS analysis of m/z 314.22919 at 78.9 min

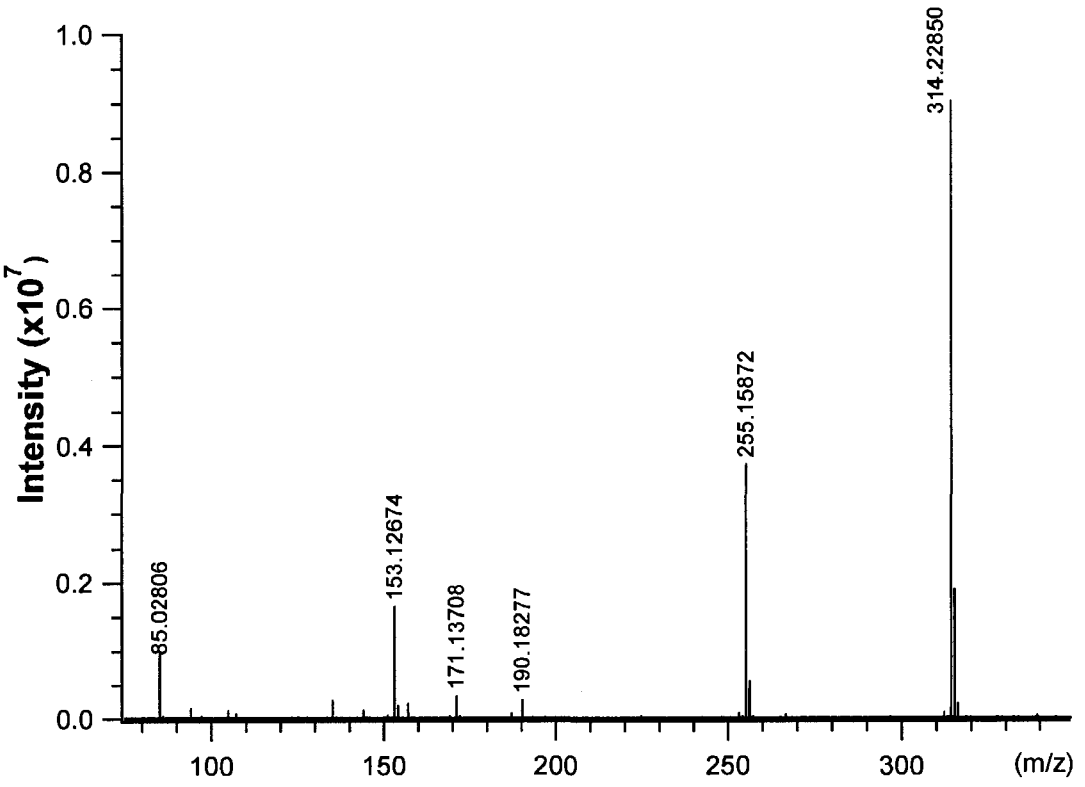

Figure 6.158 - Auto FT MS/MS analysis of m/z 314.22919 at 80.2 min

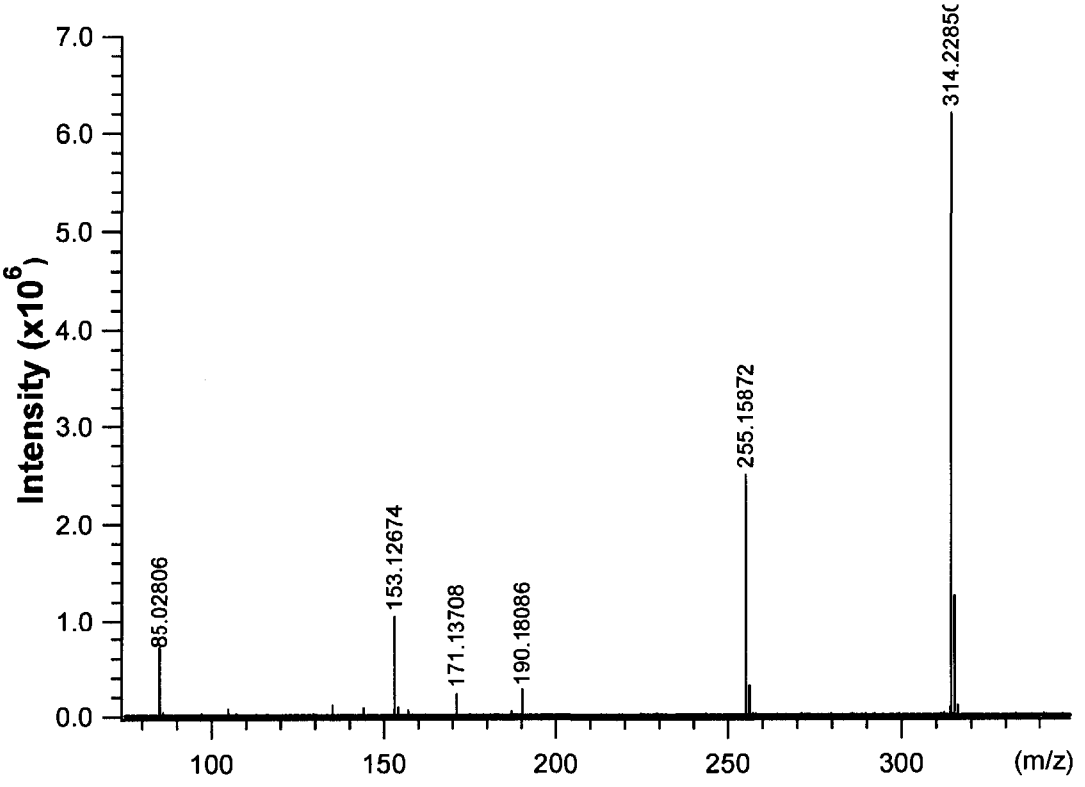

Figure 6.159 - Auto FT MS/MS analysis of m/z 314.22919 at 81.5 min

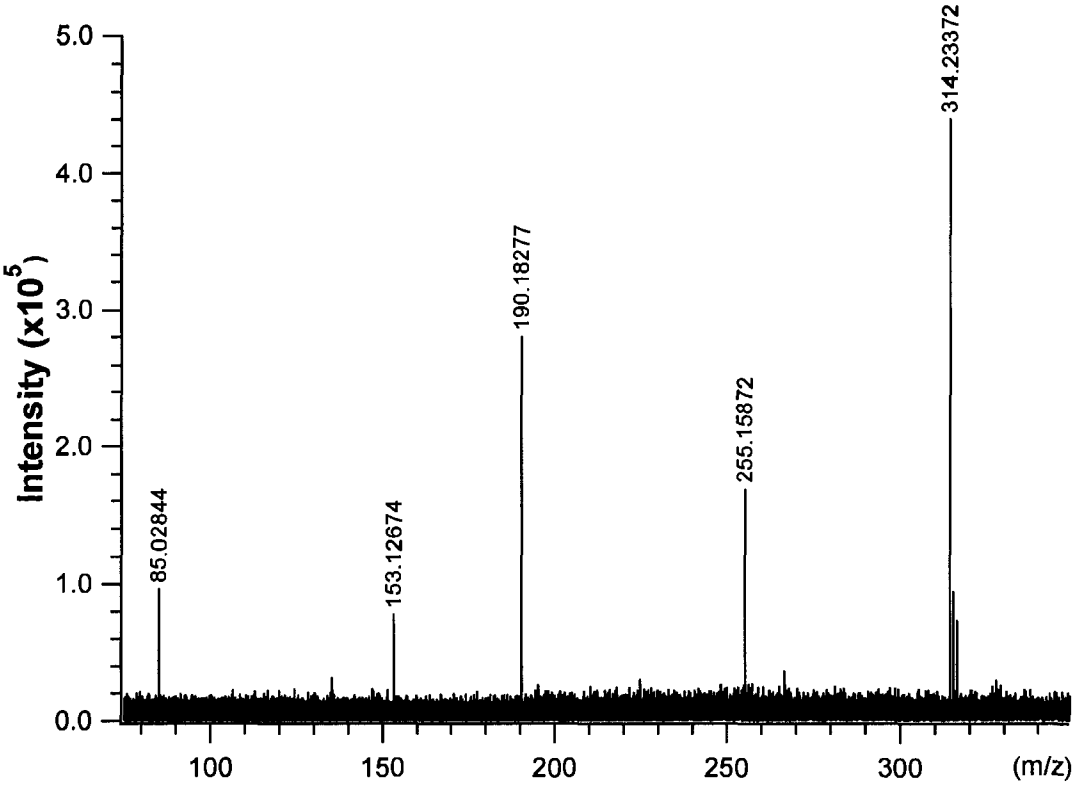

Figure 6.160 - Auto FT MS/MS analysis of m/z 314.22919 at 82.8 min

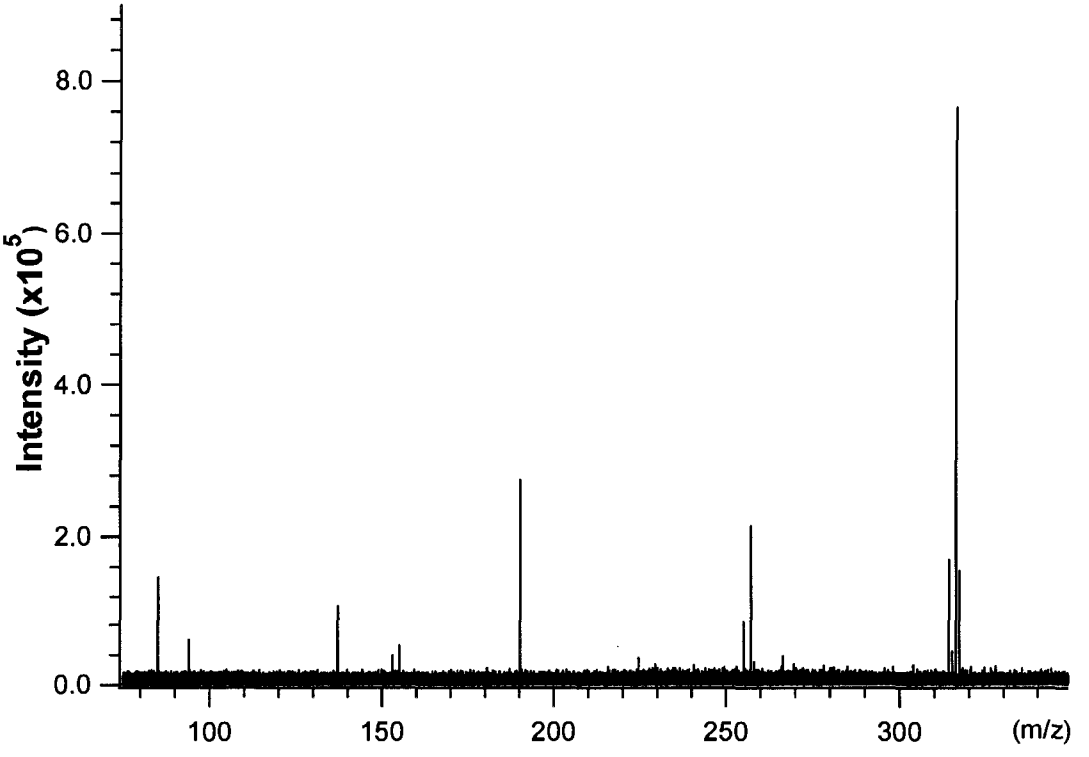

Figure 6.161 - Auto FT MS/MS analysis of m/z 316.21198 at 84.3 min

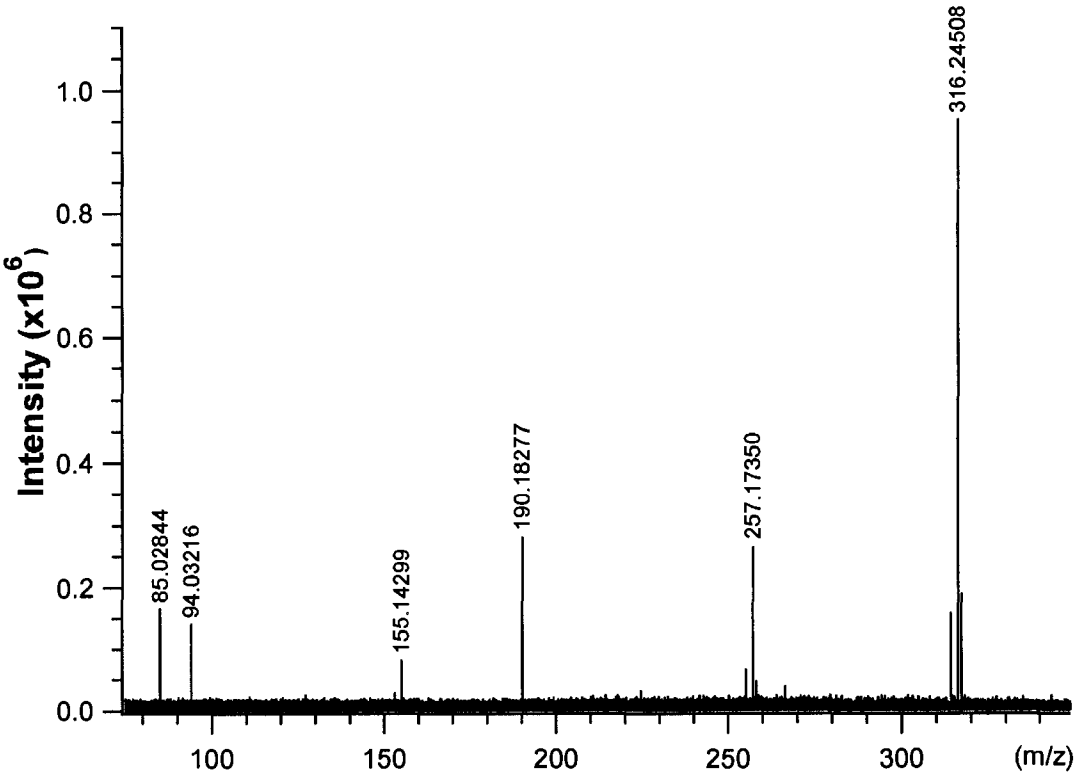

Figure 6.162 - Auto FT MS/MS analysis of m/z 316.21198 at 86.9 min

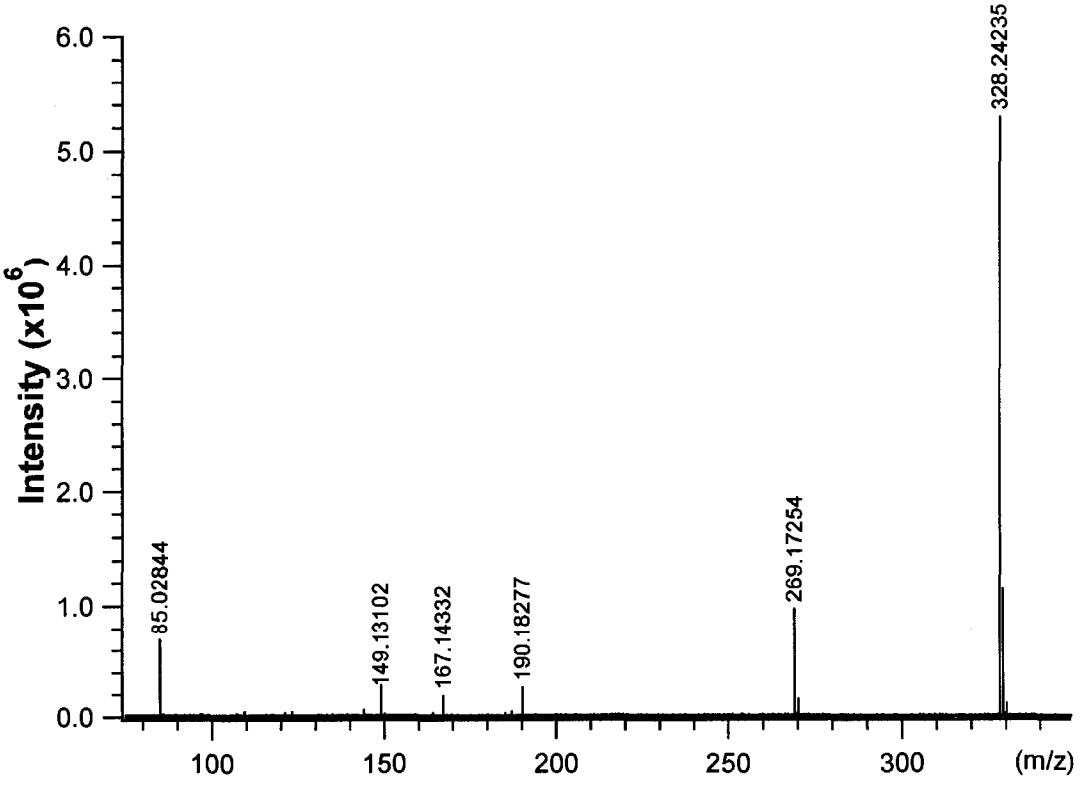

Figure 6.163 - Auto FT MS/MS analysis of m/z 328.21188 at 89.0 min

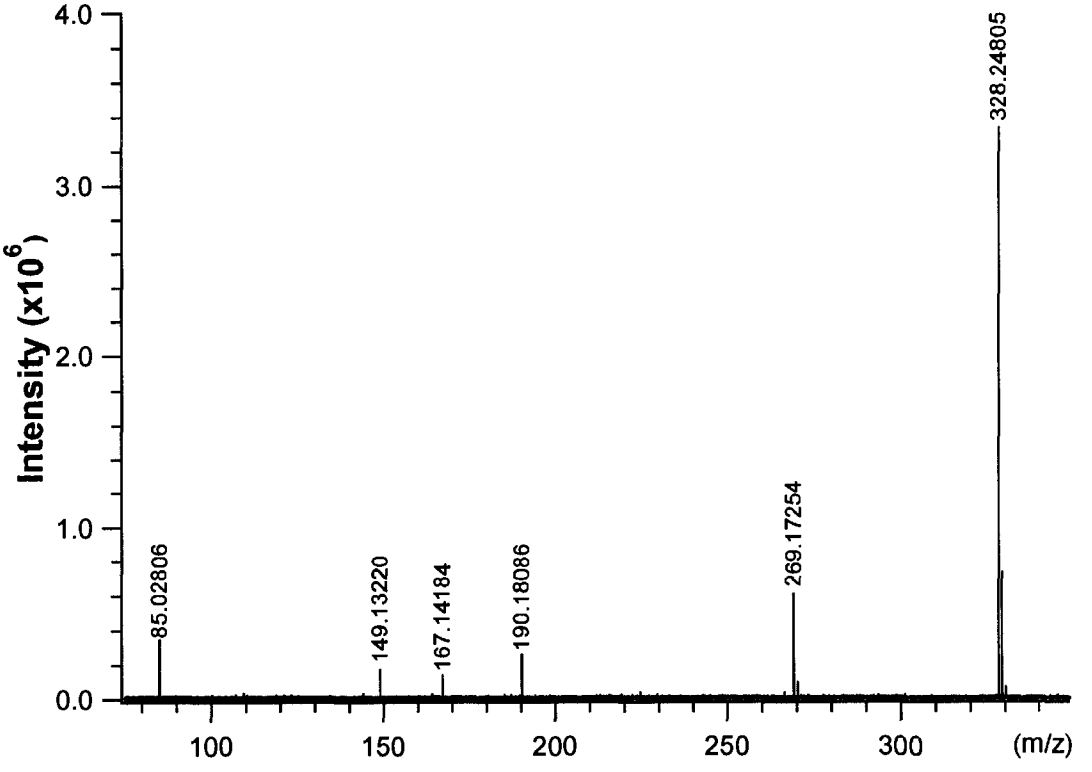

Figure 6.164 - Auto FT MS/MS analysis of m/z 328.21188 at 90.5 min

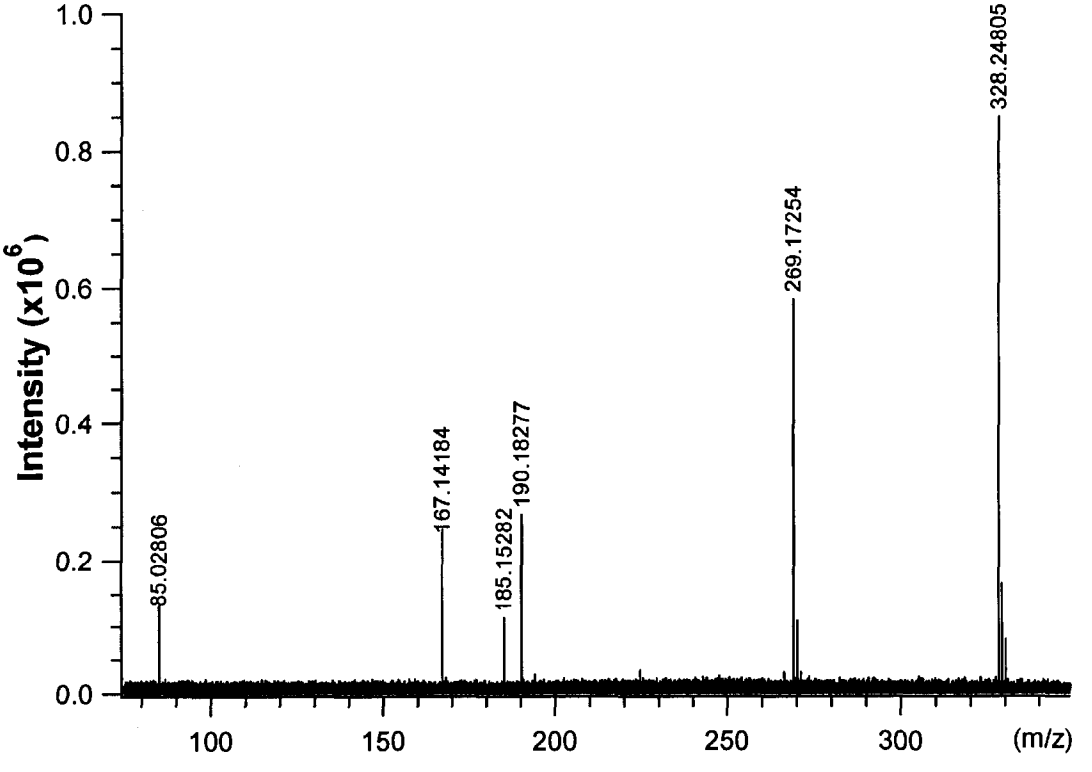

Figure 6.165 - Auto FT MS/MS analysis of m/z 328.21188 at 93.1 min